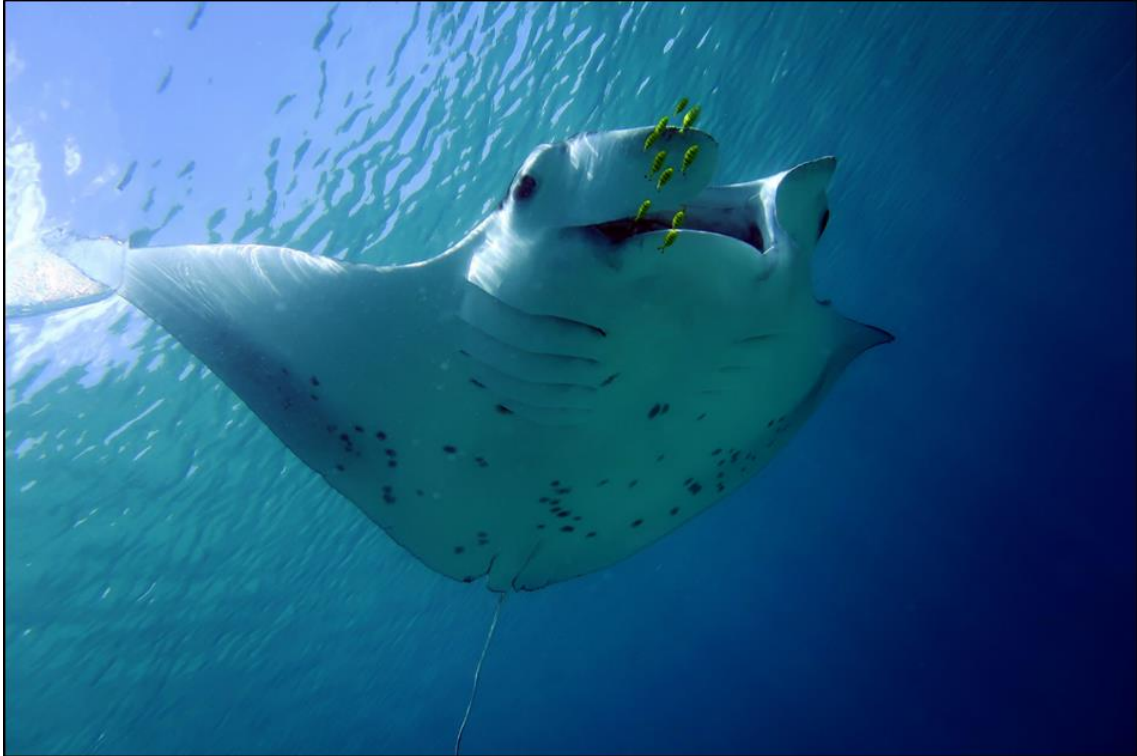


# Movement patterns and feeding ecology of the reef manta ray (*Mobula alfredi*) in Seychelles



by

**Lauren Renee Peel**

BSc (Hons.), University of Western Australia



THE UNIVERSITY OF  
**WESTERN  
AUSTRALIA**

This thesis is presented for the degree of  
*Doctor of Philosophy*  
of The University of Western Australia  
Faculty of Science  
School of Biological Sciences

2019



# Thesis declaration

I, Lauren Renee Peel, certify that:

This thesis has been substantially accomplished during enrolment in this degree.

This thesis does not contain material which has been submitted for the award of any other degree or diploma in my name, in any university or other tertiary institution.

In the future, no part of this thesis will be used in a submission in my name, for any other degree or diploma in any university or other tertiary institution without the prior approval of The University of Western Australia and, where applicable, any partner institution responsible for the joint-award of this degree.

This thesis does not contain any material previously published or written by another person, except where due reference has been made in the text and, where relevant, in the Authorship Declaration that follows.

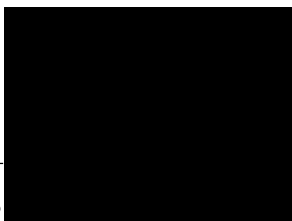
This thesis does not violate or infringe any copyright, trademark, patent, or other rights whatsoever of any person.

The research involving animal data reported in this thesis was assessed and approved by The University of Western Australia Animal Ethics Committee. Approval #: RA/3/100/1480 and RA/3/100/1541. The research involving animals reported in this thesis followed The University of Western Australia and national standards for the care and use of laboratory animals.

The following approvals were obtained prior to commencing the relevant work described in this thesis: permission from The Seychelles Bureau of Standards and The Seychelles Ministry of Environment, Energy and Climate Change to conduct all field work in Seychelles.

This thesis contains published work and/or work prepared for publication, some of which has been co-authored.

\_\_\_\_\_  
Lauren R P





# Abstract

Reef manta rays (*Mobula alfredi*) are large, filter-feeding elasmobranchs that are currently undergoing global population declines. Targeted fishing practises that aim to supply manta gill plates to the market for traditional Asian medicine have contributed significantly to population losses in recent decades, and the impacts of by-catch, accidental entanglement and boat strikes further contribute to observed declines. The development of appropriate strategies to adequately manage and protect this species, which is long-lived, late-maturing and slow to reproduce, requires an understanding of their movement patterns and feeding ecology. However, this information can be difficult to obtain as many populations occur in remote, offshore locations that are both complex to access and susceptible to unsustainable fishing pressures.

Here, I examine the size, movement patterns and feeding ecology of a population of *M. alfredi* in Seychelles. Photo-identification techniques applied over three spatio-temporal scales revealed a small, but highly resident, population of 236 individual *M. alfredi* (Chapter 2). The majority of individuals were sighted at the primary study site, D'Arros Island and St. Joseph Atoll (67%; Amirante Island Group), and 23% were sighted at St. François Atoll (Alphonse Island Group). The use of a remote camera system deployed at a key aggregation site for *M. alfredi* at D'Arros Island provided insight into the patterns of habitat use by this species at this location. It also highlighted the value of remote monitoring systems to studies of *M. alfredi* aggregations at isolated field sites. Passive acoustic telemetry was used to examine the patterns of movement and residency of *M. alfredi* at the Amirante Islands across medium (10 – 100 km) and small (< 10 km) spatial scales (Chapter 3). Telemetry data indicated that *M. alfredi* displayed a high level of residency to the Amirante Islands, particularly at D'Arros Island and St. Joseph Atoll, regardless of the size and sex of tagged individuals. Stable isotope analyses were then used to examine the feeding ecology of *M. alfredi* at the coral reefs surrounding D'Arros Island and St. Joseph Atoll, and the possible influence that foraging strategies may have on the movement patterns of the species (Chapter 4). The significant contribution of pelagic, emergent and mesopelagic zooplankton to the diet of *M. alfredi* provided support for the hypothesis that this large elasmobranch occupies a unique trophic role at this locality, and can act as a vector for horizontal transport of nutrients into reef systems from mesopelagic environments. Processing techniques for *M. alfredi* muscle tissue were also optimised to guide future studies of the foraging ecology of this species using stable isotope analyses. Finally, archival satellite telemetry was used to examine the potential large scale (> 100 km) movements of *M. alfredi* throughout Seychelles (Chapter 5). Tagged individuals did not leave the boundary of the Seychelles Exclusive Economic Zone for the entire period that they were tracked (up to 180 days), and transmitted data further supported the high residency of individuals to the Amirante Islands.

Collectively, these findings highlight the significance of D'Arros Island and St. Joseph Atoll to the small population of *M. alfredi* in Seychelles. These data also indicate that the establishment of Marine Protected Areas at the key aggregation areas for *M. alfredi* at D'Arros Island and St. Joseph Atoll (Amirante Island Group), and St. François Atoll (Alphonse Island Group), would benefit management and conservation efforts for all cohorts of the population. Continued monitoring of this population through photo-identification techniques by an increasing network of researchers and citizen scientists spread across the archipelago will ensure that *M. alfredi* is protected at an appropriate spatio-temporal scale in Seychelles in the future.

# Acknowledgements

First and foremost, I would like to thank my supervisors, Dr Mark Meekan, Prof. Shaun Collin, Dr Guy Stevens, Dr Ryan Daly, Mrs Clare Keating Daly and Dr Jane Prince, for all of their support and guidance over the past three and a half years. Mark, I am at a loss for words when it comes to expressing my gratitude to you for the opportunity to lead the Seychelles Manta Ray Project. My PhD experience has exceeded everything I could have ever expected, and I wouldn't change it for the world. Thank you for all of your advice, your mentorship, and for laughing with me while we navigated every curve ball of this crazy adventure. Thanks also for all of the drafts, forms, reports and permit applications you have read, and for the invaluable writing and presentation skills that you have taught me. I am a better scientist for all of it. Shaun, I will always be grateful for your career and life advice, and for your feedback on all of my work. Thank you for always making time to meet, regardless of how busy you were, and for always being excited about my research. Guy, thank you for answering my endless questions, for providing field work and writing advice, and for sharing your manta wisdom with me. I've lost track of all the ridiculous hours and places we have Skyped each other from, but I am grateful for all of our conversations, and can't wait to see where we can take the Seychelles Manta Ray Project in the future. Ryan, your guidance and expertise made so much of this thesis possible. From setting up the satellite tags, to collecting tissue samples, to analysing a wide range of data types, you were always available to discuss ideas and methodologies, and I can't thank you enough for everything I have learned from you. Clare, my honorary supervisor, thank you for your help managing this research project and for all of your advice throughout the past few years. Whether I was writing a formal report, putting together a blog post, or just in need of someone equally as eager to walk around D'Arros Island, you were always there, and I can't wait until the next time we can catch up over some lemon-cream cookies and coffee! Last but not least, Jane. Thank you for all of your support over the past six months (as well as the last 10 years!). It has been exciting to share my PhD journey with you, and I will never tire of our endless chats about teaching, research and life in general. Finally, to all of my supervisors, thank you for believing in me. Thank you for trusting that I could get the job done, even when I suggested adding a second island to the study on top of everything else that we had planned (totally worth it!). You will never know how much I appreciate the independence you allowed me.

A huge thank you must also go to the Save Our Seas Foundation (SOSF) for funding this research, and to the SOSF – D'Arros Research Centre for supporting all aspects of fieldwork at D'Arros Island. To Dr Michael Scholl and Dr Nadia Bruyndonckx, thank you for all of your support and for allowing me to expand the Seychelles Manta Ray Project wherever possible. To Ryan and Clare, thank you again for all of your hard work during the November field trips at D'Arros. I will treasure my memories on the island (and at Rainbow House!) forever. I'd also like to thank

the entire team at The Manta Trust for their support of the Seychelles Manta Ray Project. It has been such a fantastic experience working with you all. To Dr James Lea and the Danah Divers team, thank you for the countless hours you have spent maintaining the Amirantes acoustic receiver array. Thank you to the Island Conservation Society and Blue Safari for your support of this project, and being so open and eager to develop a manta monitoring program at Alphonse Island. Finally, thank you to The Seychelles Bureau of Standards and The Seychelles Ministry of Environment, Energy and Climate Change for allowing me to conduct this research in such a unique and beautiful part of the world.

To the people who provided me with invaluable assistance in the field – Justin Blake, Luke Gordon, Joseph (Pep) Nogués, Ariadna Fernandez, Christopher Narty and Lucy Martin – thank you for always being willing to go the extra mile. Whether it was one more identification photo, another lap around the island or a final dive, you helped this research become possible. And, to the mantas that we all worked so hard to study, thank you for keeping me on my toes at all times and giving me some of the best moments in the water of my life.

In addition to the funding support I received in the field, my gratitude goes to the Australian Government for supporting this research with a Research Training Program (RTP) Scholarship, and The University of Western Australia (UWA) for my Top-Up scholarship. Additional funding from the Australian Institute of Marine Science (AIMS), the Save Our Seas Foundation, the UWA Postgraduate Student's Association, the UWA Graduate Research School, and a Robson & Robertson Award from UWA allowed me to broaden my original research plans and to travel to a number of international conferences, providing me with experiences that I am incredibly grateful for. A thank you must also go to the staff at AIMS for all of their support over the past few years. To Olwyn, Louise, Kathrine and Sabrina, thank you for helping me to keep the manta project moving forward at all times. To Dr Luciana Ferreira, thank you for being so willing to share your expertise and skills with me, and for providing feedback on my analyses and writing. I am very lucky to have been able to work with you.

Thank you to the staff at UWA for supporting me throughout my PhD, for the inspiring discussions, and for the many opportunities to develop my teaching skills throughout my candidature. To Caroline Kerr, thank you for all of your help with my permit applications and for many a coffee. To my fellow PhD students, a big thank you to all of you for sharing in this journey with me and for allowing me to be a part of yours. To the Neuroecology Group (Shaun, Caroline, Wayne, Jon, Vic, Lucille, Mike, and Marie-Lise), thanks for all the cheeky Friday wines and cake that often accompanied our chats. To the team at Zoology – Blair, Phil, Rowan, Tabs, Fabian, Jake, Peter, JP, Emily, Callum, Annie and Sarah – thank you for all of the laughs and support. To my sharky girls – Sammy, Em, Charli, Steph, Dani and Bec – I can't imagine what these past few years would have been like without you all. You are amazing. To Em and Sammy in particular,

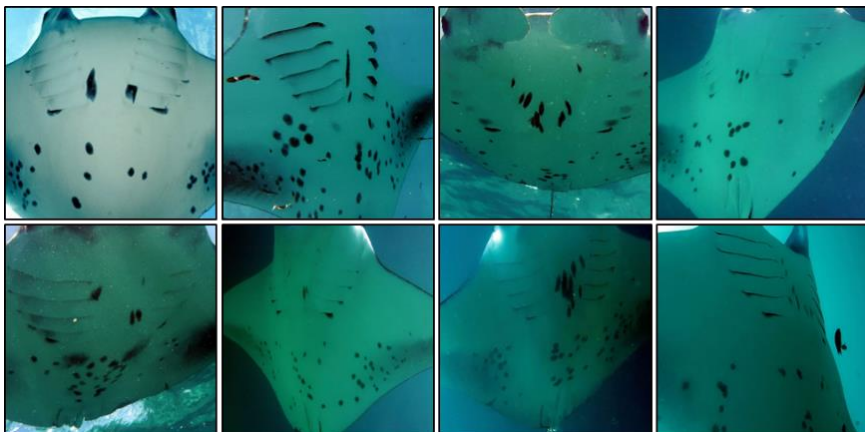


sharing an office with you both is easily one of the highlights of my PhD. Thank you for every coffee run, instant message, glass of wine, ridiculous adventure in the field, and loud cackling laugh. I can't wait until the day we are reunited again!

To all of my wonderful friends and family who have supported me throughout this journey, thank you from the bottom of my heart. To Gen, Andrew, Lauren, Abe, Crystal, Bec, Shane, David, Erin and Burke-O, thank you for always making life so much fun. To Chris, Marcia, Kirsty, Allan, Wessel, Helét, Tiaan, Ryan, Catherine and Graeme, thank you for welcoming me into your family with open arms. Your support means to world to me.

To the one and only Wesley Holm, I can't begin to express how grateful I am for everything you've done for me. Thank you for moving across an ocean to let me follow my dream, and for your endless, unwavering support through all of the highs and the lows. Thank you for every "you got this, babes", for every FaceTime call from the field, for reading my drafts, checking my figures, and for making me laugh every single day. I love you more than you will ever know, and I am so excited to see where life takes us next.

Finally, to my family in Australia, I am the person I am today because of you, and I can't explain how lucky I feel to have been able to share every experience of this PhD with you. To Tony, Sue, Mick, Heather, Marcus, Alex, Nina, Simone, Gillan, Matt, Shae, Jye, Kyra and Ruby, thank you for always asking how things were progressing, even when you knew the answer was probably going to be animated and lengthy. To Granny, thank you for always inspiring me to learn new things and for your constant support. To Grandad, thank you for all of your advice, for reminding me not to sweat the small stuff, and for your big hugs. To Hayley and Tyler, thank you for always being excited about my work and for always having my back. To Mum and Dad, you both are incredible. Thank you for teaching me to be excited about the world around me, to dream big, and to live my life to the fullest. Thank you for always encouraging me to follow my heart (even if that meant leaving home to chase fish all over the world) and for your endless support during my PhD. You have no idea how much I appreciate it all. And, to Nana. I wish more than anything you could be here to read this thesis and to celebrate with our family. I will never forget how excited you were to hear about my work and field trips, and I hope that I have made you proud. Keep watching over the mantas for me, and thank you for teaching me to be fearless, always.





# Publications from this thesis

## Chapter 2

Peel LR, Daly R, Keating Daly CA, Stevens GMW, Collin SP, Meekan MG (In preparation) Population size, habitat use and residency of manta rays at aggregation sites in Seychelles. *Marine and Freshwater Research*.

## Chapter 3

Peel LR, Stevens GMW, Daly R, Keating Daly CA, Lea JSE, Clarke CR, Collin SP, Meekan MG (2019) Movement and residency patterns of reef manta rays *Mobula alfredi* in the Amirante Islands, Seychelles. *Marine Ecology Progress Series* 621:169-184.

## Chapter 4

Peel LR, Daly R, Keating Daly CA, Stevens GMW, Collin SP, Meekan MG (2019) Stable isotope analyses reveal unique trophic role of reef manta rays (*Mobula alfredi*) at a remote coral reef. *Royal Society Open Science* 6:190599.

## Chapter 5

Peel LR, Daly R, Keating Daly CA, Stevens GMW, Collin SP, Meekan MG (In preparation) A multi-technique approach to the description of regional movements of reef manta rays (*Mobula alfredi*) in Seychelles waters. *Marine Biology*.



# Statement of candidate contributions

This thesis is presented as a series of four manuscripts in journal formats, as well as the general introduction and general discussion sections. These papers were developed by my own ideas and hypotheses, with inputs from my supervisors and co-authors.

This research was generously supported by the Save Our Seas Foundation (SOSF), and fieldwork supported by the SOSF – D’Arros Research Centre. Additional support was provided by the Australian Institute of Marine Science, The Manta Trust, The University of Western Australia (UWA), the UWA Postgraduate Student’s Association, the UWA Graduate Research School, the Island Conservation Society and Blue Safari. Tuition stipend was provided by an Australian Government Research Training Program (RTP) Scholarship and a UWA Safety Net Top-up Scholarship.

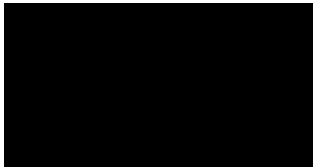
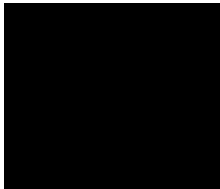
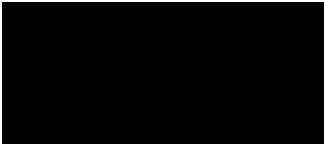


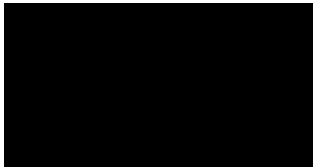
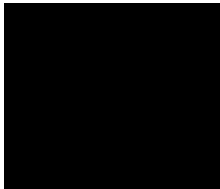
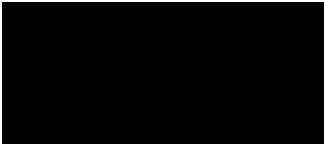


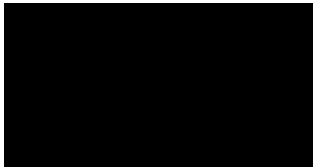
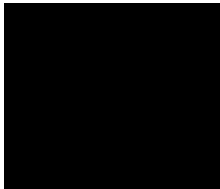
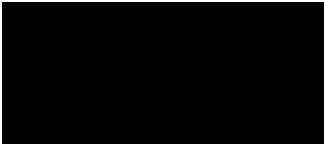


Photo-identification and acoustic telemetry data collected at D’Arros Island prior to September 2015 was contributed by Dr Guy Stevens (Manta Trust), Dr Ryan Daly (SOSF – D’Arros Research Centre) and Mrs Clare Keating Daly (SOSF – D’Arros Research Centre) for Chapters 2 and 3. Staff based at the SOSF – D’Arros Research Centre continued to provide manta ray identification photos throughout the duration of this research. Dr James Lea (University of Cambridge) managed and coordinated the maintenance and downloads of the Amiranter acoustic receiver array, and provided compiled acoustic detection data after each receiver download for Chapters 3 and 5.

The analyses described in all data chapters were carried out by myself and all chapters were written by me with feedback from Dr Mark Meekan (all chapters), Prof. Shaun Collin (all chapters), Dr Ryan Daly (all chapters), Mrs Clare Keating Daly (Chapters 1-5), Dr Guy Stevens (Chapters 3-5), Dr Jane Prince (Chapters 1, 2, 4-6), Dr James Lea (Chapter 3) and Dr Christopher Clarke (Chapter 3).



# Co-author authorisation

This thesis contains work that has been prepared for publication. By signing below, co-authors agree to the listed publication being included in the candidate's thesis and acknowledge that the candidate is the primary author, i.e. contributed greater than 50% of the content and was primarily responsible for the planning, execution and preparation of the work for publication.

<p><b>Details of the work:</b></p> <p>Peel LR, Daly R, Keating Daly CA, Stevens GMW, Collin SP, Meekan MG (In preparation) Population size, habitat use and residency of manta rays at aggregation sites in Seychelles. <i>Marine and Freshwater Research.</i></p>						
<p><b>Location in thesis:</b></p> <p>Chapter 2: Population size, habitat use and residency of manta rays at aggregation sites in Seychelles.</p>						
<p><b>Student contribution to work:</b></p> <p>I collected and analysed the data for this work and wrote the associated manuscript with critical input from co-authors.</p>						
<p><b>Co-author signatures and dates:</b></p> <table><tr><td> [1 April 2019]</td><td> Mrs Clare Keating Daly 01 April 2019</td></tr><tr><td> Dr Guy Stevens 01 April 2019</td><td> Prof. Shaun Collin 01 April 2019</td></tr><tr><td colspan="2"> Dr Mark Meekan 01 April 2019</td></tr></table>	 [1 April 2019]	 Mrs Clare Keating Daly 01 April 2019	 Dr Guy Stevens 01 April 2019	 Prof. Shaun Collin 01 April 2019	 Dr Mark Meekan 01 April 2019	
 [1 April 2019]	 Mrs Clare Keating Daly 01 April 2019					
 Dr Guy Stevens 01 April 2019	 Prof. Shaun Collin 01 April 2019					
 Dr Mark Meekan 01 April 2019						

**Details of the work:**

Peel LR, Stevens GMW, Daly R, Keating Daly CA, Lea JSE, Clarke CR, Collin SP, Meekan MG (2019) Movement and residency patterns of reef manta rays *Mobula alfredi* in the Amirante Islands, Seychelles. *Marine Ecology Progress Series* 621:169-184.

**Location in thesis:**

Chapter 3: The island life: movement and residency patterns of reef manta rays (*Mobula alfredi*) in the Amirante Island Group, Seychelles.

**Student contribution to work:**

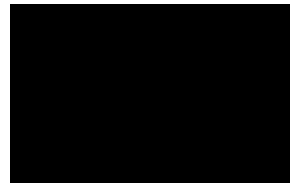
I collected and analysed the data for this work and wrote the associated manuscript with critical input from co-authors.

**Co-author signatures and dates:**

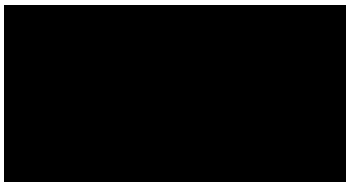


Dr Guy Stevens

01 April 2019

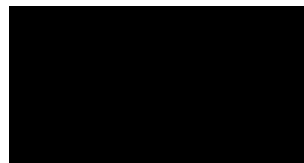


[1 April 2019]

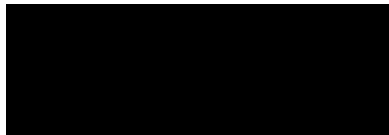


Mrs Clare Keating Daly

01 April 2019

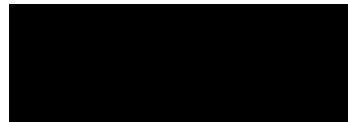


01 April 2019



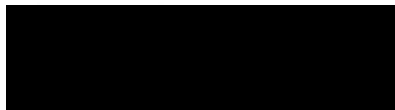
Dr Christopher Clarke

01 April 2019



Prof. Shaun Collin

01 April 2019



Dr Mark Meekan

01 April 2019



**Details of the work:**

Peel LR, Daly R, Keating Daly CA, Stevens GMW, Collin SP, Meekan MG (2019) Stable isotope analyses reveal unique trophic role of reef manta rays (*Mobula alfredi*) at a remote coral reef. *Royal Society Open Science* 6:190599.

**Location in thesis:**

Chapter 4: Trophic ecology of the reef manta ray (*Mobula alfredi*) at a remote coral reef.

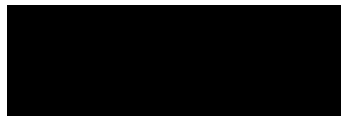
**Student contribution to work:**

I collected and analysed the data for this work and wrote the associated manuscript with critical input from co-authors.

**Co-author signatures and dates:**

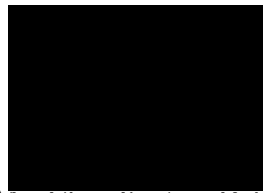


[1 April 2019]



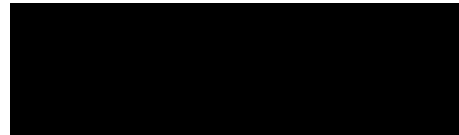
Dr Guy Stevens

01 April 2019



Mrs Clare Keating Daly

01 April 2019



Prof. Shaun Collin

01 April 2019



Dr Mark Meekan

01 April 2019

**Details of the work:**

Peel LR, Daly R, Keating Daly CA, Stevens GMW, Collin SP, Meekan MG (In preparation)  
A multi-technique approach to the description of regional movements of reef manta rays  
(*Mobula alfredi*) in Seychelles waters. *Marine Biology*.

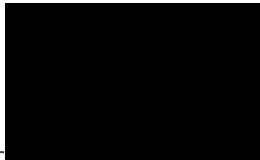
**Location in thesis:**

Chapter 5: A multi-technique approach to the description of regional movements of reef manta rays (*Mobula alfredi*) in Seychelles waters.

**Student contribution to work:**

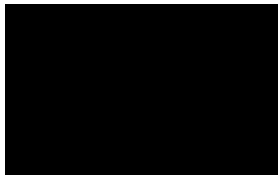
I collected and analysed the data for this work and wrote the associated manuscript with critical input from co-authors.

**Co-author signatures and dates:**



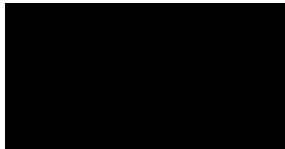
Dr Ryan Daly

[1 April 2019]



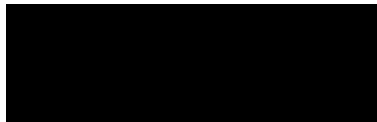
Mrs Clare Keating Daly

01 April 2019



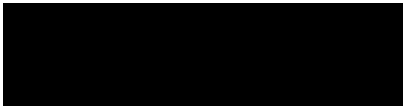
Dr Guy Stevens

01 April 2019



Prof. Shaun Collin

01 April 2019



Dr Mark Meekan

01 April 2019

**Student signature:**

**Date:** 01 April 2019

I, Dr Jane Price, certify that the student's statements regarding their contribution to each of the works listed above are correct.

**Coordinating supervisor signature:**

**Date:** 08 April 2019

# Table of Contents

Thesis declaration.....	iii	
Abstract .....	v	
Acknowledgements .....	vii	
Publications from this thesis .....	xi	
Statement of candidate contributions .....	xiii	
Co-author authorisation.....	xv	
Table of Contents .....	xix	
List of Figures .....	xxiii	
List of Tables.....	xxix	
Chapter 1	General Introduction .....	1
1.1	The significance of movement .....	1
1.2	Manta rays.....	1
1.3	The Western Indian Ocean.....	3
1.4	Seychelles.....	5
1.5	Thesis outline .....	5
1.6	Thesis structure .....	6
Chapter 2	Population size, habitat use and residency of manta rays at aggregation sites in Seychelles .....	9
2.1	Abstract .....	9
2.2	Introduction.....	9
2.3	Methods.....	11
2.3.1	Study site.....	11
2.3.2	Data collection .....	12
2.3.3	Survey frequency .....	14
2.3.4	MantaCam.....	15
2.3.5	Statistical analyses .....	16
2.3.5.1	Sighting frequency .....	16
2.3.5.2	Visits to the cleaning station .....	16
2.3.5.3	Abundance models .....	17
2.4	Results.....	19
2.4.1	Overview .....	19
2.4.2	Cleaning station.....	19
2.4.2.1	Sighting summary.....	19
2.4.2.2	Behaviour at the cleaning station .....	21
2.4.2.3	Patterns of visits .....	21

2.4.3	D'Arros Island and St. Joseph Atoll .....	23
2.4.3.1	Population size and composition .....	23
2.4.3.2	Size distribution.....	23
2.4.3.3	Patterns of habitat use.....	23
2.4.3.4	Abundance of reef manta rays at D'Arros Island.....	24
2.4.3.5	Injuries and anthropogenic impacts.....	24
2.4.4	Alphonse and other Island Groups.....	26
2.4.4.1	Oceanic manta rays .....	26
2.4.4.2	Reef manta rays .....	26
2.4.4.2.1	Sighting summary .....	26
2.4.4.2.2	Sex and maturity .....	28
2.4.4.2.3	Behaviour.....	28
2.4.4.2.4	Movements between Island Groups.....	28
2.4.4.2.5	Injuries and anthropogenic impacts .....	29
2.5	Discussion .....	29
2.5.1	Cleaning station.....	30
2.5.2	D'Arros Island and St. Joseph Atoll .....	31
2.5.3	Amirante, Alphonse and other Island Groups.....	32
2.5.3.1	Manta ray conservation in Seychelles .....	33
2.6	Supplementary material .....	35
Chapter 3	The island life: movement and residency patterns of reef manta rays ( <i>Mobula alfredi</i> ) in the Amirante Island Group, Seychelles.....	41
3.1	Abstract.....	41
3.2	Introduction.....	41
3.3	Methods.....	43
3.3.1	Study site.....	43
3.3.2	Tag deployment.....	44
3.3.3	Acoustic receiver array .....	45
3.3.4	Spatio-temporal analyses .....	46
3.3.5	Environmental modelling.....	48
3.4	Results.....	50
3.4.1	Detection summary .....	50
3.4.2	Spatial movements .....	50
3.4.3	Residency in the Amirantes .....	53
3.4.3.1	Broad scale (10 – 100 km) .....	53
3.4.3.2	Local scale (1 – 10 km) .....	55
3.4.4	Temporal and environmental patterns.....	55
3.5	Discussion .....	58
3.5.1	Spatial movements through the Amirantes .....	58
3.5.2	Residency and array use.....	59

3.5.3	Environmental and temporal patterns .....	59
3.6	Summary .....	62
3.7	Supplementary material .....	64
Chapter 4	Trophic ecology of the reef manta ray ( <i>Mobula alfredi</i> ) at a remote coral reef .....	69
4.1	Abstract .....	69
4.2	Introduction .....	69
4.3	Methods.....	71
4.3.1	Study site.....	71
4.3.2	Sample collection.....	72
4.3.2.1	Reef manta rays .....	72
4.3.2.2	Reef fishes .....	73
4.3.2.3	Zooplankton.....	73
4.3.2.3.1	Pelagic .....	73
4.3.2.3.2	Emergent.....	73
4.3.2.4	Seagrass .....	74
4.3.3	Sample processing.....	74
4.3.4	Stable isotope analysis .....	75
4.3.5	Statistical analyses .....	75
4.4	Results.....	77
4.4.1	Extraction treatment effects .....	77
4.4.2	Stable isotopes.....	78
4.4.2.1	Reef manta rays .....	78
4.4.2.2	Reef fishes .....	80
4.4.2.3	Zooplankton.....	80
4.4.3	Feeding ecology of reef manta rays at D'Arros Island .....	83
4.5	Discussion .....	83
4.5.1	Feeding ecology of reef manta rays .....	83
4.5.2	Zooplankton as prey for reef manta rays.....	86
4.5.3	Extraction procedures for reef manta ray muscle tissue .....	89
4.5.4	Limitations .....	89
4.5.5	Conclusions.....	90
4.6	Supplementary material .....	91
Chapter 5	A multi-technique approach to the description of regional movements of reef manta rays ( <i>Mobula alfredi</i> ) in Seychelles waters .....	95
5.1	Abstract .....	95
5.2	Introduction.....	95
5.3	Methods.....	98
5.3.1	Study site.....	98
5.3.2	Photo-identification.....	99

5.3.3	Satellite telemetry .....	100
5.3.3.1	Tag deployment .....	100
5.3.3.2	Geolocation .....	101
5.3.3.2.1	Inclusion of acoustic data .....	101
5.3.3.3	Horizontal movement .....	102
5.3.3.4	Vertical movement .....	102
5.4	Results .....	103
5.4.1	Photo-identification .....	103
5.4.2	Satellite telemetry .....	104
5.4.3	Horizontal movement .....	105
5.4.3.1	Inclusion of acoustic data in HMM .....	105
5.4.4	Vertical movement .....	107
5.5	Discussion .....	110
5.5.1	Horizontal movement .....	110
5.5.1.1	Photo-identification .....	110
5.5.1.2	Satellite telemetry .....	111
5.5.1.2.1	Inclusion of acoustic data .....	112
5.5.2	Vertical movement .....	113
5.5.3	Conclusion .....	114
5.6	Supporting material .....	115
Chapter 6	General Discussion .....	117
6.1	Overview of findings .....	117
6.2	Movement patterns .....	118
6.2.1	D'Arros Island .....	119
6.2.2	Amirante Islands .....	120
6.2.3	Wider Seychelles .....	121
6.3	Feeding ecology .....	123
6.4	Implications for conservation .....	124
6.5	Limitations and future directions .....	126
6.5.1	Extent of movement of reef manta rays in Seychelles .....	126
6.5.2	Additional aggregation and nursery areas for reef manta rays in Seychelles ...	127
6.5.3	Composition of zooplankton communities at the Amirantes Bank .....	127
6.5.4	Connectivity of reef manta ray populations in the Western Indian Ocean .....	128
6.6	Concluding remarks .....	129
References	.....	130
Appendix A	.....	149

# List of Figures

Figure 1.1 Distribution of manta ray aggregations and established mobulid fisheries in the Western Indian Ocean (Heinrichs et al. 2011, Moazzam 2018, Temple et al. 2018). The Exclusive Economic Zone (EEZ) of Seychelles is shaded in blue (A). Reef manta rays ( <i>Mobula alfredi</i> ) occur through the Island Groups of Seychelles (B), and are known to aggregate at D’Arros Island (black arrow) of the Outer Islands. D’Arros Island is neighboured closely by the St. Joseph Atoll (C), and is the focal study site for my thesis.....	4
Figure 2.1 The six Island Groups of Seychelles (A). D’Arros Island and St. Joseph Atoll (St. J; B) are located within the Amirante Island Group. Manta ray photo-identification surveys conducted at D’Arros Island (C) targeted nine sites during surface-based searches (yellow circles), while dive-based searches were conducted at the manta ray cleaning station to the north of the island (orange diamond). ▼, St. François Atoll. ✕, position of the Victoria Fish Market on Mahé Island. ....	12
Figure 2.2 Injury types recorded on reef manta rays ( <i>Mobula alfredi</i> ) in Seychelles. C: cephalic fin injury. D: dorsal fin injury. G: gill infection. P: pectoral fin injury. T: tail injury.....	13
Figure 2.3 MantaCam (A; black arrows) was deployed on the northern edge of the manta ray cleaning station (B; white arrow) at D’Arros Island, Seychelles, to monitor manta ray visits to this location and to capture identification photographs. N, north. S, south.....	15
Figure 2.4 Discovery curve of reef manta ray ( <i>Mobula alfredi</i> ) sightings in Seychelles (green circles), at D’Arros Island and St. Joseph Atoll (Amirante Island Group; blue diamonds), and at St. François Atoll (Alphonse Island Group; orange triangles). Blue shading indicates timing of three November sampling periods at D’Arros Island. Orange shading indicates timing of the single sampling period at St. François Atoll. ....	20
Figure 2.5 Frequency of visits by reef manta rays ( <i>Mobula alfredi</i> ) to a cleaning station at D’Arros Island, Seychelles, recorded using a remote camera system (‘MantaCam’), relative to time of day (h) and survey day (2 to 27 November 2017; numbered 1 – 26; A). Contour lines indicate the magnitude of summed effects of both variables on the occurrence of manta rays at this site. Cumulative number of manta visits to the cleaning station across all MantaCam deployments are also presented (29 September (yellow) to 27 November 2017 (purple); B).....	22
Figure 2.6 Proportion of occurrence and distribution of feeding, courtship, cleaning and cruising behaviour by reef manta rays ( <i>Mobula alfredi</i> ) at ten sites around D’Arros Island, Seychelles. Values within pie charts indicate the total number of behavioural records collected at each site. Eastern survey sites located within the channel between D’Arros Island and St. Joseph Atoll (St. J). Colour allocations to behaviours are described in figure legend.....	25
Figure 2.7 Distribution of oceanic ( <i>Mobula birostris</i> ; white text) and reef ( <i>Mobula alfredi</i> ; black text) manta ray sightings throughout the Island Groups of Seychelles. For <i>M. birostris</i> , value indicates number of individuals recorded across six sightings during this study. For <i>M. alfredi</i> , bold value indicates number of individuals sighted, and value in brackets indicates number of recorded sightings. ‘★’ is the position of the main study site; D’Arros Island and St. Joseph Atoll. ‘▼’ indicates the position of St. François Atoll (St. F). ‘✕’ is the position of the Victoria Fish Market on Mahé Island. ....	27

Figure 3.1 Located in the Western Indian Ocean (A), Republic of Seychelles (B) is an archipelago of 115 islands. The Amirante Island Group, located upon the Amirantes Bank, is one of six Island Groups identified within the country. Reef manta rays ( <i>Mobula alfredi</i> ) are known to aggregate in the Amirante Group at D’Arros Island and St. Joseph Atoll (St. J; C; Georeferenced drone imagery © Save Our Seas Foundation); the focal site for this acoustic telemetry study. Maps created in ArcGIS 10.3 ( <a href="http://www.esri.com/">http://www.esri.com/</a> ) using GEBCO_08 (version 20100927) bathymetry data. ....	44
Figure 3.2 Distribution of acoustic receivers (n = 70) throughout the Amirante Island Group, with inset indicating increased receiver density around D’Arros Island and St. Joseph Atoll. Receiver locations marked with $\odot$ . Maps created in ArcGIS ( <a href="http://www.esri.com/">http://www.esri.com/</a> ) using GEBCO_08 (version 20100927) bathymetry data. Georeferenced drone imagery © Save Our Seas Foundation. ....	46
Figure 3.3 Summary of reef manta ray ( <i>Mobula alfredi</i> ) detections recorded across the Amirantes receiver array between November 2013 and October 2017 for individual tracks lasting longer than seven days. Colour shows sex (male, blue; female, red) and life stage (light shaded colour – juvenile; average shaded colour – sub-adult; dark – adult) of each individual. Tag deployment dates are also indicated ( $\blacktriangle$ ). ....	53
Figure 3.4 Network map of the Amirantes receiver array indicating the proportion of reef manta ray ( <i>Mobula alfredi</i> ) detections recorded at each receiver (nodes; n = 70) between November 2013 and October 2017. Edges represent the frequency of subsequent detections between receivers. Symbology is described in the legend. Location of cleaning station at D’Arros Island indicated by $\star$ . Maps created in ArcGIS 10.3 ( <a href="http://www.esri.com/">http://www.esri.com/</a> ) using GEBCO_08 (version 20100927) bathymetry data. Georeferenced drone imagery © Save Our Seas Foundation. ....	54
Figure 3.5 Marginal effect plots derived from the top ranked binomial GAMM indicating the significant effects of day of year (A; <i>letters</i> above represent months of year), prevailing wind direction (B; <i>letters</i> above represent cardinal directions), time of day (C), water temperature (D), fraction of moon illumination (E), tidal range (F), time relative to high tide (G), and wind speed (H) on the probability of detecting acoustically tagged reef manta rays ( <i>Mobula alfredi</i> ) at D’Arros Island and St. Joseph Atoll, Seychelles, between November 2016 and October 2017. Blue shading indicates periods of north-west monsoon. Grey shading indicates 95% confidence interval. Horizontal dashed lines indicate $y = 0$ . ....	56
Figure 4.1 D’Arros Island and St. Joseph Atoll, located on the Amirantes Bank within the Republic of Seychelles, Western Indian Ocean. Position of St. Joseph Channel indicated by $\star$ . Maps created in ArcGIS 10.3 ( <a href="http://www.esri.com/">http://www.esri.com/</a> ) using GEBCO_08 (version 20100927) bathymetry data. Georeferenced drone imagery © Save Our Seas Foundation. ....	72
Figure 4.2 Comparison of urea and lipid extraction treatment effects on the mean values $\pm$ S.E. of $\delta^{15}\text{N}$ (A), $\delta^{13}\text{C}$ (B) and C:N (C) ratios of reef manta ray ( <i>Mobula alfredi</i> ) muscle tissue samples. Treatments with different letters are significantly different ( $p < 0.05$ ). Control, untreated; DIW, urea extraction only; LE, lipid extraction only; LE+DIW, lipid and urea extraction. ....	79
Figure 4.3 Isoscape of $\delta^{15}\text{N}$ and $\delta^{13}\text{C}$ values for reef manta ray ( <i>Mobula alfredi</i> ) muscle tissue collected in 2016 (black, n = 13) and 2017 (white, n = 36) at D’Arros Island, Seychelles. ....	80
Figure 4.4 Photographs of representative pelagic (A-C) and emergent (D-F) zooplankton samples collected at D’Arros Island, Seychelles. Pelagic samples were	



collected during daylight hours using a towed plankton-net and were dominated by copepods (A), fish-eggs (B), and crab zoea (C). Emergent samples were collected using a light trap deployed after sunset for 2.5 hours and were dominated by polychaetes and ostracods (D), polychaete worms (E), and crab megalopae (F). Scale bar (approximate sizes; a-f): 1 mm, 0.5 mm, 1 mm, 2 mm, 2 mm, 2 mm..... 82

Figure 4.5 Mean values  $\pm$  S.D. of  $\delta^{13}\text{C}$  and  $\delta^{15}\text{N}$  for samples of reef manta ray (*Mobula alfredi*), 20 species of fishes, zooplankton and seagrass collected at D'Arros Island and St. Joseph Atoll, Seychelles. Representative mean values of mesopelagic fishes (Meso.) sampled in the Western Indian Ocean are also included. Figure legend outlines allocation of symbols to sample types and colours to trophic guild of sampled fish species. Asterisks represent lipid-normalised  $\delta^{13}\text{C}$  values. *Mobula alfredi*: faeces, MA (Fe.)\*; muscle, MA (Mu.). Fishes: *Aethaloperca rogoa*, AR; *Caesio teres*, CTe; *Caesio xanthonota*, CX; *Cephalopholis miniata*, CM; *Cephalopholis sonnerati*, CSn; *Chaetodon trifasciatus*, CTr; *Chlorurus sordidus*, CSr; *Crenimugil crenilabis*, CC; *Katsuwonus pelamis*, KP; *Lethrinus enigmaticus*, LE; *Lethrinus lentjan*, LL; *Lethrinus nebulosus*, LN; *Lutjanus bohar*, LB; Mesopelagic, Meso.; *Parupeneus macronemus*, PM; *Pterocaesio tile*, PT; *Sarda orientalis*, SO; *Scarus rubroviolaceus*, SR; *Selar crumenophthalmus*, SC; *Thunnus albacares*, TA; *Variola louti*, VL. Zooplankton: emergent, P (E)\*; pelagic, P (P)\*. Seagrass: *Thalassodendron ciliatum*, TC..... 84

Figure 4.6 Estimated contribution of emergent and pelagic zooplankton, and mesopelagic sources (purple, blue and yellow, respectively), to the diet of the reef manta ray (*Mobula alfredi*) at D'Arros Island and St. Joseph Atoll, Seychelles, in 2017. Proportions estimated using two Bayesian stable isotope mixing models that assumed a diet-tissue discrimination factor (DTDF) of  $2.3 \pm 1.0$  ‰ and included either bulk (Model 1) or lipid-normalised (Model 2)  $\delta^{13}\text{C}$  values. The central box spans the 2.5 – 97.5% confidence intervals and the middle line denotes the median..... 85

Figure 5.1 Location of the six Island Groups of Seychelles. Reef manta rays (*Mobula alfredi*) are frequently sighted at D'Arros Island and St. Joseph Atoll within the Amirante Group, and at St. Francois Atoll within the Alphonse Group. Seventy acoustic receivers (●) are deployed within the Amirante Group. Alphonse Island located at '■'. St. Francois Atoll located at '▼'. D'Arros Island manta cleaning station located at '★'. St. Joseph Channel (depth 60 m) located at '◆'..... 98

Figure 5.2 Most-probable tracks for reef manta rays (*Mobula alfredi*) M1, M2, M4 and M5 tagged with archival pop-up satellite tags (miniPATs) at D'Arros Island, Seychelles. For M5, the 'GPE3 Only' track was estimated only from archived light, depth and temperature data, whereas the 'GPE3/A' track included an additional 481 acoustic detections from a passive receiver array. Tracks progress from green to red (100, 52, 180 and 134 d, respectively). Arrows indicate the first Argos location of each transmitting tag, and the associated numbers show the number of days that the tag is estimated to have been drifting prior to transmissions beginning. Core areas of use represented by dark (50% KUD), medium (95% KUD) and light (99% KUD) colour shading. Thick, solid coloured line represents boundary of 95% geolocation errors. '★' in M4 indicates the location of a re-sighting 184 d after tag release..... 106

Figure 5.3 Percentage of longitude estimates among four geo-located satellite tracks of reef manta rays (*Mobula alfredi*) in Seychelles. Blue shading represents longitudinal range of the Amirante Island Group, Seychelles. Asterisk represents longitude at tagging location (D'Arros Island). ..... 107

Figure 5.4 Percentage of total latitude estimates calculated for a geolocated satellite track (M5) of a reef manta ray ( <i>Mobula alfredi</i> ) in Seychelles by a Hidden Markov Model (HMM) considering either archived environmental data only (GPE3; white bars), or archived environmental data alongside 481 known locations retrieved from an acoustic array (GPE3/A; black bars; A). Asterisk represents longitude at tagging location (D'Arros Island). Estimated latitude over time also presented (B) for model excluding (GPE3; dashed line) and including (GPE3/A; solid line) acoustic data. Blue shading represents latitudinal range of the Amirante Island Group. Arrow indicates time of last recorded acoustic detection of individual. ....	108
Figure 5.5 Combined depth and temperature profiles for four reef manta rays ( <i>Mobula alfredi</i> ) tagged with archival pop-up satellite tags in Seychelles. Data interpolated for each day of data retrieved per tag. Gaps indicate data that was not retrieved from the tag prior to tag battery depletion. Manta identification number (M*), sex (F, female; M, male) and year of tag deployment indicated in lower left of each panel. Dotted line represents average depth of the Amirantes Bank (40 m), and dashed line represents average depth of St. Joseph Channel (60 m) located between D'Arros Island and St. Joseph Atoll. ....	109
Figure 5.6 Nightly average dive depth relative to moon illumination (arc-sin transformed; A and B) and over time (C and D) for two reef manta rays ( <i>Mobula alfredi</i> ; M1 and M5) tagged with archival pop-up satellite tags in Seychelles. Blue line indicates direction of relationship with moon illumination. Grey shading indicates 95% confidence interval. Dashed vertical line in lower panel for M5 (D) represents equivalent track-end date for individual M1.....	109
Figure S 2.1 Identification images for reef ( <i>Mobula alfredi</i> ; A) and oceanic ( <i>Mobula birostris</i> ; B) manta rays in Seychelles. Dashed boxes outline region of highest spot density and pigmentation for each species, arrows indicate differences in facial and pectoral fin margin colouration. Photographs © The Manta Trust (A: G. Stevens; B: Unknown). ....	37
Figure S 2.2 Frequency of visits by reef manta rays ( <i>Mobula alfredi</i> ) to the cleaning station at D'Arros Island, Seychelles, recorded by a remote camera system ('MantaCam'). Both the number of individuals present per visit and their visit duration (A), and number of visits recorded per survey day (B) are presented. Symbology for visit duration defined in legend. ....	37
Figure S 2.3 Images of reef manta ray ( <i>Mobula alfredi</i> ) courtship behaviour captured by a remote camera system, MantaCam, positioned at a cleaning station at D'Arros Island, Seychelles. White arrows identify individuals involved in courtship behaviour in groups of three (A) and four (B). The black circle displays a usable identification image, and the white circle highlights the pregnancy bulge of a pregnant female (C). ....	38
Figure S 2.4 Population composition of reef manta rays ( <i>Mobula alfredi</i> ) identified at D'Arros Island and St. Joseph Atoll, Seychelles, considering individual sex (F, female. M, male. U, unknown) and maturity status (Juv., juvenile; SA, sub-adult; A, adult). Colour allocations defined in figure legend. ....	38
Figure S 2.5 Size distribution of reef manta rays ( <i>Mobula alfredi</i> ) that could be identified as males (black) and females (white), or of unknown sex (grey) at D'Arros Island and St. Joseph Atoll, Seychelles.....	39
Figure S 2.6 Population composition of reef manta rays ( <i>Mobula alfredi</i> ) identified among the Island Groups of Seychelles considering individual sex (F, female. M, male. U, unknown) and maturity status (Juv., juvenile; SA, sub-adult; A,	

adult). Colour allocations defined in figure legend. Sightings from D’Arros Island and St. Joseph Atoll have been excluded. ....	39
Figure S 2.7 Sighting frequencies for 236 individual reef manta rays ( <i>Mobula alfredi</i> ) identified in Seychelles using photo-identification techniques. Males (black bars), females (white bars) and unknown sex (grey bars) are shown.....	39
Figure S 3.1 Non-metric multidimensional scaling plots of acoustically tagged reef manta ray ( <i>Mobula alfredi</i> ) visitation frequency (number of days; A) and proximity to (number of detections; B) receivers at the Amirante Island Group, Seychelles. Patterns examined with respect to individual sex (female, pink circle; male, blue triangle), life stage (juvenile, blue triangle; sub-adult, orange square; adult, green triangle), and the year of tag deployment (2013, green triangle; 2016, pink square). Data based on a Bray-Curtis similarity matrix with 9,999 permutations. ....	66
Figure S 3.2 Detections over time for acoustically-tagged reef manta rays ( <i>Mobula alfredi</i> ) relative to the latitude of detection within the Amirantes receiver array, Seychelles. Latitude of northern-most (African Banks) and southern-most (Desnoeuufs) acoustic receivers are indicated by red and purple horizontal lines, respectively. Orange horizontal lines represent latitude of receiver at Remire. Yellow horizontal lines represent northern- and southern-most receivers of D’Arros Island and St. Joseph Atoll. Green horizontal lines represent northern- and southern-most receivers of Poivre. Light and dark blue horizontal lines represent latitude of receivers at Boudeuse and Marie Louise, respectively. ....	67
Figure S 4.1 Isoscapes presenting the core (SEA <sub>c</sub> , solid lines) and total (TA, dashed lines) trophic niche areas of male (grey) and female (black) reef manta rays ( <i>Mobula alfredi</i> ) sampled at D’Arros Island, Seychelles, in November 2016 (A) and November 2017 (B). ....	93
Figure S 4.2 A reef manta ray ( <i>Mobula alfredi</i> ) defecates over the cleaning station at D’Arros Island, Seychelles. Arrow indicates faecal material. ....	93
Figure S 5.1 Percentage of time spent at temperature by four reef manta rays ( <i>Mobula alfredi</i> ) tagged with archival pop-up satellite tags in Seychelles. M* indicates manta identification number.....	115
Figure S 5.2 Percentage time at depth during the day (white bars) and night (grey bars) for reef manta ray ( <i>Mobula alfredi</i> ) M5 in Seychelles tagged with an archival pop-up satellite tag. ‘n(periods)’ indicate the number of days that depth data were available for within the track. Error bars represent standard deviation....	115
Figure S 5.3 Average hourly ( $\pm$ S.E.) dive depth for four reef manta rays ( <i>Mobula alfredi</i> ) tagged with archival pop-up satellite tags in Seychelles. Asterisks represent individuals that performed deeper dives during the night (dark grey bars) than during the day (light grey bars). ....	116



# List of Tables

Table 2.1 Location, year and duration of targeted manta ray field surveys in Seychelles. Effort is summarised by number of surface-based searches, number of dive-based searches (i.e. Manta Dives), and hours spent conducting searches. Alp., Alphonse Group. Am., Amirante Group.....	14
Table 2.2 Distribution of reef manta ray ( <i>Mobula alfredi</i> ) sightings recorded in Seychelles across three spatio-temporal scales and using varying survey techniques (effort types). St. F: St. François Atoll.....	19
Table 2.3 Top ten highest-ranked GAMs for the influence of hour of day and day of survey (h and 1-26, respectively; H D), current speed ( $\text{m s}^{-1}$ ; C), temperature ( $^{\circ}\text{C}$ ; M), tidal range (m; R) and time to high tide (h; T) on visits of manta rays to a cleaning station at D'Arros Island, Seychelles. df, degrees of freedom. AICc, Akaike's Information Criterion corrected for sample size. $\Delta\text{AICc}$ , change in AICc in comparison to model with lowest AICc. wAICc, relative AICc weight. DE (%): percent deviance explained by model. Bold text indicates selected top model.....	22
Table 2.4 Estimated total abundance ( $\hat{N} \pm \text{S.E.}$ ) of female (F), male (M) and all reef manta rays ( <i>Mobula alfredi</i> ) at D'Arros Island and St. Joseph Atoll, Seychelles, across three sampling years. Estimates derived from open POPAN models ( $\hat{c} = 1$ ) considered sexes as separate groups. 'd': number of sampling days within each survey year. 'Identified': number of unique individuals identified within each survey year. Lower (LCL) and upper (UCL) confidence intervals. ....	25
Table 2.5 Distribution of injury types throughout the reef manta ray ( <i>Mobula alfredi</i> ) population identified at D'Arros Island and St. Joseph Atoll, Seychelles. ....	26
Table 3.1 Description of variables used in GAMM analysis of reef manta ray ( <i>Mobula alfredi</i> ) occurrence at D'Arros Island and St. Joseph Atoll, Seychelles.....	49
Table 3.2 Summary of acoustic tag deployments on reef manta rays ( <i>Mobula alfredi</i> ) at D'Arros Island, Seychelles, from November 2013 to October 2017 (DSTJ = D'Arros Island and St. Joseph Atoll). ....	51
Table 3.3 Summary of the GAMM constructed to assess the influence of temporal, biological and environmental variables on the occurrence of reef manta rays ( <i>Mobula alfredi</i> ) at D'Arros Island and St. Joseph Atoll, Seychelles. Values are provided for predictors included in the final selected GAMM only. Degrees of freedom (df); p-value from $\chi^2$ test ( $p$ ); percent of deviance explained (% DE).....	57
Table 4.1 Summary of values of $\delta^{15}\text{N}$ , $\delta^{13}\text{C}$ and C:N (mean $\pm$ S.D.) ratios reported for reef manta ray ( <i>Mobula alfredi</i> ), reef fishes, zooplankton and seagrass sampled at D'Arros Island and St. Joseph Atoll, Seychelles. Values in bold indicate presence of a significant relationship between isotope composition and size in fishes (fork length, cm) are highlighted in bold. Asterisks indicate lipid-adjusted $\delta^{13}\text{C}$ values. ....	81
Table 4.2 Outputs of mixing models estimating the proportional contribution ( $\pm$ S.D.) of pelagic and emergent zooplankton and mesopelagic sources to the diet of reef manta rays ( <i>Mobula alfredi</i> ) at D'Arros Island, Seychelles, based on samples collected in November 2017. Model 1 used bulk $\delta^{13}\text{C}$ values of zooplankton samples, whereas Model 2 used values mathematically normalised for lipids. Both models assumed a diet-tissue discrimination	

factor (DTDF) of $2.3 \pm 1.0$ ‰. The mean values were calculated as an average between the two mixing models. ....	82
Table 5.1 Summary of satellite tag deployments on reef manta rays ( <i>Mobula alfredi</i> ) in Seychelles, including length of track (duration in days) and percentage of archived data decoded via satellite. Asterisk indicates an individual that was carrying an active acoustic tag at the time of satellite tagging. ‡ indicates the tag that transmitted insufficient and unreliable data for analysis. F, female. M, male. DNR, did not respond. ....	100
Table 5.2 Sighting histories and locations of six individual reef manta rays ( <i>Mobula alfredi</i> ) that were tracked in the waters of Seychelles using archival pop-up satellite tags. ....	103
Table 5.3 Horizontal and vertical movement metrics for reef manta rays ( <i>Mobula alfredi</i> ) tracked using archival pop-up satellite tags (miniPATs) in Seychelles. F, female. M, male. Pop. Dist., distance between deployment location and estimated end position of track. Max. Lat. Range, maximum latitudinal range covered by the individual. GPE3, geolocated track path including geolocated positions only. <i>Italicised metric data</i> , indicates value and difference of M5-GPE3 model to M5-GPE3/A. Diel Depth Distribution, p-value from K-S test for difference in depth distribution between day and night. Diel Dive Depth, p-value from t-test for difference in average dive depth between day and night. Lunar cycle, p-value for relationship between average night-time depth by individuals and level of moon illumination; ‡ represents p-value derived from Spearman's Rank Correlation test. GPE3/A, geolocated track path including additional positions recorded by an acoustic tag. Significant p-values presented in bold. ....	104
Table S 2.1 Top ten POPAN models of abundance for reef manta ray ( <i>Mobula alfredi</i> ) sighting data collected at D'Arros Island, Seychelles, in November/December 2013. Models allowed for apparent survival ( $\phi$ ), capture probability ( $p$ ), and probability of entry ( $P_{ent}$ ) parameters to remain constant ( $\cdot$ ), or to vary by time ( $t$ ), by sex ( $s$ ), or by time and sex ( $t+s$ ). Capture probability was also allowed to vary with sampling effort ( $e$ ). Partial closure to gains was set by $P_{ent(\cdot)=0}$ . Model selection performed using Akaike's Information Criterion corrected for small sample sizes (AICc). $\Delta$ AICc, difference in AICc value between each model and the model with the lowest AICc. Weight, calculated strength of model relative to all other candidate models. Models in bold represent selected top models that were subsequently averaged to estimate abundance. ....	35
Table S 2.2 Top ten POPAN models of abundance for reef manta ray ( <i>Mobula alfredi</i> ) sighting data collected at D'Arros Island, Seychelles, in November 2016. Models allowed for apparent survival ( $\phi$ ), capture probability ( $p$ ), and probability of entry ( $P_{ent}$ ) parameters to remain constant ( $\cdot$ ), or to vary by time ( $t$ ), by sex ( $s$ ), or by time and sex ( $t+s$ ). Capture probability was also allowed to vary with sampling effort ( $e$ ), and sampling effort and sex ( $e+s$ ). Partial closure to gains was set by $P_{ent(\cdot)=0}$ . Model selection performed using Akaike's Information Criterion corrected for small sample sizes (AICc). $\Delta$ AICc, difference in AICc value between each model and the model with the lowest AICc. Weight, calculated strength of model relative to all other candidate models. Model in bold represents selected top model used to estimate abundance. ....	35
Table S 2.3 Top ten POPAN models of abundance for reef manta ray ( <i>Mobula alfredi</i> ) sighting data collected at D'Arros Island, Seychelles, in November 2017. Models allowed for apparent survival ( $\phi$ ), capture probability ( $p$ ), and probability of entry ( $P_{ent}$ ) parameters to remain constant ( $\cdot$ ), or to vary by	

time ( <i>t</i> ), by sex ( <i>s</i> ), or by time and sex ( <i>t+s</i> ). Model selection performed using Akaike’s Information Criterion corrected for small sample sizes (AICc). $\Delta$ AICc, difference in AICc value between each model and the model with the lowest AICc. Weight, calculated strength of model relative to all other candidate models. Models in bold represent selected top models that were subsequently averaged to estimate abundance. ....	36
Table S 2.4 Distribution of injury types throughout the reef manta ray ( <i>Mobula alfredi</i> ) population identified in Seychelles, excluding sightings from D’Arros Island and St. Joseph Atoll. ....	36
Table S 3.1 Correlation matrix for continuous predictors considered in generalised additive mixed models (GAMMs) of reef manta ray ( <i>Mobula alfredi</i> ) occurrence at D’Arros Island and St. Joseph Atoll, Seychelles. ....	64
Table S 3.2 Top ten candidate GAMMs for predicting the occurrence of acoustically tagged reef manta rays ( <i>Mobula alfredi</i> ) within 2.5 km of D’Arros Island and St. Joseph Atoll, Seychelles. Best model (highlighted in bold) selected using differences in Akaike’s Information Criteria corrected for sample size (AICc) among models ( $\Delta$ AICc), and AICc weights (wAICc). Variables considered in models include: day of year (Dy), time of day (Hr), fraction of moon illuminated (Mn), time to high tide (Th), tidal range (Tr), wind speed (Ws), water temperature (Tp), sex (Sx), wingspan (Sp), and manta ray ID (Id).....	65
Table S 4.1 Summary of reef fishes sampled at D’Arros Island and St. Joseph Atoll, Seychelles, for stable isotope analysis. Estimated trophic level (TL; <a href="http://www.fishbase.org">www.fishbase.org</a> , 29/10/2018) and fork length given as mean $\pm$ standard error.....	91
Table S 4.2 Summary of values of $\delta^{15}\text{N}$ and $\delta^{13}\text{C}$ , and ratios of C:N reported for lipid and urea extracted reef manta ray ( <i>Mobula alfredi</i> ) muscle tissues relative to sample collection year, sex and life stage class. ....	92
Table S 4.3 Summary of total (TA), core (SEAc) and overlapping trophic niche areas for male and female reef manta rays ( <i>Mobula alfredi</i> ) over two sampling years at D’Arros Island, Seychelles. Overlap is based upon ellipses encompassing 95% of the data. ....	92
Table S 5.1 Movements of reef manta rays ( <i>Mobula alfredi</i> ) between the Island Groups of Seychelles recorded using photo-identification. ....	115





# Chapter 1 General Introduction

## 1.1 The significance of movement

Our ability to understand the conservation needs of marine megafauna (> 45 kg max. mass; Estes et al. 2016) is strongly dependent on our knowledge of their patterns of movement (Lea et al. 2016, Sequeira et al. 2018, Hays et al. 2019). Records of movement over time represent more than just positions in space. These data reflect the environments that were encountered by animals, the areas that may be of biological importance to them, where and how individuals forage, as well as where and how widely they may search for a mate (Meyer et al. 2010b, Papastamatiou et al. 2012, Sequeira et al. 2013, Papastamatiou et al. 2015a, Braun et al. 2018b). Collectively, this information can be used to broaden our understanding of the biology and ecological role of a species, and improve the planning of conservation and management strategies aimed at protecting vulnerable populations (Hays et al. 2019). The inherently visual nature of movement data also provides benefits to members of the general public. Maps of animal tracks (Barkley et al. 2019), home range areas (Udyawer et al. 2018), and/or locations where individuals are most threatened (White et al. 2019) can effectively convey complex data sets to wide and varied audiences (Hazen & Harris 2006), often without the restrictions imposed by language barriers (Amano & Sutherland 2013). Where the species of interest are particularly charismatic or iconic, access to these movement data may enhance the engagement of the general public in conservation efforts (Friedrich et al. 2014, Stewart et al. 2016a). This can be particularly beneficial for species suffering population declines on a global scale, such as manta rays.

## 1.2 Manta rays

Manta rays are large zooplanktivorous elasmobranchs belonging to the Family Mobulidae (the devil rays; Notarbartolo di Sciara 1987, Couturier et al. 2012, White et al. 2017), and two species are currently recognised. Oceanic manta rays (*Mobula birostris*) are the larger of the two, reaching a maximum size of 7 m and typically being sighted in offshore, deep water environments (Marshall et al. 2009, Stewart et al. 2016a). In contrast, reef manta rays (*Mobula alfredi*) reach a maximum size of 5.5 m, and are most frequently encountered in coastal reef environments (Marshall et al. 2009). Both species reliably aggregate at numerous locations circumtropically (Kashiwagi et al. 2011, Couturier et al. 2012), however, despite their large size and charismatic nature, little is known about their general biology (Stewart et al. 2018a; Appendix A). Prior to the redescription of these individual species in 2009, all manta ray sightings were recorded as being *Manta birostris* (Marshall et al. 2009). A decade later, the genus *Manta* is no longer recognised

(White et al. 2017, Hosegood et al. 2019), and the existence of a third putative species of manta ray in Gulf of Mexico has been proposed (Hinojosa-Alvarez et al. 2016, Hosegood et al. 2019). Debate over the taxonomy of the Mobulidae remains ongoing, but is being refined as a result of the increasing attention that this group is receiving from both scientists and the general public (O'Malley et al. 2013, Town et al. 2013, Lawson et al. 2017).

Public interest in marine megafauna and the identification of aggregation sites of manta rays in shallow tropical waters around the world has led to the establishment of a large ecotourism industry in recent years (Anderson et al. 2011b, Cisneros-Montemayor et al. 2013, O'Malley et al. 2013). This industry is estimated to generate USD 100 million per annum (Heinrichs et al. 2011), and in addition to stimulating local economies (Anderson et al. 2011b, Zimmerhackel et al. 2019), it effectively increases public awareness of manta rays and the role that they play within marine ecosystems (Lawson et al. 2017, Zimmerhackel et al. 2018). As a result, numerous research programs that are based on citizen science now exist in many countries, and encourage the engagement of local communities through the reporting of manta sightings and the collection of identification photographs of individuals (Couturier et al. 2011, Town et al. 2013, Germanov & Marshall 2014). Such contributions are significant given the current lack of knowledge about the population sizes, movement patterns and connectivity of manta rays on a global scale, and the need to understand these characteristics in order to effectively conserve populations (Couturier et al. 2012, Stewart et al. 2018a). Unfortunately, the increased attention to manta rays by researchers and the general public has coincided with an increase in the number of established fisheries targeting these species, which now threaten populations throughout their range (Ward-Paige et al. 2013, Croll et al. 2016, O'Malley et al. 2017).

Demand by fisheries for gill plates to supply the market for traditional Asian medicine have driven global declines of manta ray populations in recent decades (Heinrichs et al. 2011, Croll et al. 2016, O'Malley et al. 2017, Rohner et al. 2017b). The impacts of these fishing practices on populations is intensified by the life history strategies that are characteristic of manta rays (Couturier et al. 2012). As a result of reaching maturity at a late age, displaying long gestation periods and producing few (1 – 2) young (Homma et al. 1999, Couturier et al. 2012), populations require extended periods of time to recover from losses. Furthermore, fatalities resulting from by-catch, accidental entanglement, boat strikes and marine debris place additional anthropogenic pressures on populations (Heinrichs et al. 2011, Croll et al. 2016, Germanov et al. 2018). In response to observed population declines and in consideration of their life-history, manta rays were recently listed on three global conventions that aim to benefit their international protection. Both *M. alfredi* and *M. birostris* are currently listed as 'Vulnerable' on the International Union for the Conservation of Nature's Red List of Threatened Species (Marshall et al. 2018a, Marshall et al. 2018b) and on Appendix II of the Convention of the International Trade of Endangered Species. Additionally, both species are listed on Appendix I and II of the Convention of Migratory

Species. Although useful incentives, these measures do not enforce protective legislation for manta rays on a regional basis (Lawson et al. 2017). Studies that examine the conservation needs of populations around the world relative to local threats and pressures are therefore required to ensure that efficient management strategies are promptly implemented on appropriate spatio-temporal scales.

### 1.3 The Western Indian Ocean

The Western Indian Ocean (WIO) provides a unique opportunity to examine the biology and ecology of manta rays. Numerous aggregations have been identified throughout the region at both coastal and offshore locations (Figure 1.1A), yet measures of population sizes and the degree of connectivity within the meta-population are currently lacking (Marshall et al. 2011, Marshall et al. 2018b). Additionally, the establishment of mobulid fisheries throughout the WIO raises concerns over the longevity of manta aggregations in the region (Heinrichs et al. 2011). The intensive pressures imposed by targeted fisheries, coupled with the fatalities resulting from by-catch in the small-scale fisheries that operate in these waters (Temple et al. 2019), place manta populations under significant threat. These threats are particularly relevant for *M. alfredi*, as aggregations of this species often occur at coastal, inshore locations, where the likelihood of encountering areas of high occupancy and concomitant use by humans is greater than at remote, offshore sites (Stewart et al. 2010, Kashiwagi et al. 2011, White et al. 2019). The severe impact that coastal fisheries can have on *M. alfredi* in the WIO is particularly apparent in Mozambique, where sightings of these animals have declined by 98% in the past two decades (Rohner et al. 2017b). The opportunity to study the populations of *M. alfredi* that aggregate at remote, offshore locations of the WIO, such as in the waters of Seychelles, is therefore significant for two reasons. Firstly, these populations are likely to be somewhat protected from the intensive anthropogenic pressures faced by more coastal aggregations (Stewart et al. 2010), and thus provide insight into the biology and ecological role of this species in the (relative) absence of acute human disturbances. Secondly, pre-emptive conservation measures implemented for *M. alfredi* at these offshore locations may also benefit coastal aggregations should populations be connected within the WIO to some extent (Palumbi 2003, Gaines et al. 2010, Graham et al. 2012, Oliver et al. 2019). To date, research on *M. alfredi* in the WIO has been focussed on the coastal population of Mozambique (Marshall & Bennett 2010b, Marshall et al. 2011, Rohner et al. 2013), and little data is available regarding individual abundance, movement patterns and residency elsewhere. My thesis addresses this knowledge gap by examining the biology, ecology and movement patterns of *M. alfredi* in the waters of Seychelles.

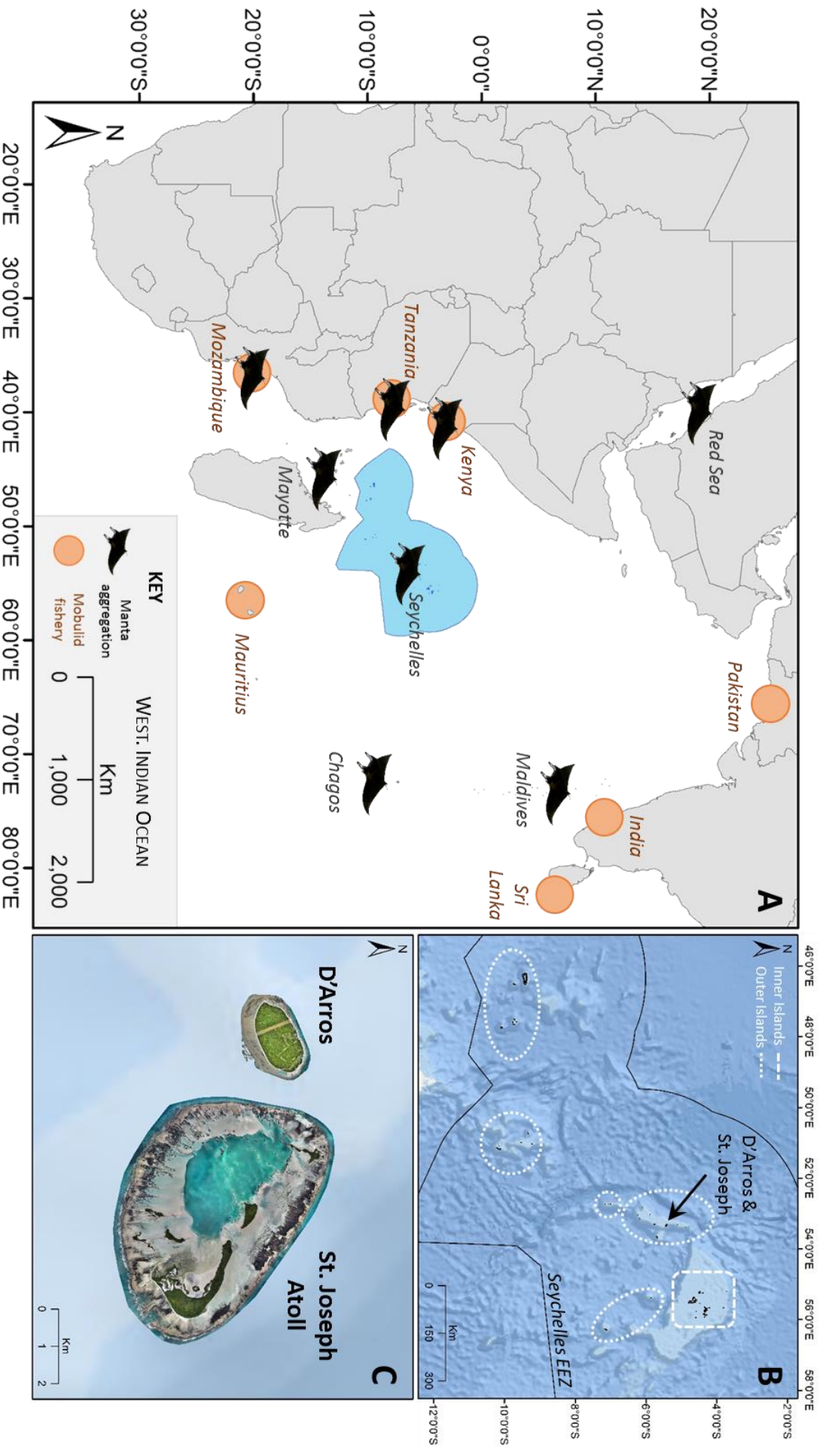


**Figure 1.1** Distribution of manta ray aggregations and established mobulid fisheries in the Western Indian Ocean (Heinrichs et al. 2011, Moazzam 2018, Temple et al. 2018). The Exclusive Economic Zone (EEZ) of Seychelles is shaded in blue (A). Reef manta rays (*Mobula affredi*) occur through the Island Groups of Seychelles (B), and are known to aggregate at D'Arros Island (black arrow) of the Outer Islands. D'Arros Island is neighboured closely by the St. Joseph Atoll (C), and is the focal study site for my thesis.

## 1.4 Seychelles

The Republic of Seychelles is an archipelago of 115 tropical islands (total area 459 km<sup>2</sup>) located to the east of Tanzania, and possesses the largest Exclusive Economic Zone (EEZ) of any African country (1.34 million km<sup>2</sup>; Figure 1.1A). Six Island Groups are recognised within the archipelago, five of which are collectively referred to as the coralline Outer Islands, and the sixth, the granitic Inner Islands (Figure 1.1B). Despite historic records of manta rays being hunted for their meat in the populated Inner Islands (Keynes 1959), the lack of an established mobulid fishery or market for mobulid products in Seychelles (Temple et al. 2019) results in the near-absence of targeted fishing pressures for mobulid rays today. Anecdotal evidence also suggests that *M. alfredi* occur infrequently around the Inner Islands. Instead, it is more likely that *M. alfredi* aggregate in the waters surrounding isolated islands and atolls within the Outer Island Group, which are often uninhabited or sparsely populated. These observations collectively suggest that *M. alfredi* in Seychelles may represent a population that is removed from current fishing pressures in the WIO, and may benefit from conservation measures that protect the population from any future threats (Temple et al. 2019). Should this population act as a ‘stepping stone’ between other isolated populations of *M. alfredi* in the region, the appropriate management and conservation of these animals may also benefit a broader proportion of the global population (Graham et al. 2012, Arauz et al. 2019).

## 1.5 Thesis outline

The overall aim of my thesis is to describe the movement patterns and feeding ecology of *M. alfredi* in Seychelles, with a focus on the aggregation at D’Arros Island and St. Joseph Atoll within the Amirante Island Group (Figure 1.1C). My research aims to:

1. Assess the population size and composition of *M. alfredi* in Seychelles and identify aggregation areas for this species throughout the archipelago.
2. Determine the level of residency of *M. alfredi* to D’Arros Island and St. Joseph Atoll, and quantify the extent of movement of individuals throughout the Amirante Island Group.
3. Describe the foraging ecology and trophic role of *M. alfredi* within the reef system surrounding D’Arros Island and St. Joseph Atoll.
4. Examine how widely *M. alfredi* travel throughout Seychelles and the broader WIO region.

Collectively, my thesis aims to expand the current understanding of the ecology of *M. alfredi*, and provide information regarding the conservation needs of this species in a remote region of the WIO.

## 1.6 Thesis structure

Preliminary sighting records collected in Seychelles indicated that the waters of D'Arros Island and the neighbouring St. Joseph Atoll may represent a significant aggregation area for *M. alfredi*. This site, located within the Amirante Island Group of the Outer Islands, was therefore selected as the primary study site for my research. In Chapter 2, I use photo-identification techniques to examine the occurrence and abundance of *M. alfredi* at D'Arros Island and St. Joseph Atoll over multiple spatio-temporal scales. Firstly, I examine the environmental and temporal variables that may influence the occurrence of *M. alfredi* at a cleaning station to the north of D'Arros Island. I also describe the habitat use patterns of *M. alfredi* at this site. Secondly, I use a photo-identification approach to collect data at multiple sites around D'Arros Island in order to assess the population composition and abundance of individuals at this location, and discuss my findings relative to observations of *M. alfredi* reported elsewhere. Finally, I use photo-identification records of *M. alfredi* collected opportunistically throughout Seychelles to examine the patterns of movement and residency of this species through the Amirante and other Island Groups. The implications of these patterns for the conservation needs of *M. alfredi* in Seychelles are then discussed.

In Chapter 3, I use passive acoustic telemetry to monitor the residency of *M. alfredi* at D'Arros Island and St. Joseph Atoll, and the other islands of the Amirante Group. I describe the recorded patterns of movement and residency for tagged individuals alongside potential biological, environmental and temporal drivers of these behaviours. This work contributes to global efforts to understand the movement ecology of *M. alfredi*, and to improve current abilities to predict where individuals may aggregate, and when they may face the greatest risk of encountering threats.

In addition to providing insight into the movement patterns of *M. alfredi*, I also use acoustic telemetry data to investigate how the feeding behaviour of this species may vary at D'Arros Island and St. Joseph Atoll throughout the diel cycle. I describe these potential foraging strategies in Chapter 4, alongside the findings of stable isotope analyses that I used to examine the trophic role of *M. alfredi* within the coral reef system surrounding this location. In contrast to previous studies that have only considered the feeding ecology of *M. alfredi* relative to potential prey items (Couturier et al. 2013a, McCauley et al. 2014), this work considered the foraging behaviour of

*M. alfredi* at an ecosystem level. By sampling a wide range of reef fishes of varying dietary niches at D'Arros Island and St. Joseph Atoll, and considering the isotopic signature of each species relative to *M. alfredi*, it was possible to describe the potential for *M. alfredi* to act as a horizontal vector of nutrient transport on two scales: (1) across the reefs surrounding D'Arros Island, and (2) between the reefs and offshore mesopelagic systems.

In Chapter 5, I describe the broad scale (> 100 km) movement patterns of *M. alfredi* from D'Arros Island and throughout Seychelles, which were monitored using a combination of satellite and acoustic telemetry, and photo-identification techniques. An understanding of how widely individuals disperse from these sites is crucial to ensuring that the extent of future conservation measures, and the habitats that they encompass, are appropriate. I also use data retrieved from pop-up archival satellite tags that were deployed on *M. alfredi* to describe the vertical movement patterns of this pelagic species. Specifically, I examine whether the diving behaviour of *M. alfredi* varies with respect to diel and lunar cycles, and discuss how such patterns of vertical habitat use may relate to the susceptibility of these animals to pressures from mobulid fisheries throughout the WIO.

Finally, in Chapter 6, I synthesise the findings of my thesis and look forward to future directions for research. I discuss how each component of this thesis has broadened the current understanding of the movement patterns and feeding ecology of *M. alfredi*, and the relevance of each finding to the conservation of this species in Seychelles. Additionally, I describe the potential ecological benefits of protecting *M. alfredi* at D'Arros Island and St. Joseph Atoll, given the unique trophic role that this zooplanktivore plays within the reef system surrounding this location. Based on the success of the various research techniques used within this thesis, I then outline future research directions regarding the study of *M. alfredi* throughout Seychelles and describe my continued efforts to monitor this population. Lastly, I describe the global significance of my findings to manta ray conservation efforts, and highlight the importance of collaboration in future research endeavours in Seychelles.





# Chapter 2 Population size, habitat use and residency of manta rays at aggregation sites in Seychelles

## 2.1 Abstract

Understanding the aggregation and habitat use patterns of a species can improve the design of management strategies that aim to conserve vulnerable populations. Here, we examined the population size and patterns of residency and habitat use of oceanic (*Mobula birostris*) and reef (*Mobula alfredi*) manta rays in Seychelles. We did this using photo-identification techniques and with a focus on the aggregation at D'Arros Island and St. Joseph Atoll. Sightings of *M. birostris* were infrequent, suggesting that if aggregation areas for this species exist, they occur outside of the boundary of our study. A total of 236 *M. alfredi* were identified across all surveys, 66.5% of which were sighted at D'Arros Island and St. Joseph Atoll (Amirante Island Group). A further 22.5% of individuals were sighted at St. François Atoll (Alphonse Island Group). The novel use of a remote camera system deployed at a cleaning station at D'Arros Island revealed that time of day influenced the occurrence of *M. alfredi* at this site, with visits more likely to occur around midday than around dawn and dusk. This suggests that *M. alfredi* adopts a crepuscular foraging strategy focused on emergent zooplankton communities. Males visited the cleaning station more frequently than females, however, both sexes were equally represented within the identified population. The apparent isolation of *M. alfredi* at D'Arros Island, St. Joseph Atoll and St. François Atoll from the acute anthropogenic pressures commonly observed at more coastal localities, and the distance of these aggregations from identified mobulid fisheries in the Western Indian Ocean, suggests that the establishment of Marine Protected Areas at these sites will aid in conserving this vulnerable species in Seychelles.

## 2.2 Introduction

Mobulid rays (Family Mobulidae; Couturier et al. 2012, Poortvliet et al. 2015) are medium to large (1.1 – 7.0 m; White et al. 2017) filter-feeding elasmobranchs that aggregate predictably in coastal waters at tropical locations around the world (Couturier et al. 2012, Stevens et al. 2018a). There is a general consensus that populations of these animals are now declining on a global scale (Croll et al. 2016, Lawson et al. 2017, Stewart et al. 2018a). Targeted fisheries that supply

mobulid gill plates to the market for traditional Asian medicines have largely driven this phenomenon (Croll et al. 2016, O'Malley et al. 2017, Rohner et al. 2017b), although by-catch, accidental entanglement and boat strikes are also significant sources of mortality (Croll et al. 2016). The conservative life history strategies of these species, including low fecundity, late maturation and long gestation periods (Couturier et al. 2012), prolong the period of time required for populations to recover from the loss of individuals. This highlights the need to identify key aggregation areas and to understand the role that these habitats play in the life history of mobulid rays.

Manta rays are the largest of the mobulids (White et al. 2017, Hosegood et al. 2019). The oceanic manta ray (*Mobula birostris*) attains a maximum wingspan of 7.0 m and is typically observed at offshore locations (Marshall et al. 2009, Kashiwagi et al. 2011), whereas reef manta rays (*Mobula alfredi*) have smaller wing spans (maximum 5.5 m), and frequently aggregate at coastal, inshore locations (Marshall et al. 2009). Both species are currently listed as 'Vulnerable' on the International Union for the Convention of Nature's Red List (Marshall et al. 2018a, Marshall et al. 2018b), on Appendix II of the Convention for the International Trade for Endangered Species, and on Appendices I and II of the Convention on Migratory Species.

Aggregations of manta rays are thought to be driven by food availability (Couturier et al. 2012) and the presence of cleaning stations (Couturier et al. 2018) that provide an opportunity for individuals to have external parasites removed from their bodies by resident reef fishes (Potts 1973, Côté 2000). Cleaning stations also facilitate social interactions between individuals, including courtship and mating behaviours (Deakos et al. 2011, Stevens et al. 2018b). The significance of these stations is further shown by the repeated visits of the same individuals over prolonged periods of time (years), despite the ability of manta rays to routinely travel large distances (10s – 100s km; Dewar et al. 2008, Marshall et al. 2011, Germanov & Marshall 2014, Couturier et al. 2018, Germanov et al. 2019).

The relative predictability of the formation of aggregations by manta rays has greatly benefited global efforts to determine the drivers of their behaviour and movement in recent decades, as sampling can be aligned with aggregation events (Deakos et al. 2011, Jaine et al. 2012). The information collected during targeted surveys is particularly valuable in dispersed, archipelagic reef systems such as Seychelles, where it can be challenging to obtain continuous access to remote study sites throughout the year. The presence of unique patterns of pigmentation on the ventral surface of individual manta rays allows photo-identification to be used to assess the sizes and distributions of populations at aggregation sites (Dewar et al. 2008, Marshall et al. 2011, Deakos 2012, Jaine et al. 2012) over long periods of time (> 20 years; Marshall & Pierce 2012, Couturier et al. 2014). Environmental data can also be collected simultaneously with sighting records to determine potential drivers of movements (O'Shea et al. 2010, Jaine et al. 2012, Rohner et al.

2013, Couturier et al. 2018). Additionally, identification photographs can be collected by citizen scientists across large spatial scales (Town et al. 2013, Couturier et al. 2014, Germanov & Marshall 2014), providing insight into the broader (> 100 km) patterns of movement of individuals and the wider distribution of their populations. Collectively, these data can expand our understanding of the biology of manta ray populations at key aggregation areas and inform conservation and management strategies aimed at protecting them.

Here, we used photo-identification techniques and underwater monitoring to examine the population size, and patterns and potential drivers of movement and residency of *M. birostris* and *M. alfredi* at D'Arros Island and St. Joseph Atoll, Seychelles. Despite facing increasing pressures from targeted and small-scale fisheries in the Western Indian Ocean (Temple et al. 2019), little is currently known about manta ray populations in Seychelles because individuals of these species tend to aggregate around remote and isolated islands of the archipelago. In light of this, we aimed to (1) use a novel remote camera system to investigate the influence of environmental and temporal factors on patterns of manta ray visits to a cleaning station located to the north of D'Arros Island, (2) assess the population composition, abundance and habitat use patterns of manta rays in the coral reef environments surrounding these sites, and (3) use photo-identification data collected throughout Seychelles to examine the patterns of residency and movement of manta rays at aggregation areas across the archipelago as a whole, and to examine the significance of the reef system at D'Arros Island to this globally 'Vulnerable' species.

## 2.3 Methods

### 2.3.1 Study site

Seychelles is a remote archipelago located in the Western Indian Ocean that is comprised of 115 tropical islands (Figure 2.1A). These islands cover a total land mass of approximately 459 km<sup>2</sup>, which encompasses just 0.03% of the Exclusive Economic Zone of the country. The islands of Seychelles form six Island Groups based on their geography and composition. The populous Inner Island Group includes 41 granitic islands that are situated upon the Mahé Plateau. All remaining islands constitute the coralline Outer Islands, and are grouped based on their location and proximity to one another. The focus of this study was the manta ray aggregation at D'Arros Island and St. Joseph Atoll (Figure 2.1B) of the Amirante Island Group, and the patterns of visitation by individuals to a cleaning station to the north of D'Arros Island (Figure 2.1C).

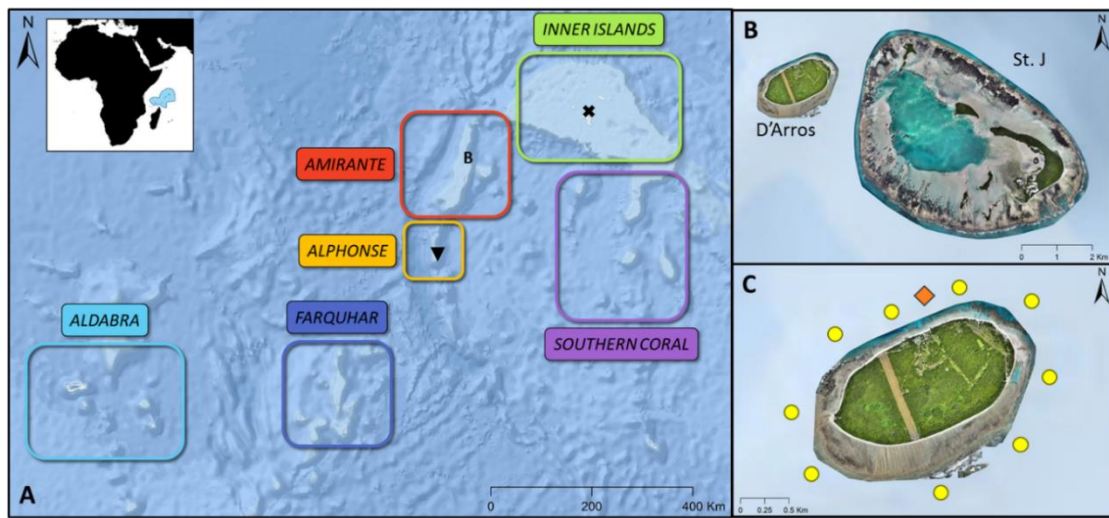


**Figure 2.1** The six Island Groups of Seychelles (A). D’Arros Island and St. Joseph Atoll (St. J; B) are located within the Amirante Island Group. Manta ray photo-identification surveys conducted at D’Arros Island (C) targeted nine sites during surface-based searches (yellow circles), while dive-based searches were conducted at the manta ray cleaning station to the north of the island (orange diamond). ▼, St. François Atoll. ✕, position of the Victoria Fish Market on Mahé Island.

## 2.3.2 Data collection

Photographs of the unique pigmentation patterns on the ventral surface of manta rays were used to identify individuals (Marshall et al. 2011, Marshall & Pierce 2012). All individual sighting records included a clear identification photograph, location and GPS position (where possible), date and time information. Species identification was based on the physical characteristics described by Marshall et al. (2009), typically by the distribution and density of pigmentation on the ventral surface, the colouration of the pectoral fin margin, and the shape of the dorsal shoulder patches. Assignment of individuals to a colour morph type – common (i.e. chevron), black (i.e. melanistic), or white (i.e. leucistic) – also followed Marshall et al. (2009). Where possible, the presence (male) or absence (female) of claspers was used to determine the sex of individuals (Marshall & Bennett 2010b). The disc width (DW; m) of each individual was estimated visually to the nearest 0.1 m and used as a proxy to assess the maturity status of *M. alfredi* based on the following metrics: juvenile ( $\leq 2.4$  m), sub-adult (male, 2.5 – 2.8 m; female, 2.5 – 3.1 m), or adult (male,  $\geq 2.9$  m; female,  $\geq 3.2$  m) (Stevens 2016). The presence of mating scars and pregnancy bulges on females, and the degree of calcification of the claspers of males, were also considered during the assignment of maturity status, as these characteristics are indicative of sexually active individuals (Marshall & Bennett 2010b, Stevens et al. 2018b). The size of pregnancy bulge in females was used to estimate length of gestation (Marshall & Bennett 2010b). Physical injuries were also noted during sightings but were used only as a secondary means for identification (Marshall & Bennett 2010a). Likely sources of injuries were categorised as natural (e.g. shark

bite to a pectoral fin) or anthropogenic (e.g. fishing line scarring around cephalic fin; Figure 2.2) where possible.

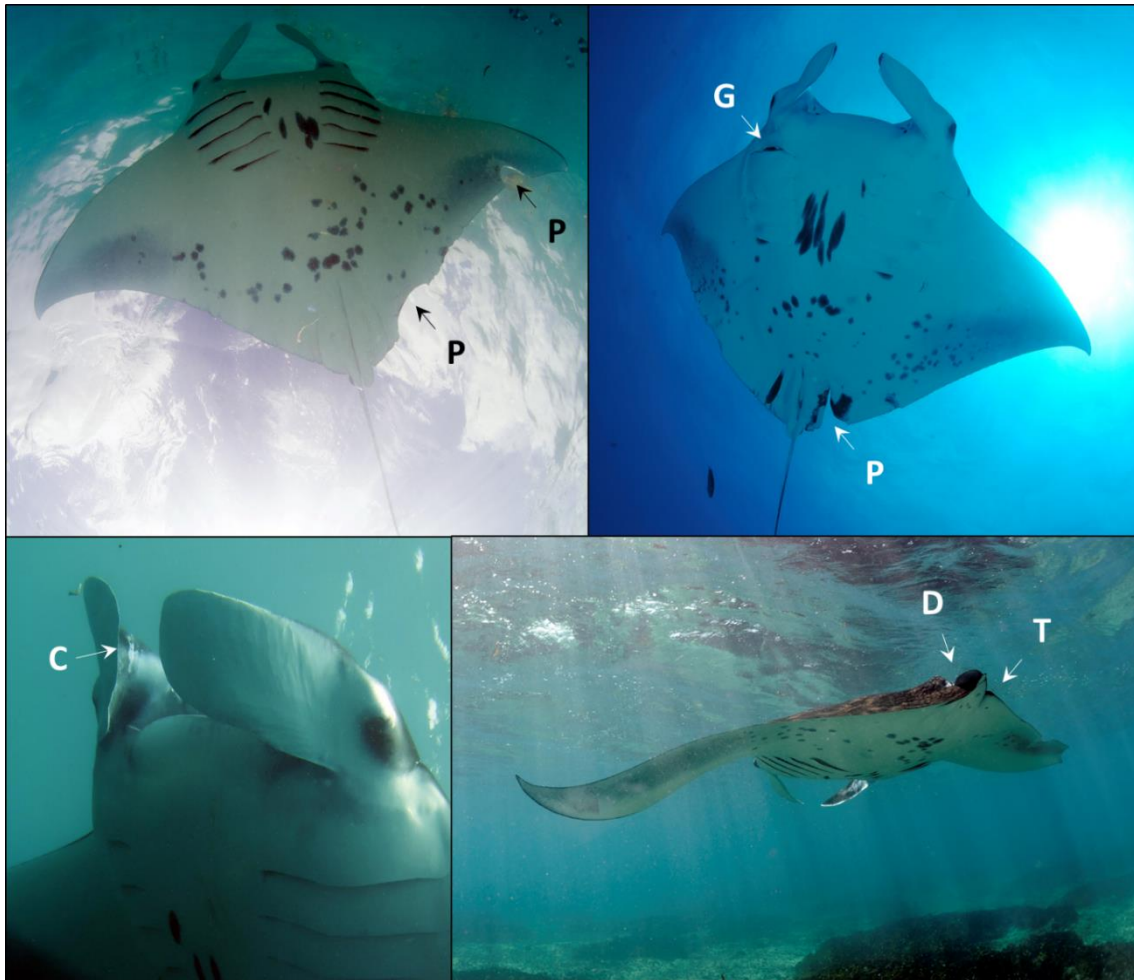


**Figure 2.2** Injury types recorded on reef manta rays (*Mobula alfredi*) in Seychelles. C: cephalic fin injury. D: dorsal fin injury. G: gill infection. P: pectoral fin injury. T: tail injury.

The behaviour of individuals throughout sighting events was noted wherever possible. Four primary behaviours were recognised: feeding, courtship, cleaning and cruising. Feeding occurred when individual manta rays had unfurled their cephalic fins while swimming with the mouth open. When feeding, individuals often formed “chains” where individuals swam in a single file one behind another. They also occasionally performed somersaults when feeding (Stevens et al. 2018a), and this behaviour was noted when observed. The movements of individuals involved in courtship were notably faster than those involved in feeding. Courtship was characterised by multiple males actively pursuing a single female, while not engaging in feeding, cleaning, or cruising behaviours (Stevens et al. 2018b). Cleaning behaviour occurred when manta rays reduced their speed to linger over sections of reef, where cleaner fishes removed external parasites from their skin. Individuals often unfurled their cephalic fins during this process. Behaviour was classified as cruising when manta rays swam through the water column with their cephalic fins

furled and their mouth closed. Where multiple behaviours occurred during a sighting, the behaviour that occupied the most time was reported.

### 2.3.3 Survey frequency

Identification photographs of manta rays were collected across three spatio-temporal scales in Seychelles. Firstly, a remote camera system (hereafter, MantaCam; described below) was used to continuously monitor manta ray visits to a cleaning station at D'Arros Island over a two-month period (29 September to 27 November 2017). Data collected by MantaCam were used to identify individuals visiting the cleaning station, to monitor the frequency of visits, and examine the behaviour of individuals at this site.

Secondly, three intensive surveys were conducted at D'Arros Island and St. Joseph Atoll by the authors during November 2013, 2016 and 2017 (Table 2.1). Collected photo-identification data were used to examine the level of residency that manta rays displayed at this location, and to estimate their abundance at D'Arros Island during each of the survey years. Observations of manta ray behaviour were also recorded at ten sites around D'Arros Island (Figure 2.1C) during surface-based and dive-based searches to examine patterns of habitat use by manta rays at this locality.

Lastly, sighting records of manta rays were collected opportunistically by the authors, collaborators and citizens throughout Seychelles between 2006 and 2018 to identify other key aggregation areas for these species and to assess the range of individual movements among islands and reefs. A week-long pilot study was also completed by the authors and collaborators at St. François Atoll (Alphonse Island Group; 2-9 December 2017; Figure 2.1A; Table 2.1) to investigate the occurrence of manta rays at this location and to examine their use of the lagoon system within the atoll. The total combined count of identified individuals across the three spatio-temporal scales of this study was used to provide a minimum estimate of population size for manta rays in Seychelles.

**Table 2.1** Location, year and duration of targeted manta ray field surveys in Seychelles. Effort is summarised by number of surface-based searches, number of dive-based searches (i.e. Manta Dives), and hours spent conducting searches. Alp., Alphonse Group. Am., Amirante Group.

Survey Location (Island Group)	Year	Field Days	Surface Searches	Manta Dives	Approx. Search Hours
D'Arros Island/St. Joseph Atoll (Am.)	2013	20	24	24	47.2
	2016	26	29	24	76.0
	2017	28	28	35	70.3
Alphonse Island/St. François Atoll (Alp.)	2017	8	6	8	53.5



### 2.3.4 MantaCam

MantaCam was used to monitor manta ray activity at a cleaning station located to the north of D'Arros Island (Figure 2.1C & 2.3) and to collect identification photographs at this site. The camera system consisted of a single GoPro Hero4 (GoPro; CA, USA) with a Blink time-lapse controller, which was attached by a USB splitter cable to two Voltaic LiPo 44Wh batteries with an 'always-on' feature. The camera and batteries were housed within a 17 x 29 cm PVC cylinder, which was sealed with a 2.3 cm thick acrylic lid with an o-ring and metal latches. The time lapse for the GoPro was set to take an image every 10 seconds, allowing for deployment periods of approximately 48 hours prior to battery depletion. Constant monitoring of the cleaning station was made possible through the use of two MantaCam systems, whereby one camera was deployed as the other was retrieved. This cycle was repeated during October and November 2017.

MantaCam was deployed on the northern edge of the cleaning station facing southwards (Figure 2.3). The camera was positioned at an upwards angle from the seafloor to capture an image of the water directly above the cleaning station and towards the surface of the water column. All images captured during the day were analysed, and the number of photographs containing a manta ray counted and used to record visits. The frequency and duration of manta ray visits to the cleaning station were measured using the timestamps on captured photographs. A visit was deemed to begin with the appearance of a manta ray in a photograph, and end 10 minutes after the last photograph of a manta ray was captured and all individuals were assumed to have left the vicinity of the station. When MantaCam was able to capture an image of the ventral surface of a manta ray, the individual was identified and the sighting recorded alongside those from the other surveys of this research.

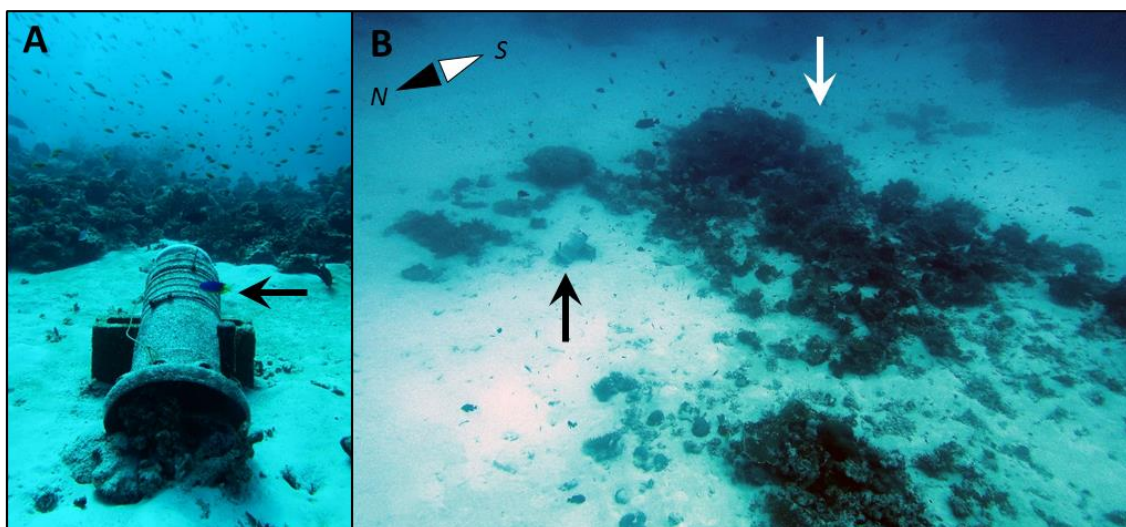


**Figure 2.3** MantaCam (A; black arrows) was deployed on the northern edge of the manta ray cleaning station (B; white arrow) at D'Arros Island, Seychelles, to monitor manta ray visits to this location and to capture identification photographs. N, north. S, south.

A current meter and CTD probe (Valeport; Devon, United Kingdom) were deployed approximately 15 m to the north of the cleaning station at D'Arros Island at a depth of approximately 20 m to examine possible environmental drivers of manta ray visits to this site. Current speed ( $\text{m s}^{-1}$ ) and temperature ( $^{\circ}\text{C}$ ) records were collected every 15 minutes while the logger was deployed (07-12 October, and 02-28 November 2017) and data averaged over each hour of MantaCam deployment. Tidal data were also collected at D'Arros Island and used to calculate tidal range (metres) and time relative to high tide (hours) at the cleaning station. Measures of tidal height were calculated using a tidal model built with the Oregon State University Tidal Model Driver (Egbert & Erofeeva 2002, Lea 2017), which was based on the harmonics recorded at St. Joseph Atoll. The model predicted tidal height in metres every ten minutes, and these data were also averaged over each hour that MantaCam was deployed. All aforementioned environmental variables have been shown to influence manta ray visitation rates and/or movement patterns in previous studies (Jaine et al. 2012, Rohner et al. 2013), and were included here to facilitate inter-population comparisons.

## 2.3.5 Statistical analyses

### 2.3.5.1 Sighting frequency

Photo-identification and sighting data were managed in an online database, through which count-based summary statistics were calculated. All other analyses used R (version 3.4.1; R Core Team 2017). Chi-squared tests were used to determine whether the proportion of males and females, and/or the three maturity classes, differed significantly across the three spatial scales considered in this study.

### 2.3.5.2 Visits to the cleaning station

A Generalised Additive Model (GAM) with a binomial error structure was constructed using the package *mgcv* (Wood 2017) to examine the influence of current speed, temperature, hour of day, tidal range, and time to high tide on the occurrence of manta ray visits to the cleaning station. Manta ray visits were analysed on an hourly basis across MantaCam deployments over 26 survey days (02 November to 27 November 2017). Each hour per day (05:00 – 18:00) was assigned either a '1' for a visit occurring or a '0' for no recorded visit, generating a binomial dataset that was used as the response variable within the GAM. Given the restriction of MantaCam data collection to daylight hours and the relatively short (< 1 month) monitoring period of this study, a tensor product smooth was fitted for hour of day and survey day number (numbered from 1 to 26) to consider potential interactions occurring between the two. Hourly environmental data were then



aligned with hourly visit data where possible, and all were fitted in the GAM using thin plate splines. This produced a dataset of 277 complete observations of the full suite of variables that were included in the final GAM. No strong correlation was found to be present between any tested predictors ( $r < 0.8$ ; Sleeman et al. 2010) and an AR(1) correlation structure was used to account for temporal autocorrelation occurring in the data (Zuur et al. 2009).

All potential combinations of predictor variables were considered during the model selection process. Akaike's Information Criterion corrected for sample size (AICc) and AICc weight (wAICc) were used to select the highest-ranking model. The values of wAICc were able to vary from 0 (no support) to 1 (complete support) for each model (Ferreira et al. 2017). Models within 2 AICc units of each other were considered to be equally ranked. When the model with the highest support was equally ranked with other candidate models, the model containing the lowest number of explanatory variables (i.e. the most parsimonious) was selected to be most appropriate for the data. The percentage of deviance explained by models was used as a measure of goodness of fit. The function 'vis.gam' from the package *mgcv* was used to visualise the summed effects of the tensor product smooth included in the final GAM. Contour values within this plot indicated the predicted magnitude of the effect of the combined variables on manta ray visits to the cleaning station. Summed effect plots were then compared to cumulative histograms of manta ray visits to the cleaning station throughout the full monitoring period (29 September – 27 November) for further examination of visitation patterns.

### 2.3.5.3 Abundance models

Sighting data collected through targeted surveys and by MantaCam were used to estimate manta ray abundance at D'Arros Island and St. Joseph Atoll, Seychelles, during surveys in November 2013, 2016 and 2017 (Table 2.1). An estimate of population abundance for all of Seychelles could not be calculated, given the largely opportunistic, unstructured and sparse nature of the data collected at the broadest spatial scale. Sighting data from D'Arros Island were collated by day within each survey year, with individuals either being present or absent across sampling days. Sighting histories of males and females were considered separately within each year, and the number of searches completed on each day used as a measure of sampling effort. A search was classified as one of three sampling techniques: a surface-based circumnavigation of D'Arros Island, a dive at the cleaning station, or a full-day of MantaCam deployment.

Open Jolly-Seber population models with a POPAN formulation (hereafter, POPAN models) were fitted to sighting data collected during the three November surveys at D'Arros Island using the package *RMark* in R (Laake 2013). The POPAN model structure allowed for the data collected within each survey to be examined independently, removing the uncertainties associated with

modelling animal population dynamics across sampling periods that are unevenly spaced (Brown et al. 2016). POPAN models provided an estimate of the total number of animals that visited D'Arros at any time during each survey year, and recognised that encountered individuals were a random sub-sample of the total 'super-population' ( $\hat{N}$ ) available for capture (Brown et al. 2016).

Three additional parameters were estimated in each POPAN model; apparent survivorship of individuals between sampling events ( $\phi$ ), the probability of capturing individuals ( $p$ ), and the probability that an unsighted individual will enter from the super-population and be sighted ( $P_{ent}$ ). For each period (i.e. survey year), a total of 150 models were fitted that imposed various constraints on parameter estimation. Apparent survival and probability of entry were allowed to vary with time ( $t$ ), sex ( $s$ ), time and sex ( $t + s$ ), or were set to remain constant (.) within each period (Marshall et al. 2011, Brown et al. 2016). Capture probability was modelled in a similar manner, with the addition of variation with effort ( $e$ ), or effort and sex ( $e + s$ ).

Population closure at D'Arros Island was assessed by fitting fully and partially closed models within each period alongside the full sets of open models. Closure to loss (i.e. to emigration or deaths) was achieved by fixing  $\phi$  at 1 ( $=1$ ), while closure to gains (i.e. to immigration or births) was achieved by fixing  $P_{ent}$  at 0 ( $=0$ ). Both  $\phi$  and  $P_{ent}$  were fixed in the fully closed models (Brown et al. 2016). A comparison of closed versus open population structure within each period was completed during the model selection process.

All models were subject to the same set of assumptions throughout the study (White & Burnham 1999). These included that sampling was instantaneous throughout a constant study area (Brown et al. 2016), and that all individual manta rays were identified correctly from their ventral markings (Kitchen-Wheeler 2010, Marshall et al. 2011). It was also assumed that the unique pigmentation patterns of individuals were permanent, allowing complete tag retention so that the ability to identify individuals did not change over time (Couturier et al. 2014). Importantly for the Jolly-Seber model structure, the probability of capture and apparent survival of marked (sighted) and unmarked (unsighted) individuals was assumed to be equal.

The goodness-of-fit of sighting data for each period to the POPAN models was assessed using the function 'release.gof' in *RMark* (Lebreton et al. 1992). Overdispersion was examined through the variance inflation factor,  $\hat{c}$ , which was calculated by dividing the combined Test 2 and Test 3 chi-square statistic by the total degrees of freedom (Deakos et al. 2011, Marshall et al. 2011). A  $\hat{c} > 1$  indicates overdispersion in the data and potential violation of the equal catchability assumption. Overdispersion was not observed in any sampling years at D'Arros Island, so the default  $\hat{c}$  settings ( $\hat{c} = 1$ ) were used for all analyses.

The top POPAN model within each survey year was identified using AICc and wAICc values. A gross estimate of  $\hat{N}$  was subsequently derived for male and female manta rays from the top model.

Where the top model was within 2 AICc units of other candidate models ( $\Delta\text{AICc}$ ), all were deemed to be equally ranked. Estimates of male and female  $\hat{N}$  at D'Arros Island were derived from model-averaged estimates based on normalised wAICc values in these cases. Closure assumptions were examined by noting the prevalence of fixed  $\phi$  and  $P_{ent}$  parameters in the top ten models as ranked by AICc values.

## 2.4 Results

### 2.4.1 Overview

A total of 1,583 sightings of 241 individual manta rays were reported throughout Seychelles between July 2006 and December 2018 across the three spatio-temporal scales of this study. Of these 241, only five individuals were *M. birostris* (Figure S 2.1), and the remaining 236 were *M. alfredi* (Table 2.2; Figure 2.4). No melanistic or leucistic individuals of either species were sighted.

**Table 2.2** Distribution of reef manta ray (*Mobula alfredi*) sightings recorded in Seychelles across three spatio-temporal scales and using varying survey techniques (effort types). St. F: St. François Atoll.

Scale	Effort Type	Time Frame & Survey Dates	No. sightings (% total)	No. individuals (No. resighted)
Cleaning Station (D'Arros Island)	MantaCam	29-Sep-2017 to 27-Nov-2017	341 (21.6%)	83 (51)
D'Arros Island & St. Joseph Atoll	Opportunistic + 3 x Surveys	2013-2018 Surveys: Nov-2013-2016-2017	1,076 (68.2%)	151 (114)
Wider Seychelles	Opportunistic + 1 x Survey (St. F)	2006-2018 Survey (St.F): Dec 2017	160 (10.2%)	98 (46)
<b>All Records</b>			<b>1,577 (100%)</b>	<b>236 (157)</b>

### 2.4.2 Cleaning station

#### 2.4.2.1 Sighting summary

MantaCam captured 203,277 photographs during the 599.5 hours that it was deployed and active at the D'Arros cleaning station, of which 3,146 (1.5%) contained images of *M. alfredi*. These latter images contributed 341 confirmed sightings of 83 individuals to the Seychelles database

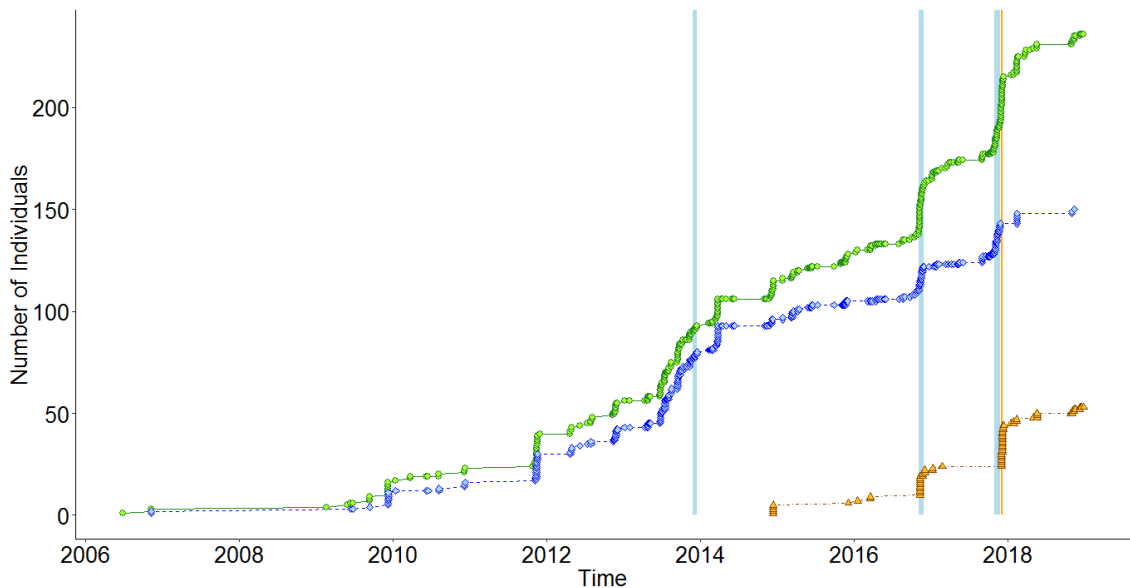


**Figure 2.4** Discovery curve of reef manta ray (*Mobula alfredi*) sightings in Seychelles (green circles), at D'Arros Island and St. Joseph Atoll (Amirante Island Group; blue diamonds), and at St. François Atoll (Alphonse Island Group; orange triangles). Blue shading indicates timing of three November sampling periods at D'Arros Island. Orange shading indicates timing of the single sampling period at St. François Atoll.

(21.6% of total), of which seven were new. No *M. birostris* were recorded at the cleaning station by MantaCam. The largest number of photographs containing *M. alfredi* collected during a single day was 174 on 10 November 2017. The maximum number of individuals estimated to be photographed by MantaCam in a single day was 18 (27 November 2017). Of these, 15 were individually identified and three were unidentifiable.

Males ( $n = 217$ , 63.6%) were sighted more frequently at the cleaning station than females ( $n = 124$ , 36.4%;  $\chi^2 = 25.36$ ,  $df = 1$ ,  $p < 0.001$ ). Additionally, the cleaning station was more frequently visited by adult and sub-adult individuals, than by juveniles (53.1, 38.7 and 8.2%, respectively;  $\chi^2 = 31.54$ ,  $df = 2$ ,  $p < 0.001$ ).

Visits of *M. alfredi* to the cleaning station lasted an average of  $4.92 \pm 6.84$  (S.D.) minutes, although visits lasting one minute occurred most frequently. MantaCam recorded a total of 392 visits by *M. alfredi* to the cleaning station during the full deployment period (Figure S 2.2). The largest number of individuals recorded at the cleaning station at the same time was seven (26 November 2017), and the highest number of visits that were recorded in a single day was 14 (17 November 2017).

### 2.4.2.2 Behaviour at the cleaning station

Cleaning dominated behavioural records at the station (90.7% of observations), although feeding, courtship and cruising were also reported (3.1%, 3.7%, and 2.5%, respectively). Courtship had not been observed at this site prior to the deployment of MantaCam in 2017. Images collected by MantaCam were used to contribute 12 additional courtship events to the existing database of records at D'Arros Island (Figure S 2.3), where only four observations of courtship had been recorded during previous years. In some instances, identification images were captured during courtship events (Figure S 2.3A), allowing identification of participants. The largest number of individuals observed engaging with each other in a single courtship event was four (Figure S 2.3B), although events involving only two ( $n = 9$ ) or three ( $n = 2$ ) individuals were more common.

MantaCam captured images of one pregnant female (DW = 3.6 m) on 12 October 2017 (Figure S 2.3C). It is estimated that this individual was in the fourth trimester of a 12-month pregnancy based on the extent of the ventral stomach bulge (G. Stevens, pers. comm.). In total, four pregnant females were identified throughout Seychelles during this study, and an additional 16 individuals were seen with mating scars on the tip of their left pectoral fin. These individuals accounted for 17.4% of the population of female *M. alfredi* identified in Seychelles to-date.

### 2.4.2.3 Patterns of visits

The top-ranked GAM explained 14.8% of the variation in the data, and included only the tensor product spline of time of day and day of survey as a driver of manta visits to the cleaning station (Table 2.3). Current speed, water temperature, tidal range and time to high tide did not have a significant effect on the frequency of visits. Visits by *M. alfredi* to the cleaning station varied significantly with the hour of the day, and were more likely to occur during the middle of the day (10:00 – 15:00) than in the hours following dawn or preceding dusk (Figure 2.5A). This pattern of visitation was most consistent during the first two weeks of November, with a greater amount of variation observed in the visit times recorded in during the last two weeks of the month (Figure 2.5A). The same pattern was also observed when *M. alfredi* visits were considered cumulatively per hour over all MantaCam deployments (29 September – 27 November 2017), where the majority of visits occurred between 10:00 and 14:00 (Figure 2.5B).

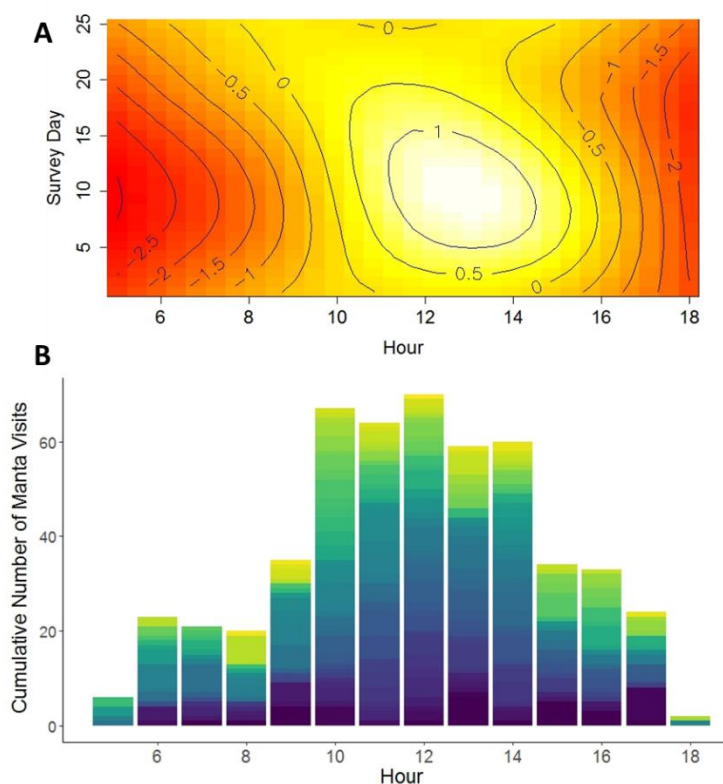


**Figure 2.5** Frequency of visits by reef manta rays (*Mobula alfredi*) to a cleaning station at D'Arros Island, Seychelles, recorded using a remote camera system ('MantaCam'), relative to time of day (h) and survey day (2 to 27 November 2017; numbered 1 – 26; A). Contour lines indicate the magnitude of summed effects of both variables on the occurrence of manta rays at this site. Cumulative number of manta visits to the cleaning station across all MantaCam deployments are also presented (29 September (yellow) to 27 November 2017 (purple); B).

**Table 2.3** Top ten highest-ranked GAMs for the influence of hour of day and day of survey (h and 1-26, respectively; H|D), current speed ( $\text{m s}^{-1}$ ; C), temperature ( $^{\circ}\text{C}$ ; M), tidal range (m; R) and time to high tide (h; T) on visits of manta rays to a cleaning station at D'Arros Island, Seychelles. df, degrees of freedom. AICc, Akaike's Information Criterion corrected for sample size.  $\Delta\text{AICc}$ , change in AICc in comparison to model with lowest AICc. wAICc, relative AICc weight. DE (%): percent deviance explained by model. Bold text indicates selected top model.

Model	df	AICc	$\Delta\text{AICc}$	wAICc	DE (%)
~ H D + M	15.21	324.61	0.00	0.21	14.81
~ <b>H D</b>	<b>13.43</b>	<b>324.81</b>	<b>0.20</b>	<b>0.19</b>	<b>14.76</b>
~ H D + R	18.68	326.19	1.58	0.09	14.40
~ H D + M + T	16.38	326.67	2.06	0.07	14.27
~ H D + C + M	16.12	326.81	2.20	0.07	14.24
~ H D + T	14.76	326.84	2.22	0.07	14.23
~ H D + C	14.32	326.89	2.28	0.07	14.22
~ H D + M + R	19.93	326.96	2.35	0.06	14.20
~ H D + R + T	19.77	328.21	3.60	0.03	13.87
~ H D + C + R	19.61	328.47	3.86	0.03	13.80

## 2.4.3 D'Arros Island and St. Joseph Atoll

### 2.4.3.1 Population size and composition

Collective survey efforts identified a total of 157 individual *M. alfredi* at D'Arros Island and St. Joseph Atoll. Of these individuals, 150 were first sighted at this locality (63.6% of Seychelles total) and 122 (78.0% of D'Arros total) have been resighted on at least one occasion.

Male *M. alfredi* were sighted more frequently than females across surveys conducted at D'Arros Island ( $\chi^2 = 38.37$ ,  $df = 1$ ,  $p < 0.001$ ). Males ( $n = 79$ , 50.3%) and females ( $n = 76$ , 48.4%) were equally represented within the population ( $\chi^2 = 0.06$ ,  $df = 1$ ,  $p = 0.81$ ), and only two individuals (1.3%) were unable to be assigned a sex (Figure S 2.4). Mature ( $n = 75$ , 47.8%) and sub-adult ( $n = 62$ , 39.5%) individuals encompassed the majority of the *M. alfredi* sightings recorded at D'Arros Island, with a significantly lower number of juveniles ( $n = 20$ , 12.7%) identified by all survey methods at this location ( $\chi^2=31.58$ ,  $df = 2$ ,  $p < 0.001$ ). All individuals at D'Arros Island were assigned a maturity status.

The relative abundance of different maturity classes (juvenile, sub-adult, adult) did not differ by sex at D'Arros Island ( $p > 0.05$ ). Additionally, there was no significant difference in resighting rates between identified males ( $n = 66$ , 83.5%) or females ( $n = 76$ , 73.7%;  $\chi^2 = 0.62$ ,  $df = 1$ ,  $p = 0.43$ ), or among juveniles ( $n = 12$ , 66.7%), sub-adults ( $n = 47$ , 75.8%), and adults ( $n = 63$ , 81.8%;  $\chi^2 = 1.55$ ,  $df = 2$ ,  $p = 0.46$ ).

### 2.4.3.2 Size distribution

Almost half (44.6%) of the *M. alfredi* identified at D'Arros Island and St. Joseph Atoll had disc widths of 2.5 – 3.0 m, with an average disc width of  $2.9 \pm 0.5$  m (Figure S 2.5). Six individuals were < 2 m wide, the majority of them males ( $n = 4$ , 66.7%), with the smallest estimated to be 1.5 m for an individual for whom sex could not be determined. Females had significantly larger disc width than males (3.06 and 2.82 m, respectively;  $t = -3.52$ ,  $df = 121.71$ ,  $p < 0.001$ ). A mature female was the only individual to exceed a disc width of 4.0 m.

### 2.4.3.3 Patterns of habitat use

Surface-feeding accounted for 53.6% of the 1,391 behavioural observations of *M. alfredi* at D'Arros Island and was recorded at all sites (Figure 2.6). Sites towards the north-east of D'Arros Island displayed the highest frequency of feeding behaviour, with surface-feeding observed during 96.7, 97, and 100% of sightings of *M. alfredi* at the northern, north-eastern, and eastern

sites, respectively. Courtship behaviour was observed 22 times at the cleaning station to the north of D'Arros Island, accounting for 3.7% of the total behavioural observations recorded at this site. Cleaning behaviours were observed 545 times (39.7%) along the northern shoreline of D'Arros Island, most frequently at the cleaning station ( $n = 534$ ). Cleaning behaviour was only reported once at Airstrip North and eight times at Jetty. Cruising behaviour constituted 5.1% ( $n = 70$ ) of all behavioural observations at D'Arros Island and was most frequently observed along the western and southern coastlines (range 2.5 to 16.7% of records across sites).

#### 2.4.3.4 Abundance of reef manta rays at D'Arros Island

POPAN models were fitted separately to sighting data of *M. alfredi* collected at D'Arros Island during each of the November 2013, 2016 and 2017 surveys (Tables S 2.1 – 2.3). Males and females were considered separately within each POPAN model, and combined to produce an overall estimate of the abundance of individuals at D'Arros Island during each survey.

Abundance estimates for *M. alfredi* at D'Arros Island were lower in 2013 than they were in the subsequent years, but remained consistent between 2016 and 2017 (Table 2.4). Little difference ( $\leq 10$  individuals) was observed between estimated  $\hat{N}$  for males and females in all years. None of the top selected models across the three survey periods included fixed (i.e. closed) parameters (Tables S 2.1-2.3).

#### 2.4.3.5 Injuries and anthropogenic impacts

Almost half ( $n = 76$ ; 48.4%) of the individual *M. alfredi* sighted at D'Arros Island and St. Joseph Atoll had an injury to their body. Males ( $n = 35$ , 44.0%) and females ( $n = 40$ , 52.6%) displayed similar extents of injuries. Adults (41 of 75 individuals, 54.7%) were more frequently injured than juveniles (6 of 20 individuals, 30.0%;  $\chi^2 = 7.15$ ,  $df = 1$ ,  $p = 0.01$ ), but there was no significant difference in injury rates between sub-adults (29 of 62 individuals, 46.8%) and either juveniles or adults ( $\chi^2 = 3.68$ ,  $df = 1$ ,  $p = 0.06$  and  $\chi^2 = 0.60$ ,  $df = 1$ ,  $p = 0.44$ , respectively).

Injuries to pectoral fins were most common, followed by injuries to the tail and/or dorsal fin, gills, and cephalic fins (43.3, 13.4, 5.1 and 3.8% of those injured, respectively; Table 2.5). Natural causes were responsible for the majority of injuries to these individuals (76.3%), with anthropogenic threats - namely, damage caused by fishing line – accounting for 3.9% of injuries. Injuries from a combination of natural and anthropogenic causes were observed on four individuals (5.3%), whereas the likely causes of injury were unknown on 11 individuals (14.5%). Anthropogenic causes were most frequently associated with injuries to cephalic fins.



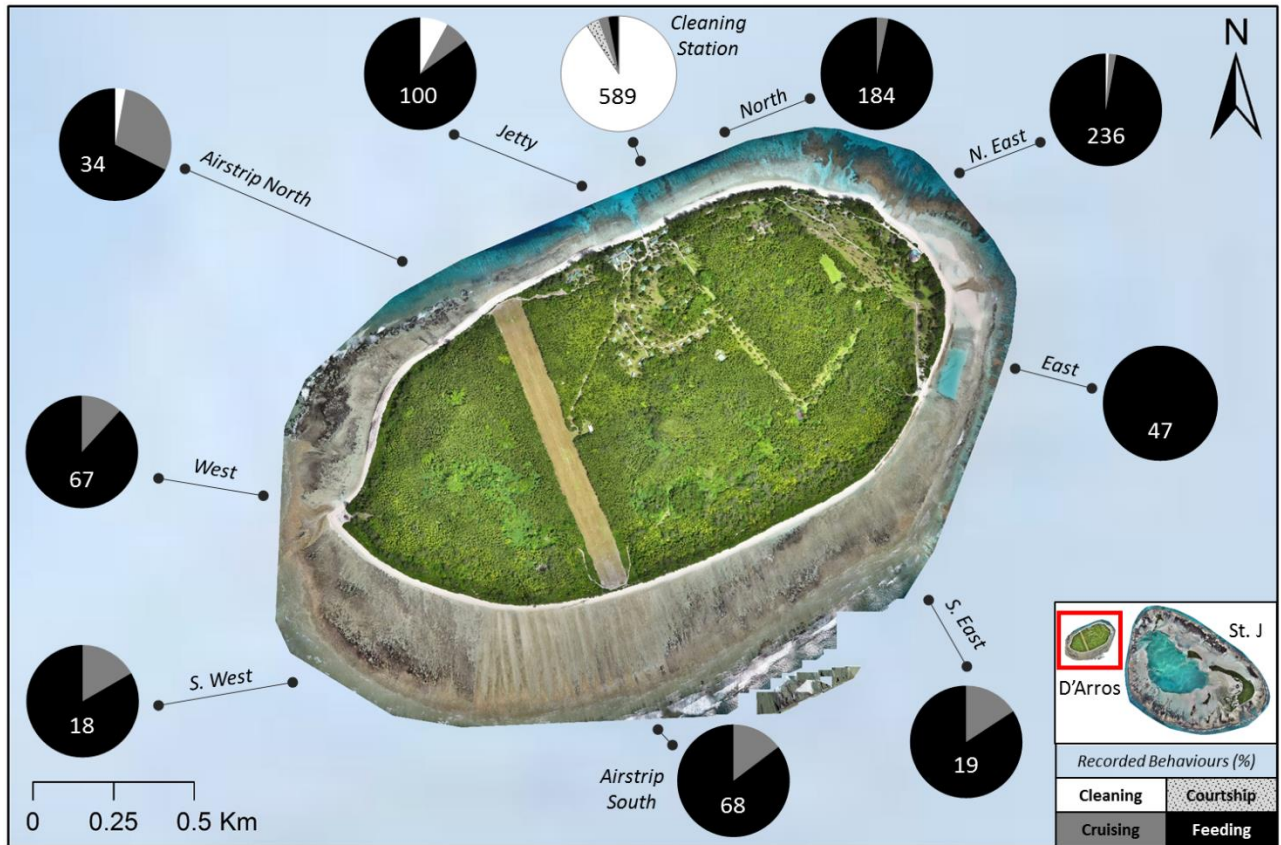


**Figure 2.6** Proportion of occurrence and distribution of feeding, courtship, cleaning and cruising behaviour by reef manta rays (*Mobula alfredi*) at ten sites around D’Arros Island, Seychelles. Values within pie charts indicate the total number of behavioural records collected at each site. Eastern survey sites located within the channel between D’Arros Island and St. Joseph Atoll (St. J). Colour allocations to behaviours are described in figure legend.

**Table 2.4** Estimated total abundance ( $\hat{N} \pm \text{S.E.}$ ) of female (F), male (M) and all reef manta rays (*Mobula alfredi*) at D’Arros Island and St. Joseph Atoll, Seychelles, across three sampling years. Estimates derived from open POPAN models ( $\hat{c} = 1$ ) considered sexes as separate groups. ‘d’: number of sampling days within each survey year. ‘Identified’: number of unique individuals identified within each survey year. Lower (LCL) and upper (UCL) confidence intervals.

Sampling Dates (d)	Identified (F, M)	Sex	$\hat{N}$	LCL	UCL
29 Nov-18 Dec 2013 (20)	35 (15,20)	F	18 ± 1.88	14.46	21.85
		M	23 ± 1.89	19.46	26.87
		<b>All</b>	<b>41 ± 2.67</b>		
04 Nov-29 Nov 2016 (21)	73 (37,36)	F	54 ± 5.37	43.49	64.55
		M	53 ± 5.37	42.49	63.55
		<b>All</b>	<b>107 ± 7.60</b>		
01 Nov-28 Nov 2017 (28)	88 (39,49)	F	48 ± 2.69	42.59	53.15
		M	58 ± 2.71	52.72	63.34
		<b>All</b>	<b>106 ± 3.82</b>		

**Table 2.5** Distribution of injury types throughout the reef manta ray (*Mobula alfredi*) population identified at D'Arros Island and St. Joseph Atoll, Seychelles.

Damaged Region	No. Individuals (% Population)	Suspected Cause of Injury (No. Individuals Affected, % of Population)			
		Anthropogenic	Natural	Anthropogenic & Natural	Unknown Cause
Pectoral Fin/s	68 (43.3)	2 (1.6%)	53 (41.7%)	4 (3.1%)	7 (7.1%)
Cephalic Fin/s	6 (3.8)	2 (1.6%)	2 (1.6%)	2 (1.6%)	0 (0%)
Tail and/or Dorsal Fin	21 (13.4)	2 (1.6%)	14 (11.0%)	0 (0%)	5 (3.9%)
Gill/s	8 (5.1)	0 (0%)	6 (4.7%)	1 (0.8%)	1 (0.8%)

## 2.4.4 Alphonse and other Island Groups

### 2.4.4.1 Oceanic manta rays

Only six sightings of *M. birostris* were recorded throughout the study period (0.4% of total). All sightings of *M. birostris* were reported in the Inner Island Group of Seychelles, and none of the five identified individuals (3 female, 1 male, 1 unknown sex) that were cruising at the time of each encounter were resighted (Figure 2.7).

### 2.4.4.2 Reef manta rays

#### 2.4.4.2.1 Sighting summary

A total of 160 sightings of 98 individual *M. alfredi* were recorded throughout the remaining Island Groups of Seychelles during this study, with the exception of the Southern Coral Group where no sightings were reported (Figure 2.7). These sightings added a further 79 individuals to the population of *M. alfredi* in Seychelles. Sightings of *M. alfredi* within the Aldabra and Farquhar Groups comprised just 1.7 and 2.1% of the identified population, and none of the individuals in either region were resighted ( $n = 4$  and  $5$ , respectively). Of the 11 (4.7%) individuals sighted in the Inner Island Group, only one was resighted and this occurred within 24 hours of the first encounter. An additional 22 sightings of *M. alfredi* were reported in the Amirante Island Group at Desroches and Poivre Islands. The remaining sighting records for 53 (22.5%) individuals were collected at St. François Atoll (Alphonse Island Group), of which 33 (62.3%) were resighted. Collectively, the 236 individual *M. alfredi* identified throughout Seychelles serve as a minimum estimate for the total population size of this archipelago.

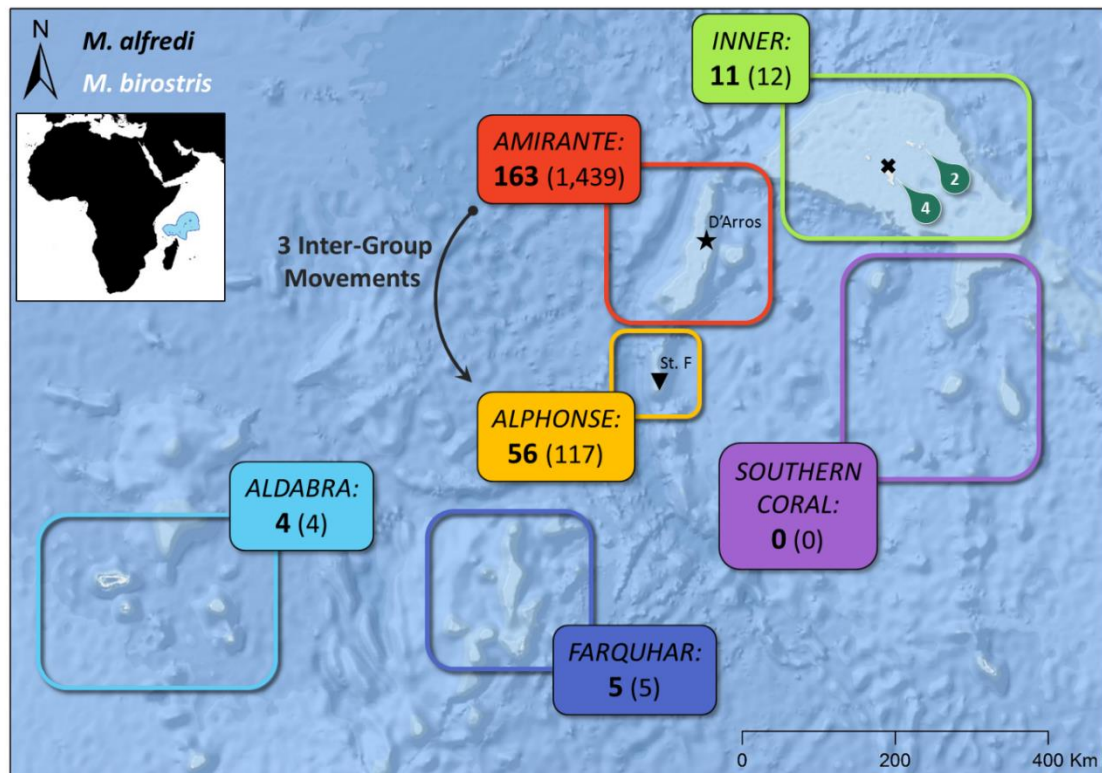


**Figure 2.7** Distribution of oceanic (*Mobula birostris*; white text) and reef (*Mobula alfredi*; black text) manta ray sightings throughout the Island Groups of Seychelles. For *M. birostris*, value indicates number of individuals recorded across six sightings during this study. For *M. alfredi*, bold value indicates number of individuals sighted, and value in brackets indicates number of recorded sightings. ‘★’ is the position of the main study site; D’Arros Island and St. Joseph Atoll. ‘▼’ indicates the position of St. François Atoll (St. F). ‘✕’ is the position of the Victoria Fish Market on Mahé Island.

The largest aggregation of *M. alfredi* occurred at St. François Atoll (Alphonse Island Group) on 19 December 2018, where approximately 40 individuals were observed feeding at the surface (L. Martin, pers. comm.). The second largest event occurred at D’Arros Island (Amirante Island Group) on 4 November 2017 when a group of 25 individuals were observed. The pilot study conducted within the Alphonse Group in December 2017 contributed 43 confirmed sightings of 29 individual *M. alfredi* to the Seychelles records. Eighteen of these individuals were new to the database at the time of the encounters (Figure 2.4). Additionally, a number of incidental sightings of *M. alfredi* within the St. François Atoll lagoon system were noted. Poor water visibility (< 0.5 m) prohibited the collection of identification images from this location, where up to 15 large *M. alfredi* (DW > 2.5 m) were observed swimming in the main lagoon channel, and a small individual (DW ~ 1 m) was sighted feeding within the northernmost lagoon. The discovery curves for the Alphonse Island Group, D’Arros Island and St. Joseph Atoll, and Seychelles as a whole, have not yet reached an asymptote.

#### 2.4.4.2.2 Sex and maturity

Male and female *M. alfredi* were encountered at similar frequencies away from D'Arros Island and St. Joseph Atoll ( $\chi^2 = 0.24$ ,  $df = 1$ ,  $p = 0.63$ ). They also remained equally represented within the identified population ( $n = 43$  and  $48$  individuals, respectively;  $\chi^2 = 0.27$ ,  $df = 1$ ,  $p = 0.60$ ). Seven individuals (3.8%) were unable to be assigned a sex based on photographs (Figure S 2.6). Mature ( $n = 36$ , 36.8%) and sub-adult ( $n = 40$ , 40.8%) individuals continued to account for the majority of the identified *M. alfredi* population, with a significantly lower number of juveniles ( $n = 16$ , 16.3%) being sighted ( $\chi^2 = 10.78$ ,  $df = 2$ ,  $p = 0.005$ ) than the sub-adults or adults. Maturity status could not be assigned to six individuals (6.1%).

Sighting frequencies for all individuals throughout Seychelles varied from a single sighting, to a maximum of 60 re-sightings of an adult male between July 2012 and November 2018 at D'Arros Island (Figure S 2.7). The most frequently sighted female was a sub-adult sighted 47 times between December 2015 and November 2017 at D'Arros Island. Of the top 10 most re-sighted individuals in this study, seven were males (Figure S 2.7). The longest time between two sightings of the same individual was 2,808 days (7.75 years), where a juvenile male was first sighted at D'Arros Island on 09 August 2010, and next resighted on 17 April 2018 at Poivre Island of the Amirante Island Group. An updated maturity status was unable to be assigned to this individual during the latter sighting.

#### 2.4.4.2.3 Behaviour

As at D'Arros Island and St. Joseph Atoll, typical surface-feeding behaviour was reported most frequently across sightings of *M. alfredi* at other Island Groups ( $n = 135$ , 84.4% records). Only five observations of somersault feeding were recorded, all of which occurred at St. François Atoll (Alphonse Island Group; 3.1% of records). This behaviour was also noted within the large feeding aggregation of 40 individuals sighted in December 2018. Cruising behaviour was observed on 17 occasions (10.6%), and cleaning behaviour was reported eight times (5.0%). No records of courtship behaviour currently exist for *M. alfredi* outside of the Amirante Island Group.

#### 2.4.4.2.4 Movements between Island Groups

Three individuals were recorded to move between the Amirante Island Group and the Alphonse Island Group. All individuals travelled an average of  $198 \pm 2$  km from D'Arros Island to St. François Atoll, over timeframes of 14 to 1,624 days (Figure 2.7). Return journeys were not

observed in any of these cases, and no additional movements of individuals among other Island Groups were recorded in this study.

#### 2.4.4.2.5 Injuries and anthropogenic impacts

Thirty eight (37.8%) of the 98 individual *M. alfredi* sighted elsewhere than D'Arros Island and St. Joseph Atoll displayed an injury to their body. Male (n = 20, 47%) and female (n = 16, 33.3%) *M. alfredi* at these locations displayed similar extents of injury. Adults (17 of 36 individuals, 47.2%) and sub-adults (15 of 40 individuals, 16.7%) were more frequently injured than juveniles (10 of 35 individuals, 28.6%) ( $\chi^2 = 8.17$ , df = 1,  $p = 0.017$  and  $\chi^2 = 8.05$ , df = 1,  $p = 0.005$ , respectively). There was no significant difference in injury rates between sub-adults and adults ( $\chi^2 = 0.125$ , df = 1,  $p = 0.724$ ). The occurrence and type of injuries reported for these *M. alfredi* were similar to those reported for individuals at D'Arros Island and St. Joseph Atoll (Table S 2.4), with injuries to the pectoral fins being most common, and anthropogenic impacts being most frequently associated with cephalic fin injuries.

Four deceased *M. alfredi* were reported in the Victoria Fish Market on Mahé Island (Inner Island Group) by collaborators during the course of this study. Landings occurred in 2015 (n = 2), 2016 (n = 1) and 2018 (n = 1), and included either finned individuals (n = 2), or pieces of pectoral fin (n = 2). Additionally, two lethal entanglements of *M. alfredi* were reported from the Inner Islands, one involving a discarded fishing line (March 2009), and the other, a mooring line (December 2017).

## 2.5 Discussion

Sightings of manta rays in Seychelles recorded using photo-identification techniques were dominated by a relatively small, but resident population of 236 individual *M. alfredi*. Larger *M. birostris* were only occasionally sighted within the Inner Island group of Seychelles. The combination of surveying techniques used in this study allowed us to examine the drivers of visits by *M. alfredi* to a cleaning station at D'Arros Island. They also allowed us to assess patterns of residency and habitat use of *M. alfredi* at the coral reefs surrounding this location. Together with the sighting records collected throughout the other Island Groups of Seychelles, these data provide important information regarding the conservation needs of this globally vulnerable species in a remote region of the Western Indian Ocean.

## 2.5.1 Cleaning station

Individual *M. alfredi* were more likely to be sighted at the D'Arros Island cleaning station during the middle hours of the day than at dawn or dusk. A similar pattern of visits has been reported for *M. alfredi* at cleaning stations at other locations around the world, including Hawaii, eastern Australia and Indonesia (Dewar et al. 2008, Couturier et al. 2018, Setyawan et al. 2018). This may be due to cleaner fishes at cleaning stations only being active during daylight hours (Potts 1973, Lenke 1988). Additionally, such patterns of visitation may be the result of the feeding behaviour of *M. alfredi*. Stable isotope analyses have revealed that emergent zooplankton comprises a large proportion of the diet of this species at D'Arros Island (38%; Peel et al. 2019a) and in eastern Australia (Couturier et al. 2013b). The crepuscular movement of these benthic zooplankton communities may trigger foraging by *M. alfredi* at dawn and dusk (Armstrong et al. 2016), and subsequently reduce the frequency of visits by individuals to the D'Arros Island cleaning station during these times. Studies using passive acoustic telemetry further support this hypothesis, with *M. alfredi* more likely to be detected during the day than at night at D'Arros Island and elsewhere (Couturier et al. 2018, Setyawan et al. 2018, Peel et al. 2019b). These telemetry data also overcome the restriction of data collection by MantaCam to daylight hours only, and provide insight into the patterns of movement of *M. alfredi* throughout the full diel cycle.

Current speed, water temperature, tidal range and time to high tide did not influence the frequency of *M. alfredi* visits to the cleaning station at D'Arros Island. This was unexpected given the importance of environmental drivers at aggregation sites for *M. alfredi* on the Great Barrier Reef (O'Shea et al. 2010, Jaine et al. 2012), in the coastal waters of Mozambique (Rohner et al. 2013), and at D'Arros Island and St. Joseph Atoll as a whole (Peel et al. 2019b). Additionally, in-water observations of *M. alfredi* at the D'Arros Island cleaning station suggested that current speed may influence how individuals visit this location, with sightings frequently being reported at the onset of, and during a slack tide under minimal current speeds. It seems likely, however, that the relatively short (approximately one month) deployment period of MantaCam contributed to our result. The fortnightly variation observed in *M. alfredi* visits during this study suggests that tidal cycles may play a role in manta ray visitations to cleaning sites, however, were unable to be clearly identified here. Furthermore, the ~85% of deviance yet to be explained by our model suggests that other, un-measured variables (e.g. prey distribution and availability) may also be playing a role in how *M. alfredi* visit and use cleaning stations. Longer deployment times may be required to identify important environmental drivers for *M. alfredi* occurring at tidal and lunar scales (Couturier et al. 2018).

Despite the short duration of sampling, the deployment of MantaCam at the cleaning station to the north of D'Arros Island quadrupled the number of courtship records for *M. alfredi* at this

locality. Previously, courtship behaviour had not been recorded at the cleaning station, despite numerous dive-based manta searches at the site. This finding suggests that the significance of D'Arros Island to the courtship and reproductive behaviours of *M. alfredi* may have been underestimated by previous survey efforts. It also highlights the value of using remote monitoring systems at key aggregation sites for *M. alfredi* to examine patterns of habitat use (O'Shea et al. 2010) and to increase the number of collected identification images. Despite only being deployed for two months, sightings from MantaCam accounted for 22% of the total sighting database for Seychelles at the completion of this study. The ability of this camera system to facilitate a rapid accumulation of data over a short time frame underscores its value for establishing baseline population estimates of manta rays in remote locations.

## 2.5.2 D'Arros Island and St. Joseph Atoll

A total of 78% of individuals identified at D'Arros Island and St. Joseph Atoll were resighted on at least one occasion, and population models suggested that similar numbers of individuals used this area during the month of November in 2016 and 2017. D'Arros Island may provide critical habitat to *M. alfredi* on the shallow Amirantes Bank (< 40 m; Stoddart et al. 1979) and provide refuge for individuals across the extensive reef flats (Couturier et al. 2014, McCauley et al. 2014). Additionally, the presence of cleaning stations may facilitate important social interactions among individuals at this locality (Deakos et al. 2011, Stevens et al. 2018b). It is also possible that the unique bathymetry of the relatively deep St. Joseph Channel (60 m; Stoddart et al. 1979) between D'Arros Island and St. Joseph Atoll enhances zooplankton aggregation at this location, allowing cost-efficient foraging (Anderson et al. 2011a, Armstrong et al. 2016). Regardless of the mechanisms driving the observed residency patterns, the prolonged and frequent visits of *M. alfredi* to this location highlights its significance to this small population.

Females and males were equally represented at D'Arros Island and St. Joseph Atoll. Equal sex ratios have been reported for manta ray populations in Japan and Hawaii (Homma et al. 1999, Deakos et al. 2011), although higher proportions of males are observed in Indonesia (Germanov et al. 2019), and higher proportions of females are observed in the Maldives (1.8:1; Kitchen-Wheeler et al. 2012) and at Lady Elliot Island on the Great Barrier Reef (1.32:1; Couturier et al. 2011). The largest female bias has been reported in Mozambique, where it is hypothesised that mature females use the surrounding habitat for pupping and mating (3.55:1; Marshall et al. 2011). A lack of female bias in the D'Arros Island population might therefore suggest that birthing and breeding grounds for *M. alfredi* exist elsewhere in Seychelles (Deakos et al. 2011), however, the sighting of pregnant females in MantaCam images implies that this is not necessarily the case.

Adult and sub-adult *M. alfredi* comprised the majority of the population at D'Arros Island and St. Joseph Atoll. Juveniles were observed infrequently throughout the wider region of Seychelles, with the smallest individual (DW ~ 1.0 m) being sighted within the lagoon of the St. François Atoll. Although this is a single sighting, lagoon habitats are thought to provide refuges and food sources for *M. alfredi* (Papastamatiou et al. 2012, McCauley et al. 2014), so this region may function as a pupping area for the species in this Island Group. Additionally, the observation of large numbers of individual *M. alfredi* feeding within the main channel of the St François Atoll lagoon suggests that this locality may provide significant foraging opportunities to individuals in the Alphonse Group. Further sampling at St. François Atoll will be required to confirm or refute the hypothesis that this location serves as a nursery area for *M. alfredi*, and to quantify the importance of the lagoon system to the foraging ecology of the species.

### 2.5.3 Amirante, Alphonse and other Island Groups

The population of *M. alfredi* currently identified in Seychelles is relatively small at 236 individuals, with the majority of individuals sighted within the Amirante and Alphonse Island Groups (n = 216, 91.5%). Similar population sizes for *M. alfredi* have been observed in the waters of Hawaii and the Yaeyama Islands of Japan (290 and 300 individuals, respectively; Homma et al. 1999, Deakos et al. 2011). In contrast, a population of 3,570 individuals has been identified in the Maldives, located 2,200 km to the north-east of Seychelles (Stevens 2016). To a large extent, this difference in population sizes likely reflects the spread of human populations (observers) within Seychelles and the Maldives. In the former, many Island Groups are remote and difficult to access (e.g. Aldabra), whereas in the latter, numerous atolls have human settlements. Additionally, the economy of the Maldives is based in large part on marine ecotourism (Zimmerhackel et al. 2018, Zimmerhackel et al. 2019), and this creates an incentive to locate aggregations of manta rays as attractions for divers (Anderson et al. 2011b, O'Malley et al. 2013, Ward-Paige et al. 2013). The lack of access to other remote Island Groups in Seychelles, where mantas are known to occur, means that our study has recorded only a fraction of the population of *M. alfredi* likely to exist in the region. It is also possible that we underestimated the size of the aggregations in the Amirante and Alphonse Groups, where our sampling effort was focussed, since discovery curves did not reach an asymptote (Couturier et al. 2011, Deakos et al. 2011). However, our finding of the comparative rarity of sightings of *M. birostris* is consistent across many localities, including the Maldives, Indonesia and Hawaii (Clark 2010, Kashiwagi et al. 2011, Stevens et al. 2018b). This is likely due to the occurrence of *M. birostris* in deeper, offshore environments, in contrast to the shallow coastal reef sites where *M. alfredi* aggregations tend to occur (Couturier et al. 2012, Stewart et al. 2016a). For the most part, sightings of *M. birostris* are



probably serendipitous events, where observers crossed paths with animals transiting coastal or shelf environments.

Individual *M. alfredi* appeared to move infrequently between the Amirante and Alphonse Island Groups. Although our study was limited by the small size of the photo-identification database from Alphonse, this conclusion was supported by the results of passive acoustic (Peel et al. 2019b) and satellite telemetry (Chapter 5) studies, which also indicate that this species displays restricted patterns of movement. Deep water (> 1,000 m) occurs between these Island Groups and is thought to act as a barrier to the movements of *M. alfredi* (Deakos et al. 2011), despite individuals displaying the ability to undertake large scale movements in locations including Japan, Indonesia and eastern Australia (> 300 km; Homma et al. 1999, Germanov & Marshall 2014, Jaine et al. 2014, Armstrong et al. 2019). It has been hypothesised that deep water may increase the threat of predation (Marshall & Bennett 2010a, Deakos et al. 2011) and reduce the likelihood of encountering prey in offshore locations (Gove et al. 2016). It is equally possible, however, that foraging and social opportunities afforded to *M. alfredi* within these Island Groups in Seychelles reduce the need for animals to transit the distances between aggregation sites (Couturier et al. 2018).

### 2.5.3.1 Manta ray conservation in Seychelles

The lack of anthropogenic injuries observed on individual *M. alfredi* in our study contrasts with aggregations in other locations, such as Mozambique, Sri Lanka and Indonesia, where the population of humans is larger and denser than Seychelles. In comparison to *M. alfredi* in the Amirante and Alphonse Island Groups, the incidence of reported physical injuries, targeted fisheries catch, and frequency of by-catch and accidental entanglement at these other localities is far greater (Heinrichs et al. 2011, Couturier et al. 2012, Croll et al. 2016). This suggests that *M. alfredi* aggregating at D'Arros Island and St. Joseph Atoll, and also at St. François Atoll, are removed from the acute anthropogenic pressures typically encountered by mobulid populations that aggregate in coastal, highly populated areas (Lawson et al. 2017). The relatively pristine nature of the *M. alfredi* population identified in Seychelles therefore provides a unique opportunity to gather important baseline information about the biology and ecology of these animals in the absence of such anthropogenic disturbances. The increasing impact of small fisheries in the Western Indian Ocean, however, raises concerns over the longevity of *M. alfredi* aggregations at D'Arros Island, St. Joseph Atoll, and St. François Atoll, and their currently reduced level of exposure to the threat of exploitation (Stewart et al. 2010, Temple et al. 2019). Should demand for mobulid products increase in the region, it is possible that these predictable aggregations could be easily and rapidly impacted by targeted fisheries (Temple et al. 2019). This concern, alongside the findings presented here for this small, resident population, highlights the

importance of establishing Marine Protected Areas for *M. alfredi* at D'Arros Island, St. Joseph Atoll and St. François Atoll, which appear to represent key aggregation areas for these animals in Seychelles. Such pre-emptive conservation measures would serve not only to protect individuals of a globally vulnerable species from future threat, but prolong our ability to study this small population of *M. alfredi*, and use the collected data to inform the establishment of management strategies for aggregations occurring elsewhere in the Western Indian Ocean and beyond.

## 2.6 Supplementary material

**Table S 2.1** Top ten POPAN models of abundance for reef manta ray (*Mobula alfredi*) sighting data collected at D'Arros Island, Seychelles, in November/December 2013. Models allowed for apparent survival ( $\phi$ ), capture probability ( $p$ ), and probability of entry ( $P_{ent}$ ) parameters to remain constant ( $\cdot$ ), or to vary by time ( $t$ ), by sex ( $s$ ), or by time and sex ( $t+s$ ). Capture probability was also allowed to vary with sampling effort ( $e$ ). Partial closure to gains was set by  $P_{ent}(\cdot=0)$ . Model selection performed using Akaike's Information Criterion corrected for small sample sizes (AICc).  $\Delta$ AICc, difference in AICc value between each model and the model with the lowest AICc. Weight, calculated strength of model relative to all other candidate models. Models in bold represent selected top models that were subsequently averaged to estimate abundance.

Model	AICc	$\Delta$ AICc	Weight	No. parameters
$\phi(s) p(\cdot) P_{ent}(s)$	<b>469.01</b>	<b>0.00</b>	<b>0.10</b>	<b>6</b>
$\phi(s) p(\cdot) P_{ent}(\cdot)$	<b>469.14</b>	<b>0.14</b>	<b>0.10</b>	<b>5</b>
$\phi(\cdot) p(\cdot) P_{ent}(\cdot)$	<b>469.53</b>	<b>0.53</b>	<b>0.08</b>	<b>4</b>
$\phi(\cdot) p(\cdot) P_{ent}(s)$	<b>469.54</b>	<b>0.54</b>	<b>0.08</b>	<b>5</b>
$\phi(s) p(\cdot) P_{ent}(t+s)$	<b>470.26</b>	<b>1.25</b>	<b>0.06</b>	<b>5</b>
$\phi(s) p(s) P_{ent}(\cdot)$	<b>470.27</b>	<b>1.26</b>	<b>0.06</b>	<b>6</b>
$\phi(s) p(s) P_{ent}(s)$	471.05	2.05	0.04	7
$\phi(s) p(e) P_{ent}(s)$	471.31	2.30	0.03	7
$\phi(s) p(e) P_{ent}(\cdot)$	471.38	2.38	0.03	6
$\phi(s) p(s) P_{ent}(\cdot=0)$	471.56	2.55	0.03	3

**Table S 2.2** Top ten POPAN models of abundance for reef manta ray (*Mobula alfredi*) sighting data collected at D'Arros Island, Seychelles, in November 2016. Models allowed for apparent survival ( $\phi$ ), capture probability ( $p$ ), and probability of entry ( $P_{ent}$ ) parameters to remain constant ( $\cdot$ ), or to vary by time ( $t$ ), by sex ( $s$ ), or by time and sex ( $t+s$ ). Capture probability was also allowed to vary with sampling effort ( $e$ ), and sampling effort and sex ( $e+s$ ). Partial closure to gains was set by  $P_{ent}(\cdot=0)$ . Model selection performed using Akaike's Information Criterion corrected for small sample sizes (AICc).  $\Delta$ AICc, difference in AICc value between each model and the model with the lowest AICc. Weight, calculated strength of model relative to all other candidate models. Model in bold represents selected top model used to estimate abundance.

Model	AICc	$\Delta$ AICc	Weight	No. parameters
$\phi(t+s) p(s) P_{ent}(t)$	<b>710.61</b>	<b>0.00</b>	<b>0.39</b>	<b>13</b>
$\phi(t+s) p(e+s) P_{ent}(t)$	712.92	2.31	0.12	14
$\phi(t) p(s) P_{ent}(t)$	713.51	2.90	0.09	13
$\phi(t+s) p(e+s) P_{ent}(t+s)$	715.12	4.51	0.04	15
$\phi(t) p(t+s) P_{ent}(\cdot=0)$	715.74	5.14	0.03	26
$\phi(t) p(e+s) P_{ent}(t)$	715.79	5.19	0.03	14
$\phi(t) p(s) P_{ent}(t+s)$	715.88	5.27	0.03	14
$\phi(t) p(t+s) P_{ent}(\cdot)$	716.17	5.56	0.02	29
$\phi(t) p(t+s) P_{ent}(t)$	716.23	5.62	0.02	32
$\phi(t) p(e) P_{ent}(t)$	716.60	5.99	0.02	12

**Table S 2.3** Top ten POPAN models of abundance for reef manta ray (*Mobula alfredi*) sighting data collected at D'Arros Island, Seychelles, in November 2017. Models allowed for apparent survival ( $\phi$ ), capture probability ( $p$ ), and probability of entry ( $P_{ent}$ ) parameters to remain constant ( $\cdot$ ), or to vary by time ( $t$ ), by sex ( $s$ ), or by time and sex ( $t+s$ ). Model selection performed using Akaike's Information Criterion corrected for small sample sizes (AICc).  $\Delta$ AICc, difference in AICc value between each model and the model with the lowest AICc. Weight, calculated strength of model relative to all other candidate models. Models in bold represent selected top models that were subsequently averaged to estimate abundance.

Model	AICc	$\Delta$ AICc	Weight	No. parameters
<b><math>\phi(\cdot) p(t+s) P_{ent}(\cdot)</math></b>	<b>1410.86</b>	<b>0.00</b>	<b>0.51</b>	<b>32</b>
<b><math>\phi(s) p(t+s) P_{ent}(\cdot)</math></b>	<b>1412.31</b>	<b>1.45</b>	<b>0.25</b>	<b>33</b>
$\phi(\cdot) p(t+s) P_{ent}(s)$	1413.25	2.40	0.15	33
$\phi(s) p(t+s) P_{ent}(s)$	1414.70	3.84	0.07	34
$\phi(\cdot) p(t+s) P_{ent}(t)$	1419.19	8.33	0.01	41
$\phi(s) p(t+s) P_{ent}(t)$	1421.11	10.25	<0.01	42
$\phi(\cdot) p(t+s) P_{ent}(t+s)$	1421.69	10.83	<0.01	42
$\phi(\cdot) p(t) P_{ent}(\cdot)$	1422.12	11.26	<0.01	31
$\phi(s) p(t+s) P_{ent}(t+s)$	1423.66	12.80	<0.001	43
$\phi(\cdot) p(t) P_{ent}(s)$	1424.37	13.51	<0.001	32

**Table S 2.4** Distribution of injury types throughout the reef manta ray (*Mobula alfredi*) population identified in Seychelles, excluding sightings from D'Arros Island and St. Joseph Atoll.

Damaged Region	No. Individuals (% of Sighted)	Suspected Cause of Injury (No. Individuals Affected, % of Injured)			
		Anthropogenic	Natural	Anthropogenic & Natural	Unknown Cause
Pectoral Fin/s	32 (32.7)	1 (2.7)	28 (75.7)	0 (0.0)	3 (8.1)
Cephalic Fin/s	2 (2.0)	2 (5.4)	0 (0.0)	0 (0.0)	0 (0.0)
Tail and/or Dorsal Fin	3 (3.1)	0 (0.0)	3 (8.1)	0 (0.0)	0 (0.0)
Gill/s	2 (2.0)	0 (0.0)	2 (5.4)	0 (0.0)	0 (0.0)

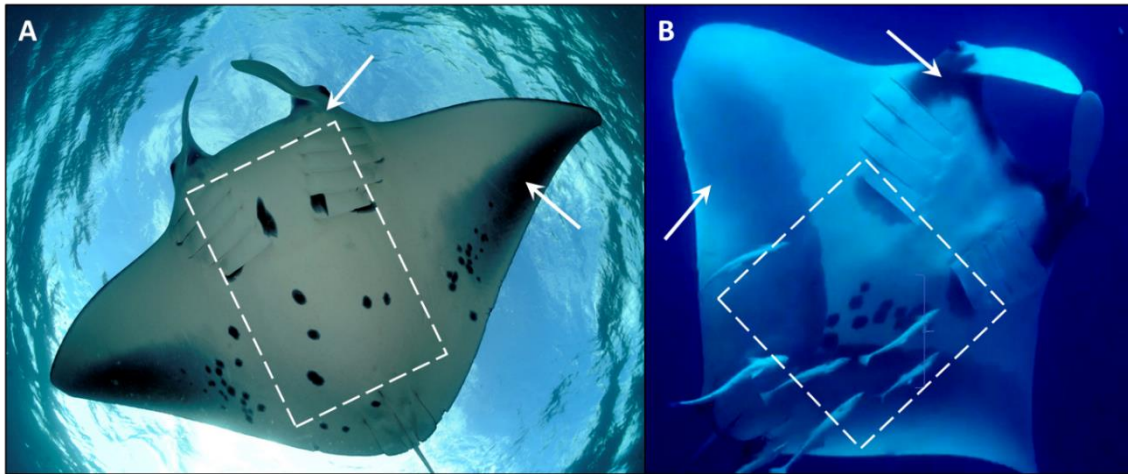


**Figure S 2.1** Identification images for reef (*Mobula alfredi*; A) and oceanic (*Mobula birostris*; B) manta rays in Seychelles. Dashed boxes outline region of highest spot density and pigmentation for each species, arrows indicate differences in facial and pectoral fin margin colouration. Photographs © The Manta Trust (A: G. Stevens; B: Unknown).

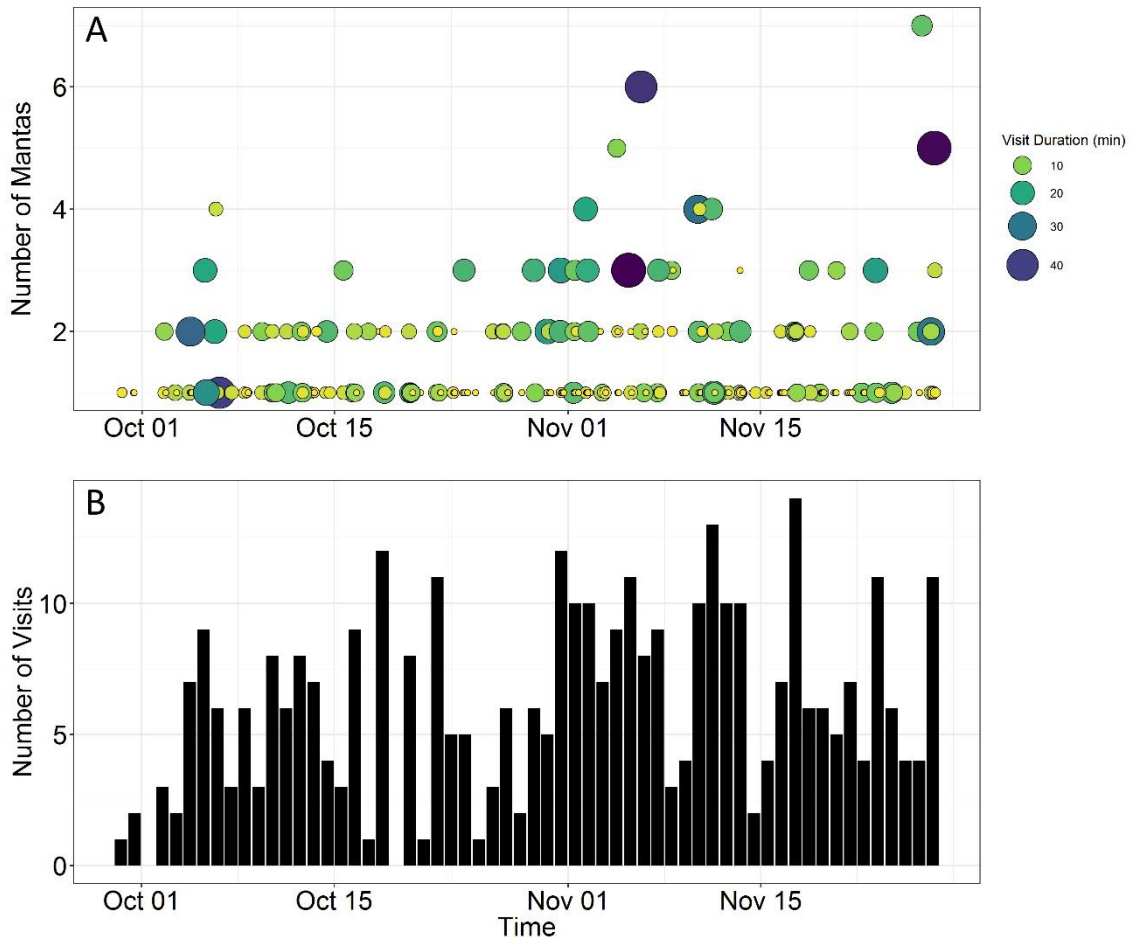


**Figure S 2.2** Frequency of visits by reef manta rays (*Mobula alfredi*) to the cleaning station at D'Arros Island, Seychelles, recorded by a remote camera system ('MantaCam'). Both the number of individuals present per visit and their visit duration (A), and number of visits recorded per survey day (B) are presented. Symbology for visit duration defined in legend.

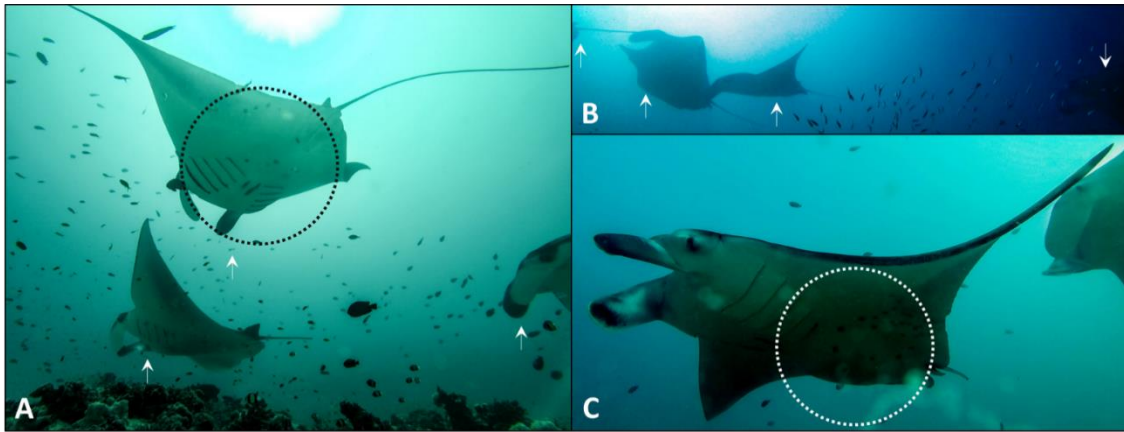


**Figure S 2.3** Images of reef manta ray (*Mobula alfredi*) courtship behaviour captured by a remote camera system, MantaCam, positioned at a cleaning station at D'Arros Island, Seychelles. White arrows identify individuals involved in courtship behaviour in groups of three (A) and four (B). The black circle displays a usable identification image, and the white circle highlights the pregnancy bulge of a pregnant female (C).

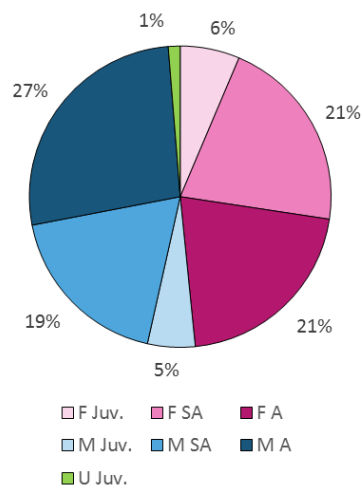


**Figure S 2.4** Population composition of reef manta rays (*Mobula alfredi*) identified at D'Arros Island and St. Joseph Atoll, Seychelles, considering individual sex (F, female. M, male. U, unknown) and maturity status (Juv., juvenile; SA, sub-adult; A, adult). Colour allocations defined in figure legend.

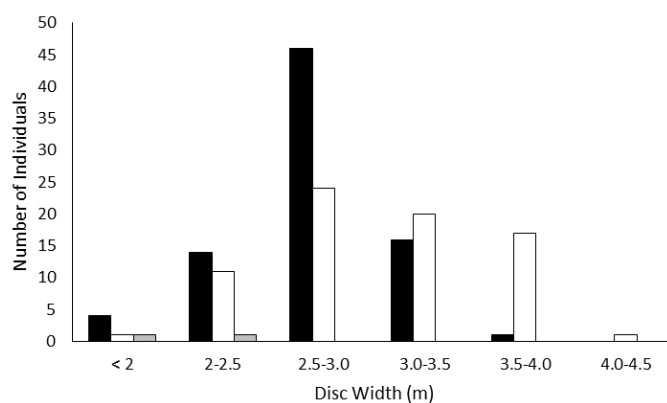


**Figure S 2.5** Size distribution of reef manta rays (*Mobula alfredi*) that could be identified as males (black) and females (white), or of unknown sex (grey) at D'Arros Island and St. Joseph Atoll, Seychelles.

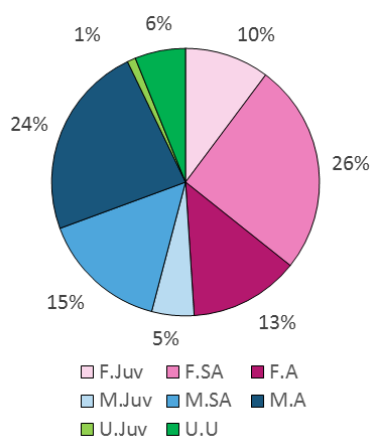


**Figure S 2.6** Population composition of reef manta rays (*Mobula alfredi*) identified among the Island Groups of Seychelles considering individual sex (F, female. M, male. U, unknown) and maturity status (Juv., juvenile; SA, sub-adult; A, adult). Colour allocations defined in figure legend. Sightings from D'Arros Island and St. Joseph Atoll have been excluded.

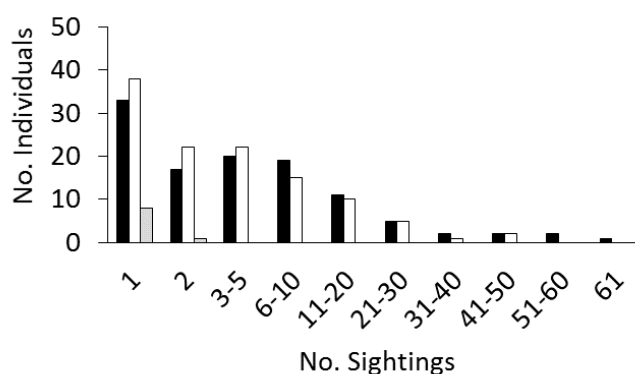


**Figure S 2.7** Sighting frequencies for 236 individual reef manta rays (*Mobula alfredi*) identified in Seychelles using photo-identification techniques. Males (black bars), females (white bars) and unknown sex (grey bars) are shown.





# Chapter 3 The island life: movement and residency patterns of reef manta rays (*Mobula alfredi*) in the Amirante Island Group, Seychelles

## 3.1 Abstract

Reef manta rays (*Mobula alfredi*) are large filter-feeding elasmobranchs that are undergoing substantial population declines on a global scale. In order to effectively conserve and manage populations, it is crucial that the drivers of their occurrence are defined and that key aggregation areas for this species are identified and protected. Here, we used passive acoustic telemetry to monitor and assess the movement ecology of *M. alfredi* in the remote Amirante Island Group, Republic of Seychelles. Acoustic transmitters were externally deployed on *M. alfredi* at D'Arros Island (n = 42), and movement data retrieved from an array of 70 acoustic receivers deployed throughout the Amirantes between November 2013 and October 2017. Individuals were detected year-round, with a peak in detections occurring between November and April coinciding with the arrival and departure of the north-west monsoon. Individuals were most likely to be detected within the array during the day, at low wind speeds, and when water temperatures were approximately 28°C. Additionally, individuals were more likely to be detected during a new moon, when the tidal range was at its highest, and on the slack of high tide. *M. alfredi* travelled widely within the Amirantes, with larger individuals travelling greater distances per day than smaller individuals and juveniles. The majority of detections (89%) were recorded within 2.5 km of the shoreline of D'Arros Island and the neighbouring St. Joseph Atoll, highlighting the importance of these sites to *M. alfredi* in the Amirantes, and supporting the proposed development of a Marine Protected Area at this location.

## 3.2 Introduction

Reef manta rays (*Mobula alfredi*; Marshall et al. 2009, White et al. 2017), are large planktivorous elasmobranchs of the family Mobulidae (the devil rays; Notarbartolo di Sciara 1987, Couturier et al. 2012, White et al. 2017). Conservative life history strategies are characteristic of this group, with the majority of species exhibiting slow growth rates, late entry to maturity and low fecundity (Couturier et al. 2012, Lawson et al. 2017, Stewart et al. 2018a). These reproductive traits greatly

increase the susceptibility of mobulid populations to local and broad scale extinctions resulting from unsustainable fishing pressures, and minimise the rate at which populations can recover from loss (Holden 1974, Musick et al. 2000, Dulvy et al. 2014).

Targeted fishing practises aiming to supply mobulid gill plates to the market for traditional Asian medicine have resulted in the decline of *M. alfredi* populations on a global scale in recent decades (Ward-Paige et al. 2013, Whitcraft et al. 2014, Lawson et al. 2017, O'Malley et al. 2017). This is particularly notable in the Indian Ocean where three of the five most intensive fisheries for mobulids in the world are located (Sri Lanka, India, and Indonesia; Heinrichs et al. 2011). The by-catch of mobulids in the gear of other fisheries contributes additional pressures to these populations, with individuals becoming entangled in gill and purse-seine nets (Rohner et al. 2017b, Temple et al. 2019). Given that mobulid fisheries have now been identified in Mozambique (Heinrichs et al. 2011, Dent & Clarke 2015), and mobulid landings by small-scale fisheries are reported in Pakistan (Moazzam 2018) and throughout eastern Africa (Kenya, Mauritius and Tanzania; Temple et al. 2018), there is an urgent need to identify and protect key aggregation areas for *M. alfredi* in the Western Indian Ocean to ensure the conservation of their populations.

Marine Protected Areas (MPAs) provide a relatively simple, regional-scale conservation and management strategy for populations of *M. alfredi* (Graham et al. 2012, Stewart et al. 2016a, Couturier et al. 2018) that complement international efforts to restrict their global trade (Listing on CITES Appendix II; Marshall et al. 2018b). In addition to preventing targeted fishing efforts towards this 'Vulnerable' species (IUCN Red List of Threatened Species; Marshall et al. 2018b), MPAs also serve to reduce the risk of by-catch, accidental entanglement and boat strikes to individuals (Heinrichs et al. 2011, Moazzam 2018, Stewart et al. 2018a). By specifically targeting key aggregation sites for *M. alfredi*, MPAs are able to direct resources and effort to places where populations will most greatly benefit from protection (Kessel et al. 2017, Lawson et al. 2017). However, the successful design and implementation of MPAs relies on an understanding of the movement and residency patterns of target species, and it is for this reason that an increasing number of studies focusing on the ecology of manta rays have incorporated an element of animal tracking using telemetry (Dewar et al. 2008, Deakos et al. 2011, Braun et al. 2014, Jaine et al. 2014, Stewart et al. 2016a, Kessel et al. 2017, Stewart et al. 2018a).

Passive acoustic telemetry is a popular tool for the assessment of movement and connectivity patterns of populations of *M. alfredi* because it is cost effective, allows collection of records of individual movements for up to a decade and can be implemented in remote locations (Hussey et al. 2015, Stewart et al. 2018a). Such studies of *M. alfredi* in Hawaii (Clark 2010), Palmyra Atoll (McCauley et al. 2014), the Red Sea (Braun et al. 2015), eastern Australia (Couturier et al. 2018), and Indonesia (Setyawan et al. 2018) have emphasised the typically coastal and limited nature of

the movement patterns of this species, which displays high levels of residency and site fidelity. With the exception of the aggregations in the waters of Mozambique, such movement data are currently limited for *M. alfredi* in the Western Indian Ocean, where numerous populations exist, but are afforded little to no national-scale protections from commercial or artisanal fisheries (Marshall et al. 2011, Temple et al. 2018).

Here, we used passive acoustic telemetry to investigate the presence and movement patterns of *M. alfredi* in the Amirante Island Group of the Republic of Seychelles. Little is currently known about the movement ecology of *M. alfredi* within this region of the Western Indian Ocean, as the islands and atolls around which they aggregate are often remote and difficult to access. The lack of an established manta fishery in Seychelles – despite records of historic fishing practises and occasional landings of by-catch (Keynes 1959, Temple et al. 2018) – is also significant, as it provides an opportunity for our study to assess the movement and residency patterns of *M. alfredi* at a locality where there is likely little to no targeted fishing at present, but where increasing market demand may occur in the future (Temple et al. 2018). Telemetry data were used to examine patterns of residency and site fidelity of *M. alfredi* throughout the Amirante Islands, and to investigate how the observed patterns varied with the sex and maturity status of tagged individuals. Trends in patterns of occurrence with respect to environmental, temporal, and biological variables were also examined. Finally, detection data were used to assess the potential benefits of a proposed MPA at D’Arros Island and St. Joseph Atoll to *M. alfredi* within the Amirante Island Group, and the significance of this location to a globally vulnerable species currently afforded no national-scale protection in Seychelles (Temple et al. 2018).

## 3.3 Methods

### 3.3.1 Study site

The Republic of Seychelles is an archipelago of 115 islands located in the tropical Western Indian Ocean (Figure 3.1A). Two seasons (monsoons) shape the climate of the nation, with the lighter and less-persistent winds of the wet north-west monsoon blowing from October to March, and the stronger, steadier south-easterly winds of the dry south-east monsoon, prevailing from April through September (Schott & McCreary Jr 2001, Komdeur & Daan 2005). Despite encompassing an Exclusive Economic Zone of 1.4 million km<sup>2</sup>, the total land mass of Seychelles covers just 459 km<sup>2</sup>. Given the sparse distribution of islands throughout the region, each is therefore considered to fall within one of six discrete Island Groups based on its geography (Figure 3.1B; Stoddart et al. 1979).

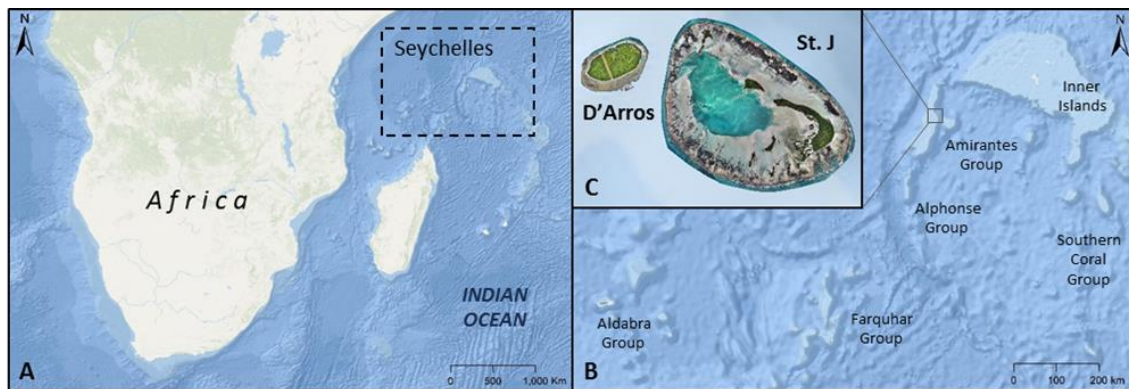


**Figure 3.1** Located in the Western Indian Ocean (A), Republic of Seychelles (B) is an archipelago of 115 islands. The Amirante Island Group, located upon the Amirantes Bank, is one of six Island Groups identified within the country. Reef manta rays (*Mobula alfredi*) are known to aggregate in the Amirante Group at D'Arros Island and St. Joseph Atoll (St. J; C; Georeferenced drone imagery © Save Our Seas Foundation); the focal site for this acoustic telemetry study. Maps created in ArcGIS 10.3 (<http://www.esri.com/>) using GEBCO\_08 (version 20100927) bathymetry data.

The focal area for our study was the Amirante Island Group; a cluster of 24 small islands and islets located on the Amirantes Bank approximately 250 km south-west of the capital, Victoria, and extending over a distance of approximately 152 km (Hamylton et al. 2012). On the Bank, water depths reach a maximum of 70 m in the centre before rising to a shallower outer rim of 11 to 27 m, and then steeply dropping to depths greater than 1,000 m (Hamylton et al. 2012).

D'Arros Island (S 5°24.9', E 53°17.9') is a small (1.71 km<sup>2</sup>) coralline island located midway along the Amirantes Bank within the Amirante Island Group, neighbored closely to the east by the St. Joseph Atoll (Figure 3.1C). These two land masses are surrounded by insular platform reefs and sea grass beds, and are separated by a one kilometre wide channel that reaches a depth of 60 m in the centre (Stoddart et al. 1979). Aggregations of *M. alfredi* have been observed nearly year-round at this location, and for this reason, it was chosen as the focal site for this study within the Amirantes.

### 3.3.2 Tag deployment

Forty-two acoustic tags (Vemco; Nova Scotia, Canada) were externally deployed on *M. alfredi* at D'Arros Island across two tagging periods; November 2013 – March 2014 (Period One; n = 20) and November 2016 (Period Two; n = 22). All tags deployed in Period One were V16-5H tags, and during Period Two, thirteen V16-5H and nine V16TP-5H (temperature and depth sensor tags) were deployed. Tag anchors were made of either titanium (n = 15) or stainless steel (n = 27), and all were of a similar design to the Wildlife Computers large titanium anchor (Wildlife Computers, Redmond, WA, USA). Tags were deployed *in situ* using a modified Hawaiian sling, and positioned towards the posterior dorsal surface of each manta ray such that the tag was not trailing

over the back edge of the pectoral fin and the anchor would not pose a risk to the body cavity of the individual. All tagged animals were photographed and identified prior to being tagged, and their size and sex recorded with the tag identification number (ID). Individuals were identified from the unique pattern of pigmentation on their ventral surface, which does not vary throughout their lifetime (Marshall et al. 2009, Marshall et al. 2011, Couturier et al. 2014, Germanov & Marshall 2014). The sex of each tagged individual was assigned based on the observed presence (males) or absence (females) of claspers (Marshall et al. 2009). Wingspan was visually estimated to the nearest 0.1 m and used as a proxy to estimate maturity status. Individuals were classified into one of the following three 'life stage' groups based on their estimated size: juvenile (any individual,  $\leq 2.4$  m), sub-adult (male, 2.5 – 2.8 m; female, 2.5 – 3.1 m), or adult (male,  $\geq 2.9$  m; female,  $\geq 3.2$  m; Stevens 2016). The presence of mating scars (females only) and degree of calcification of the claspers (males only) were also considered during assignment of maturity status.

### 3.3.3 Acoustic receiver array

An array of 70 acoustic receivers (model VR2W; Vemco; Nova Scotia, Canada) were deployed around the islands of the Amirante Group between 2012 and 2016. A large proportion of the receivers ( $n = 32$ , 46%) were positioned within 2.5 km of the shorelines of D'Arros Island and St. Joseph Atoll, with the remaining receivers located around other islands of the Group, or at key locations across the Bank (Figure 3.2). Detections of tagged *M. alfredi* were recorded and monitored between November 2013 and October 2017. Deployed tags were detected within approximately 150 m of the receivers as determined by preliminary range testing ( $\bar{x} = 165 \pm 33$  m; Lea et al. 2016). Data from receivers in close proximity to D'Arros Island were downloaded every six months, with offshore receivers being downloaded annually each November to coincide with calm weather conditions. Once a year, the battery of each receiver was replaced and the receiver inspected for damage or clock drift. Upon import of the detection data into a Microsoft Access database (Microsoft Corporation, Redmond, USA), false positive detections were removed through filtration for active tag ID's, and any receiver clock-drift time corrections calculated assuming linear drift (Lea et al. 2016). Four tags were removed from the dataset prior to analysis because they were lost from individuals within one week. Tag loss was confirmed through re-sightings of these individuals. Detection data for the remaining tags were visually examined to ensure that tags had not been shed within range of any receivers. Where continuous detections were recorded for a tag at a single receiver over a long period of time ( $> 24$  h), the tag was deemed to have fallen from the animal, and detection data from that receiver subsequently removed from the dataset prior to analysis. For all analyses, values of the standard deviation were presented with means unless otherwise stated.

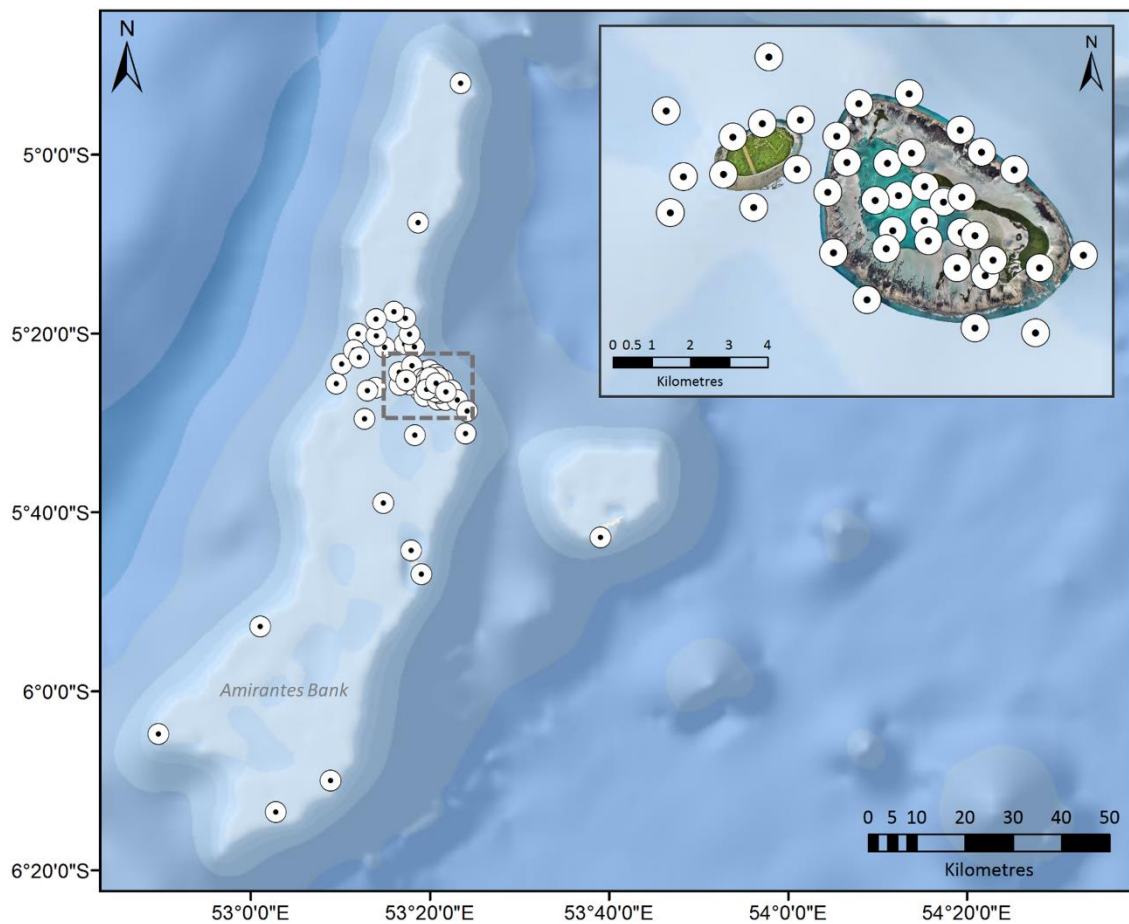


**Figure 3.2** Distribution of acoustic receivers ( $n = 70$ ) throughout the Amirante Island Group, with inset indicating increased receiver density around D'Arros Island and St. Joseph Atoll. Receiver locations marked with  $\odot$ . Maps created in ArcGIS (<http://www.esri.com/>) using GEBCO\_08 (version 20100927) bathymetry data. Georeferenced drone imagery © Save Our Seas Foundation.

### 3.3.4 Spatio-temporal analyses

The distribution and connectivity of detections throughout the receiver array were visualised and analysed using the packages *igraph* (Csardi & Nepusz 2006) and *ggplot2* (Wickham 2016) in R (version 3.4.1; R Core Team 2017), before being presented in ArcMap 10.3<sup>®</sup> (ESRI Inc., Redlands, California). Briefly, each acoustic receiver was considered to be a node within a network, and the size of each node was drawn to represent the number of detections recorded at that receiver. The line thickness of the edges connecting the nodes were then drawn relative to the frequency at which *M. alfredi* travelled between each pair of receivers (Jacoby et al. 2012). The sequential detection of tagged *M. alfredi* throughout the receiver array from the first detection to the last is hereafter referred to as the 'track' for each individual.

The mean distance travelled per day by each individual was calculated by averaging the cumulative distance between detections across receivers within a 24-hour period. This metric represented the minimum distance travelled per day for each *M. alfredi*, as the extent of movement

of any individual that travelled beyond the detection boundary of the receiver array could not be quantified. A one-way ANOVA was used to determine whether female and male *M. alfredi* travelled the same mean distance per day, and linear regression was used to examine the potential relationship between wingspan (i.e. maturity status) and distance travelled per day. Data homogeneity and normality were confirmed through Levene's tests and Shapiro-Wilk tests, respectively.

Broad scale residency was measured using a residency index (RI; Daly et al., 2014) defined as:

$$RI = \left( \frac{\text{Number of days detected within the Amirantes array}}{\text{Number of days between first and last detection}} \right) * 100$$

On five occasions, an individual that had shed a tag deployed in Period One was re-tagged in Period Two. For these mantas, RI values were averaged across both deployment periods. Residency indices were used to infer the amount of time that tagged *M. alfredi* spent inshore of the islands of the Amirante Group, and at D'Arros Island and St. Joseph Atoll. One- and two-way ANOVAs were used to determine whether residency indices differed significantly with the sex and wingspan (i.e. life stages) of tagged individuals. Assumptions of normality and homogeneity were found to be met in all cases through Shapiro-Wilk and Levene's tests, respectively.

Differences in patterns of local residency to the Amirantes between the sexes and life stages of *M. alfredi* were further investigated by considering at which receivers, and how frequently, individuals were detected within the array. The number of track days that individuals were detected at each receiver was calculated to examine the extent of array use (A), and the proportion of total detections recorded at each receiver per individual was used as a measure of residency to each site (B; Papastamatiou et al. 2010). Prior to analysis, counts of detection days were  $\log(x+1)$  transformed to allow for better comparisons among individuals with differing track lengths, whereas proportion data were transformed to arcsine-square root values (Meyer et al. 2010a, Papastamatiou et al. 2010). Bray-Curtis similarity matrices were then constructed (PRIMER-E, Version 6; Plymouth, UK) and non-metric multidimensional scaling plots used to visualise potential differences in A and B among tagged individuals. Analysis of Similarity (ANOSIM) measures were used to assess whether array use or residency varied significantly between male and female *M. alfredi* of various life stages, and if these patterns were the same between the two deployment periods of this study. All ANOSIMs were programmed to process up to 9,999 permutations of the data, and significant differences between groups was taken at  $p < 0.05$ .

### 3.3.5 Environmental modelling

Generalised additive mixed models (GAMMs) were used to investigate how temporal, biological and environmental factors may influence the occurrence of *M. alfredi* at D'Arros Island and St. Joseph Atoll. Models considered the presence of *M. alfredi* at receivers within 2.5 km of these locations between November 2016 and September 2017, and this time frame was selected because it provided the greatest availability of environmental data within the overall study period. Nine continuous variables were examined during the modelling process: day of the year, time of day, fraction of moon illuminated, time relative to high tide, tidal range, water temperature, prevailing wind direction, wind speed, and wingspan (Table 3.1). Sex of individual was also included as a categorical factor. All predictors were selected for inclusion because they have been shown to influence the occurrence (Couturier et al. 2018, Setyawan et al. 2018) and behaviour (O'Shea et al. 2010, Jaine et al. 2012) of *M. alfredi* at other locations. Behavioural differences among individuals that may influence the frequency of occurrence at D'Arros Island were accounted for by including manta ray identification number (ID) as a random effect in all models. Inclusion of this random factor also controlled for pseudo-replication arising from the repeated measure of the same individuals throughout the study period (Couturier et al. 2018).

Day of the year (Julian Day) and hourly values were extracted from detection data, whereas daily lunar illumination data for Seychelles were obtained from the United States Naval Observatory website (<http://aa.usno.navy.mil/data/docs/MoonFraction.php>). Both tidal metrics – tidal range and time relative to high tide – were assigned to hourly detection periods based on measures of tidal height as calculated by a tidal model built using the Oregon State University Tidal Model Driver (Egbert & Erofeeva 2002, Lea 2017). Modelled tidal cycles were based on the harmonics for St. Joseph Atoll's location, with the final model predicting tidal heights in metres every 10 minutes, which were averaged over each hour of the study period. Wind speed and direction data were collected every 30 minutes by a weather station (Davis 6152 Wireless Vantage Pro2; Davis Instruments Australia, Australia) deployed at D'Arros Island. Water temperature data were collected every 10 minutes by a temperature logger (Onset HOBO Water Temperature Pro-v2; Bourne, MA) deployed to the north of D'Arros Island at approximately 15 m depth. These records were subsequently averaged over each hour of the study period and aligned with the acoustic detection data.

GAMMs were constructed with a binomial error structure and log link function using maximum likelihood estimations in the package *mgcv* (Wood 2017). The presence of individual manta rays within the array was quantified as either '1' (present) or '0' (absent) for each hour of the study period, based on whether or not a detection had been recorded for that individual during that time. Harmonic polynomials were fitted to the cyclical factors 'time of day', 'day of year' and 'wind direction' to ensure continuity between records (Jaine et al. 2012), whereas the square root values



of wind speed were used to normalise the skewed distribution of data available for that predictor. The function ‘cor’ in R was used to ensure that there was no strong cross-correlation between continuous predictors (Table S 3.1).

Significant predictors of *M. alfredi* occurrence at D’Arros Island and St. Joseph Atoll were identified from the complete suite of variables through a full-subset model selection approach using the package *MuMIn* (Barton & Barton 2018). All potential combinations of predictor variables were considered, and each fitted within a separate GAMM. Akaike’s Information Criterion corrected for sample size (AICc) and AICc weights (wAICc) were then used to select the highest ranking model, with wAICc able to vary between 0 (no support) and 1 (complete support; Ferreira et al. 2017). Models within 2 AICc units of each other were considered to be equally ranked. When the difference in AICc values ( $\Delta$ AICc) between top candidate models was  $< 2$ , the model containing the lowest number of explanatory variables (i.e. the most parsimonious) was selected as the appropriate model for the data.

**Table 3.1** Description of variables used in GAMM analysis of reef manta ray (*Mobula alfredi*) occurrence at D’Arros Island and St. Joseph Atoll, Seychelles.

<b>Variable</b>	<b>Type of effect</b>	<b>Units/Levels</b>	<b>Description</b>
Sex	Fixed - categorical	Female, male	Sex of tagged individuals
Wingspan	Fixed – continuous, fitted with natural spline (k = 5)	0.1 m	Wingspan of tagged individuals
Day of year	Fixed – continuous, fitted with harmonic polynomial (k = 5)	1-365	Julian day
Hour of day	Fixed – continuous, fitted with harmonic polynomial (k = 5)	0 – 23	Hour of day
Moon Illumination	Fixed – continuous, fitted with natural spline (k = 5)	0.00 – 1.00	Fraction of moon illuminated by the sun
Time to high Tide	Fixed – continuous, fitted with natural spline (k = 5)	1 h	Time relative to most recent or next high tide
Tidal range	Fixed – continuous, fitted with natural spline (k = 5)	0.01 m	Tidal range measured between subsequent high and low tides
Wind speed	Fixed – continuous, fitted with natural spline (k = 5)	0.1 km h <sup>-1</sup>	Square root of hourly wind speed
Wind direction	Fixed – continuous, fitted with harmonic polynomial (k = 5)	1°	Hourly wind direction
Water Temperature	Fixed – continuous, fitted with natural spline (k = 5)	0.1 °C	Hourly water temperature at cleaning station north of D’Arros Island
Manta ID	Random	Individual Tag ID	Identifies individual manta rays

The contribution of each significant predictor variable to the final GAMM was assessed using likelihood-ratio tests that compared the fit of the final model to a model omitting the respective predictor variable as described by Jaime et al. (2012). Marginal effects for each predictor in the final model were visualised using the ‘plot.gam’ function from the *mgcv* package, where the scale on the y-axis was relative to the magnitude of the effect, and the shape indicated the direction of influence of that predictor on *M. alfredi* occurrence at D’Arros Island and St. Joseph Atoll (Jaime et al. 2012).

## 3.4 Results

### 3.4.1 Detection summary

Of the 42 acoustic tags deployed on *M. alfredi* for this study, 38 tags returned usable tracks from 33 individuals (Table 3.2). A total of 164,336 detections were recorded across the full study period, with females accounting for 34.6% of detections and males for 65.4% ( $n = 16$  and  $17$ , respectively; Figure 3.3). Of the females that were tagged, one was juvenile, four were sub-adults, and eleven were adults (4.0, 5.9, and 18.5% of total detections, respectively). Of the males that were tagged, two were juvenile, six were sub-adults, and nine were adults (41.0, 12.1, and 18.4% of total detections, respectively). Tags remained on individuals for an average of  $247 \pm 170$  days, with a minimum retention time of 19 days and a maximum retention time of 776 days.

### 3.4.2 Spatial movements

Individuals moved widely throughout the Amirantes receiver array (Figure 3.4), travelling mean distances of  $13.3 \pm 2.9$  km per day and a maximum of 89.3 km per day. There were no significant differences in the average daily distances travelled by males and females ( $F_{1,36} = 0.68$ ,  $p = 0.41$ ), but daily distance travelled was found to increase with increasing wingspan (i.e. maturity level;  $F_{1,36} = 3.39$ ,  $p = 0.07$ , adj.  $R^2 = 0.06$ ). Only a single tagged individual with a wingspan  $< 3.0$  m was found to travel an average of  $> 20$  km per day (SC-MA-0020; juvenile male). When this individual was removed from the analysis, the relationship between wingspan and average daily distance travelled became even more apparent ( $F_{1,35} = 6.16$ ,  $p = 0.02$ , adj.  $R^2 = 0.13$ ).

**Table 3.2** Summary of acoustic tag deployments on reef manta rays (*Mobula alfredi*) at D'Arros Island, Seychelles, from November 2013 to October 2017 (DSTJ = D'Arros Island and St. Joseph Atoll).

Manta ID	Sex	Size (m)	Tag ID (Tag Type)	Deployment Date	Last Detection	Total # Det.	Total Track Days	Total Det. Days	Residency Index (%)	Av. Dist. (km d <sup>-1</sup> )	Tracking Days at DSTJ (%)	Detection Days at DSTJ (%)
SC-MA-0001	M	2.8	28222 (V16-5H)	30/11/2013	15/04/2014	5,681	137	133	97.1	14.7	91.2	94.0
SC-MA-0002	M	3	28248 (V16-5H)	15/11/2016	23/10/2017	7,070	343	204	59.5	12.1	51.3	86.3
SC-MA-0005	M	2.7	28240 (V16-5H)	17/12/2013	31/01/2016	30,504	776	685	88.3	15.7	72.3	81.9
SC-MA-0006	M	3	28245 (V16-5H)	15/11/2016	30/04/2017	1,554	167	97	58.1	13.1	28.7	49.5
SC-MA-0011	F	3.8	28227 (V16-5H)	08/12/2013	30/05/2014	5,589	174	151	86.8	12.7	78.7	90.7
SC-MA-0012	F	3.5	28239 (V16-5H)	16/12/2013	04/08/2014	4,451	232	162	69.8	9.6	55.2	79.0
SC-MA-0014	F	3.1	28242 (V16-5H)	18/12/2013	07/03/2015	20,655	445	395	88.8	12.7	76.2	85.8
SC-MA-0016	M	3.1	28224 (V16-5H) & 27120 (V16-5H)	06/12/2013 & 13/11/2016	28/02/2015 & 13/01/2017	11,289	512	334	65.2	12.2	36.3	55.7
SC-MA-0017	F	3.5	15038 (V16TP-5H)	22/11/2016	04/03/2017	1,016	103	83	80.6	13.5	68.9	85.5
SC-MA-0019	M	2.5	28229 (V16-5H)	12/12/2013	17/11/2014	14,198	341	305	89.4	12.7	68.6	76.7
SC-MA-0020	M	2.8	28228 (V16-5H) & 28246 (V16-5H)	11/12/2013 & 17/11/2016	17/05/2017 & 27/12/2016	6,559	199	162	81.4	17.7	71.9	88.3
SC-MA-0021	F	3.1	27121 (V16-5H)	14/11/2016	22/03/2017	2,229	129	90	69.8	9.6	64.3	92.2
SC-MA-0025	F	3.6	15042 (V16TP-5H)	25/11/2016	20/01/2017	425	57	34	59.6	19.7	38.6	64.7
SC-MA-0026	M	3.2	28244 (V16-5H)	14/11/2016	02/12/2016	161	19	8	42.1	9.3	26.3	62.5
SC-MA-0027	F	3.7	27118 (V16-5H)	15/11/2016	23/10/2017	353	343	38	11.1	19.4	1.7	15.8
SC-MA-0031	M	2.4	28220 (V16-5H)	16/11/2013	13/04/2014	2,344	149	98	65.8	13.6	12.1	18.4
SC-MA-0044	M	3	27117 (V16-5H)	11/11/2016	20/05/2017	3,288	191	150	78.5	10.7	70.2	89.3
SC-MA-0052	M	2.6	28241 (V16-5H) & 28236 (V16-5H)	18/12/2013 & 14/11/2016	15/04/2014 & 21/06/2017	8,683	339	265	78.2	13.0	72.3	92.5
SC-MA-0053	M	2.9	15044 (V16TP-5H)	25/11/2016	16/10/2017	1,297	326	138	42.3	12.9	36.5	86.2
SC-MA-0073	M	3.3	28234 (V16-5H)	15/03/2014	06/10/2014	1,575	206	116	56.3	11.3	20.4	36.2
SC-MA-0075	M	2.9	28231 (V16-5H)	15/12/2013	10/10/2014	3,409	300	150	50.0	13.4	24.0	48.0
SC-MA-0077	F	3.6	28226 (V16-5H)	08/12/2013	23/04/2014	1,232	228	66	28.9	14.6	14.5	50.0
SC-MA-0078	F	3.8	15036 (V16TP-5H)	18/11/2016	12/10/2017	747	329	99	30.1	15.0	15.8	52.5
SC-MA-0079	F	3.7	28223 (V16-5H)	06/12/2013	22/03/2014	963	107	49	45.8	12.4	2.8	6.1
SC-MA-0084	F	2.4	28221 (V16-5H) & 15040 (V16TP-5H)	30/11/2013 & 24/11/2016	19/01/2014 & 25/10/2017	6,581	387	339	87.6	10.7	82.2	93.8
SC-MA-0087	M	2.6	28232 (V16-5H)	16/12/2013	23/07/2014	1,836	220	116	52.7	14.1	17.7	33.6
SC-MA-0094	M	3	28238 (V16-5H)	14/11/2016	17/02/2017	607	96	60	62.5	10.9	17.7	28.3

Manta ID	Sex	Size (m)	Tag ID (Tag Type)	Deployment Date	Last Detection	Total # Det.	Total Track Days	Total Det. Days	Residency Index (%)	Av. Dist. (km d <sup>-1</sup> )	Tracking Days at DSTJ (%)	Detection Days at DSTJ (%)
SC-MA-0101	F	3.5	28237 (V16-5H)	14/11/2016	14/07/2017	915	243	89	36.6	18.2	11.1	30.3
SC-MA-0107	F	3	15050 (V16TP-5H)	26/11/2016	20/10/2017	3,579	329	266	80.9	12.3	72.3	89.5
SC-MA-0110	F	2.6	15048 (V16TP-5H)	26/11/2016	25/10/2017	3,960	334	274	82.0	11.8	76.9	93.8
SC-MA-0115	M	2.7	27119 (V16-5H)	11/11/2016	25/10/2017	7,401	349	253	72.5	8.5	69.6	96.0
SC-MA-0128	F	3.5	28235 (V16-5H) & 15046 (V16TP-5H)	22/03/2014 & 26/11/2016	24/04/2016 & 07/05/2017	3,856	928	269	29.0	13.9	7.2	24.9
SC-MA-0134	F	3.7	15034 (V16TP-5H)	18/11/2016	18/10/2017	329	335	52	15.5	16.3	7.2	46.2
<b>Average:</b>						4,979.9	284.0	173.6	61.9	13.3	44.3	64.4



**Figure 3.3** Summary of reef manta ray (*Mobula alfredi*) detections recorded across the Amirantes receiver array between November 2013 and October 2017 for individual tracks lasting longer than seven days. Colour shows sex (male, blue; female, red) and life stage (light shaded colour – juvenile; average shaded colour – sub-adult; dark – adult) of each individual. Tag deployment dates are also indicated (▲).

The majority of detections ( $n = 145,677$ ; 89% of total) of *M. alfredi* were recorded at the receivers located within 2.5 km of D’Arros Island and St. Joseph Atoll (inset, Figure 3.4). No detections were recorded inside the St. Joseph Atoll lagoon, and only four detections from a single individual (SC-MA-0027; mature female) were recorded at the easternmost Desroches receiver. *M. alfredi* were most frequently detected on the northern side of D’Arros Island in proximity to a site where *M. alfredi* were consistently observed to visit and clean (hereafter, ‘cleaning station’; Potts (1973);  $n_{\text{detections}} = 48,766$ ; 29.7% of total; Figure 3.4). A large amount of activity was also recorded in the St. Joseph Channel between D’Arros Island and the St. Joseph Atoll, where *M. alfredi* are often seen feeding at the surface.

### 3.4.3 Residency in the Amirantes

#### 3.4.3.1 Broad scale (10 – 100 km)

On average, tagged *M. alfredi* were detected throughout the Amirantes on 62% of the days that they were tracked ( $\bar{x}_{\text{RI}} = 61.9 \pm 23.0\%$ ), with a minimum RI of 11.1% and maximum RI of 97.1% (Table 3.2). A two-way ANOVA suggested that there was no difference in RI according to sex

( $F_{1,31} = 1.81, p = 0.19$ ), but that RI decreased significantly with increasing wingspan (i.e. maturity level;  $F_{1,31} = 13.58, p < 0.001$ ). Juvenile *M. alfredi* were observed to spend a greater amount of time ( $\bar{x}_{RI} = 76.0 \pm 14.2\%$ ) within range of the receiver array than adults ( $\bar{x}_{RI} = 45.6 \pm 23.8\%$ ), regardless of their sex ( $F_{3,29} = 4.77, p_{wingspan*sex} = 0.52$ ).

Multivariate analyses indicated that when tagged *M. alfredi* were present within the Amirantes receiver array, there was no significant difference in the frequency at which either sex, or any of the maturity groups, visited the different receivers ( $R = -0.02, p = 0.77$ , and  $R = -0.02$  and  $p = 0.35$ , respectively), or in the amount of time spent in proximity to the receivers ( $R = 0.01, p = 0.35$  and  $R = -0.04, p = 0.67$ , respectively; Figure S 3.1). Additionally, there were no differences in receiver visitation patterns, or time spent in proximity to receivers, between the two deployment periods ( $R = 0.05, p = 0.09$  for both metrics; Figure S 3.1).

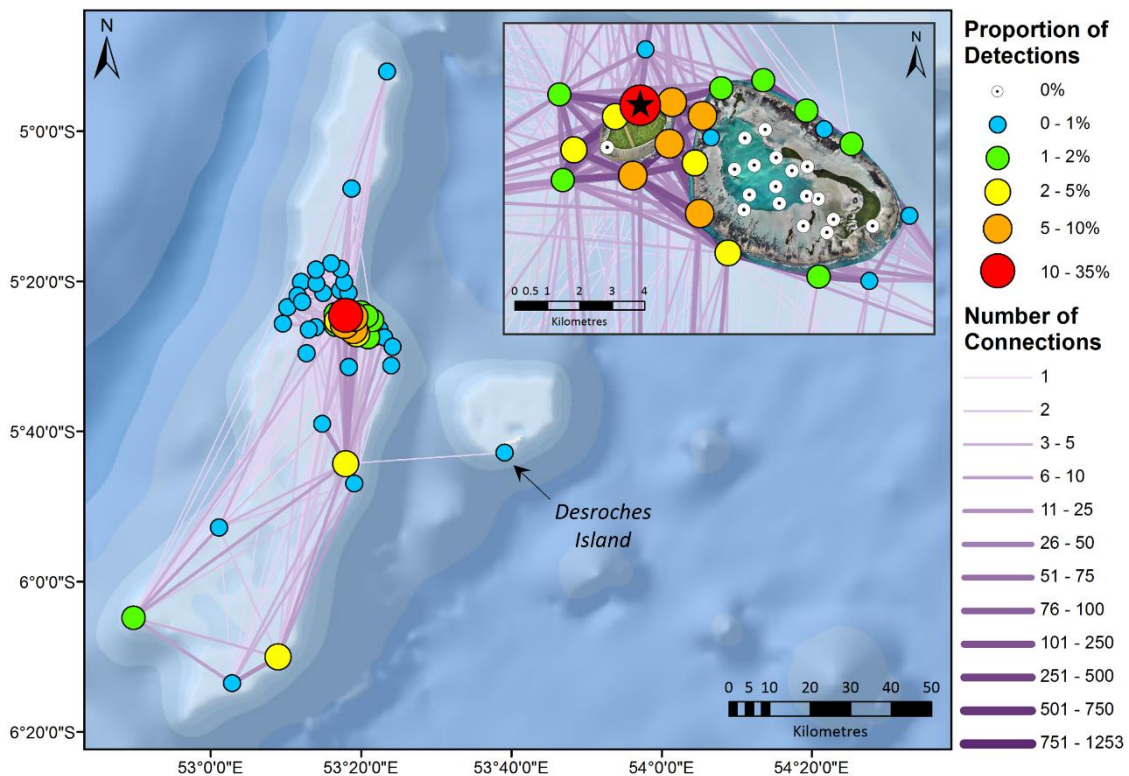


**Figure 3.4** Network map of the Amirantes receiver array indicating the proportion of reef manta ray (*Mobula alfredi*) detections recorded at each receiver (nodes;  $n = 70$ ) between November 2013 and October 2017. Edges represent the frequency of subsequent detections between receivers. Symbology is described in the legend. Location of cleaning station at D'Arros Island indicated by  $\star$ . Maps created in ArcGIS 10.3 (<http://www.esri.com/>) using GEBCO\_08 (version 20100927) bathymetry data. Georeferenced drone imagery  $\copyright$  Save Our Seas Foundation.

### 3.4.3.2 Local scale (1 – 10 km)

Individual *M. alfredi* appeared to be largely resident to D'Arros Island and the neighbouring St. Joseph Atoll. On average, individuals were recorded at the receivers positioned within 2.5 km of these islands on 48% of all of the days that they were tracked ( $\bar{x} = 47.6 \pm 30.6\%$ ), and on 67% of all days that they were detected within the entirety of the Amirantes array ( $\bar{x} = 66.7 \pm 28.0\%$ ; Table 3.2). During the first deployment period, one juvenile female (SC-MA-0084) was recorded only at the inshore receivers around D'Arros Island and St. Joseph Atoll for the 51 days that it was tracked. Of the other 32 individuals that were tagged across both deployment periods and were observed to have left this area, all except one (SC-MA-0079, mature female) returned to D'Arros Island and St. Joseph Atoll on at least one occasion while being tracked (Figure S 3.2).

### 3.4.4 Temporal and environmental patterns

The final GAMM developed through the model selection process considered 77,414 observations of *M. alfredi* presence and absence at D'Arros Island and St. Joseph Atoll and described 15.0% of the variation present in these data (wAIC = 0.22; Table S 3.2). All temporal and environmental predictors considered during the model selection process were included in the final model, while the biological predictors, sex and wingspan, were excluded (Table 3.3).

The probability *M. alfredi* being detected within 2.5 km of D'Arros Island and St. Joseph Atoll peaked between November and April (Figure 3.5A); coinciding with arrival and departure of the north-west monsoon and the prevailing wind (Figure 3.5B) that occurs during these months in Seychelles. Individuals were more likely to be detected during the day (06:00 – 18:00) than at night (18:00 – 06:00; Figure 3.5C). Water temperature ranged from 25.3 to 30.6°C during the study period, and detection frequencies for *M. alfredi* peaked when the water temperature was approximately 28°C (Figure 3.5D). Additionally, individuals were more likely to be detected during a new moon (Figure 3.5E), when the tidal range was at its highest (Figure 3.5F), and on the slack of high tide (Figure 3.5G). Individuals were less likely to be detected at this location as wind speed increased (Figure 3.5H). Finally, differences in visitation patterns among individuals explained the largest amount of variation in these data (10.2%; Table 3.3).

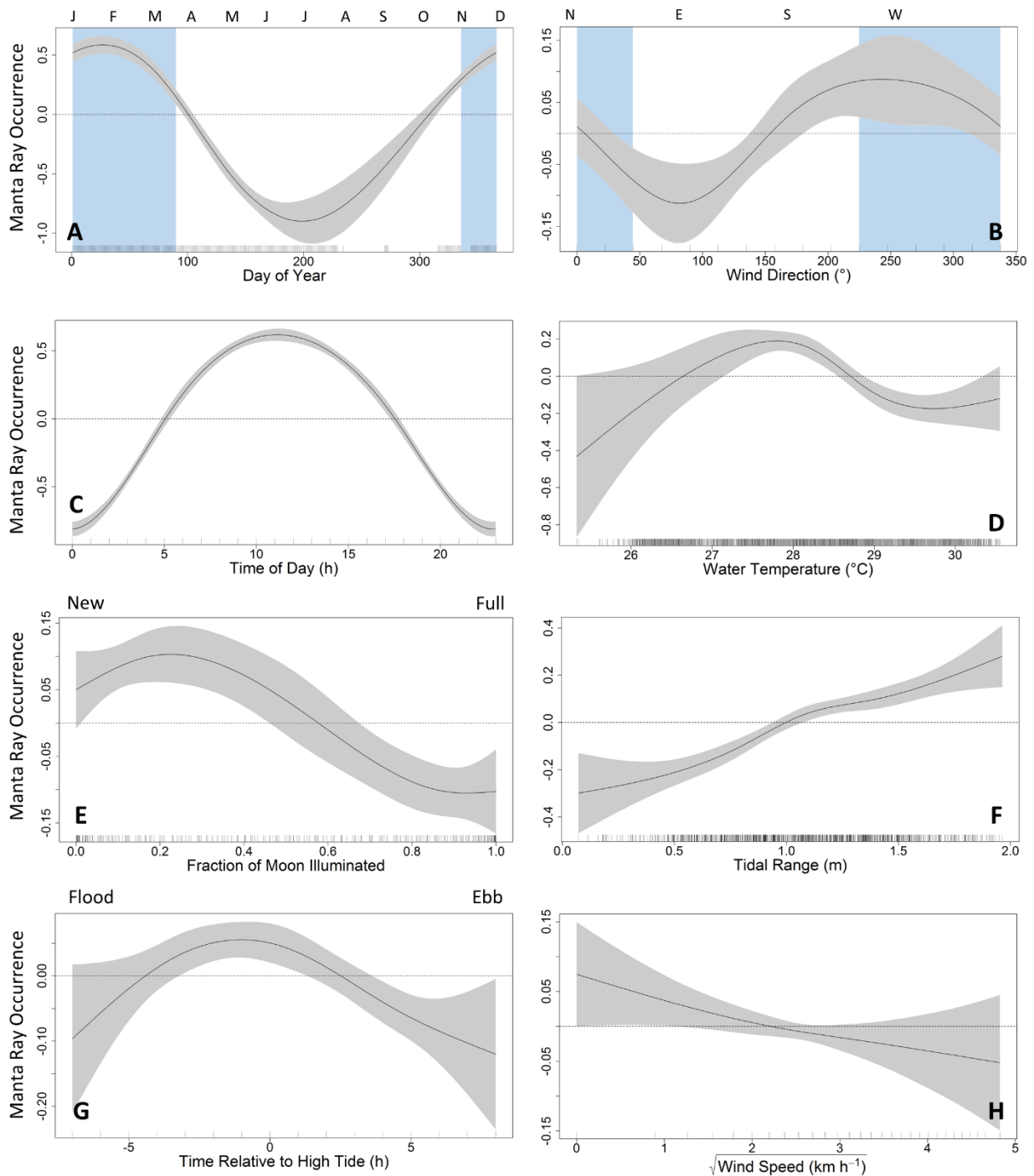


**Figure 3.5** Marginal effect plots derived from the top ranked binomial GAMM indicating the significant effects of day of year (A; *letters* above represent months of year), prevailing wind direction (B; *letters* above represent cardinal directions), time of day (C), water temperature (D), fraction of moon illumination (E), tidal range (F), time relative to high tide (G), and wind speed (H) on the probability of detecting acoustically tagged reef manta rays (*Mobula alfredi*) at D'Arros Island and St. Joseph Atoll, Seychelles, between November 2016 and October 2017. Blue shading indicates periods of north-west monsoon. Grey shading indicates 95% confidence interval. Horizontal dashed lines indicate  $y = 0$ .



**Table 3.3** Summary of the GAMM constructed to assess the influence of temporal, biological and environmental variables on the occurrence of reef manta rays (*Mobula alfredi*) at D'Arros Island and St. Joseph Atoll, Seychelles. Values are provided for predictors included in the final selected GAMM only. Degrees of freedom (df); p-value from  $\chi^2$  test ( $p$ ); percent of deviance explained (% DE).

<b>Predictor added to model</b>	<b>Deviance</b>	<b>df</b>	<b><math>p</math> (<math>\chi^2</math>)</b>	<b>% DE</b>
Sex	-	-	-	-
Wingspan (m)	-	-	-	-
Day of year	330.42	2.54	< 0.001	0.68
Time of day (h)	1,599.40	2.32	< 0.001	3.30
Fraction of moon illuminated	46.10	5.57	< 0.001	0.10
Time to high tide (h)	20.72	3.57	< 0.001	0.04
Tidal range (m)	71.32	4.61	< 0.001	0.15
Water temperature (°C)	57.33	4.30	< 0.001	0.12
Wind direction (°)	18.23	2.05	< 0.001	0.04
Wind speed (km h <sup>-1</sup> )	6.18	2.17	0.05	0.01
Manta ID	4,955.40	18.98	<0.001	10.24
<b>Full Model</b>	<b>48,409.44</b>	<b>77,372.01</b>	<b>-</b>	<b>15.00</b>

## 3.5 Discussion

### 3.5.1 Spatial movements through the Amirantes

Tagged *M. alfredi* were resident to the area of D'Arros Island and St. Joseph Atoll, spending an average of 64.4% of the days they were tracked within 2.5 km of these locations. Movements of individuals along the length of the Amirantes Bank (152 km) were infrequent and tended to favour the eastern ridge of the Bank. Although reef manta rays have a circumtropical distribution (Couturier et al. 2012), such patterns of high residency and relatively restricted movements away from aggregation sites appear to be typical of most localities (Jaine et al. 2014, Couturier et al. 2018, Stewart et al. 2018a). Broad scale movements do occur, for example in the waters of eastern Australia, where *M. alfredi* travelled across a range of up to 1,035 km (Jaine et al. 2014), however, movements of individuals are typically limited to < 500 km (Couturier et al. 2011, Germanov & Marshall 2014, Braun et al. 2015, Setyawan et al. 2018).

Only one *M. alfredi* was detected at Desroches Island (50 km from D'Arros Island; Figure 3.4) during our four year study. This individual (SC-MA-0027; a mature female) travelled 40 km across waters up to 1,500 m in depth from northern Poivre (17 November 2016) to Desroches Island (19 November 2016), where two detections were recorded over a period of two minutes. The same individual briefly returned to Desroches Island on 21 February 2017 when another two detections were recorded, and was detected again on the main Amirantes Bank six days later. This was the first confirmed movement of *M. alfredi* between D'Arros Island and Desroches Island, and only one additional movement has been recorded since using photo-identification techniques (L. Peel, unpub. data). Evidence from Japan and Indonesia suggests that *M. alfredi* are easily capable of movements at this spatial scale (350 – 450 km; Homma et al. 1999, Germanov & Marshall 2014), however, such movements of individuals between the Amirante Islands appear to be infrequent.

The small number of detections of *M. alfredi* recorded at Desroches Island could be the result of the single receiver at this location being placed in an area that was not suitable habitat for *M. alfredi*, and so failing to record their presence. Alternatively, the channel (up to 1,500 m deep) between the main Amirantes Bank and Desroches Island may act as a barrier to movement, possibly because it places individuals at greater risk of predation (Marshall & Bennett 2010a, Deakos et al. 2011). It is also possible that sufficient food resources may exist on the Amirantes Bank, so that it is unnecessary for individuals to travel elsewhere (Deakos et al. 2011). A lack of cross-channel movements of *M. alfredi* has similarly been noted in Hawaii, where none of the 435 individually identified mantas were found to have traversed the 47 km wide and 2,000 m deep channel between Maui and the Big Island during a ten-year study (Deakos et al. 2011). The

present study provides further support to the possibility that deep water may act as a barrier to the movements of this species.

### 3.5.2 Residency and array use

Tagged individuals showed high levels of residency to the Amirante Island Group ( $\bar{x}_{RI} = 61.9\%$ ), with a maximum recorded residency index of 97.1% recorded over 137 tracking days (SC-MA-0001; sub-adult male). Similar levels of residency have been reported for *M. alfredi* using passive acoustic telemetry in the Red Sea ( $\bar{x}_{RI} = 65.1\%$ ; Braun et al. 2015), but the residency indices recorded in this study are much higher than those recorded from arrays in eastern Australia ( $\bar{x}_{RI} = 15\%$ ; Couturier et al. 2018) and Hawaii ( $\bar{x}_{RI} = 39.1\%$ ; Clark 2010). These latter studies also included receivers that were placed at known cleaning stations, but deployed fewer receivers compared to the Amirante array (six and forty-three, respectively), which may have contributed to a lower likelihood of detection and thus apparent residency.

Juvenile *M. alfredi* displayed greater residency to the Amirantes Bank than adults. A variety of factors might contribute to this pattern, including the possibility that juveniles face an increased threat of predation when travelling away from the refuge of the reef flats of D'Arros Island and St. Joseph Atoll (Heupel et al. 2007, Cerutti-Pereyra et al. 2014, Heupel et al. 2018, Stewart et al. 2018b). Juveniles may also lack experience in locating foraging opportunities offshore and, due to smaller body mass, may have limited abilities to forage in the deeper, cooler waters associated with such environments (Ware 1978, Sims et al. 2006). Alternatively, or in addition, the lower swimming efficiency of juvenile *M. alfredi* due to their smaller size might also restrict their movements in comparison to the larger adults (Weihs 1973, Nøttestad et al. 1999).

Movement patterns between, and duration of visitation events to, the islands of the Amirantes did not differ between the sexes and life stages of *M. alfredi*. D'Arros Island and St. Joseph Atoll, in particular the St. Joseph Channel between them and the northern coast of D'Arros Island, were key locations for all tagged individuals. The high use of this restricted area by all individuals in this study suggests that the establishment of an MPA covering D'Arros Island and St. Joseph Atoll would provide conservation and management benefits for *M. alfredi*.

### 3.5.3 Environmental and temporal patterns

The occurrence of tagged *M. alfredi* varied with the shifting trade winds of the annual monsoons, with a steep decline in detection probability from March through to July when the north-western monsoon begins to subside, and higher detection frequencies occurring during southern winds.

Given that the trade winds play a critical role in the development of surface currents and subsequently how plankton accumulates in the water column (Gove et al. 2016), it is possible that these changing wind regimes alter zooplankton accumulation at D'Arros Island and St. Joseph Atoll as it does across the islands of the Maldives (Anderson et al. 2011a). The resulting fluctuation in food availability for *M. alfredi* may drive the subsequent changes of presence of individuals at this location.

Tidal phase also had a significant influence on the presence of *M. alfredi* at D'Arros Island and St. Joseph Atoll. Occurrence was highest in the hours before and during a high tide, and when the tidal range was at a maximum (approximately 2 m). These trends in detections were additionally supported by sighting and photo-identification records collected at D'Arros Island (L. Peel, unpub. data). Tides also influenced the cleaning and foraging behaviours of *M. alfredi* on the Great Barrier Reef (O'Shea et al. 2010, Jaine et al. 2012, Couturier et al. 2018), where cleaning behaviour was most commonly observed at, and after, a high tide, and foraging behaviour frequently reported on large, ebbing tides (Jaine et al. 2012). As our receivers were located close to a cleaning station, and in the St. Joseph Channel where feeding behaviour is commonly observed, similar behaviours could account for the increase in detections around high tide at D'Arros Island and St. Joseph Atoll. A slack tide may also increase the frequency of tag detection by reducing the amount of ambient noise present in the surrounding environment through diminished current speeds (Mathies et al. 2014). However, this should occur on both the high and low tides, thus is unlikely to account for our results.

Increasing wind speeds were associated with a reduction in the occurrence of *M. alfredi* around D'Arros Island and St. Joseph Atoll. Similar patterns during high winds have been recorded on the Great Barrier Reef (Jaine et al. 2012, Couturier et al. 2018), with decreased prey concentration, reduced visibility, and increased predation risk being suggested as potential reasons for *M. alfredi* to avoid rough conditions at the surface (Couturier et al. 2018). Additionally, it is possible that these rough sea conditions caused a reduction of receiver efficiency and contributed to the observed pattern of occurrence at D'Arros Island and St. Joseph Atoll (Cagua 2012). The consistency of response by *M. alfredi* to increasing wind speeds at various study sites, however, suggests that this is a component of their behaviour rather than an artefact of ambient noise (Jaine et al. 2012, Couturier et al. 2018).

Detection frequencies of *M. alfredi* at D'Arros Island and St. Joseph atoll were greater during the day than at night. This pattern suggests that individuals move beyond the boundary of the receiver array at night, potentially travelling offshore and beyond the Amirantes Bank where the majority of the receivers were located. This finding also supports the hypothesis that *M. alfredi* vary their foraging strategy throughout the diel cycle. Individuals are thought to feed at the surface of shallow reef flats during the day, before venturing into deeper waters during the night, where they

forage on emergent and benthic zooplankton communities (Couturier et al. 2013a, Burgess et al. 2016). This pattern of foraging has been recorded in numerous localities, including Indonesia (Dewar et al. 2008, Setyawan et al. 2018), Hawaii (Clark 2010, Deakos et al. 2011), the Red Sea (Braun et al. 2014), and eastern Australia (Couturier et al. 2018). Alternatively, or in addition, higher detection frequencies during the day may also be driven by the physiological needs of individuals. Occupation of the shallow waters of the reef flats during the day might allow *M. alfredi* to warm their regionally endothermic bodies (Alexander 1996, Thorrold et al. 2014) to favourable temperatures prior to undertaking deep or offshore feeding behaviours at night (Braun et al. 2014).

The strong diel cycle observed in the inshore visitation pattern of *M. alfredi* might also be explained by their use of cleaning stations during daylight hours. Visits by *M. alfredi* to cleaning stations elsewhere have tended to occur from late morning to early afternoon (Dewar et al. 2008, Clark 2010, O'Shea et al. 2010, Jaine et al. 2012, Couturier et al. 2018, Setyawan et al. 2018), since cleaner fishes are only active and therefore available for parasite removal during the daytime (Potts 1973, Lenke 1988, Côté 2000, Marshall & Bennett 2010a, Couturier et al. 2018). Additionally, manta cleaning stations are thought to facilitate important social interactions among individuals (O'Shea et al. 2010, Deakos et al. 2011, Marshall et al. 2011, Stevens et al. 2018b). Attendance at the cleaning station at D'Arros Island for either or both of these reasons would have brought acoustically-tagged *M. alfredi* close to receiver stations during the day, increasing the likelihood of tag detections. It is also important to acknowledge that a reduced detection range of receivers resulting from increased levels of biological noise on the coral reef at night may have contributed to the observed pattern of detection (Cagua 2012, How & de Lestang 2012). However, given the consistency of diurnal movement patterns of *M. alfredi* among studies using a combination of observational records (Anderson et al. 2011a), active (Clark 2010) and passive (Deakos et al. 2011, Couturier et al. 2018, Setyawan et al. 2018) acoustic telemetry, and satellite telemetry (Braun et al. 2014, Jaine et al. 2014), fluctuating receiver efficiency is unlikely to be the primary driver of the observed pattern in the present study.

*M. alfredi* were detected more frequently during the new moon than the full moon at D'Arros Island and St. Joseph Atoll. Numerous studies have recorded changes in the occurrence of manta rays with lunar phase (Dewar et al. 2008, Clark 2010, Jaine et al. 2012, Rohner et al. 2013). Both sharks and rays tend to occupy deeper waters during the full moon (Vianna et al. 2013, Hammerschlag et al. 2017), a pattern that may be driven by changes in food availability, predation pressure and foraging. At D'Arros Island, a need to occupy or forage in deeper water may drive tagged individuals beyond the boundary of the receiver array and subsequently reduce detection frequencies during this time. Lower detection frequencies for acoustically-tagged *M. alfredi* have also been observed during a full moon on the Great Barrier Reef (Couturier et al. 2018), and in the Red Sea, satellite tagged *M. alfredi* were found to dive deeper during a full moon than a new

moon when in offshore waters (Braun et al. 2014). Collectively, this suggests that such a pattern of movement is common for *M. alfredi*.

Finally, it is important to note that 68% of the deviance explained by the final GAMM in this study was attributed to differences between individual *M. alfredi*. This may be due to some individuals being largely resident to D'Arros Island and St. Joseph Atoll, whereas others are more transient throughout the Amirante Islands but display high levels of site fidelity to these locations (Chapman et al. 2015, Germanov et al. 2019). It is likely that the generality of movement patterns for the species would become more apparent with the deployment of more tags in the region (Sequeira et al. 2019). Furthermore, 85% of the variation in the detection data included in the GAMM remained unexplained, suggesting that the spatial resolution of the considered environmental variables was at a scale different to that of the movement decisions made by *M. alfredi* (Ferreira 2017). The inclusion of data relating to prey fields and prey availability at D'Arros Island and St. Joseph Atoll in future models of *M. alfredi* movement patterns is expected to increase the explanatory power of such analyses, particularly given the frequency of feeding behaviour observed in the St. Joseph Atoll relative to that at the cleaning station (Chapter 2). Should environmental conditions influence patterns of behaviour for *M. alfredi* at D'Arros Island and St. Joseph Atoll, as has been reported to occur in eastern Australia (Jaine et al. 2012), data collected from temperature loggers and current meters deployed at multiple sites around these locations would also benefit future models of movement patterns. Despite these caveats, however, the collective results outlined above represent a significant first step in understanding the drivers of movement and residency patterns for *M. alfredi* at D'Arros Island and St. Joseph Atoll, and in a remote region of the Western Indian Ocean.

## 3.6 Summary

The patterns of high residency and similarity of movements of all cohorts of the population of *M. alfredi* at D'Arros Island and St. Joseph Atoll suggests that the establishment of a MPA at this locality would be a benefit conservation and management efforts for this species in the Amirante Island Group of Seychelles. This is particularly true for juvenile *M. alfredi*, which displayed the highest levels of residency, regardless of their sex. In addition to protecting *M. alfredi* from targeted fishing pressures, accidental entanglement and boat strikes at D'Arros Island and St. Joseph Atoll, such a MPA would also serve to protect the cleaning station to the north of D'Arros Island and the surrounding coral reef ecosystem. Satellite telemetry and photo-identification data will assist in expanding our current understanding of the movement patterns of this species in the future by providing insight into the broader movements of *M. alfredi* throughout Seychelles as a whole. To date, few confirmed sightings of *M. alfredi* have been recorded outside of the Amirante

Island Group and the neighbouring Alphonse Island Group in Seychelles (< 2% of all records, L. Peel, unpub. data), despite considerable effort to collect data in these locations. This observation further supports the hypothesis that the Amirante Islands, in particular D'Arros Island and St. Joseph Atoll, are key areas for this vulnerable species. Continued monitoring of *M. alfredi* movement throughout Seychelles will ensure that this species is protected at appropriate scales across this remote area of the Western Indian Ocean.

### 3.7 Supplementary material

**Table S 3.1** Correlation matrix for continuous predictors considered in generalised additive mixed models (GAMMs) of reef manta ray (*Mobula alfredi*) occurrence at D’Arros Island and St. Joseph Atoll, Seychelles.

	Day of year	Time of day	Fraction of moon illuminated	Time to high tide	Tidal range	$\sqrt{\text{Wind Speed}}$	Water temperature	Wind direction
Day of year	1	-0.01	-0.02	0.01	-0.04	0.05	-0.30	-0.17
Time of day	-0.01	1	0.00	0.02	0.02	-0.01	0.02	0.01
Fraction of moon illuminated	-0.02	0.00	1	0.00	0.02	-0.02	-0.06	-0.12
Time to high tide	0.01	0.02	0.00	1	0.01	0.00	0.00	-0.01
Tidal range	-0.04	0.02	0.02	0.01	1	-0.10	0.01	-0.03
$\sqrt{\text{Wind speed}}$	0.05	-0.01	-0.02	0.00	-0.10	1	-0.27	0.07
Water temperature	-0.30	0.02	-0.06	0.00	0.01	-0.27	1	0.10
Wind direction	-0.17	0.01	-0.12	-0.01	-0.03	0.07	0.10	1



**Table S 3.2** Top ten candidate GAMMs for predicting the occurrence of acoustically tagged reef manta rays (*Mobula alfredi*) within 2.5 km of D'Arros Island and St. Joseph Atoll, Seychelles. Best model (highlighted in bold) selected using differences in Akaike's Information Criteria corrected for sample size (AICc) among models ( $\Delta$ AICc), and AICc weights (wAICc). Variables considered in models include: day of year (Dy), time of day (Hr), fraction of moon illuminated (Mn), time to high tide (Th), tidal range (Tr), wind speed (Ws), water temperature (Tp), sex (Sx), wingspan (Sp), and manta ray ID (Id).

<b>Candidate Model Set</b>	<b>AICc</b>	<b><math>\Delta</math>AICc</b>	<b>wAICc</b>
<b>Dy + Hr + Mn + Th + Tr + Ws + Tp + Wd + Id</b>	<b>48,499.77</b>	<b>0.00</b>	<b>0.22</b>
Sx + Dy + Hr + Mn + Th + Tr + Ws + Tp + Wd + Id	48,499.84	0.07	0.21
Dy + Hr + Mn + Th + Tr + Ws + Tp + Wd + Sp + Id	48,500.06	0.29	0.19
Sx + Dy + Hr + Mn + Th + Tr + Ws + Tp + Wd + Sp + Id	48,500.06	0.29	0.19
Dy + Hr + Mn + Th + Tr + Tp + Wd + Id	48,502.49	2.72	0.06
Sx + Dy + Hr + Mn + Th + Tr + Tp + Wd + Id	48,502.55	2.78	0.05
Dy + Hr + Mn + Th + Tr + Tp + Wd + Sp + Id	48,502.84	3.07	0.05
Sx + Dy + Hr + Mn + Th + Tr + Tp + Wd + Sp + Id	48,502.84	3.07	0.05
Dy + Hr + Mn + Th + Tr + Ws + Tp + Id	48,513.12	13.35	0.00
Sx + Dy + Hr + Mn + Th + Tr + Ws + Tp + Id	48,513.19	13.42	0.00

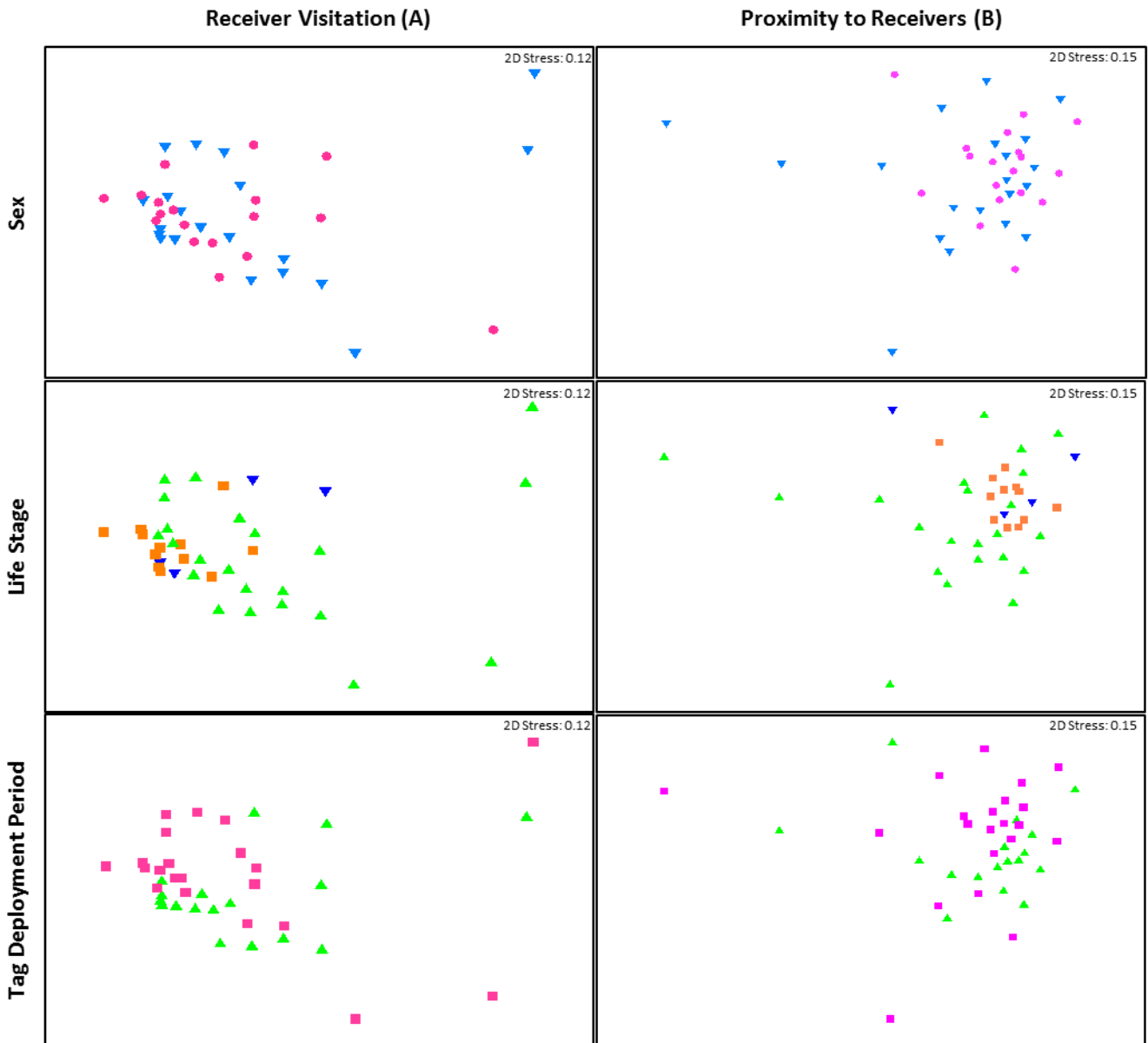


**Figure S 3.1** Non-metric multidimensional scaling plots of acoustically tagged reef manta ray (*Mobula alfredi*) visitation frequency (number of days; A) and proximity to (number of detections; B) receivers at the Amirante Island Group, Seychelles. Patterns examined with respect to individual sex (female, pink circle; male, blue triangle), life stage (juvenile, blue triangle; sub-adult, orange square; adult, green triangle), and the year of tag deployment (2013, green triangle; 2016, pink square). Data based on a Bray-Curtis similarity matrix with 9,999 permutations.

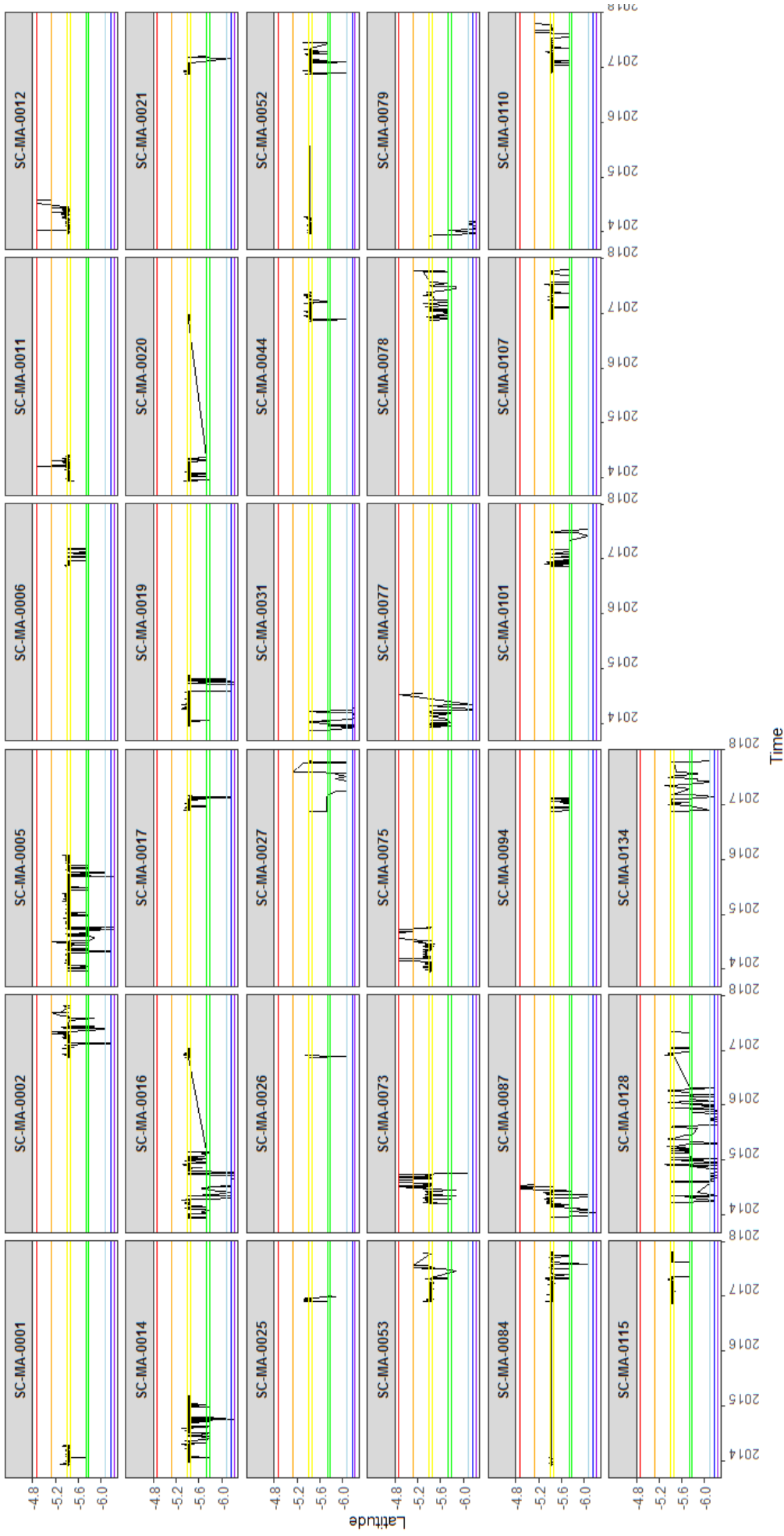


**Figure S 3.2** Detections over time for acoustically-tagged reef manta rays (*Mobula alfredi*) relative to the latitude of detection within the Amirantes receiver array, Seychelles. Latitude of northern-most (African Banks) and southern-most (Desnoeuufs) acoustic receivers are indicated by red and purple horizontal lines, respectively. Orange horizontal lines represent latitude of receiver at Remire. Yellow horizontal lines represent northern- and southern-most receivers of D'Arros Island and St. Joseph Atoll. Green horizontal lines represent northern- and southern-most receivers of Poivre. Light and dark blue horizontal lines represent latitude of receivers at Boudeuse and Marie Louise, respectively.



# Chapter 4 Trophic ecology of the reef manta ray (*Mobula alfredi*) at a remote coral reef

## 4.1 Abstract

Stable isotope analyses provide the means to examine the trophic role of animals in complex food webs. Here, we used stable isotope analyses to characterise the feeding ecology of reef manta rays (*Mobula alfredi*) at a remote coral reef in the Western Indian Ocean. Muscle samples of *M. alfredi* were collected from D'Arros Island and St. Joseph Atoll, Republic of Seychelles, in November 2016 and 2017. Prior to analysis, lipid and urea extraction procedures were tested on freeze-dried muscle tissue in order to standardise sample treatment protocols for *M. alfredi*. The lipid extraction procedure was effective at removing both lipids and urea from samples and should be used in future studies of the trophic ecology of this species. The isotopic signatures of nitrogen ( $\delta^{15}\text{N}$ ) and carbon ( $\delta^{13}\text{C}$ ) for *M. alfredi* differed by year, but did not vary by sex or life stage, suggesting that all individuals occupy the same trophic niche at this coral reef. Furthermore, the isotopic signatures for *M. alfredi* differed to those for co-occurring planktivorous fish species also sampled at D'Arros Island and St. Joseph Atoll, suggesting that the ecological niche of *M. alfredi* is unique. Pelagic zooplankton were the main contributor (45%) to the diet of *M. alfredi*, combined with emergent zooplankton (38%) and mesopelagic prey items (17%). Given the extent of movement that would be required to undertake this foraging strategy, individual *M. alfredi* are implicated as important vectors of nutrient supply around and to the coral reefs surrounding D'Arros Island and St. Joseph Atoll, particularly where substantial site fidelity is displayed by these large elasmobranchs.

## 4.2 Introduction

Coral reefs support high levels of marine biodiversity and host intricate food webs (Bellwood et al. 2005, Roff et al. 2016). Many reef systems are isolated, dispersed across tropical waters where they form hotspots of increased productivity in otherwise oligotrophic oceans (Gove et al. 2016). Part of this productivity may be supported by highly mobile marine megafauna, such as sharks, rays, seabirds, turtles and whales, whose foraging movements and residency patterns can facilitate significant nutrient transport and recycling between reef and offshore environments (McCauley et al. 2012b, Moss 2017, Graham et al. 2018, Williams et al. 2018).

Reef manta rays (*Mobula alfredi*; Marshall et al. 2009, White et al. 2017) are large filter-feeding elasmobranchs that display high levels of site fidelity and residency at circum-tropical reef locations (Dewar et al. 2008, Anderson et al. 2011a, Couturier et al. 2018, Setyawan et al. 2018). Individuals are often observed feeding on pelagic zooplankton that accumulates near the surface of the water column (< 5 m) during daylight hours, and this foraging behaviour has been found to be linked to zooplankton density in eastern Australia (Armstrong et al. 2016). During the night, demersal zooplankton emerge from the seabed, where they vertically migrate towards the surface (Allredge & King 1980), and become potential prey items for *M. alfredi* (Couturier et al. 2013a). These emergent zooplankton communities are thought to be particularly significant for *M. alfredi* that occupy lagoon systems (McCauley et al. 2014). Furthermore, *M. alfredi* have been observed to travel offshore to feed on mesopelagic zooplankton before returning to inshore coral reefs during the day where they may excrete waste products (Clark 2010, Couturier et al. 2013a, Braun et al. 2014, Jaine et al. 2014). In this way, *M. alfredi* may be able to create links between shallow coral reefs and deeper water ecosystems, potentially facilitating the horizontal transport of nutrients between these environments (Papastamatiou et al. 2015a).

Stable isotope analyses provide a means to examine the trophic role of manta rays and other marine megafauna in coral reef environments (Fleming et al. 2018, Munroe et al. 2018, Pethybridge et al. 2018). The isotopic ratios of nitrogen ( $^{14}\text{N}/^{15}\text{N}$ , or  $\delta^{15}\text{N}$ ) and carbon ( $^{12}\text{C}/^{13}\text{C}$ , or  $\delta^{13}\text{C}$ ) in the muscle tissues of manta rays provide information on both the trophic level and foraging locations of these animals. This is possible as values of  $\delta^{15}\text{N}$  increase with increasing trophic position (Post 2002, Hussey et al. 2014), and values of  $\delta^{13}\text{C}$  display predictable changes with habitat (Pitt et al. 2008) and location (Prebble et al. 2018). Few studies to-date have used this analytical approach to examine the feeding ecology of reef and oceanic (*Mobula birostris*) manta rays, but those published have shown that emergent ( $\delta^{13}\text{C} > -17\%$ ; Pitt et al. 2008) and mesopelagic zooplankton (> 200 m depth in the water column) comprise a significant proportion of the diet of *M. alfredi* along the coast of eastern Australia (Couturier et al. 2013a), and of *M. birostris* in Ecuador (Burgess et al. 2016), respectively. Emergent zooplankton have also been reported to be a significant contributor to the diet of *M. alfredi* within the lagoon of Palmyra Atoll in the central Pacific (McCauley et al. 2014). Coupled with the potential for *M. alfredi* to travel large distances (300 – 1150 km; Homma et al. 1999, Germanov & Marshall 2014, Jaine et al. 2014, Armstrong et al. 2019), these findings suggest that manta rays may act as a vector for the horizontal transport of nutrients between offshore and coastal reef ecosystems. Additionally, the high site fidelity displayed by *M. alfredi* at aggregation sites may serve to increase the significance of such nutrient transfer processes, and of the trophic role of this species within reef environments as a whole.

Although previous research suggests that manta rays may be important to nutrient flows in oligotrophic seas (Couturier et al. 2013a, McCauley et al. 2014), the context of their trophic role

within reef communities is not fully understood (Stewart et al. 2018a). Since most isotope-based studies of manta ray trophic ecology have used restricted sampling regimes that included only the target species and putative species of prey (Couturier et al. 2013a, Burgess et al. 2016, Stewart et al. 2017), it may be that mantas are simply one species of a much larger guild of fishes that perform similar functions. Alternatively, by moving across habitats over larger distances than most other planktivorous reef fishes (Carpenter 1988), it could be that manta rays occupy a unique role in nutrient transport in reef systems. Insight into this issue requires contemporaneous sampling and isotope analysis across a wide range of species from multiple guilds of reef fishes.

Here, we describe the feeding ecology and trophic role of *M. alfredi* at the coral reefs surrounding D'Arros Island and St. Joseph Atoll (hereafter, D'Arros Island), Republic of Seychelles, using stable isotope analyses. In order to facilitate comparisons across species at D'Arros Island and among studies in other locations (Stewart et al. 2018a), we firstly optimised sample treatment procedures by assessing the effect of lipid and urea extraction procedures on the  $\delta^{15}\text{N}$  and  $\delta^{13}\text{C}$  values obtained from *M. alfredi* muscle tissue. Our study then assessed the extent to which foraging *M. alfredi* targeted pelagic, emergent and mesopelagic zooplankton communities, given the findings of earlier work (Pitt et al. 2008, Couturier et al. 2013a, Burgess et al. 2016). The values of  $\delta^{15}\text{N}$  and  $\delta^{13}\text{C}$ , and ratios of C:N, for *M. alfredi* were then compared to that of zooplankton, reef fishes and seagrass samples collected at D'Arros Island to understand the broader trophic role of the species within the reef community. Lastly, we examined the role that this species may play in the horizontal transport of nutrients across ecosystems within this region of the Western Indian Ocean.

## 4.3 Methods

### 4.3.1 Study site

The Republic of Seychelles is an archipelago located in the Western Indian Ocean and encompasses an Exclusive Economic Zone (EEZ) of 1.4 million km<sup>2</sup>. It is comprised of 115 islands that collectively occupy 459 km<sup>2</sup> of land (Kawaley 1998). These tropical islands are divided into two main groups based on their geography and composition; the granitic islands to the north comprise the Inner Islands, and the dispersed coralline islands to the south-west comprise the Outer Islands. The Amirante Island Group, located upon the predominantly shallow (< 40 m depth) Amirantes Bank, lies within the Outer Island region and is made up of 11 low-lying sand cays (Stoddart et al. 1979). D'Arros Island (1.71 km<sup>2</sup>) and the St. Joseph Atoll (1.63 km<sup>2</sup>) occur in the central region of the Bank (5°24.9'S, 53°17.9'E), and are separated by a 1 km wide and 60 m deep channel (Figure 4.1; Stoddart et al. 1979). Aggregations of *M. alfredi* are observed year-round in the waters surrounding D'Arros Island, which is significant given the

infrequency of sightings of this species at other islands and Island Groups throughout the rest of Seychelles (L. Peel, unpub. data).

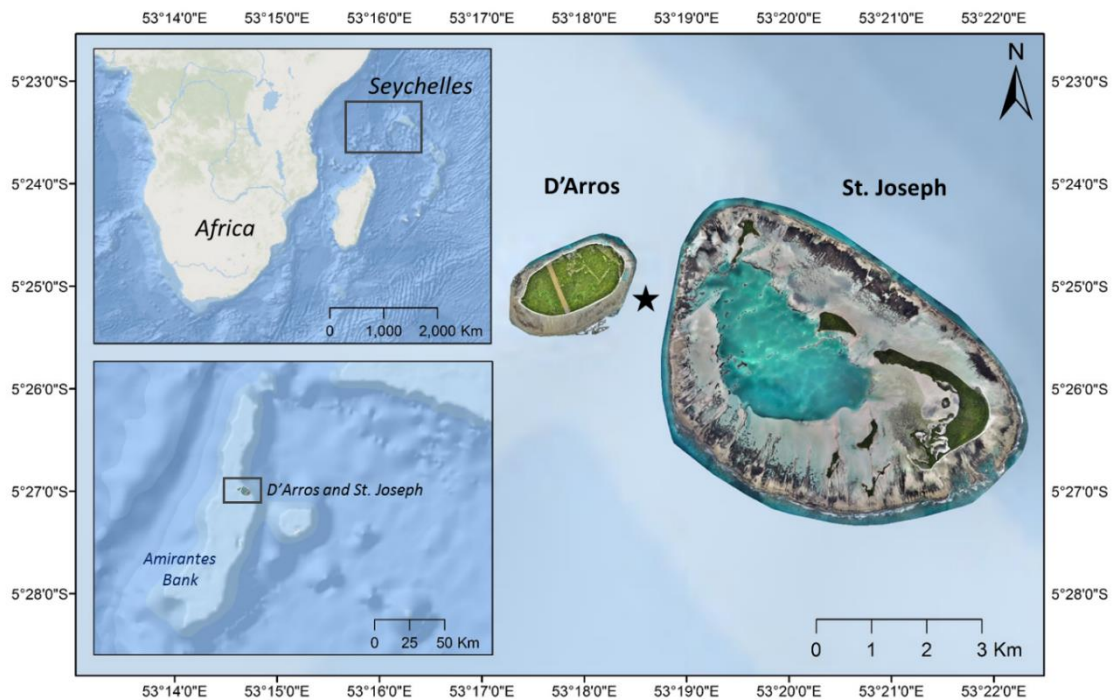


**Figure 4.1** D'Arros Island and St. Joseph Atoll, located on the Amirantes Bank within the Republic of Seychelles, Western Indian Ocean. Position of St. Joseph Channel indicated by ★. Maps created in ArcGIS 10.3 (<http://www.esri.com/>) using GEBCO\_08 (version 20100927) bathymetry data. Georeferenced drone imagery © Save Our Seas Foundation.

## 4.3.2 Sample collection

### 4.3.2.1 Reef manta rays

Small tissue samples (approximately 50 mg;  $n = 50$ ) were collected from the posterior dorsal surface of *M. alfredi* at D'Arros Island in November 2016 ( $n = 13$ ) and November 2017 ( $n = 37$ ) using a biopsy probe mounted onto the end of a modified Hawaiian sling (Couturier et al. 2013a). Individual *M. alfredi* were identified by the unique pigmentation patterns present on their ventral surface (Marshall et al. 2011, Marshall & Pierce 2012) prior to all sampling to ensure that the sex, size and identification number of each animal could be associated with all collected samples and to minimise the likelihood of re-sampling the same individual. Sex was determined from the presence (male) or absence (female) of claspers (Marshall et al. 2009, Ebert et al. 2013). Wingspan (m) was visually estimated to the nearest 0.1 m, and individuals subsequently categorised into one of three life-stage classes indicative of increasing maturity status (Stevens 2016): juvenile ( $\leq 2.4$  m), sub-adult (male, 2.5 – 2.8 m; female, 2.5 – 3.1 m), and adult (male,  $\geq 2.9$  m; female,  $\geq 3.2$  m). The presence of mating scars on females, and the extent of calcification



of the claspers of males, were used as additional aids to assess maturity status (Marshall & Bennett 2010b, Stevens et al. 2018b). Biopsy samples were kept on ice until return to land, where the white muscle of the sample was separated from the skin, and tissues were stored at -20°C. A single sample of *M. alfredi* faeces was also collected opportunistically from a surface-feeding individual at D'Arros Island, and subsequently stored at -20°C.

#### 4.3.2.2 Reef fishes

Samples of the dorsal musculature of 20 fish species, representative of nine trophic guilds ranging from herbivore to carnivore, were collected at D'Arros Island in November 2017 ( $n = 157$ ; Table S 4.1). Species were assigned to trophic guilds based on information about their primary diet obtained from FishBase (Froese et al. 2018). Capture method, mean size (fork length; cm) and diet of each species are summarised in Table S 4.1. Tissue samples of white muscle collected in the field were stored on ice until being stored at -20°C.

#### 4.3.2.3 Zooplankton

Zooplankton samples ( $n_{\text{total}} = 24$ ) were collected from near the surface of the water column around D'Arros Island during the day and at night.

##### 4.3.2.3.1 Pelagic

During the day, zooplankton samples were collected within the uppermost two metres of the water column using a small plankton net towed behind an 18 ft research boat. The net (202  $\mu\text{m}$  mesh, 50 cm diameter; General Oceanics, FL, USA) was deployed when *M. alfredi* were sighted feeding over the reef flats of D'Arros Island or the along the reef edge of the St. Joseph Channel during November 2016 ( $n = 7$ ) and 2017 ( $n = 10$ ), and towed for approximately five minutes at a speed of two knots. The sample contained in the cod-end at the completion of each tow was kept on ice until it was divided into sub-samples using a Folsom plankton sample splitter (Aquatic Research Instruments, ID, USA), and stored at -20°C.

##### 4.3.2.3.2 Emergent

Samples of emergent zooplankton were collected at night using a small light trap constructed from a 300 mL plastic bottle, 200  $\mu\text{m}$  mesh net, and an underwater fishing lure light with a white

LED in November 2017 ( $n = 7$ ). The light trap was deployed 40 m offshore to the north of D'Arros Island at a depth of 2 m at sunset, and retrieved after approximately two and a half hours. The collected zooplankton sample was immediately stored at  $-20^{\circ}\text{C}$ .

#### 4.3.2.4 Seagrass

Seagrass samples (*Thalassodendron ciliatum*,  $n = 10$ ) were collected by hand within the St. Joseph Atoll lagoon in November 2017. Seagrass leaves were removed from the stems and all epiphytes removed from the exterior of the blades prior to storing the samples at  $-20^{\circ}\text{C}$ .

### 4.3.3 Sample processing

Within a month of collection, all samples were lyophilised in an Alpha 1-2 LD Plus freezer dryer (Martin Christ, Germany) for  $69.8 \pm 14.8$  hours and subsequently stored in a desiccator until required. In April 2018, all fish, zooplankton, and seagrass samples were coarsely subdivided and homogenised by hand before being ground to a fine powder using a Mixed Mill MM 200 with 6.4 mm ball bearings in preparation for stable isotope analysis. The single sample of *M. alfredi* faeces was also processed in this manner. No additional extraction procedures were performed on this subset of samples.

Freeze-dried tissue samples of *M. alfredi* were subdivided into 1 x 1 mm cubes by hand using a scalpel blade, but were not ground to a powder because of the sponge-like nature of the freeze-dried tissue. Given the recommendations made in previous studies of stable isotope ratios in elasmobranch tissues (Hussey et al. 2012b, Li et al. 2016, Marcus et al. 2017), lipids and urea were extracted from *M. alfredi* samples following the methodology of Carlisle et al. (2017) and Marcus et al. (2017), respectively. Briefly, subdivided samples were soaked in 2:1 chloroform-methanol solution for 24 hours to remove lipids. After a 24-hour air-drying period, the samples were then oven dried for 48 hours at  $60^{\circ}\text{C}$ . To remove urea, samples were then soaked in 1.5 – 1.8 mL of milliQ water for 72 hours; centrifuging each sample (Centrifuge 5810 R; Eppendorf, Hamburg, Germany) for 3 minutes at 3,000 RPM and replacing the water every 24 hours. At the completion of this process, samples were oven-dried a final time for 48 hours at  $60^{\circ}\text{C}$ .

To examine the effect of the lipid and urea extraction on *M. alfredi* muscle tissue, five samples that were collected in 2017 – four male and one female – were subdivided into quarters. One of four extraction treatments was then applied to each sub-sample. The first sub-sample was exposed to the full extraction treatment described above (lipid and urea extraction; LE + DIW), the second was exposed to only the lipid extraction treatment (LE) and the third to only the urea extraction

treatment (DIW). The last subsample was left untreated as a control according to Marcus et al. (2017).

#### 4.3.4 Stable isotope analysis

All samples were analysed for  $\delta^{15}\text{N}$  and  $\delta^{13}\text{C}$ , using a continuous flow system consisting of a Delta V Plus mass spectrometer connected with a Thermo Flush 1112 via Conflo IV (Thermo-Finnigan, Germany) at the West Australian Biogeochemistry Centre at The University of Western Australia.  $\delta^{15}\text{N}$  and  $\delta^{13}\text{C}$  (parts per million ‰) were used to express stable isotope ratios, with  $\delta^{15}\text{N}$  reported relative to atmospheric  $\text{N}_2$  and  $\delta^{13}\text{C}$  reported relative to the standard reference Vienna Pee Dee Belemnite. Samples were standardised against primary analytical standards from the International Atomic Energy Agency ( $\delta^{13}\text{C}$ : NBS22, USGS24, NBS19, LSVEC;  $\delta^{15}\text{N}$ : N1, N2, USGS32 and laboratory standards). The external error of analyses, calculated as the standard deviation of mean values, was determined to be 0.10‰ for both  $\delta^{15}\text{N}$  and  $\delta^{13}\text{C}$ .

Prior to data analysis, lipid normalisation equations were applied where the reported mean C:N ratios for sampled fauna were  $> 3.5$  (Post et al. 2007), as the presence of lipids in muscle tissue can lead to depleted values of  $\delta^{13}\text{C}$  (Hussey et al. 2012a, Daly et al. 2013). No corrections were required for *M. alfredi* or any of the reef fishes, but zooplankton  $\delta^{13}\text{C}$  values were normalised with the following equation (Syväranta & Rautio 2010, Burgess et al. 2016):

$$\delta^{13}C_{norm} = \delta^{13}C_{bulk} + 7.95 * \left( \frac{(C:N_{bulk} - 3.8)}{C:N_{bulk}} \right)$$

where  $_{norm}$  was the lipid-normalised  $\delta^{13}\text{C}$  value, and  $_{bulk}$  were the unadjusted  $\delta^{13}\text{C}$  values and C:N ratios. The same equation was applied to the sample of *M. alfredi* faeces, given the zooplankton-based diet of this species. Values of  $\delta^{13}\text{C}$  for seagrass samples were not adjusted.

#### 4.3.5 Statistical analyses

One-way ANOVAs were used to investigate the effect of extraction treatment type, sampling year, sex, and life stage on the values of  $\delta^{15}\text{N}$  and  $\delta^{13}\text{C}$  and the ratio of C:N in *M. alfredi* muscle tissue. Tukey's Honestly Significant Difference post hoc tests were used to examine group-specific values when significant differences were observed. Differences between groups were assessed using non-parametric Kruskal-Wallis (KW) tests, where data were shown to be non-normally distributed using Shapiro-Wilk normality tests, or heterogeneous in nature through Levene's tests. Dunn Tests were then used to examine group-specific differences post-hoc.

Similarly, linear models were used to examine the effect of wingspan on values of  $\delta^{15}\text{N}$  and  $\delta^{13}\text{C}$  and the ratio of C:N in *M. alfredi* muscle tissue, and of size on the same values and ratio for the muscle tissue of reef fishes. Where data were found to be non-normally distributed, Spearman's ranked-order correlation coefficients were used. All analyses were conducted in R (version 3.4.1; R Core Team 2017) and variation around the mean presented as standard deviation unless otherwise stated. Significance for all analyses was  $p < 0.05$ .

The packages *SIBER* (Jackson et al. 2011) and *nicheROVER* (Lysy et al. 2014) were used to assess the level of trophic niche overlap that occurred between male and female *M. alfredi* as described by Shipley et al. (2018). Values of  $\delta^{13}\text{C}$  and  $\delta^{15}\text{N}$  for both sexes were compared using a bi-plot, and the total area of the convex hull (TA) and core trophic niche area with small sample size correction ( $\text{SEA}_c$ ) for each sex calculated using *SIBER*. Total trophic overlap values for 95% TA were calculated using *nicheROVER*. This latter analysis is insensitive to sample size and incorporates a statistical uncertainty using Bayesian methods that differs from more traditional, geometric-based computations regarding trophic niche space (Swanson et al. 2015, Shipley et al. 2018).

Estimates of relative trophic position (TL) for *M. alfredi* were calculated using the following equation (Post 2002, Burgess & Bennett 2016):

$$\text{TL} = \left( \frac{(\delta^{15}\text{N}_{\text{consumer}} - \delta^{15}\text{N}_{\text{base}})}{\text{DTDF}} \right) + 2$$

where  $\delta^{15}\text{N}_{\text{consumer}}$  was the  $\delta^{15}\text{N}$  value for *M. alfredi*, and  $\delta^{15}\text{N}_{\text{base}}$  represented the weighted average value of  $\delta^{15}\text{N}$  for all pelagic and emergent zooplankton samples combined. The integer value of '2' was used to reflect the baseline trophic level of the zooplankton samples that were composed predominantly of primary consumers (TL = 2; Hussey et al. 2014, Burgess et al. 2016). To account for the sensitivity of TL estimations to assumptions regarding the trophic fractionation of  $\delta^{15}\text{N}$ , two estimates of TL were generated for *M. alfredi* using diet-tissue discrimination factors (DTDFs) calculated previously for other elasmobranch species (Burgess et al. 2016). The first estimate was based upon a DTDF of 2.3‰ as calculated for *Carcharias taurus* and *Negaprion brevirostris* muscle (Hussey et al. 2010), and the second based upon a DTDF of 3.7‰ as calculated for muscle of *Triakis semifasciata* (Kim et al. 2012a).

Estimates of trophic enrichment between *M. alfredi* and both pelagic and emergent zooplankton samples were calculated using the following equation (Couturier et al. 2013a):

$$\Delta X = \delta X_{\text{predator}} - \delta X_{\text{prey}}$$

where X represented either  $\delta^{15}\text{N}$  or  $\delta^{13}\text{C}$ , and using both bulk and lipid-normalised  $\delta^{13}\text{C}$  values.

Lastly, Bayesian stable isotope mixing models were constructed to determine the potential contribution of different prey sources to the diet of *M. alfredi* using the *simmr* package (Parnell 2016) in R. Other studies of the trophic ecology of both *M. alfredi* and *M. birostris* have suggested that demersal and/or mesopelagic organisms may form a key component of their diet (Couturier et al. 2013a, Burgess et al. 2016, Stewart et al. 2017). As we could not sample mesopelagic zooplankton, in this analysis, we included stable isotope data from four species of small (35.3 – 69.3 mm total length) mesopelagic fishes (*Ceratoscopelus warmingii*,  $n = 20$ ; *Diaphus splendidus*,  $n = 15$ ; *Notoscopelus caudispinosus*,  $n = 13$ ; *Vinciguerra nimbaria*,  $n = 8$ ) that were collected within the Indian South Subtropical Gyre for another study (Annasawmy et al. 2018). Each of the four species have distributions encompassing the Seychelles region and equivalent trophic positions to that of primary and secondary copepod consumers (TL = 2.1 – 2.9; Hannides et al. 2009). Mesopelagic fishes have been shown to display strong isotopic similarity to mesopelagic zooplankton (Valls et al. 2014), allowing their use as representative mesopelagic organisms in the absence of zooplankton samples (Burgess et al. 2016). The selected species had an overall mean  $\delta^{15}\text{N}$  value of  $8.23 \pm 1.27\text{‰}$  and overall mean  $\delta^{13}\text{C}$  value of  $-18.33 \pm 0.39\text{‰}$ .

The final mixing models included three potential prey sources for *M. alfredi*; pelagic and emergent zooplankton, and mesopelagic prey sources. Data for pelagic and emergent zooplankton collected at D'Arros Island were not pooled as there were significant differences between their values of  $\delta^{15}\text{N}$  and  $\delta^{13}\text{C}$ . We constructed two versions of our mixing models to overcome uncertainty in the importance of dietary lipid content and in the lipid normalisation procedures applied to the zooplankton data. The first model used the non-normalised values of  $\delta^{13}\text{C}$  for the zooplankton groups, and the second, the lipid normalised values of  $\delta^{13}\text{C}$ . Both models incorporated the DTDFs of Couturier et al. (2013) for *M. alfredi* – 1.3‰ for  $\delta^{13}\text{C}$  and 2.4‰ for  $\delta^{15}\text{N}$  – and accounted for the variation that has been observed in measurements of these values in elasmobranchs during lab-based experiments by introducing a standard deviation of 1‰ for both isotopes (Hussey et al. 2010, Kim et al. 2012a, Stewart et al. 2017). The average between the two mixing models was taken as the final estimated contribution of the three prey sources to the diet of *M. alfredi*.

## 4.4 Results

### 4.4.1 Extraction treatment effects

Lipid and urea extraction had a significant effect on values of  $\delta^{15}\text{N}$  and  $\delta^{13}\text{C}$ , and the ratios of C:N of *M. alfredi* muscle tissue (Kruskal-Wallis test,  $H(3) = 11.983$ ,  $p = 0.007$ ; Kruskal-Wallis test,  $H(3) = 10.440$ ,  $p = 0.015$ ; ANOVA,  $F(3,16) = 220.601$ ,  $p < 0.001$ , respectively). Untreated muscle tissue samples were found to have significantly lower  $\delta^{15}\text{N}$  values than the DIW, LE and

LE+DIW treatment groups, which did not differ significantly from one another (Figure 4.2A). The untreated control group was found to have similar values of  $\delta^{13}\text{C}$  to that of the LE and LE+DIW treatments, but these values were significantly higher than the  $\delta^{13}\text{C}$  values of the DIW treatment. Values of  $\delta^{13}\text{C}$  for the DIW and LE+DIW treatments did not differ significantly (Figure 4.2B). Values of  $\delta^{13}\text{C}$  encompassed an overall range of 1.09‰. The C:N ratios of the untreated muscle tissue samples of *M. alfredi* were significantly lower than those of the DIW, LE, and LE+DIW treatment groups. Ratios of C:N did not differ between the LE and LE+DIW treatments, but these two treatments had ratios that were significantly lower than the DIW treatment and higher than the control (Figure 4.2C). Ratios of C:N for the control and DIW treatments differed significantly.

## 4.4.2 Stable isotopes

### 4.4.2.1 Reef manta rays

The effect of sampling year, sex, life stage and wingspan on isotope composition was investigated for *M. alfredi* using stable isotope data collected from the set of 50 samples included in the LE+DIW treatment (Table S 4.2). Values of  $\delta^{15}\text{N}$  and  $\delta^{13}\text{C}$  differed significantly among *M. alfredi* muscle tissues collected in November 2016 ( $n = 13$ ) and 2017 ( $n = 37$ ). Values of  $\delta^{15}\text{N}$  were lower in 2016 than in 2017, whereas values of  $\delta^{13}\text{C}$  were more enriched. Consequently, ratios of C:N were lower in 2016 than in 2017 (Kruskal-Wallis tests,  $H(1) = 12.321$ ,  $P < 0.001$ ;  $H(1) = 14.821$ ,  $P < 0.001$ ;  $H(1) = 12.162$ ,  $P < 0.001$ , respectively; Figure 4.3), and all subsequent analyses considered isotope data relative to year of collection.

Values of  $\delta^{15}\text{N}$  and  $\delta^{13}\text{C}$  and ratios of C:N did not differ significantly between males (wingspan 2.1 – 3.6 m) and females (wingspan 2.4 m – 3.8 m) in 2016 or 2017 (ANOVA,  $F(1,11) = 0.991$ ,  $P = 0.341$ ;  $F(1,11) = 0.153$ ,  $P = 0.904$ ;  $F(1,11) = 0.002$ ,  $P = 0.967$ ; ANOVA,  $F(1,34) = 3.456$ ,  $P = 0.072$ ; Kruskal-Wallis test,  $H(1) = 0.146$ ,  $P = 0.702$ ; Kruskal-Wallis test,  $H(1) = 0.584$ ,  $P = 0.445$ , respectively). Males, however, displayed lower amounts of variation in all values than females (Table S 4.2).

The similarity in  $\delta^{15}\text{N}$  and  $\delta^{13}\text{C}$  values for male and female *M. alfredi* was confirmed by trophic overlap analyses. The trophic niche of females overlapped with 71.6% and 51.6% of that of males in November 2016 and 2017, respectively, whereas the trophic niche of males overlapped with 78.1% and 89.3% of the niche of females during November 2016 and 2017, respectively (Figure S 4.1). Females were found to have higher TA and  $\text{SEA}_c$  values in comparison to males during both sampling years, with the exception of  $\text{SEA}_c$  in 2016, which was slightly lower (Table S 4.3).

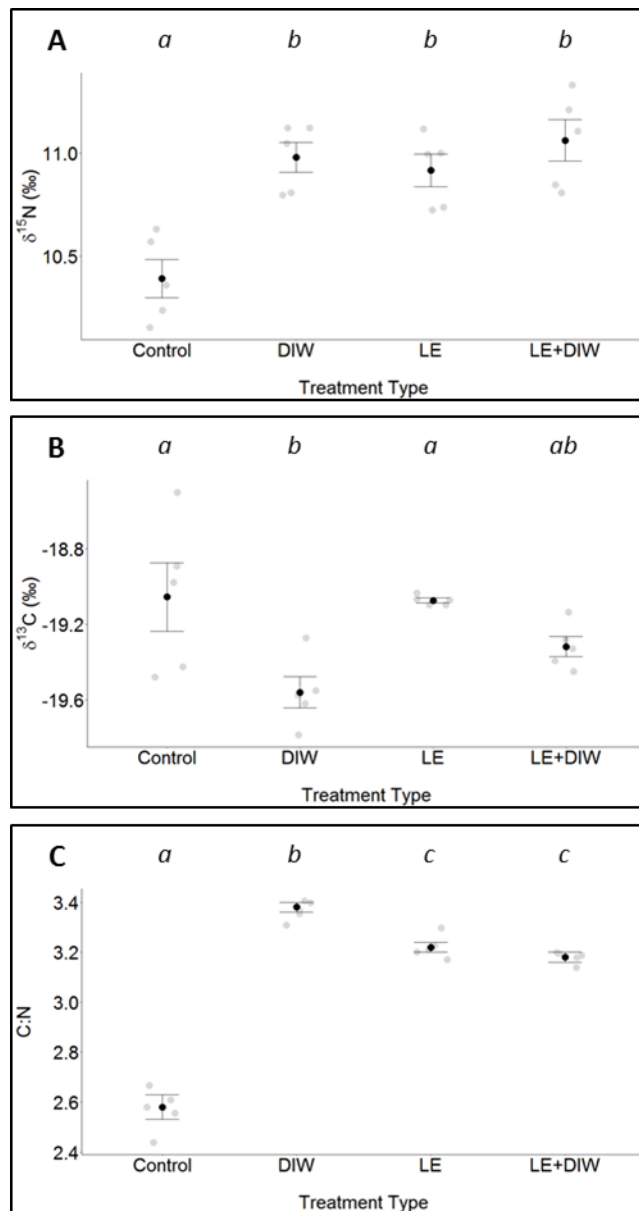


**Figure 4.2** Comparison of urea and lipid extraction treatment effects on the mean values  $\pm$  S.E. of  $\delta^{15}\text{N}$  (A),  $\delta^{13}\text{C}$  (B) and C:N (C) ratios of reef manta ray (*Mobula alfredi*) muscle tissue samples. Treatments with different letters are significantly different ( $p < 0.05$ ). Control, untreated; DIW, urea extraction only; LE, lipid extraction only; LE+DIW, lipid and urea extraction.

Life stage did not influence values of  $\delta^{15}\text{N}$ ,  $\delta^{13}\text{C}$ , or ratios of C:N for *M. alfredi* in 2016 or 2017 ( $P > 0.05$ ), whereas wingspan was found only to influence values of  $\delta^{15}\text{N}$  in 2017 (Spearman Rank Correlation,  $r_s = -0.334$ ,  $P = 0.047$ ). In November 2017,  $\delta^{15}\text{N}$  tended to be lower for individuals with larger wingspans in 2017, however, these values did not vary to the extent that the C:N ratio for *M. alfredi* also differed during this sampling year.

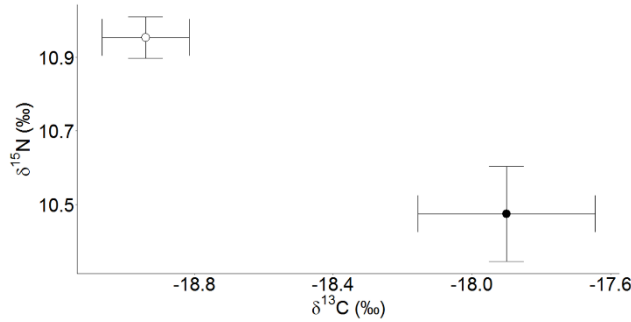


**Figure 4.3** Isoscape of  $\delta^{15}\text{N}$  and  $\delta^{13}\text{C}$  values for reef manta ray (*Mobula alfredi*) muscle tissue collected in 2016 (black,  $n = 13$ ) and 2017 (white,  $n = 36$ ) at D'Arros Island, Seychelles.

#### 4.4.2.2 Reef fishes

Of the 20 fish species sampled in this study, significant relationships between size and values of  $\delta^{15}\text{N}$ ,  $\delta^{13}\text{C}$ , and ratios of C:N were identified across seven species (Table 4.1). Values of  $\delta^{15}\text{N}$  increased significantly with size in three species: *Aethaloperca rogoa*, *Scarus rubroviolaceus*, and *Thunnus albacares* (Linear regression,  $r^2 = 0.591$ ,  $F(1,6) = 8.667$ ,  $P = 0.026$ ;  $r^2 = 0.525$ ,  $F(1,7) = 7.731$ ,  $P = 0.027$ ;  $r^2 = 0.673$ ,  $F(1,6) = 12.38$ ,  $P = 0.013$ ). Similarly, values of  $\delta^{13}\text{C}$  increased significantly with size in four species: *Chaetodon trifasciatus*, *Chlorurus sordidus*, *Lethrinus lentjan*, and *Selar crumenophthalmus* (Linear regression,  $r^2 = 0.739$ ,  $F(1,8) = 22.619$ ,  $P = 0.001$ ;  $r^2 = 0.527$ ,  $F(1,8) = 8.925$ ,  $P = 0.017$ ;  $r^2 = 0.408$ ,  $F(1,8) = 9.248$ ,  $P = 0.047$ ;  $r^2 = 0.564$ ,  $F(1,8) = 10.353$ ,  $P = 0.012$ , respectively). Ratios of C:N increased with size in two species i.e. *Lethrinus lentjan* and *Lutjanus bohar* (Linear regression,  $r^2 = 0.536$ ,  $F(1,8) = 9.248$ ,  $P = 0.016$ ; Spearman Rank Correlation,  $r_s = 0.906$ ,  $P < 0.001$ ).

#### 4.4.2.3 Zooplankton

Pelagic samples from net tows were dominated by calanoid copepods (Figure 4.4A), with one sample showing an abundance of fish eggs (Figure 4.4B) and another of crab zoea (Figure 4.4C). Emergent samples were more variable in composition, with dominant species across samples including ostracods, polychaetes, and crab megalopae (Figure 4.4D-F, respectively).

Values of  $\delta^{15}\text{N}$  and  $\delta^{13}\text{C}$  for pelagic zooplankton samples differed between collection years. Values of  $\delta^{15}\text{N}$  were larger in 2016 than 2017 ( $8.439 \pm 0.401$  and  $7.185 \pm 0.340\text{‰}$ , respectively; ANOVA,  $F(1,15) = 48.727$ ,  $P < 0.001$ ). Values of  $\delta^{13}\text{C}$  were more enriched in 2017 than in 2016 ( $-21.410 \pm 1.560$  and  $-22.476 \pm 0.380\text{‰}$ , respectively; Kruskal-Wallis test,  $H(1) = 9.482$ ,  $P =$



0.002). Ratios of C:N did not differ significantly between years (Kruskal-Wallis test,  $H(1) = 1.120$ ,  $P = 0.290$ ).

Furthermore, values of  $\delta^{15}\text{N}$  and  $\delta^{13}\text{C}$  also differed between samples of pelagic and emergent zooplankton collected in November 2017 (ANOVA,  $F(1,14) = 87.746$ ,  $P < 0.001$ ; Kruskal-Wallis test,  $H(1) = 7.868$ ,  $P = 0.005$ , respectively), with the former having higher concentrations of both isotopes than the latter (Table 4.1). Ratios of C:N were similar between these groups ( $P > 0.05$ ).

**Table 4.1** Summary of values of  $\delta^{15}\text{N}$ ,  $\delta^{13}\text{C}$  and C:N (mean  $\pm$  S.D.) ratios reported for reef manta ray (*Mobula alfredi*), reef fishes, zooplankton and seagrass sampled at D'Arros Island and St. Joseph Atoll, Seychelles. Values in bold indicate presence of a significant relationship between isotope composition and size in fishes (fork length, cm) are highlighted in bold. Asterisks indicate lipid-adjusted  $\delta^{13}\text{C}$  values.

Sample Type	Trophic Guild	Species	n	$\delta^{15}\text{N}$ (‰)	$\delta^{13}\text{C}$ (‰)	C:N
<i>Mobula alfredi</i>	Planktivore	<i>Mobula alfredi</i> (tissue)	50	10.82 $\pm$ 0.42	-18.64 $\pm$ 0.93	3.13 $\pm$ 0.16
		<i>Mobula alfredi</i> (faeces)*	1	7.88	-21.95	2.79
Reef Fishes	Herbivore	<i>Chlorurus sordidus</i>	10	9.24 $\pm$ 0.35	<b>-14.62 <math>\pm</math> 1.32</b>	3.20 $\pm$ 0.08
		<i>Scarus rubroviolaceus</i>	9	<b>9.74 <math>\pm</math> 0.25</b>	-17.04 $\pm$ 1.14	3.16 $\pm$ 0.03
	Detritivore	<i>Crenimugil crenilabis</i>	10	8.17 $\pm$ 1.05	-10.70 $\pm$ 0.53	3.19 $\pm$ 0.03
		Planktivore	<i>Caesio teres</i>	10	11.90 $\pm$ 0.18	-19.17 $\pm$ 0.42
	<i>Caesio xanthonota</i>		10	11.56 $\pm$ 0.13	-19.65 $\pm$ 0.45	3.30 $\pm$ 0.19
	<i>Pterocaesio tile</i>		1	11.37	-19.57	3.13
	Corallivore	<i>Chaetodon trifasciatus</i>	10	10.69 $\pm$ 0.33	<b>-15.23 <math>\pm</math> 0.65</b>	3.21 $\pm$ 0.03
	Invertivore	<i>Lethrinus enigmaticus</i>	7	13.42 $\pm$ 0.43	-17.75 $\pm$ 1.04	3.34 $\pm$ 0.18
		<i>Lethrinus lentjan</i>	10	13.19 $\pm$ 0.40	<b>-18.09 <math>\pm</math> 0.91</b>	<b>3.34 <math>\pm</math> 0.26</b>
		<i>Lethrinus nebulosus</i>	10	12.32 $\pm$ 0.65	-16.71 $\pm$ 2.32	3.30 $\pm$ 0.17
	Reef Carnivore	<i>Parupeneus macronemus</i>	10	11.65 $\pm$ 0.92	-17.85 $\pm$ 1.95	3.21 $\pm$ 0.07
		<i>Cephalopholis sonnerati</i>	2	13.51 $\pm$ 0.21	-19.24 $\pm$ 0.00	3.21 $\pm$ 0.01
		<i>Variola louti</i>	10	13.50 $\pm$ 0.23	-18.91 $\pm$ 0.34	3.23 $\pm$ 0.05
	Reef Piscivore	<i>Aethaloperca rogae</i>	8	<b>13.17 <math>\pm</math> 0.38</b>	-18.31 $\pm$ 0.50	3.20 $\pm$ 0.03
		<i>Cephalopholis miniata</i>	1	12.66	-19.03	3.16
<i>Lutjanus bohar</i>		10	12.98 $\pm$ 0.34	-18.59 $\pm$ 0.72	<b>3.25 <math>\pm</math> 0.06</b>	
Reef & Pelagic Piscivore	<i>Selar crumenophthalmus</i>	10	12.23 $\pm$ 0.30	<b>-19.44 <math>\pm</math> 0.36</b>	3.17 $\pm$ 0.02	
Pelagic Piscivore	<i>Katsuwonus pelamis</i>	5	12.66 $\pm$ 0.22	-19.53 $\pm$ 0.50	3.16 $\pm$ 0.07	
	<i>Sarda orientalis</i>	1	12.86	-19.46	3.54	
	<i>Thunnus albacares</i>	8	<b>12.28 <math>\pm</math> 0.25</b>	-19.50 $\pm$ 0.41	3.10 $\pm$ 0.02	
Zooplankton	Pelagic*	17	7.78 $\pm$ 0.74	-20.92 $\pm$ 1.97	2.70 $\pm$ 0.27	
	Emergent*	7	9.29 $\pm$ 0.56	-16.79 $\pm$ 1.51	1.82 $\pm$ 0.22	
Seagrass		<i>Thalassodendron ciliatum</i>	10	2.27 $\pm$ 0.79	-10.78 $\pm$ 1.13	24.27 $\pm$ 2.47

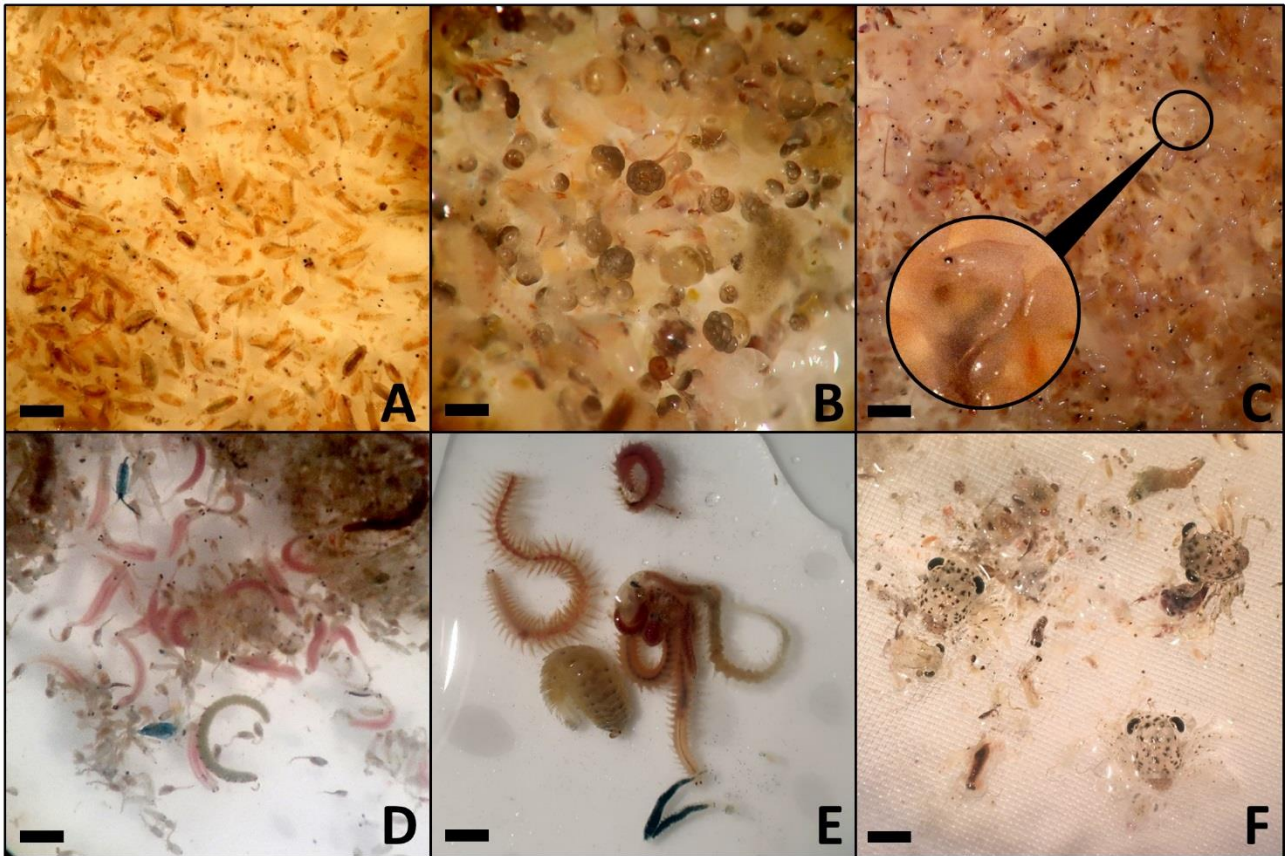


**Figure 4.4** Photographs of representative pelagic (A-C) and emergent (D-F) zooplankton samples collected at D'Arros Island, Seychelles. Pelagic samples were collected during daylight hours using a towed plankton-net and were dominated by copepods (A), fish-eggs (B), and crab zoea (C). Emergent samples were collected using a light trap deployed after sunset for 2.5 hours and were dominated by polychaetes and ostracods (D), polychaete worms (E), and crab megalopae (F). Scale bar (approximate sizes; a-f): 1 mm, 0.5 mm, 1 mm, 2 mm, 2 mm, 2 mm.

**Table 4.2** Outputs of mixing models estimating the proportional contribution ( $\pm$  S.D.) of pelagic and emergent zooplankton and mesopelagic sources to the diet of reef manta rays (*Mobula alfredi*) at D'Arros Island, Seychelles, based on samples collected in November 2017. Model 1 used bulk  $\delta^{13}\text{C}$  values of zooplankton samples, whereas Model 2 used values mathematically normalised for lipids. Both models assumed a diet-tissue discrimination factor (DTDF) of  $2.3 \pm 1.0$  ‰. The mean values were calculated as an average between the two mixing models.

Source	Model 1	Model 2	Mean
Emergent Zooplankton	$0.41 \pm 0.06$	$0.34 \pm 0.07$	<b><math>0.38 \pm 0.07</math></b>
Pelagic Zooplankton	$0.43 \pm 0.04$	$0.47 \pm 0.05$	<b><math>0.45 \pm 0.05</math></b>
Mesopelagic Sources	$0.16 \pm 0.06$	$0.19 \pm 0.08$	<b><math>0.17 \pm 0.07</math></b>
s.d. $\delta^{13}\text{C}$	$0.26 \pm 0.20$	$0.75 \pm 0.48$	<b><math>0.50 \pm 0.34</math></b>
s.d. $\delta^{15}\text{N}$	$0.13 \pm 0.10$	$0.16 \pm 0.12$	<b><math>0.14 \pm 0.11</math></b>

### 4.4.3 Feeding ecology of reef manta rays at D'Arros Island

The relative trophic position of all taxa was visualised using an isoscape comparing the values of  $\delta^{13}\text{C}$  to those of  $\delta^{15}\text{N}$  (Figure 4.5). The trophic level of *M. alfredi* was 2.92 (i.e. TL = ~ 3; secondary consumer; Hussey et al. 2014) after estimates using the conservative (2.3‰; TL = 3.13) and maximum (3.7‰; TL = 2.70) DTDF were averaged. The sample of *M. alfredi* faecal tissue closely aligned with that of the pelagic zooplankton samples. Muscle tissue samples of *M. alfredi* were positioned in a unique isotopic space within the isoscape, aligning closely with the zooplanktivorous and mesopelagic fishes, as well as emergent zooplankton. Values of  $\delta^{13}\text{C}$  for muscle tissue samples of *M. alfredi* were more enriched than those of the other zooplanktivorous fishes sampled in this study, and were similar to those of the benthic invertivore, *Parupeneus macronemus*.

Average enrichment values between *M. alfredi* and bulk emergent zooplankton samples was 1.53‰ and -0.39‰ for  $\delta^{15}\text{N}$  and  $\delta^{13}\text{C}$ , respectively. When lipids were mathematically normalised for emergent samples, the  $\delta^{13}\text{C}$  enrichment value decreased to -1.85‰. For bulk pelagic zooplankton samples, average enrichment values for *M. alfredi* were 3.05‰ and 3.27‰ for  $\delta^{15}\text{N}$  and  $\delta^{13}\text{C}$ , respectively. Following mathematical lipid normalisation, the value of  $\delta^{13}\text{C}$  decreased to 2.28‰. For both mixing models, pelagic zooplankton was the dominant contributor (around 45%) to the diet of *M. alfredi* (Table 4.2) and emergent zooplankton (~38%) contributed a larger proportion of the diet than mesopelagic sources (~17%; Figure 4.6).

## 4.5 Discussion

*M. alfredi* fed predominantly on pelagic zooplankton that accumulated at the surface of the water column (approximately 50% of diet). Emergent and mesopelagic zooplankton contributed a smaller, but significant proportion of the diet (38 and 17%, respectively). The observed pattern of foraging was consistent between sexes and the majority of individuals, and placed *M. alfredi* within a unique trophic niche relative to the other reef fishes sampled at D'Arros Island.

### 4.5.1 Feeding ecology of reef manta rays

Mean nitrogen enrichment values indicated that *M. alfredi* at D'Arros Island occupy a trophic level of approximately 3, a level representative of a secondary consumer as was expected for this zooplanktivore (Couturier et al. 2013a, Hussey et al. 2014, Stewart et al. 2016a). The average

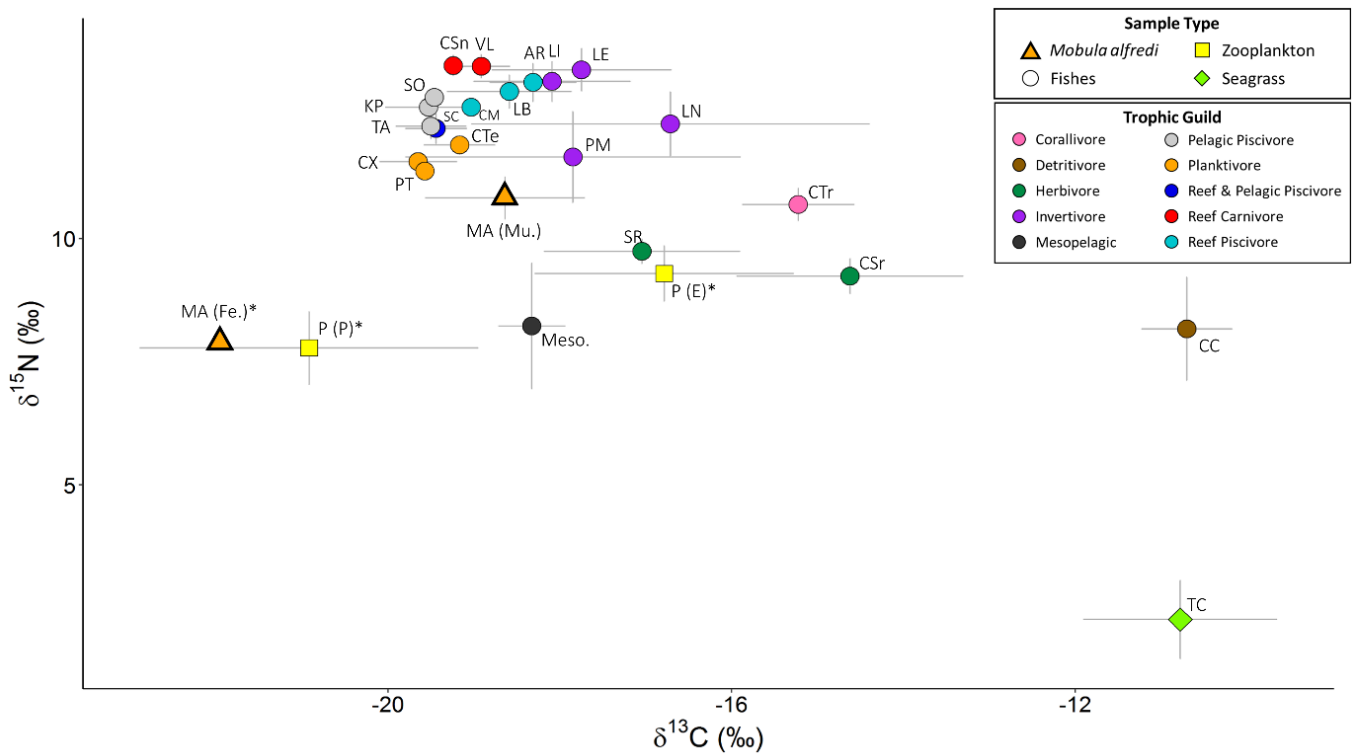


**Figure 4.5** Mean values  $\pm$  S.D. of  $\delta^{13}\text{C}$  and  $\delta^{15}\text{N}$  for samples of reef manta ray (*Mobula alfredi*), 20 species of fishes, zooplankton and seagrass collected at D'Arros Island and St. Joseph Atoll, Seychelles. Representative mean values of mesopelagic fishes (Meso.) sampled in the Western Indian Ocean are also included. Figure legend outlines allocation of symbols to sample types and colours to trophic guild of sampled fish species. Asterisks represent lipid-normalised  $\delta^{13}\text{C}$  values. *Mobula alfredi*: faeces, MA (Fe.)\*; muscle, MA (Mu.). Fishes: *Aethaloperca rogae*, AR; *Caesio teres*, CTe; *Caesio xanthonota*, CX; *Cephalopholis miniata*, CM; *Cephalopholis sonnerati*, CSn; *Chaetodon trifasciatus*, CTr; *Chlorurus sordidus*, CSr; *Crenimugil crenilabis*, CC; *Katsuwonus pelamis*, KP; *Lethrinus enigmaticus*, LE; *Lethrinus lentjan*, LL; *Lethrinus nebulosus*, LN; *Lutjanus bohar*, LB; Mesopelagic, Meso.; *Parupeneus macronemus*, PM; *Pterocaesio tile*, PT; *Sarda orientalis*, SO; *Scarus rubroviolaceus*, SR; *Selar crumenophthalmus*, SC; *Thunnus albacares*, TA; *Variola louti*, VL. Zooplankton: emergent, P (E)\*; pelagic, P (P)\*. Seagrass: *Thalassodendron ciliatum*, TC.

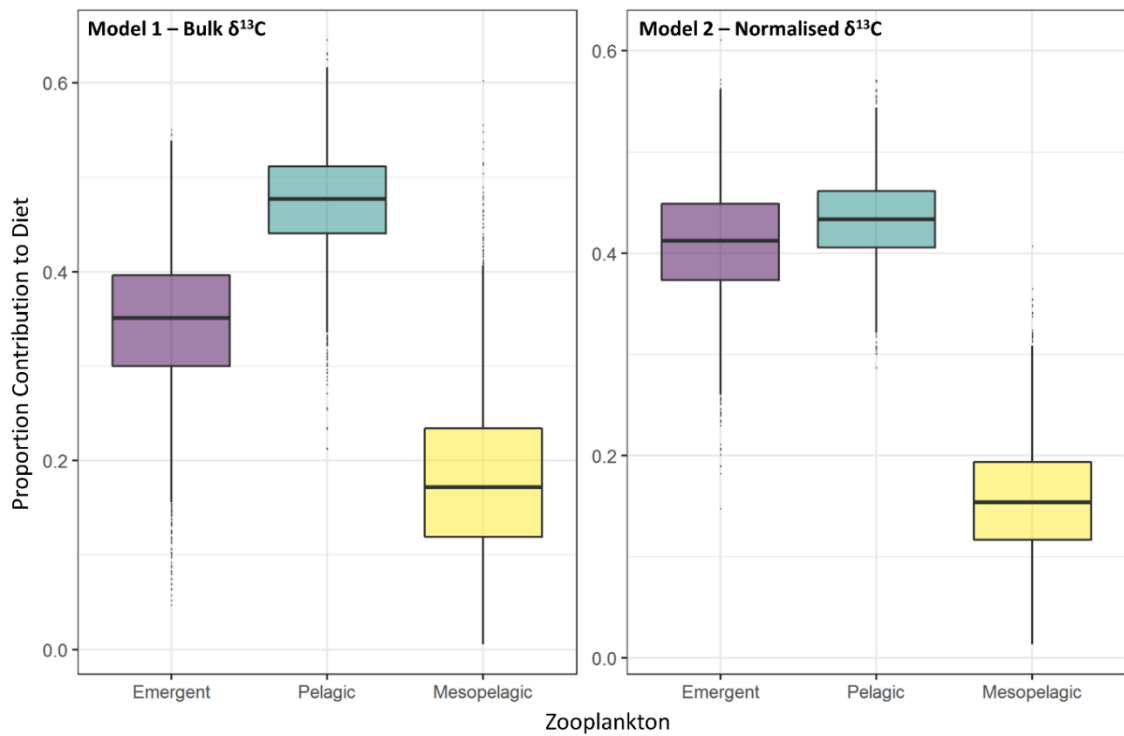


**Figure 4.6** Estimated contribution of emergent and pelagic zooplankton, and mesopelagic sources (purple, blue and yellow, respectively), to the diet of the reef manta ray (*Mobula alfredi*) at D'Arros Island and St. Joseph Atoll, Seychelles, in 2017. Proportions estimated using two Bayesian stable isotope mixing models that assumed a diet-tissue discrimination factor (DTDF) of  $2.3 \pm 1.0$  ‰ and included either bulk (Model 1) or lipid-normalised (Model 2)  $\delta^{13}\text{C}$  values. The central box spans the 2.5 – 97.5% confidence intervals and the middle line denotes the median.

enrichment value for  $\delta^{15}\text{N}$  of 2.92‰ was close to that of 2.4‰ calculated for *M. alfredi* on the Great Barrier Reef (Couturier et al. 2013a) and places *M. alfredi* within the range of DTDFs estimated for other elasmobranchs (2.29‰ for *C. taurus* and *N. brevirostris*, and 3.7‰ for *T. semifasciata*) (Hussey et al. 2010, Kim et al. 2012a, Kim et al. 2012b).

The values of  $\delta^{13}\text{C}$  in *M. alfredi* muscle tissues after lipid and urea extraction (LE+DIW) fell between those of the lipid-normalised pelagic and emergent zooplankton groups with enrichment values of -2.28‰ and -1.85‰, respectively. Isotopic signatures of carbon for *M. alfredi* were similar to those of planktivorous fishes, a benthic invertivore (*P. macronemus*), and mesopelagic zooplankton. These results suggest that *M. alfredi* may have periods of residency (often several months) in reef environments, followed by excursions between reefs into the open-ocean and movements throughout the water column (Braun et al. 2014, Jaine et al. 2014, Peel et al. 2019b).

Values of  $\delta^{15}\text{N}$  and  $\delta^{13}\text{C}$  for *M. alfredi* muscle tissue were significantly different between collection years, likely reflecting a shift in the zooplankton community structure at D'Arros Island during this time and subsequently, prey availability to *M. alfredi* (Giering et al. 2018, Benedetti et al. 2019). Within each year, values of  $\delta^{15}\text{N}$  and  $\delta^{13}\text{C}$  did not vary between the sexes, although females tended to display more variation in both isotopic concentrations. This suggests that female *M. alfredi* may forage upon a more diverse assemblage of prey items than males. In 2017, the values of  $\delta^{15}\text{N}$  for *M. alfredi* were found to decrease with increasing wingspan. Given that the level of residency displayed by *M. alfredi* to D'Arros Island decreases with increasing wingspan (Peel et al. 2019b), it is possible that this result reflects the tendency for larger individuals (mostly females) to seek alternative foraging opportunities offshore of D'Arros Island and consume zooplankton communities that occupy lower trophic positions (Giering et al. 2018).

#### 4.5.2 Zooplankton as prey for reef manta rays

Pelagic zooplankton were found to constitute the largest proportion (45%) of the diet of *M. alfredi* at D'Arros Island. The coral reefs surrounding these locations are one of the few locations in Seychelles where *M. alfredi* are known to aggregate predictably year-round (Peel et al. 2019b), and individuals are regularly sighted surface-feeding during daylight hours. This is particularly true within the St. Joseph Channel (Figure 4.1), where pelagic zooplankton is observed to accumulate along current lines (L. Peel, unpub. data). The isotopic similarity between faeces of *M. alfredi* and pelagic zooplankton reported here confirms that *M. alfredi* are consuming these communities at D'Arros Island, and estimates from faeces are likely representative of a very recent feeding event (possibly within 24 h of sampling). Similar observations of *M. alfredi* feeding on pelagic zooplankton at the surface during the day have been reported at other aggregation sites around the world (Clark 2010, Anderson et al. 2011a, Couturier et al. 2011,

Papastamatiou et al. 2012, Armstrong et al. 2016, Stevens et al. 2018a). *M. alfredi* have also been observed foraging during the day on demersal zooplankton in the Maldives (Stevens et al. 2018a), and on the Great Barrier Reef. In the latter locality, demersal zooplankton constitute a significant proportion of the diet (Couturier et al. 2013a). Such benthic-oriented feeding behaviours have, however, not been observed for *M. alfredi* at D'Arros Island during the day (L. Peel, unpub. data). Taken together, the observations reported here and the results of the isotopic mixing models suggest that pelagic zooplankton comprises the majority of the diet of *M. alfredi* at D'Arros Island.

The feeding behaviour of *M. alfredi* on pelagic zooplankton in the St. Joseph Channel may serve to increase nutrient cycling over the reefs of D'Arros Island as a whole, and enhance nutrient enrichment in particular places within the reef. After feeding on zooplankton, *M. alfredi* frequently return to cleaning stations on coral reefs for parasite removal, to socialise, and possibly to thermoregulate (O'Shea et al. 2010, Couturier et al. 2018, Stevens et al. 2018b). Defecation is often observed at these shallow (< 30 m) cleaning stations (Figure S 4.2), where the water temperature can be warmer than the surrounding habitat, possibly increasing the speed of digestion (Papastamatiou et al. 2015b, Stevens et al. 2018a). At D'Arros Island, this could result in the transfer of nutrients from St. Joseph Channel to the reef slope, with positive impacts on coral growth. Similar impacts of nutrient enrichment on coral growth have been reported for reef fishes and sharks (Meyer et al. 1983, Papastamatiou et al. 2015a, Allgeier et al. 2017, Williams et al. 2018), and for schools of small planktivorous fishes that shelter in individual coral heads (Shantz et al. 2015). The high residency and frequent use of cleaning stations by *M. alfredi* at reefs around D'Arros Island identified through acoustic telemetry (Peel et al. 2019b) and photo-identification (L. Peel, unpub. data), increases the significance of such nutrient cycling processes to these reefs.

Emergent zooplankton were estimated to comprise approximately 38% of the diet of *M. alfredi*, suggesting that the species – unlike diurnal zooplanktivorous fishes (Carpenter 1988) – also forages along the reef at D'Arros Island at night. The value of  $\delta^{13}\text{C}$  for *M. alfredi* was close to that of the invertivore, *P. macronemus*, which forages on benthic invertebrates in sand along reef edges during the day (< 40 m; Randall 2004, Rajan et al. 2012). This apparently contradictory result can be explained by the fact that the same communities consumed by benthic invertivores during the day emerge at dusk to occupy the water column, where they can become prey for *M. alfredi*. While it is possible that emergent zooplankton originating from the St. Joseph Atoll lagoon may also contribute slightly to this demersal signature, acoustic telemetry and visual observations indicate that *M. alfredi* rarely enter this habitat (Peel et al. 2019b). In contrast to the feeding behaviour of *M. alfredi* within the lagoon at Palmyra Atoll (McCauley et al. 2014), this suggests that foraging by *M. alfredi* on the emergent zooplankton community at D'Arros Island is restricted to the reef flats surrounding this location.

The emergence of benthic zooplankton from sediment and the reef at night is thought to influence the movement and foraging behaviour of *M. alfredi* in many locations, including eastern Australia (Couturier et al. 2013a, Couturier et al. 2018), Hawaii (Deakos et al. 2011), Indonesia (Setyawan et al. 2018) and Seychelles (Peel et al. 2019b). The ability to forage throughout a full diel cycle may be necessary in order for these relatively large animals to obtain sufficient food resources to satisfy metabolic requirements in the warm surface waters of a coral reef (Meekan et al. 2015). In contrast to *M. alfredi*, smaller planktivorous fishes tend to be either diurnal (e.g. caesionids, pomacentrids) or nocturnal (e.g. holocentrids, apogonids), and subsequently only forage during half of the day. The extended periods of foraging undertaken by *M. alfredi* may therefore serve to increase nutrient cycling in the reef environment over larger temporal scales, particularly at cleaning sites within the reef, where nutrient supply is expected to be enhanced.

In addition to nutrient cycling within reef systems, the possible contribution of mesopelagic zooplankton to the diet of *M. alfredi* (approximately 17%) highlights the potential for this species to act as a vector for horizontal nutrient transport between coastal and mesopelagic ecosystems. In comparison to the local-scale nutrient supply occurring across the reefs at D'Arros Island (< 1 km), the transport of nutrients derived from mesopelagic origins is estimated to occur over larger distances (> 10 km). Mesopelagic zooplankton communities perform diel vertical migrations involving movements from depths (> 200 m) during the day to shallow surface waters (< 50 m) during the night (Hays 2003). Feeding on these communities would require travel by *M. alfredi* either 10 km to the east or 20 km to the west of D'Arros Island to waters beyond the shelf edge. Such distances fall well below the maximum reported range of travel for *M. alfredi* within a 24 hour period (89.3 km d<sup>-1</sup>) (Peel et al. 2019b), and would be reduced should the mesopelagic zooplankton community migrate horizontally over the Amirantes Bank and towards D'Arros Island during the night (Benoit-Bird & Au 2002). Although the frequency at which such ventures occur cannot be assessed here, such movement behaviour could provide *M. alfredi* with additional feeding opportunities, or supplement foraging when food availability around D'Arros Island is scarce (Braun et al. 2014, Thorrold et al. 2014, Rohner et al. 2017a). The ability of *M. alfredi* to travel away from the shallow reef of D'Arros Island to consume mesopelagic zooplankton contrasts with zooplanktivorous reef fishes that tend to range over a much smaller spatial scale (m – km). The excretion of faecal matter by *M. alfredi* on return to D'Arros Island therefore represents a unique method of nutrient supply to the coral reefs at this locality, and may serve to increase horizontal nutrient transport in the region (McCauley et al. 2014, Papastamatiou et al. 2015a, Williams et al. 2018).



### 4.5.3 Extraction procedures for reef manta ray muscle tissue

There is still debate regarding the most appropriate way to treat elasmobranch tissue samples prior to analysis, despite the increasing use of stable isotopes as a means of investigating the feeding ecology of marine megafauna and the trophic structure of marine ecosystems (Munroe et al. 2018). We found that urea should be extracted at a minimum from *M. alfredi* tissue samples prior to stable isotope analysis, given the significant difference observed in all  $\delta^{15}\text{N}$  treatment groups relative to the control. Lipid extraction must also be considered in studies of *M. alfredi* stable isotope analyses (as discussed by Marcus et al. 2017), as significant differences were observed in values of  $\delta^{13}\text{C}$  across extraction procedures. No difference was observed between the final C:N ratio of the LE and LE+DIW extraction procedures, suggesting that the lipid extraction process conducted here was sufficient for the concurrent removal of lipids and urea from *M. alfredi* muscle tissues (Hussey et al. 2012b). Future studies of *M. alfredi* using stable isotope analyses should, therefore, aim to extract lipids from freeze-dried muscle tissue samples using the LE procedure described above. No additional urea-extraction treatment would then be required, and the utilisation of a consistent extraction methodology would increase the comparability of results of all studies.

### 4.5.4 Limitations

All sampling was conducted during the month of November in both 2016 and 2017, which has implications for our ability to detect seasonal shifts in the diet of *M. alfredi*, and align these measures with biological and environmental variables. White muscle tissue is estimated to represent the assimilated diet of elasmobranchs over periods of 300 – 700 days (Logan & Lutcavage 2010, Kim et al. 2012b), in contrast to shorter periods reflected by tissues such as blood plasma or skin, which exhibit higher turnover rates of  $\delta^{15}\text{N}$  and  $\delta^{13}\text{C}$  (Kim et al. 2012a, Matley et al. 2016, Wyatt et al. 2019). The restriction of our sampling to a single month of the year at D'Arros Island thus averages our view of the feeding ecology of *M. alfredi* on the zooplankton community at D'Arros Island across both the south-east (April-September) and north-west (December-March) monsoonal periods. Future studies should aim to collect tissue samples throughout the year in order to gain further insight into potential seasonal shifts in the foraging and feeding patterns of *M. alfredi* in Seychelles during the full annual cycle. Additionally, other tissues, such as skin (Ferreira et al. 2017) or mucous (Burgess et al. 2018), with higher turnover rates of isotopes could be collected and analysed together with samples of muscle tissue to provide better temporal resolution of feeding patterns. Such tissue samples would also provide more

information on the frequency and timing of mesopelagic foraging, and indicate whether pelagic zooplankton remains the primary food source for *M. alfredi* year-round.

Significant differences in the  $\delta^{15}\text{N}$  and  $\delta^{13}\text{C}$  values of pelagic zooplankton collected in 2016 and 2017 further emphasise the importance of multi-year sampling programs for studies of manta ray feeding ecology. These differences are likely to be the result of a dynamic zooplankton community existing at D'Arros Island, the composition of which may be constantly changing on both spatial and temporal scales (Giering et al. 2018, Benedetti et al. 2019). While logistical constraints limited the amount of zooplankton sampling that could be completed in the present study, future research should endeavour to repeatedly sample zooplankton communities throughout the annual cycle. Concurrently, rapid methods for community structure assessment (e.g. using ZooScan systems and Plankton ID Software) (Armstrong et al. 2016) should be developed to allow for the feeding ecology and trophic role of *M. alfredi* to be described on finer spatio-temporal scales at aggregation sites around the world.

#### 4.5.5 Conclusions

Stable isotope analyses revealed that *M. alfredi* occupy a unique trophic niche and role within the coral reef ecosystem at D'Arros Island. With a diet that includes pelagic, emergent and mesopelagic zooplankton, *M. alfredi* are able to maximise foraging opportunities at this remote locality while supplying nutrients via excretion to the coral reef over fine (< 1 km) and broad (> 10 km) spatial scales. The high level of site fidelity that *M. alfredi* exhibits at D'Arros Island (Peel et al. 2019b) increases the significance of these nutrient transport processes from mesopelagic ecosystems to local reefs by increasing the frequency at which they can occur. Collectively, the findings presented here highlight the potential for this large elasmobranch to play a unique role in nutrient transport and supply to an otherwise nutrient-poor coral reef ecosystem.

## 4.6 Supplementary material

**Table S 4.1** Summary of reef fishes sampled at D'Arros Island and St. Joseph Atoll, Seychelles, for stable isotope analysis. Estimated trophic level (TL; [www.fishbase.org](http://www.fishbase.org), 29/10/2018) and fork length given as mean  $\pm$  standard error.

Trophic Guild	Species Name	n	Est. TL	Fork Length (cm)	Capture Method (# Samples)
Herbivore	<i>Chlorurus sordidus</i>	10	2.62 $\pm$ 0.29	20.82 $\pm$ 3.89	Spearpole (10)
	<i>Scarus rubroviolaceus</i>	9	2.00 $\pm$ 0.00	31.14 $\pm$ 5.36	Spearpole (9)
Detritivore	<i>Crenimugil crenilabis</i>	10	2.29 $\pm$ 0.14	12.90 $\pm$ 6.62	Thrownet (10)
Planktivore	<i>Caesio teres</i>	10	3.40 $\pm$ 0.45	27.27 $\pm$ 1.84	Spearpole (10)
	<i>Caesio xanthonota</i>	10	3.40 $\pm$ 0.45	26.12 $\pm$ 2.10	Spearpole (10)
	<i>Pterocaesio tile</i>	1	3.33 $\pm$ 0.33	18	Spearpole (1)
Corallivore	<i>Chaetodon trifasciatus</i>	10	3.34 $\pm$ 0.61	9.67 $\pm$ 1.12	Spearpole (10)
Invertivore	<i>Lethrinus enigmaticus</i>	7	3.83 $\pm$ 0.58	36.31 $\pm$ 2.20	Spearpole (1); Hook and Line (6)
	<i>Lethrinus lentjan</i>	10	3.94 $\pm$ 0.25	32.12 $\pm$ 7.01	Spearpole (6); Hook and Line (4)
	<i>Lethrinus nebulosus</i>	10	3.76 $\pm$ 0.19	52.41 $\pm$ 8.81	Hook and Line (10)
	<i>Parupeneus macronemus</i>	10	3.50 $\pm$ 0.37	15.62 $\pm$ 3.00	Spearpole (10)
Reef Carnivore	<i>Cephalopholis sonnerati</i>	2	3.81 $\pm$ 0.60	35.25 $\pm$ 5.87	Hook and Line (2)
	<i>Variola louti</i>	10	4.33 $\pm$ 0.70	50.14 $\pm$ 4.90	Spearpole (1); Hook and Line (9)
Reef Piscivore	<i>Aethaloperca rogae</i>	8	4.20 $\pm$ 0.71	31.95 $\pm$ 7.02	Spearpole (8)
	<i>Cephalopholis miniata</i>	1	4.29 $\pm$ 0.51	25.5	Spearpole (1)
	<i>Lutjanus bohar</i>	10	4.27 $\pm$ 0.50	36.84 $\pm$ 10.93	Spearpole (4); Hook and Line (6)
Reef & Pelagic Carnivore	<i>Selar crumenophthalmus</i>	10	3.81 $\pm$ 0.18	26.83 $\pm$ 1.45	Hook and Line (10)
Pelagic Piscivore	<i>Katsuwonus pelamis</i>	5	4.43 $\pm$ 0.47	48.80 $\pm$ 3.63	Hook and Line (5)
	<i>Sarda orientalis</i>	1	4.21 $\pm$ 0.69	56	Hook and Line (1)
	<i>Thunnus albacares</i>	8	4.41 $\pm$ 0.41	68.88 $\pm$ 10.43	Hook and Line (7)
<b>Total</b>		<b>157</b>			

**Table S 4.2** Summary of values of  $\delta^{15}\text{N}$  and  $\delta^{13}\text{C}$ , and ratios of C:N reported for lipid and urea extracted reef manta ray (*Mobula alfredi*) muscle tissues relative to sample collection year, sex and life stage class.

Year	Sex	Life Stage Class	n	$\delta^{15}\text{N}$ (‰)	$\delta^{15}\text{N}$ (min/max)	$\delta^{13}\text{C}$ (‰)	$\delta^{13}\text{C}$ min/max	C:N
2016	Female		<b>8</b>	10.37 ± 0.48	9.67, 10.93	-17.87 ± 1.02	-18.98, -16.23	3.03 ± 0.16
		Juvenile	3	10.44 ± 0.39	10.00, 10.75	-18.28 ± 0.83	-18.98, -17.36	3.07 ± 0.1
		Sub-adult	4	10.31 ± 0.65	9.67, 10.93	-17.98 ± 0.93	-18.59, -16.61	3.06 ± 0.18
		Adult	1	10.44	-	-16.23	-	2.78
	Male		<b>5</b>	10.64 ± 0.44	9.87, 10.95	-17.94 ± 0.86	-19.16, -16.89	3.03 ± 0.11
		Juvenile	1	10.95	-	-18.25	-	3.07
		Sub-adult	1	9.87	-	-18.00	-	3.03
		Adult	3	10.79 ± 0.11	10.69, 10.91	-17.82 ± 1.19	-19.16, -16.89	3.02 ± 0.15
	Annual Average	-	13	10.47 ± 0.47	9.67, 10.95	-17.9 ± 0.92	-19.16, -16.23	3.03 ± 0.14
	2017	Female		<b>16</b>	10.84 ± 0.41	10.03, 11.42	-18.8 ± 1.02	-20.22, -16.53
Juvenile			2	11.07 ± 0.23	10.91, 11.23	-19.22 ± 0.06	-19.27, -19.18	3.25 ± 0.03
Sub-adult			7	10.86 ± 0.55	10.03, 11.42	-18.98 ± 1.02	-20.22, -16.97	3.21 ± 0.21
Adult			7	10.76 ± 0.29	10.2, 11.03	-18.5 ± 1.18	-19.45, -16.53	3.10 ± 0.20
Male			<b>20</b>	11.04 ± 0.23	10.61, 11.48	-19.05 ± 0.44	-19.45, -17.77	3.18 ± 0.07
		Juvenile	2	10.74 ± 0.19	10.61, 10.88	-19.04 ± 0.09	-19.11, -18.98	3.16 ± 0.06
		Sub-adult	8	11.18 ± 0.22	10.89, 11.48	-18.98 ± 0.53	-19.41, -17.77	3.19 ± 0.08
		Adult	10	11 ± 0.19	10.75, 11.31	-19.11 ± 0.42	-19.45, -18.09	3.18 ± 0.08
Unknown		-	1	10.66	-	-17.33 ± 0	-	2.82
Annual Average		-		10.95 ± 0.34	10.03, 11.48	-18.9 ± 0.79	-20.22, -16.53	3.17 ± 0.15
<b>Total Combined</b>	-	-	<b>50</b>	<b>10.82 ± 0.42</b>	<b>9.67, 11.48</b>	<b>-18.64 ± 0.93</b>	<b>-20.22, -16.23</b>	<b>3.13 ± 0.16</b>

**Table S 4.3** Summary of total (TA), core (SEAc) and overlapping trophic niche areas for male and female reef manta rays (*Mobula alfredi*) over two sampling years at D'Arros Island, Seychelles. Overlap is based upon ellipses encompassing 95% of the data.

Sampling Year	Sex	n	TA	SEAc	Total Trophic Overlap (%)
2016	Female	8	2.09	1.44	71.59
	Male	5	1.20	1.57	78.06
2017	Female	16	2.04	0.8	51.63
	Male	20	0.80	0.34	89.34

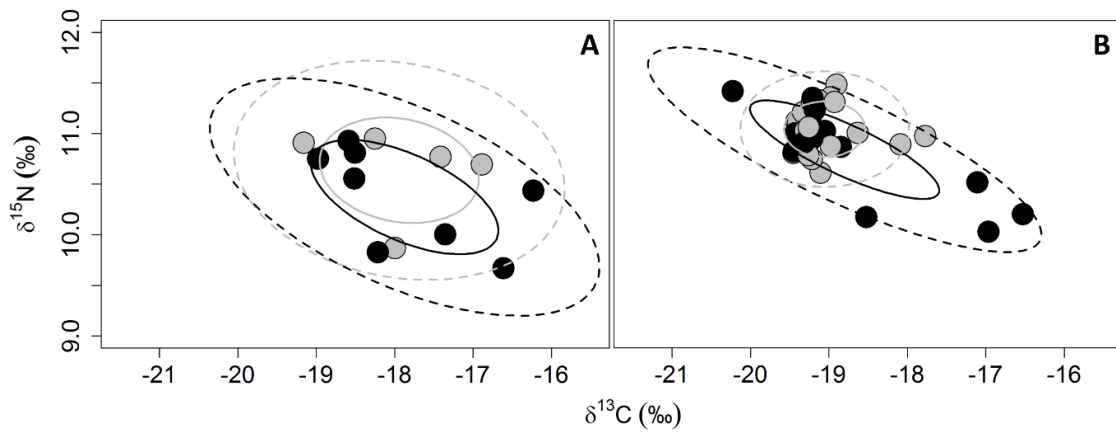


**Figure S 4.1** Isoscapes presenting the core (SEA<sub>c</sub>, solid lines) and total (TA, dashed lines) trophic niche areas of male (grey) and female (black) reef manta rays (*Mobula alfredi*) sampled at D'Arros Island, Seychelles, in November 2016 (A) and November 2017 (B).

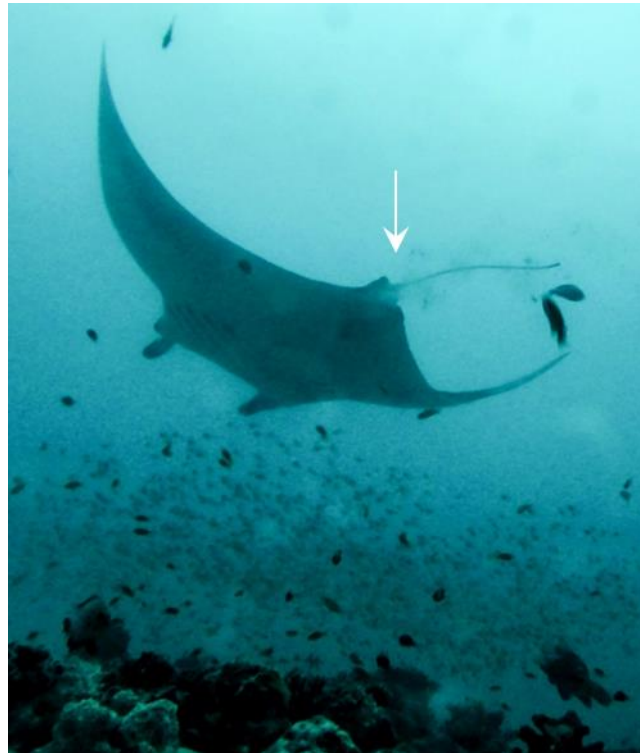


**Figure S 4.2** A reef manta ray (*Mobula alfredi*) defecates over the cleaning station at D'Arros Island, Seychelles. Arrow indicates faecal material.



# Chapter 5    A multi-technique approach to the description of regional movements of reef manta rays (*Mobula alfredi*) in Seychelles waters

## 5.1    Abstract

Understanding the movement ecology of reef manta rays (*Mobula alfredi*) is critical to the design of effective conservation strategies aimed at protecting vulnerable populations. Here, we used archival pop-up satellite tags, acoustic tags, and photo-identification approaches to examine the patterns of movement of *M. alfredi* in Seychelles, with a focus on the aggregation at D'Arros Island within the Amirante Island Group. Individuals photographed at D'Arros Island displayed a high level of site fidelity to this location, with 67% of individuals being resighted at least once. Only three movements of individuals over distances of 200 km were recorded away from D'Arros Island during photo-identification surveys. Satellite-tracked *M. alfredi* (n = 4 tracks; maximum 180 days) remained within the boundary of the Seychelles Exclusive Economic Zone, and in close proximity to the Amirante Islands, where they spent the majority of their time (91%) in the upper 50 m of the water column. The inclusion of acoustic tagging data in the models of estimated satellite-track paths significantly reduced the errors associated with the geolocation positions derived from archived light level data. The insights gained into the patterns of horizontal and vertical movements of *M. alfredi* using this multi-technique approach highlight the significance of D'Arros Island and the wider Amirante Island Group to *M. alfredi* in Seychelles, and will benefit future national-scale conservation efforts for this species.

## 5.2    Introduction

Reef manta rays (*Mobula alfredi*; Marshall et al. 2009, White et al. 2017) are large, zooplanktivorous elasmobranchs with a circumtropical distribution (Couturier et al. 2012, Stewart et al. 2018a). Aggregations of these mobulid rays (Family Mobulidae; Notarbartolo di Sciara 1987, Couturier et al. 2012, White et al. 2017) occur at numerous locations around the world (Stewart et al. 2018a). The predictability of these aggregation events and the charismatic nature of manta rays has driven the development of a large eco-tourism industry that promotes encounters with these animals through snorkelling or diving (Venables et al. 2016). Recent

estimates suggest that this industry now generates over USD 100 million in revenue per annum (O'Malley et al. 2013).

In parallel with the growth of eco-tourism, there has also been an increasing commercial harvest of *M. alfredi* for their gill plates for use in the Asian medicinal trade (White et al. 2006, O'Malley et al. 2017). This fishing pressure, coupled with the impacts of other anthropogenic threats, including boat strike, accidental entanglement and by-catch, has resulted in the decline of populations around the world (Couturier et al. 2012, Croll et al. 2016, Stewart et al. 2018a). In the last decade, positive protective measures for *M. alfredi* have been taken at the international level (Croll et al. 2016, Marshall et al. 2018b). However, at local (i.e. regional and national) scales, where intensive fishing practises can cause rapid and persistent declines in populations (Dewar 2002, Rohner et al. 2017b, Marshall et al. 2018b), management strategies are less defined and can be difficult to establish. Local management is further complicated by the ability of *M. alfredi* to travel large distances away from the aggregation sites at which they are commonly sighted (50 - 1,150 km; Couturier et al. 2011, Deakos et al. 2011, Jaine et al. 2014, Armstrong et al. 2019). Such movements highlight the difficulty associated with quantifying the magnitude of impact of anthropogenic pressures on *M. alfredi* populations throughout their range. An understanding of the movement and habitat use patterns of *M. alfredi* not only at aggregation areas, but also away from these sites, is therefore critical to the design of effective conservation measures aimed at protecting their populations from unsustainable exploitation at local scales.

Satellite tracking provides an effective means to monitor the movement patterns of megafauna (Hays et al. 2016, Sequeira et al. 2018) and is providing researchers insights into both the large (100s to 1000s of km) and fine (0.1s to 1s of km) scale movement patterns of *M. alfredi* (Braun et al. 2014, Jaine et al. 2014, Braun et al. 2015, Kessel et al. 2017). Data sets retrieved from archival pop-up satellite tags can be used to visualise the horizontal extent of movement of individuals throughout their home range, and in addition, can also reveal the drivers of vertical movements through the water column (Canese et al. 2011, Jaine et al. 2014, Kessel et al. 2017, Andrzejczek et al. 2018). By staggering tag deployments over field expeditions throughout the year, it becomes possible to consider *M. alfredi* movement patterns on seasonal and annual scales (Weng et al. 2007, Braun et al. 2018b). The prohibitive cost of satellite tags, however, limits deployment numbers and is the primary barrier to obtaining representative sample sizes for many species, including manta rays (Hays et al. 2016). Furthermore, the errors surrounding location estimates that are generated using light data reduces the accuracy of horizontal tracks provided by pop-up tags, particularly in the tropics (Teo et al. 2004, Braun et al. 2014, Braun et al. 2018a), where the majority of *M. alfredi* populations occur (Kashiwagi et al. 2011, Couturier et al. 2012).

Acoustic telemetry offers an alternative to satellite tagging as a means of describing movement patterns of *M. alfredi* (Clark 2010, Braun et al. 2015, Couturier et al. 2018, Setyawan et al. 2018).



In this approach, acoustic tags that transmit an individually-coded signal are deployed externally on animals. These transmissions are passively detected whenever the tagged individual moves within the detection radius of receivers deployed at the study site (Heupel et al. 2006). Although many more animals can be monitored using acoustic tags due to their lower cost relative to satellite tags, acoustic tracking is restricted to the spatial extent of the receiver array (Stewart et al. 2018a). Additionally, receivers must be recovered and downloaded to obtain detection data (Heupel et al. 2006).

In contrast to the cost and logistics involved with satellite and acoustic tagging, photo-identification offers a simple means to examine site fidelity and movement patterns of *M. alfredi* (Marshall & Pierce 2012). Photographs of the unique and permanent ventral markings on individual *M. alfredi* can be used to examine levels of site fidelity and residency exhibited by cohorts of a population, and to assess the frequency at which individuals travel between aggregation sites (Kitchen-Wheeler 2010, Deakos et al. 2011, Marshall et al. 2011, Marshall & Pierce 2012). This technique is, however, usually biased to areas where *M. alfredi* are already known to aggregate, and information on the fine-scale (hours to days) movements of individuals between locations is often absent (Deakos et al. 2011). Additionally, it can be logistically difficult to gain access to and continuously survey aggregation sites, particularly in remote locations. These challenges can result in seasonally-biased datasets that may not be completely representative of the annual movement patterns of the study species.

Some of the shortcomings of satellite and acoustic tagging, and photo-identification techniques, may be overcome by combining these approaches (Meyer et al. 2010b, Kneebone et al. 2014, Vianna et al. 2014, Braun et al. 2015). Detections of acoustic tags within receiver arrays individually, or combined with sighting records of tagged individuals at aggregation sites, can be used to reduce the uncertainty surrounding location estimates derived from satellite tags. This combined approach improves the accuracy of individual tracks provided by archival pop-up tags. In turn, tracking data can provide a better picture of both large-scale movement and home range of individuals, allowing researchers to determine the extent to which acoustic tagging and photo-identification techniques are likely to capture residency and movement patterns (Kneebone et al. 2014, Vianna et al. 2014).

Here, we combined satellite and acoustic tracking and photo-identification techniques to examine the movement ecology of *M. alfredi* in the remote reef systems of Seychelles. These data were used to determine the home range size and regional movement patterns of individuals, and to assess potential drivers of patterns of horizontal and vertical movement.

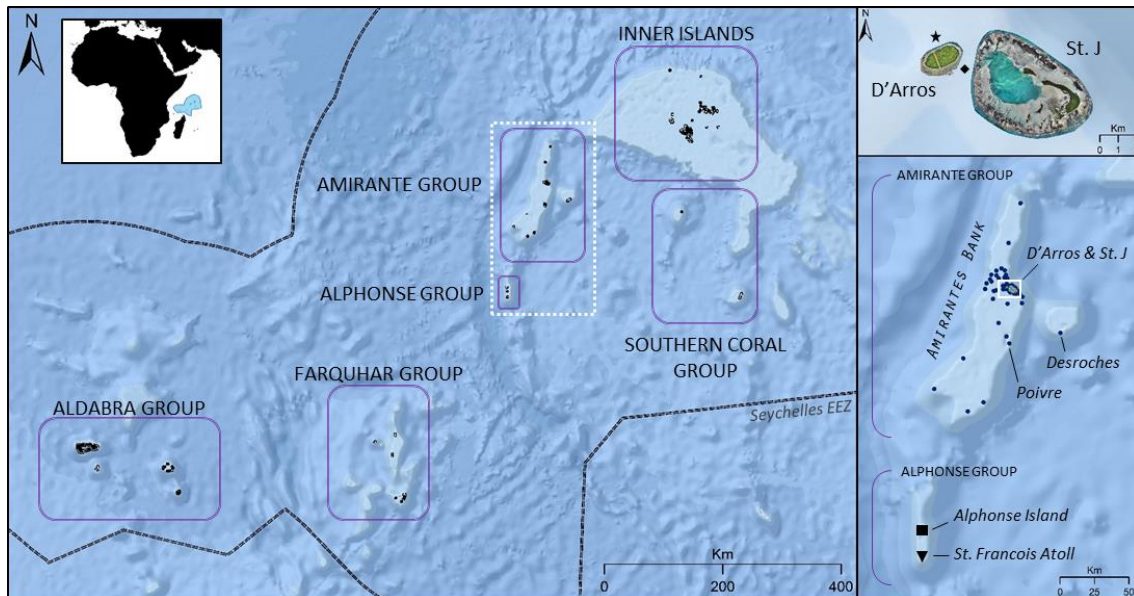


**Figure 5.1** Location of the six Island Groups of Seychelles. Reef manta rays (*Mobula alfredi*) are frequently sighted at D'Arros Island and St. Joseph Atoll within the Amirante Group, and at St. Francois Atoll within the Alphonse Group. Seventy acoustic receivers (●) are deployed within the Amirante Group. Alphonse Island located at '■'. St. Francois Atoll located at '▼'. D'Arros Island manta cleaning station located at '★'. St. Joseph Channel (depth 60 m) located at '◆'.

## 5.3 Methods

### 5.3.1 Study site

Seychelles is an archipelago nation of 115 tropical islands in the Western Indian Ocean that are divided into two main groups; the populous and granitic Inner Islands, and the remote, coralline Outer Islands. The Outer Islands are divided into 5 smaller groups – Aldabra, Alphonse, Amirante, Farquhar, and Southern Coral - based on the geographic location of the islands (Figure 5.1).

Reliable aggregations of *M. alfredi* are currently known to occur within the Amirante and Alphonse Island Groups. The 24 islands and islets of the Amirante Group are located across the Amirantes Bank (30 x 160 km); a predominantly shallow (< 40 m average depth) shelf that reaches maximum depths of 70 m in the centre, before waters descend rapidly to depths of over 1,000 m off the Bank ridge (Figure 5.1; Stoddart et al. 1979). D'Arros Island and St. Joseph Atoll are situated centrally along the eastern ridge of the Bank, and host a year-round aggregation of *M. alfredi* (see Chapters 2 and 3). Previous studies have used acoustic telemetry to study local movement and residency patterns of elasmobranchs throughout the Amirante Islands, and as a result, a network of acoustic receivers exists throughout the region (Figure 5.1; Lea et al. 2016, Peel et al. 2019b).

Alphonse Island and the St. François Atoll comprise the Alphonse Island Group, and are located 80 km to the south of the Amirantes Bank (Figure 5.1; Hamylton et al. 2012). The extensive reef flats, two islands, and three-chambered lagoon of the St. François Atoll span a collective area of 53 km<sup>2</sup>. Sightings of *M. alfredi* feeding along the edges of the reef flats and within the northernmost lagoon are common at this location, particularly during the north-west monsoon (November – March; L. Peel, unpub. data).

### 5.3.2 Photo-identification

Identification photographs of individual *M. alfredi* were collected across three spatio-temporal scales to monitor the movement patterns of this population (see Chapter 2). Broadly, sightings of *M. alfredi* were recorded opportunistically throughout Seychelles by the authors, collaborators, and members of the public between 2006 and 2018. More specifically, three dedicated manta survey periods were undertaken at D'Arros Island and St. Joseph Atoll (November 2013, November 2016 and November 2017), and one dedicated manta survey period undertaken at Alphonse Island and St. François Atoll (2-9 December 2017). These surveys were conducted to monitor *M. alfredi* occurrence, habitat use and movement patterns on a finer-scale at these locations within the archipelago. Lastly, a remote camera system was deployed at a manta ray cleaning station to the north of D'Arros Island between 29 September 2017 and 27 November 2017 in order to continuously monitor visits of *M. alfredi* to this site.

All recorded sightings of *M. alfredi* included an identification image of the unique pigmentation pattern on the ventral surface of each individual, and details of the time and location of the encounter. The presence (male) or absence (female) of claspers was used to determine the sex of each individual (Marshall et al. 2009), and the extent of calcification of the claspers used as a proxy for the maturity status of males (Marshall & Bennett 2010b). Mating scars and pregnancy bulges were used as indicators of sexual maturity in females, when present (Marshall & Bennett 2010b). The size (disc width) of all encountered individuals was visually estimated to the nearest 0.1 m and also considered when estimating maturity status. Individuals were subsequently categorised into three life history stages: juvenile (any individual,  $\leq 2.4$  m), sub-adult (male, 2.5 – 2.8 m; female, 2.5 – 3.1 m), or adult (male,  $\geq 2.9$  m; female,  $\geq 3.2$  m; Stevens 2016). All sighting records were stored in an online database, and re-sightings of individuals used to monitor the frequency at which they moved between locations over time.

## 5.3.3 Satellite telemetry

### 5.3.3.1 Tag deployment

Six archival pop-up satellite tags (miniPATs; Wildlife Computers; WA, USA) with titanium anchors and 10 cm stainless steel tethers were deployed between November 2016 and December 2017 in Seychelles (Table 5.1). Tags were externally deployed on the posterior dorsal surface of free-swimming *M. alfredi* either by SCUBA divers at a manta ray cleaning station, or by free-divers at the surface using a modified Hawaiian sling. Two tags were deployed on two mature females at D'Arros Island in November 2016 (disc widths 3.0 and 3.6 m). An additional mature female was tagged at D'Arros Island in November 2017 (disc width 3.4 m). This latter individual was carrying an external acoustic tag that was deployed in a previous study (V16TP-5H; Vemvo; Nova Scotia, Canada; Peel et al. 2019b). The remaining three tags were deployed on males; two mature males at D'Arros Island in November 2017, and a sub-adult male at St. François Atoll in December 2017 (disc widths 3.0, 3.0 and 2.5 m, respectively).

All tags were programmed to release after 180 days and to archive light level, depth and water temperature data every 5 seconds. Archived data were summarised every six hours for transmission, with the upper limits of storage bins for time-at-depth data set to 0, 1, 5, 10, 20, 35, 50, 65, 80, 100, 150, 300, 2000 m, and for time-at-temperature data to 3, 6, 9, 12, 15, 18, 21, 24, 27, 30, 33, 45°C. In the event of an early release, tags were programmed to transmit summarised data via the Argos satellite system after a period of 36 h (tags deployed in 2016), or 24 h (tags deployed in 2017), at a constant depth ( $\pm 1.5$  m) until battery failure or tag retrieval.

**Table 5.1** Summary of satellite tag deployments on reef manta rays (*Mobula alfredi*) in Seychelles, including length of track (duration in days) and percentage of archived data decoded via satellite. Asterisk indicates an individual that was carrying an active acoustic tag at the time of satellite tagging. ‡ indicates the tag that transmitted insufficient and unreliable data for analysis. F, female. M, male. DNR, did not respond.

Manta ID	PTT	Sex	Disc Width (m)	Tag Date	Deployment Location		Track End Date	Duration (d)	Decoded (%)	Days with Light Data (%)
					Lat (°S)	Long (°E)				
M1	166070	F	3.0	27 Nov 2016	-5.409	53.299	07 Mar 2017	100	88	100
M2	166071	F	3.6	28 Nov 2016	-5.409	53.299	19 Jan 2017	52	88	100
M3 <sup>‡</sup>	41817	M	3.0	17 Nov 2017	-5.409	53.301	06 Apr 2018	140	68	9
M4	41818	M	3.0	17 Nov 2017	-5.409	53.301	16 May 2018	180	44	29
M5*	41819	F	3.4	22 Nov 2017	-5.441	53.315	05 Apr 2018	134	84	100
M6	44321	M	2.5	03 Dec 2017	-7.066	52.757	-	DNR	-	-

### 5.3.3.2 Geolocation

Data retrieved via satellite from all miniPATs were decoded using Wildlife Computers' online portal-based software and quality checked prior to analysis. Three tags were noted to have drifted at the surface for a period longer than scheduled (i.e. > 36 or 24 h) before transmitting data. Retrieved depth and temperature data were therefore examined to confirm accurate tag release times for all tags. The end time of each track was deemed to be the time before which all subsequent depth records from the tag were < 0.5 m. No GPS locations were assigned to the final estimated track end times for each tag, because we could not quantify the true distance between the first reported pop-up location of the tag and the real release location. Light level data were then examined to ensure that only single time estimates of dawn and dusk were recorded per day of each track. Where duplicate estimates were presented for either event, the later time was removed from the dataset. Lastly, for individual M4, an additional location point from a re-sighting event recorded through photo-identification was included in the final data set.

Geolocation processing was completed using a Hidden Markov Model (HMM, WC-GPE3, Wildlife Computers) that considered archived light level, temperature and depth data alongside sea surface temperature (NOAA OI SST V2 High Resolution; <http://www.esri.noaa.gov/psd/>) and bathymetric constraints (ETOPO1-Bedrock). After collating the available data, the HMM calculated a posterior probability distribution that estimated the most likely position of each individual at every time point of the track (Skomal et al. 2017). The diffusion parameter (i.e. most-probable speed) for *M. alfredi* was set to 1.2 m s<sup>-1</sup> for all individuals, based on maximum speeds reported for this species moving through a coastal acoustic receiver array in the eastern Indian Ocean (F. McGregor, pers. comm.). Track paths were only estimated for tags that had light level data for > 10% of the tracking days (n = 4) to avoid excessive interpolation occurring in tracks.

#### 5.3.3.2.1 Inclusion of acoustic data

A total of 481 acoustic detections were retrieved throughout the Amirantes acoustic receiver array from the acoustic tag concurrently deployed alongside the miniPAT on individual M5. A second HMM was constructed for this individual, which included these acoustic data as known positions (error radius 165 ± 33 m; Lea et al. 2016) alongside the positions estimated from the archived data set. The same quality checks and model parameters were used to construct this secondary HMM, and this facilitated a comparison between the metrics of a geolocated track considering light level data alone (GPE3), to one that was based upon light level data and a substantial amount of additional location information (GPE3/A).

### 5.3.3.3 Horizontal movement

Patterns of horizontal movement were visualised in ArcGIS 10.3® (ESRI, Redlands, California) and analysed in ArcGIS and R (version 3.4.1; R Core Team 2017). Firstly, the most-probable track for each individual was mapped in order to visualise the extent of movement of each individual away from the tagging location and throughout the waters of Seychelles. The 50% error radii associated with the geolocated positions for each individual were averaged as a measure of geolocation accuracy relative to the acoustic detection data retrieved for individual M5. The 95% error radii associated with each geolocated position were then imported into ArcGIS, where they were used to determine the total possible area of occupancy by each individual. Core areas of use were calculated from the most-probable track positions for each individual using kernel utilisation density (KUD) analyses through the ‘kernelUD’ function of *adehabitatHR* (Calenge 2006) in R, before being mapped in ArcGIS.

### 5.3.3.4 Vertical movement

Transmitted depth and temperature data were analysed using the package *RchivalTag* (Bauer 2018) in R. Kolmogorov–Smirnov (K-S) tests were used to investigate whether depth distribution varied between day (06:00 – 18:00) and night (18:00 – 06:00), and t-tests were used to determine if individual *M. alfredi* dived to deeper depths on average during the day than at night. Generalised linear models (GLMs) were used to determine whether average nightly dive depth varied with respect to the lunar cycle. Moon illumination data for this latter investigation were accessed from the ‘SunCalc.net’ project (<http://suncalc.net>) using the package *suncalc* (Agafonkin & Thieurmel 2018) in R, and arcsin transformed prior to analysis. Where dive and moon illumination data were found to be non-normally distributed through a Shapiro Wilk test for normality, a Spearman’s rank correlation was used to investigate the relationship. Lastly, transmitted depth data were examined relative to the average depth of the Amirantes Bank (~ 40 m) and the depth of the St. Joseph Channel between D’Arros Island and St. Joseph Atoll (~ 60 m; Figure 5.1). This was done by considering the proportion of depth records reported above each of these depths for all tagged individuals.

## 5.4 Results

### 5.4.1 Photo-identification

Photo-identification was successfully used in Seychelles to identify 236 individual *M. alfredi* throughout the Republic (see Chapter 2). A total of 157 (66.5%) of these individuals were resighted on at least one occasion, the vast majority within the same Island Group that they were first sighted in (99.8% of all recorded re-sightings).

Only three individuals were recorded to move between Island Groups on single occasions based on the 1,579 confirmed sightings of *M. alfredi* in Seychelles (Table S 5.1). All of these movements were from D'Arros Island (Amirante Island Group) to St. François Atoll (Alphonse Island Group), and the time between re-sightings ranged from 14 to 1,624 days (~ 4.5 years). The shortest of these journeys was 14 days, during which time the sighted individual would have travelled at a minimum straight-line speed of 13.9 km d<sup>-1</sup> (0.16 m s<sup>-1</sup>).

The six *M. alfredi* satellite-tagged in this study had varying sighting histories prior to the deployment of the miniPATs (Table 5.2), but all had only been recorded within a single Island Group. As of January 2019, only two individuals were resighted through photo-identification after the release of their tags. Tagged individual M4 was resighted in the Amirante Island Group at Poivre Island on 15 November 2018, after being tagged 40 km away at D'Arros Island 364 days earlier. Individual M6, whose tag failed to respond, was also resighted. This individual was observed feeding in a large aggregation event at St. François Atoll on 19 December 2018, 382 days after it was tagged in the same location.

**Table 5.2** Sighting histories and locations of six individual reef manta rays (*Mobula alfredi*) that were tracked in the waters of Seychelles using archival pop-up satellite tags.

Manta ID	First Sight (Location)	# Resights Pre-Tag	Tag Date	# Resights With Tag	# Resights Post-Tag
M1	15 Nov 2012 (D'Arros)	4	27 Nov 2016	0	0
M2	27 Sep 2013 (D'Arros)	6	28 Nov 2016	0	0
M3	20 Nov 2011 (D'Arros)	12	17 Nov 2017	1 (D'Arros)	0
M4	7 Dec 2010 (D'Arros)	22	17 Nov 2017	1 (D'Arros)	1 (Poivre)
M5	18 Nov 2016 (D'Arros)	1	22 Nov 2017	0	0
M6	11 Nov 2016 (St. François)	2	03 Dec 2017	1 (St. François)	1 (St. François)

## 5.4.2 Satellite telemetry

Five of the six miniPATs deployed on *M. alfredi* in Seychelles successfully transmitted data, all of which were deployed at D'Arros Island (Table 5.3). The single tag deployed at St. François Atoll did not respond and the reason for this tag failure remains unknown. Only one of the five reporting tags released from the manta ray on schedule (180 d, individual M5), with the remaining four tags releasing prematurely for unknown reasons (retention time 66 – 151 d). No tags were able to be physically recovered, and three of the tags drifted for an extended period of time at the surface prior to commencing data transmission (6 d, M2; 23 d, M4; 5 d, M5). Between 44 and 88% of all archived data were retrieved via the Argos satellite system from the five successful tags, of which four provided adequate data for horizontal and vertical movement analyses. Data from individual M3 were excluded from further analysis as a result of a lack of light-level data (< 10%; Table 5.1).

**Table 5.3** Horizontal and vertical movement metrics for reef manta rays (*Mobula alfredi*) tracked using archival pop-up satellite tags (miniPATs) in Seychelles. F, female. M, male. Pop. Dist., distance between deployment location and estimated end position of track. Max. Lat. Range, maximum latitudinal range covered by the individual. GPE3, geolocated track path including geo-located positions only. Italicised metric data, indicates value and difference of M5-GPE3 model to M5-GPE3/A. Diel Depth Distribution, p-value from K-S test for difference in depth distribution between day and night. Diel Dive Depth, p-value from t-test for difference in average dive depth between day and night. Lunar cycle, p-value for relationship between average night-time depth by individuals and level of moon illumination; ‡ represents p-value derived from Spearman's Rank Correlation test. GPE3/A, geolocated track path including additional positions recorded by an acoustic tag. Significant p-values presented in bold.

	Metric	M1	M2	M4	M5-GPE3/A	M5-GPE3
<i>Individual Information</i>	PTT	166070	166071	41818	41819	<i>41819</i>
	Sex	F	F	M	F	<i>F</i>
	Disc Width (m)	3.0	3.6	3.0	3.4	<i>3.4</i>
<i>Horizontal Movements</i>	Pop. Dist. (km)	323	193	33	132	<i>295 (x2.2)</i>
	Travelled Length (km)	887	278	1,454	1,632	<i>1466 (x0.9)</i>
	Min. Distance/Day (km)	8.9	5.3	8.1	12.2	<i>10.9 (x0.9)</i>
	Max. Lat. Range (km)	364	180	560	334	<i>548 (x1.6)</i>
	50% KUD (km <sup>2</sup> )	12,319	1,798	34,155	5,937	<i>22,353 (x3.8)</i>
	95% KUD (km <sup>2</sup> )	45,491	8,585	114,985	37,033	<i>84,158 (x2.3)</i>
	Error Area (km <sup>2</sup> )	48,668	27,081	229,424	66,928	<i>121,557 (x0.55)</i>
<i>Vertical Movements</i>	Max Depth (m)	184	280	240	224	-
	Min. Temp (°C)	14.6	17.1	16.9	12	-
	Max. Temp (°C)	30.7	30.4	30.3	31.7	-
	Diel Depth Distribution ( <i>p</i> )	0.72	0.92	0.26	0.72	-
	Diel Dive Depth ( <i>p</i> )	< <b>0.001</b>	0.28	<b>0.02</b>	<b>0.007</b>	-
	Lunar Cycle ( <i>p</i> )	<b>0.03</b>	0.66 <sup>‡</sup>	0.50	<b>0.04<sup>‡</sup></b>	-



### 5.4.3 Horizontal movement

Satellite tracked individuals (three female, one male) moved an average of 8.6 km d<sup>-1</sup> (range 5.3 – 12.2 km d<sup>-1</sup>) throughout Seychelles. The longest recorded track path was 1,632 km for individual M5 over a period of 180 d (GPE3/A; Table 5.3), and the estimated end position of each track varied between 33 and 323 km from the original deployment location (Figure 5.2). The average error radius for geolocated positions was 29.8 ± 12.2 km. Areas of core habitat use varied greatly between individuals, with an average 50% KUD area of 13,612 km<sup>2</sup> and 95% KUD area of 51,688 km<sup>2</sup> (ranges of 1,798 to 34,394 km<sup>2</sup>, and 8,585 to 115,643 km<sup>2</sup>, respectively). All tagged *M. alfredi* were found to remain within the boundary of the Seychelles Exclusive Economic Zone (EEZ), where the Amirantes Bank represented a key area of use for all individuals. The 50% KUD areas for tagged individuals spanned across just 0.99 ± 0.91% of the Seychelles EEZ. The average maximum area inhabited by each individual for the duration of the tracks was 93,025 km<sup>2</sup> (27,081 to 229,424 km<sup>2</sup>), encompassing on average 6.8 ± 5.8% of the EEZ of Seychelles.

The majority (89.7%) of geolocation-derived track positions were estimated to occur within a similar longitudinal range (52.8°E to 54.2°E). Of the 4,724 geolocated positions considered here, a total of 3,744 (79.2%) fell within the same longitudinal range of the Amirante Island Group (52.87 to 53.76°E), and 1,342 (28.4%) fell within the longitudinal range of D'Arros Island and St. Joseph Atoll (53.29 to 53.37°E; Figure 5.3).

#### 5.4.3.1 Inclusion of acoustic data in HMM

The estimated latitudinal range covered by *M. alfredi* ranged from 179 to 559 km within Seychelles, with track paths for individuals tagged in 2016 (M1 and M2) generally moving in a southerly direction, and track paths for individuals tagged in 2017 (M4 and M5) tending to travel northwards. The inclusion of additional location data collected from the acoustic tag of M5 in the HMM for this individual (GPE3/A) constricted the latitudinal distance encompassed by the resulting geo-located track path by 39.1% in comparison to the model that considered transmitted light level data alone (GPE3; Table 5.3). Although the total distance moved by M5 during the most-probable track in the GPE3/A model remained similar to that predicted by the GPE3 model (1,632 and 1,466 km, respectively), the GPE3/A model estimated the release location of the tag to be 163 km closer to the tagging location. The KUD areas estimated for M5 also differed greatly between models GPE3/A and GPE3, with the 50% and 95% KUD areas constricting by 73.4 and 56.0%, respectively. The total area of possible inhabitation by M5 in model GPE3/A was 55% smaller than that calculated in model GPE3, most notably due to a reduction in latitudinal range for this individual of 214 km (Figure 5.2). The percentage of geolocation positions falling within the latitudinal range of the Amirantes Bank for M5 increased from 43.6% in the GPE3 model,

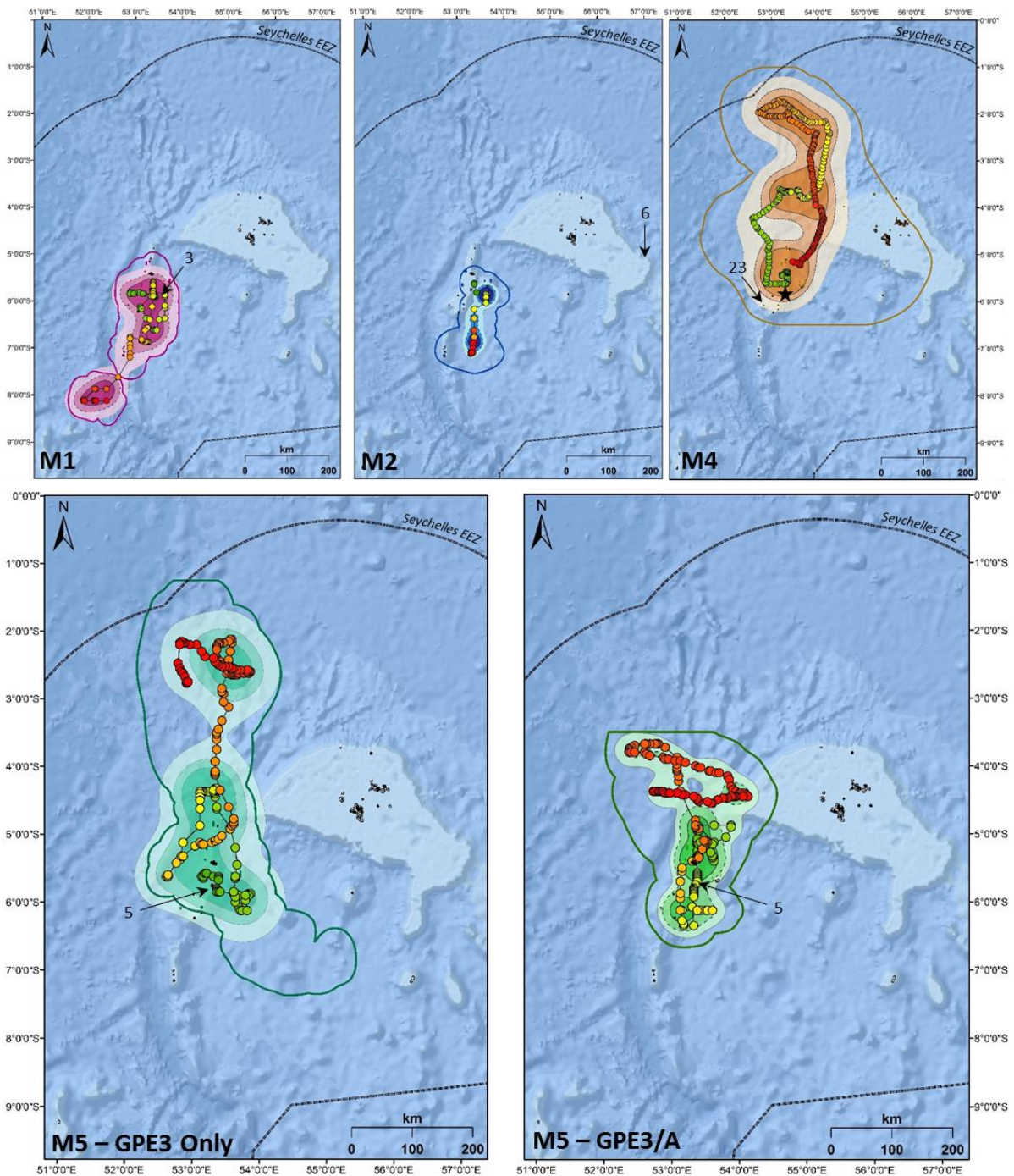


**Figure 5.2** Most-probable tracks for reef manta rays (*Mobula alfredi*) M1, M2, M4 and M5 tagged with archival pop-up satellite tags (miniPATs) at D'Arros Island, Seychelles. For M5, the 'GPE3 Only' track was estimated only from archived light, depth and temperature data, whereas the 'GPE3/A' track included an additional 481 acoustic detections from a passive receiver array. Tracks progress from green to red (100, 52, 180 and 134 d, respectively). Arrows indicate the first Argos location of each transmitting tag, and the associated numbers show the number of days that the tag is estimated to have been drifting prior to transmissions beginning. Core areas of use represented by dark (50% KUD), medium (95% KUD) and light (99% KUD) colour shading. Thick, solid coloured line represents boundary of 95% geolocation errors. '★' in M4 indicates the location of a re-sighting 184 d after tag release.

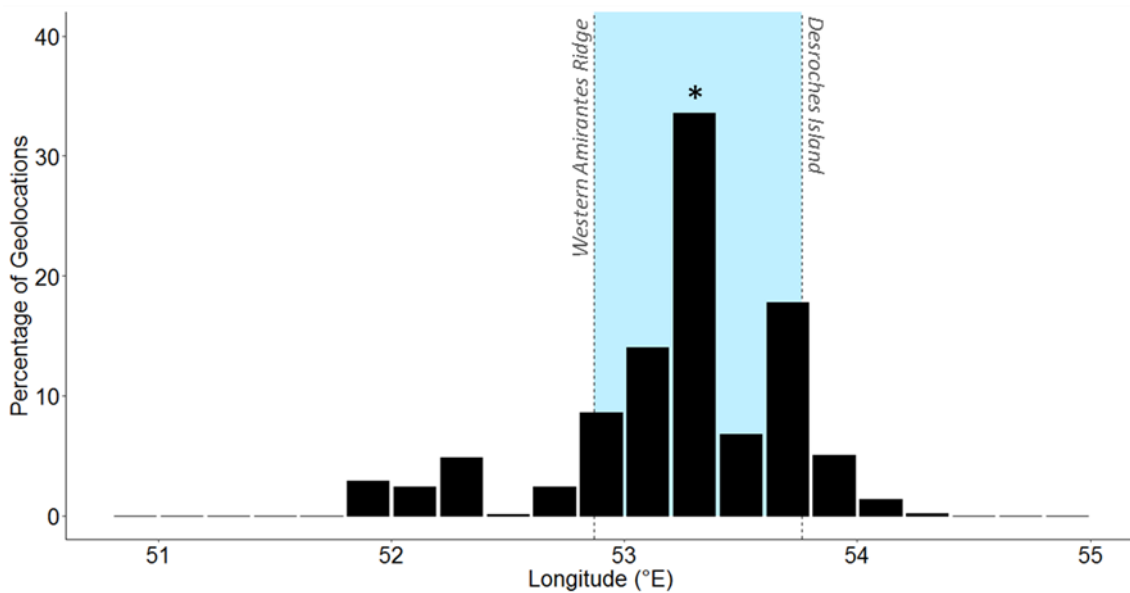


**Figure 5.3** Percentage of longitude estimates among four geo-located satellite tracks of reef manta rays (*Mobula alfredi*) in Seychelles. Blue shading represents longitudinal range of the Amirante Island Group, Seychelles. Asterisk represents longitude at tagging location (D'Arros Island).

to 69.4% in the GPE3/A model, (Figure 5.4A), after the 481 known locations of this individual within the Amirantes acoustic receiver array between 22 November 2017 and 06 February 2018 were accounted for (Figure 5.4B).

#### 5.4.4 Vertical movement

Tagged *M. alfredi* spent an average of 91% of their time in the top 50 m of the water column (range 81.4% - 95.8%; Figure 5.5), infrequently performing deeper dives that reached maximum depths of approximately 232 m (range 184 – 280 m; Table 5.3). Individuals spent approximately 83.2% of their time at temperatures between 27 and 29°C (range 73.6 – 94.0%), and 95.9% of their time at temperatures between 24 and 29°C (range 92.9 – 99.3%; Figure 5.5 and S 5.1). The minimum temperature experienced by a tagged individuals was 12.0°C, and the maximum temperature experienced was 31.7°C.

Tagged *M. alfredi* spent an average of  $82.8 \pm 5.3\%$  of their time at depths shallower than the average depth of the Amirantes Bank (40 m; Figure 5.5). This increased to  $94.6 \pm 3.4\%$  when depth data were examined relative to the depth of the St. Joseph Channel (60 m), located between D'Arros Island and St. Joseph Atoll.

Patterns of depth use did not differ between the day and night for any individual (K-S test,  $p > 0.05$ ; Table 5.3; example provided in Figure S 5.2). Average dive depths were deeper during

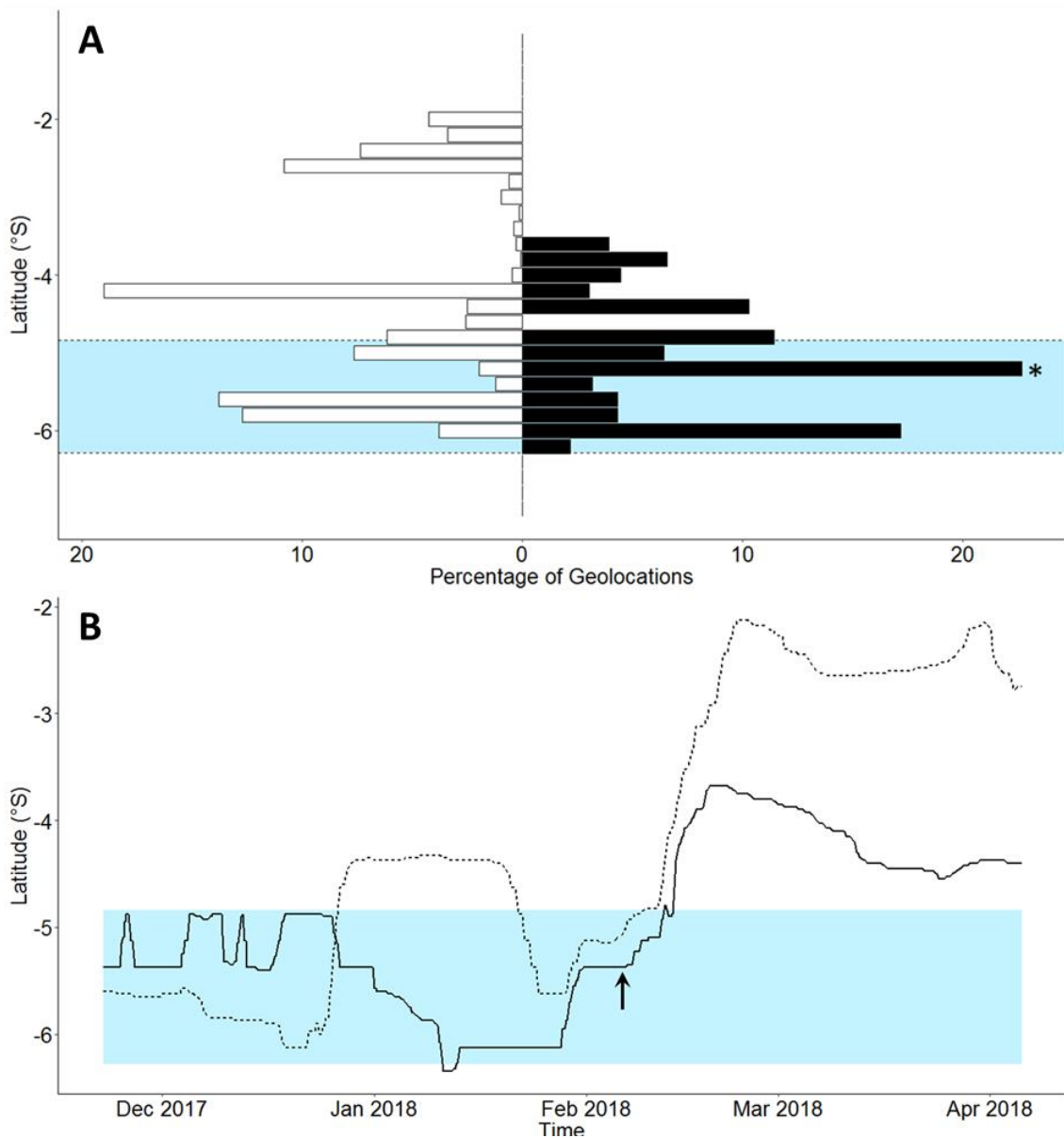


**Figure 5.4** Percentage of total latitude estimates calculated for a geolocated satellite track (M5) of a reef manta ray (*Mobula alfredi*) in Seychelles by a Hidden Markov Model (HMM) considering either archived environmental data only (GPE3; white bars), or archived environmental data alongside 481 known locations retrieved from an acoustic array (GPE3/A; black bars; A). Asterisk represents longitude at tagging location (D'Arros Island). Estimated latitude over time also presented (B) for model excluding (GPE3; dashed line) and including (GPE3/A; solid line) acoustic data. Blue shading represents latitudinal range of the Amirante Island Group. Arrow indicates time of last recorded acoustic detection of individual.

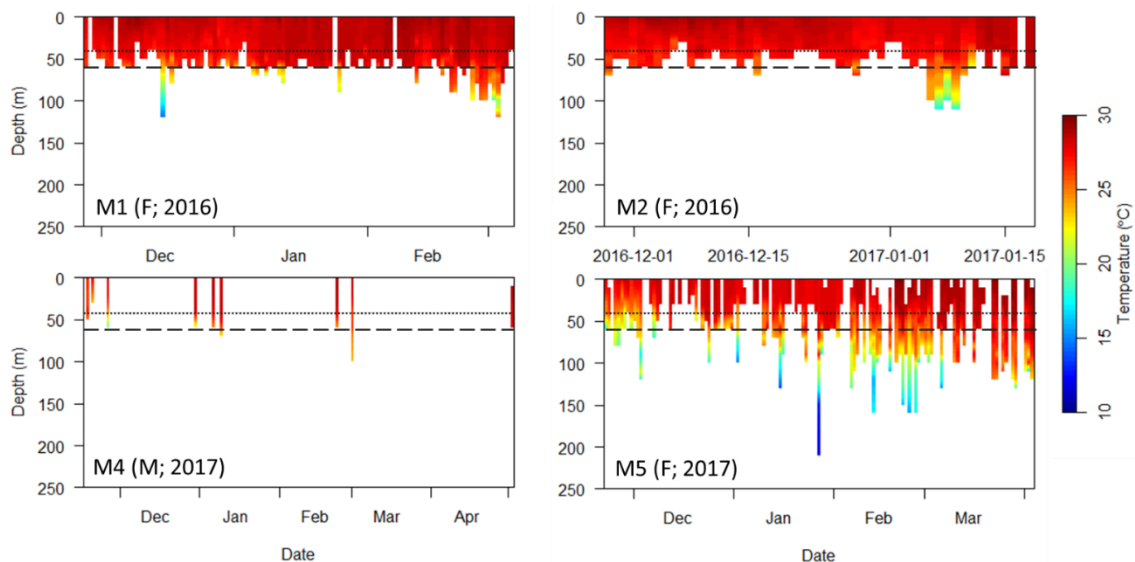


**Figure 5.5** Combined depth and temperature profiles for four reef manta rays (*Mobula alfredi*) tagged with archival pop-up satellite tags in Seychelles. Data interpolated for each day of data retrieved per tag. Gaps indicate data that was not retrieved from the tag prior to tag battery depletion. Manta identification number (M\*), sex (F, female; M, male) and year of tag deployment indicated in lower left of each panel. Dotted line represents average depth of the Amirantes Bank (40 m), and dashed line represents average depth of St. Joseph Channel (60 m) located between D'Arros Island and St. Joseph Atoll.

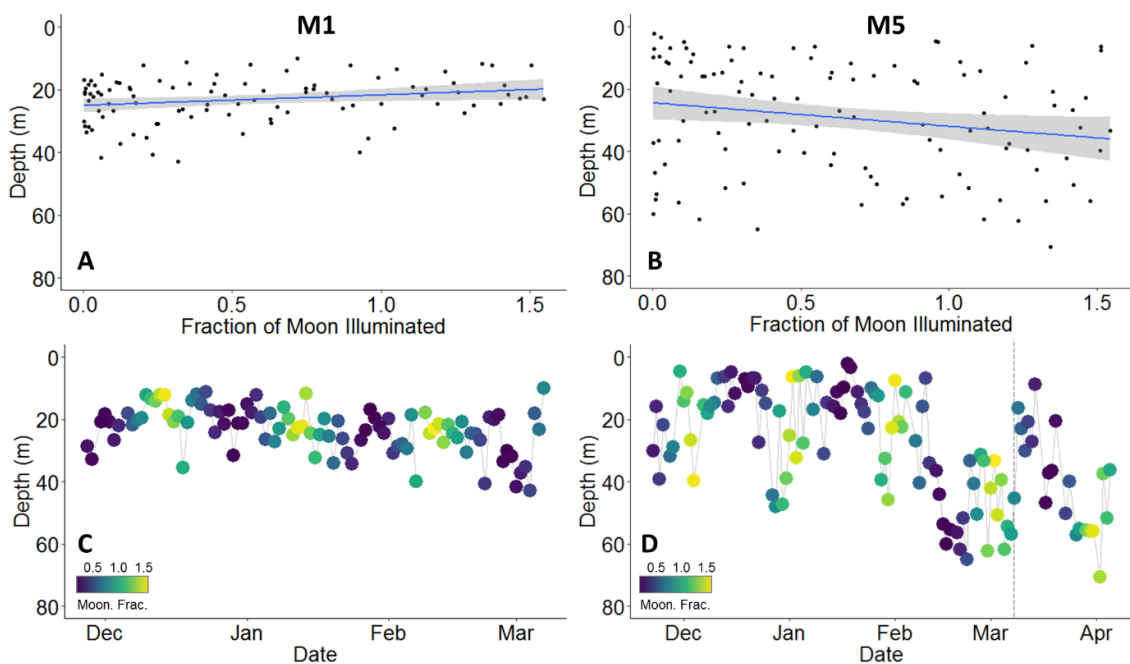


**Figure 5.6** Nightly average dive depth relative to moon illumination (arc-sin transformed; A and B) and over time (C and D) for two reef manta rays (*Mobula alfredi*; M1 and M5) tagged with archival pop-up satellite tags in Seychelles. Blue line indicates direction of relationship with moon illumination. Grey shading indicates 95% confidence interval. Dashed vertical line in lower panel for M5 (D) represents equivalent track-end date for individual M1.

the night than the day for three individuals (two females, one male;  $t = -5.19$ ,  $df = 191$ ,  $p < 0.001$ ;  $t = -2.49$ ,  $df = 219$ ,  $p = 0.01$ ;  $t = -2.15$ ,  $df = 50.6$ ,  $p = 0.02$ , respectively; Table 5.3; Figure S 5.3). Average nightly dive depth varied slightly with increasing levels of moon illumination for two of four individuals (two females; Table 5.3). Individual M1 dived slightly shallower during a full moon than a new moon (M1, GLM,  $F_{1,95} = 4.87$ ,  $p = 0.03$ ,  $R^2 = 0.04$ ) at depths between 10.15 to 43.01 m, and individual M5 dived deeper (Spearman Rank Correlation,  $r_s = 0.20$ ,  $p = 0.04$ ) at depths between 2.13 and 70.69 m (Figure 5.6).

## 5.5 Discussion

Reef manta rays that were photographed and satellite tagged at D'Arros Island displayed restricted movements away from this location, and appeared to be largely resident to the waters surrounding the Amirante Islands. The Amirantes Bank was a key habitat for all tagged individuals, with photo-identification revealing high residency and limited inter-island movements of the species across the rest of the archipelago. Satellite tagged *M. alfredi* spent the majority of their time in the upper 50 m of the water column, with 95% of all depth records found to be shallower than the maximum depth of the St. Joseph Channel (60 m) upon the Amirantes Bank.

### 5.5.1 Horizontal movement

#### 5.5.1.1 Photo-identification

Photo-identification data suggested that *M. alfredi* display high site fidelity to sighting locations, with over half of all identified individuals being re-sighted on at least one occasion. This technique found evidence of only three movements of  $> 200$  km being recorded away from D'Arros Island in four years. Additionally, two of the six satellite-tagged individuals were resighted close to their tagging location after shedding their tags. Similar levels of site fidelity have been reported for *M. alfredi* at other localities using photo-identification, with food availability and deep-water barriers to movement thought to contribute to the extended site occupancy of individuals (Couturier et al. 2011, Deakos et al. 2011, Marshall et al. 2011, Germanov & Marshall 2014). In Seychelles, the bathymetry of the Amirantes Bank may drive increased zooplankton accumulation in an otherwise oligotrophic region, subsequently generating reliable food sources for *M. alfredi* and contributing to the observed residency of this species at the Amirante Islands (Gove et al. 2016, Peel et al. 2019b). Continued efforts to monitor the patterns of movement of *M. alfredi* in Seychelles using photo-identification will provide additional insight into the distribution and connectivity of this population, and strengthen the

current understanding of residency and site fidelity in this species. Furthermore, the impact of these data will be maximised if records can be collected by a network of citizen scientists throughout the region. Such a network will assist in overcoming the challenges associated with surveying the substantial area encompassed by the Seychelles EEZ and the large distances that separate islands of the archipelago (maximum 1,200 km), which were faced in the present study.

### 5.5.1.2 Satellite telemetry

The suggestion of prolonged residency of *M. alfredi* to the Island Groups of Seychelles provided by the photo-identification study was confirmed by satellite tagging. All tagged *M. alfredi* remained in close proximity to the Amirantes Bank while they were tracked, and no individual was recorded to exit the boundary of the Seychelles EEZ. The residency of tagged *M. alfredi* to the Amirante Island Group, and potentially to D'Arros Island and St. Joseph Atoll, was highlighted by the frequency at which track positions were estimated to occur within the latitudinal and longitudinal ranges of these locations. Similar patterns of restricted movement have been reported for satellite tagged *M. alfredi* elsewhere (Jaine et al. 2014, Braun et al. 2015, Kessel et al. 2017). Individuals in eastern Australia, for example, dispersed up to 520 km from their tagging location (Jaine et al. 2014), but all were observed to travel back towards this location prior to the end of their track. A higher level of site fidelity was noted for *M. alfredi* tagged in the Red Sea, where the repeated visitation of individuals to a coastal aggregation area was recorded, and regional movements occurred within 200 km of the tagging site (Braun et al. 2015, Kessel et al. 2017). The similar spatial scales of tracks reported for *M. alfredi* across these other locations, and as now recorded in Seychelles, supports the hypothesis that limited dispersal and high residency to aggregation areas are characteristic of this species.

The patterns of movement of male (n = 1) and female (n = 3) *M. alfredi* were considered collectively in this study. Two of the three miniPATs deployed on male *M. alfredi* in Seychelles failed to report a reliable data set, so a comparison between the movement patterns of the sexes was not attempted. Tag failure has been reported in numerous studies of the movement ecology of elasmobranchs (Braun et al. 2015, Ferreira et al. 2015, Skomal et al. 2017, Domeier et al. 2019). Indeed, it is an unavoidable component of telemetry-based research given the suite of factors in the marine environment that can lead to tag damage, loss or computational error (Hammerschlag et al. 2011). The deployment of a larger number of tags on *M. alfredi* in Seychelles in the future will reduce the impact of these two tag failures on the cumulatively collected dataset for this region. Additional tags may also provide insight into the frequency of occurrence of large-scale movements by *M. alfredi* throughout the archipelago.



All four of the tracks estimated in this study were associated with tags deployed on mature *M. alfredi*. Mature individuals were hypothesised to travel further than immature individuals at the time of tag deployment. This was because of the reduced energy requirements that are associated with travel for larger fishes (Ware 1978) and the observation of size-based variation in movement patterns in other elasmobranch species (Bansemer & Bennett 2011, Chapman et al. 2015). Larger *M. alfredi* were therefore anticipated to encompass the widest possible home range for this species in Seychelles, and were selectively targeted during tagging. Juvenile *M. alfredi* were subsequently confirmed to display a higher level of residency and site fidelity to D'Arros Island than larger individuals monitored passively through an acoustic receiver array in the Amirante Island Group (Peel et al. 2019b). For this reason, future studies aiming to deploy additional satellite tags on *M. alfredi* in Seychelles should continue to focus efforts on mature males and females, and endeavour to tag individuals at other Island Groups. This will facilitate a comparison of movement patterns between the sexes (Sequeira et al. 2019), and across a wider region of Seychelles.

#### 5.5.1.2.1 Inclusion of acoustic data

The inclusion of acoustic detection data in the HMM of one satellite-tagged individual significantly restricted the latitudinal range encompassed by the associated track by reducing geolocated-position error from an approximate radius of 29.8 km to only 165 m. In addition to highlighting the magnitude of error present in the HMM models based upon geolocation-position estimates alone, the inclusion of acoustic detection data also increased the frequency at which the position estimates for this individual fell within the range of D'Arros Island and St. Joseph Atoll. Geolocation errors are known to increase with increasing proximity to the equator because of the lack of seasonal variation in the timing of sunrise and sunset, and the consistency of sea surface temperature throughout the equatorial zone (Nielsen et al. 2006, Nielsen & Sibert 2007, Braun et al. 2015, Braun et al. 2018a). Future studies of *M. alfredi* movement patterns in Seychelles should therefore consider using alternative satellite tag types at this location. For example, tags that incorporate GPS and Argos technology alongside geolocation capabilities (e.g. SPLASH or GPS Fastloc tags; Doherty et al. 2017), or fin-mounted or towed tags that provide live updates of location via satellite (SPOT tags; Kessel et al. 2017). These tags may also help to increase the amount of archived high-resolution data that can be transmitted via satellite; a useful function in a remote archipelago, where land is scarce (459 km<sup>2</sup>), and detached satellite tags are unlikely to wash ashore for easy retrieval as has occurred elsewhere (Braun et al. 2014, Jaine et al. 2014).



## 5.5.2 Vertical movement

Little variation was observed in the vertical movement patterns of *M. alfredi* tagged at D'Arros Island. Individuals spent the majority of their time in the top 50 m of the water column at temperatures between 27 and 29°C, and infrequently completed dives to depths of > 150 m (n = 6). Average dive depth increased at night for three of the four individuals that were successfully tagged, a behaviour consistent with the results of similar studies in the Red Sea (Braun et al. 2014). Such changes in patterns of vertical habitat use by manta rays and other elasmobranchs have been attributed to foraging behaviour (Couturier et al. 2013a, Burgess et al. 2016) and/or predator aversion (Gliwicz 1986, Hays 2003, Webster et al. 2015). Given the relatively coarse nature of the movement data retrieved in this study, however, additional tag deployments on *M. alfredi* in Seychelles will be required to further explore the mechanisms underlying the patterns of vertical habitat use by this species.

Weak and conflicting relationships between average nightly dive depth and moon illumination level were noted for two of the four *M. alfredi* successfully tagged in this study. One individual dived slightly deeper during a new moon, whereas the other dived deeper during a full moon. In the Red Sea, dive depth was found to increase with moon illumination for *M. alfredi* when individuals moved from inshore waters (< 15 km from coastline;  $R^2 = 0.10$ ,  $p = 0.01$ ), to offshore waters (> 15 km from coastline;  $R^2 = 0.503$ ,  $p < 0.001$ ; Braun et al. 2014). The increased illumination of the full moon is thought to restrict the extent of diel vertical migration of zooplankton through the water column in these deeper, offshore locations, subsequently altering the vertical movement patterns of foraging *M. alfredi* (Hays 2003, Couturier et al. 2013a, Braun et al. 2014). It is therefore possible, that the weak influence of moon illumination on the dive profiles of *M. alfredi* reported here is a result of the residency displayed by individuals to the typically shallow Amirantes Bank (average depth 40 m; Stoddart et al. 1979), where increased prey availability may reduce their need to forage in deep, offshore sites during the night. Future tagging efforts that allow for the collection of higher resolution depth and position data for *M. alfredi* over multiple lunar cycles are required to confirm this hypothesis, and to quantify the extent to which vertical movement patterns vary at an individual level.

The consistent and shallow (< 50 m) habitat use of *M. alfredi* increases the likelihood of individuals encountering anthropogenic threats (Dulvy et al. 2014). These include, but are not limited to, boat strikes, accidental entanglements in fishing gear, and targeted fishing practises (Heinrichs et al. 2011, Croll et al. 2016, Stewart et al. 2018a). The reliable aggregation of individuals at specific locations in Seychelles, particularly within the Amirante Island Group (Peel et al. 2019b), further increases these risks for *M. alfredi*. This is because the predictability of these aggregation events in both time and space increases the risk of exploitation for a substantial number of individuals. Although a dedicated mobulid fishery does not currently exist

in Seychelles (Temple et al. 2019), the large impact of small-scale fisheries on elasmobranch populations in the Western Indian Ocean region is becoming increasingly apparent (Temple et al. 2018, Temple et al. 2019). Should the demand for mobulid products – specifically gill plates (Whitcraft et al. 2014, Lawson et al. 2017, O'Malley et al. 2017) – increase in this region, it is highly likely to increase the susceptibility of this *M. alfredi* population to exploitation and decline (Temple et al. 2019). In the absence of national-scale protective legislature for this globally vulnerable species in Seychelles (Marshall et al. 2018b), these anthropogenic threats raise concerns regarding the longevity of *M. alfredi* aggregations at D'Arros Island and St. Joseph Atoll, and emphasise the importance of establishing appropriate management and conservation strategies at this site.

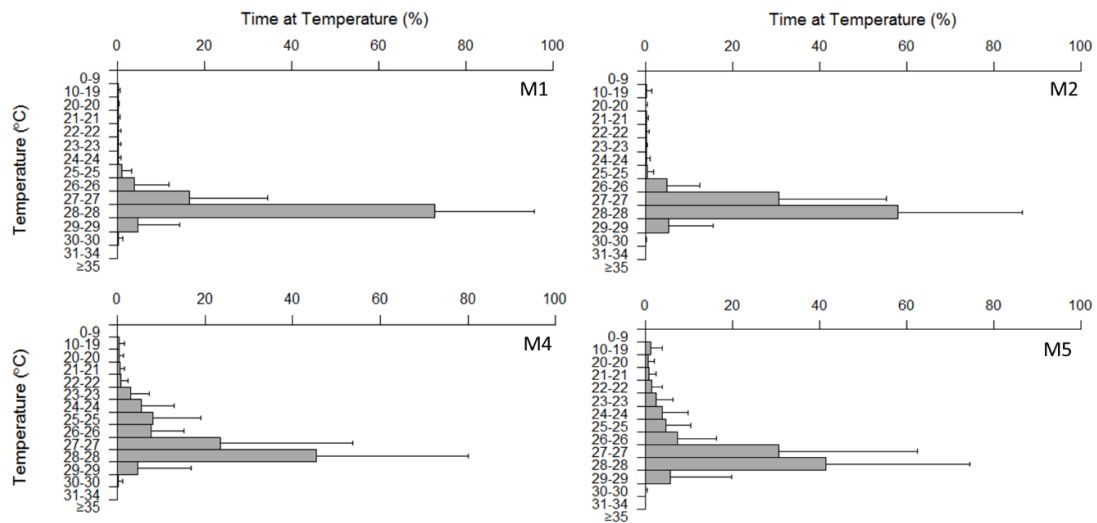
### 5.5.3 Conclusion

Photo-identification, and satellite and acoustic telemetry, have revealed that *M. alfredi* photographed and tagged at D'Arros Island were largely resident to the Amirante Island Group of Seychelles. Tagged individuals spent the majority of the time that they were tracked in the upper 50 m of the water column, likely over the shallow Amirantes Bank, where they may face increasing exposure to anthropogenic threats from small-scale fisheries in the Western Indian Ocean in the future. These findings suggest that the development of a Marine Protected Area at D'Arros Island and St. Joseph Atoll, and more broadly across the Amirantes Bank as a whole, would benefit *M. alfredi* conservation efforts in Seychelles. Continued monitoring of the movement patterns of this remote population across the archipelago will be crucial to the assessment of national-scale management strategies for this globally vulnerable species.

## 5.6 Supporting material

**Table S 5.1** Movements of reef manta rays (*Mobula alfredi*) between the Island Groups of Seychelles recorded using photo-identification.

Manta ID	Sex	Maturity	D'Arros Island (Amirante Group)	St. François Atoll (Alphonse Group)	Time between resightings (days)	Approx. Distance (km)
SC-MA-0021	Female	Sub-adult	13 Mar 2017	14 Dec 2018	641	198
SC-MA-0032	Female	Adult	28 Jun 2013	8 Dec 2017	1,624	200
SC-MA-0190	Male	Adult	26 Nov 2017	10 Dec 2017	14	195



**Figure S 5.1** Percentage of time spent at temperature by four reef manta rays (*Mobula alfredi*) tagged with archival pop-up satellite tags in Seychelles. M\* indicates manta identification number.

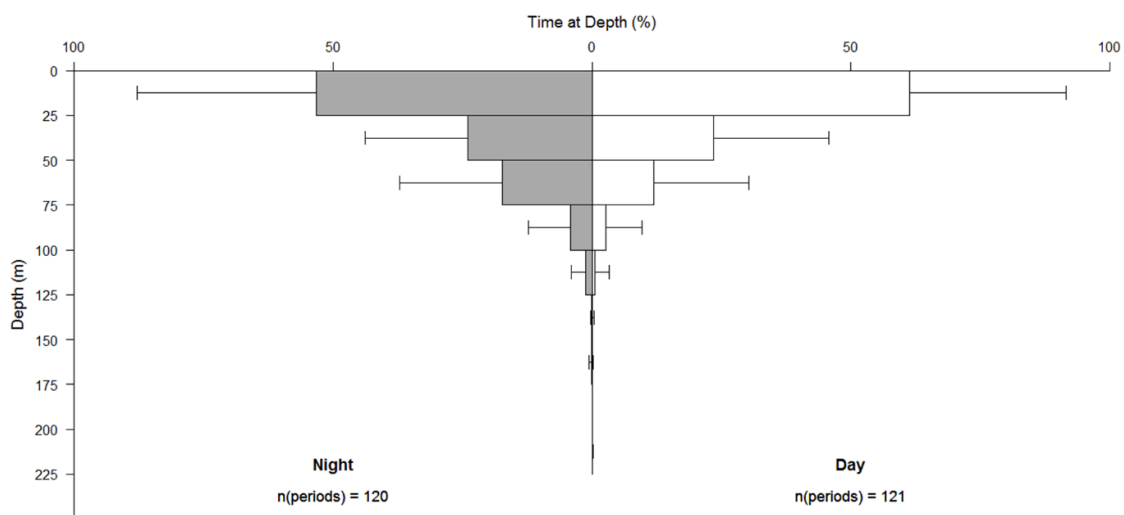


**Figure S 5.2** Percentage time at depth during the day (white bars) and night (grey bars) for reef manta ray (*Mobula alfredi*) M5 in Seychelles tagged with an archival pop-up satellite tag. 'n(periods)' indicate the number of days that depth data were available for within the track. Error bars represent standard deviation.

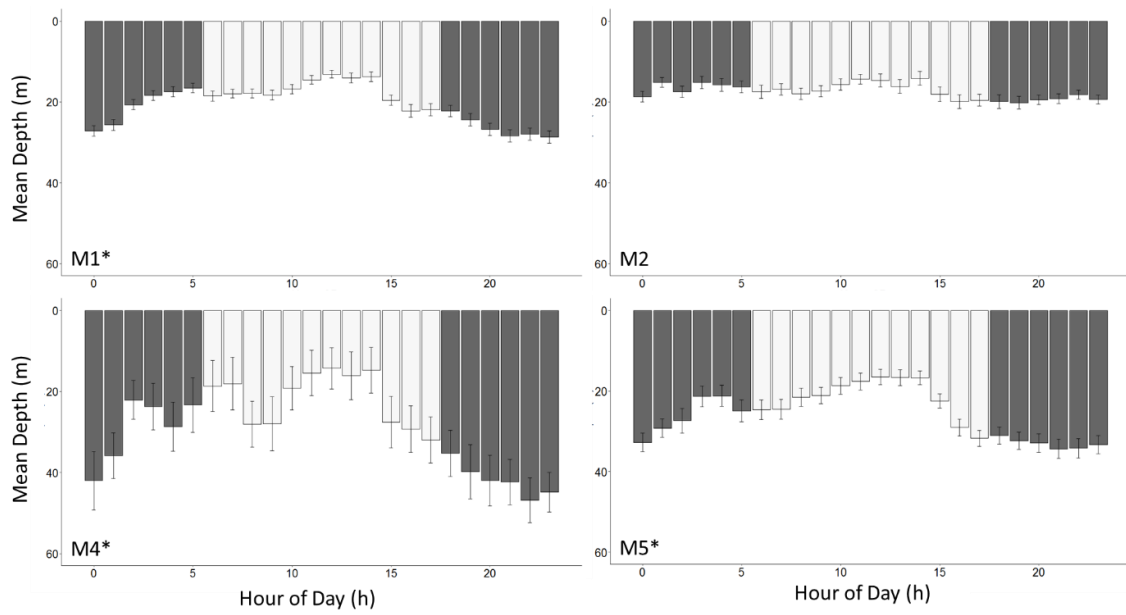


**Figure S 5.3** Average hourly ( $\pm$  S.E.) dive depth for four reef manta rays (*Mobula alfredi*) tagged with archival pop-up satellite tags in Seychelles. Asterisks represent individuals that performed deeper dives during the night (dark grey bars) than during the day (light grey bars).

## Chapter 6 General Discussion

An understanding of the movement patterns and feeding ecology of reef manta rays (*Mobula alfredi*) is essential to the design of effective conservation measures aimed at protecting vulnerable populations from future declines (Stewart et al. 2018a, Hays et al. 2019). In the Western Indian Ocean, numerous aggregations of *M. alfredi* have been identified, however, little data is available regarding population sizes and distributions in the region, complicating the establishment of appropriate management strategies. In this study, I used a combination of research techniques to examine the population size, patterns of movement and residency and feeding ecology of *M. alfredi* in the remote archipelago of Seychelles, with a focus on the aggregation at D'Arros Island and St. Joseph Atoll (hereafter D'Arros Island). These data broaden our current understanding of the biology and ecology of this globally vulnerable species, and will aid in the development of future management strategies for the species in Seychelles and wider Western Indian Ocean region.

### 6.1 Overview of findings

I used photo-identification techniques to examine the population size and distribution of *M. alfredi* in Seychelles, with a focus on the aggregation at D'Arros Island, and identified a small, but resident, population of 236 individuals (Chapter 2). The majority of individuals were sighted at D'Arros Island (67%; Amirante Island Group), and 23% were sighted at St. François Atoll (Alphonse Island Group). A camera system deployed at a cleaning station to the north of D'Arros Island provided insights into the temporal variation in patterns of habitat use by *M. alfredi* at this location. This work also highlighted the value of remote camera systems as a means of monitoring this species at isolated aggregation sites. I also used passive acoustic telemetry to examine the patterns of movement and residency of *M. alfredi* around D'Arros Island, and throughout the Amirante Island Group (Chapter 3). Telemetry data indicated that *M. alfredi* displayed a high level of residency to the Amirante Islands, particularly to D'Arros Island, regardless of the size and sex of individuals.

I then used stable isotope analyses to examine the feeding ecology of *M. alfredi* at D'Arros Island (Chapter 4). The significant contribution of pelagic, emergent and mesopelagic zooplankton to the diet of *M. alfredi* provided support for the hypothesis that these large elasmobranchs occupy a unique trophic role at this locality, and may act as a vector for the horizontal transport of nutrients into reef systems from mesopelagic environments. In addition, I optimised lipid-extraction procedures for muscle tissue of *M. alfredi* to ensure that the results of future analyses

using stable isotopes to examine the foraging ecology of this species would be comparable among populations.

Lastly, I used archival satellite telemetry alongside acoustic telemetry and photo-identification data to examine the potential large scale (> 100 km) patterns of movement of *M. alfredi* in Seychelles (Chapter 5). Satellite-tagged *M. alfredi* did not leave the boundary of the Seychelles Exclusive Economic Zone (EEZ) for the entire period that they were tracked (maximum 180 days), and geolocation data further indicated a high level of residency of individuals to the Amirante Islands.

Collectively, these findings highlight the significance of D'Arros Island to the small, resident population of *M. alfredi* currently identified in Seychelles. These data also indicate that the establishment of Marine Protected Areas at the aggregation sites for *M. alfredi* currently recognised at D'Arros Island (Amirante Island Group) and St. François Atoll (Alphonse Island Group), would benefit management and conservation efforts for all cohorts of this population. Furthermore, the apparent removal of *M. alfredi* aggregations in Seychelles from the pressures of mobulid fisheries and acute anthropogenic threats (by-catch, boat strike, entanglement etc.) that are associated with more coastal sites in the Western Indian Ocean, emphasises the relatively pristine nature of this population and its potential to provide baseline data regarding the biology and ecology of this species. Moving into the future, photo-identification techniques should be used by an increasing network of citizen science collaborators spread across the archipelago to monitor the population of *M. alfredi* in Seychelles, and to ensure that management strategies are established at appropriate spatio-temporal scales for this population.

## 6.2 Movement patterns

The aggregative behaviour of manta rays facilitates studies of their biology and ecology, but challenges the need to conserve threatened populations. The residency of *M. alfredi* at aggregation sites allows intensive studies to be conducted on population dynamics and patterns of movement and habitat use, which can then inform the design of protective strategies. Additionally, aggregation sites can be used to direct the focus of management and conservation efforts to locations where the largest number of individuals will benefit. This is particularly significant for populations of *M. alfredi*, given that the area of their aggregation sites is much smaller than the area encompassed by their overall distribution. Conversely, the predictability of aggregations of *M. alfredi* increases the susceptibility of large numbers of individuals to exploitation by mobulid fisheries, and to acute anthropogenic threats including by-catch, boat strike, entanglement and marine debris (Heinrichs et al. 2011, Croll et al. 2016, Germanov et al. 2018). The concurrent identification of aggregation sites for *M. alfredi*, and development of an understanding of the level

of connectivity between them, is thus key to efficiently establishing conservation measures for populations on appropriate spatio-temporal scales.

## 6.2.1 D'Arros Island

In the scattered archipelago of Seychelles, D'Arros Island is one of the few locations where *M. alfredi* are known to reliably form aggregations. Acoustic and satellite telemetry data collected in this study indicated that *M. alfredi* tagged at D'Arros Island were highly resident at this location, and to the Amirante Islands as a whole (Chapters 3 and 5), regardless of their size and sex (Chapter 3). This finding was further supported by the photo-identification component of this study (Chapter 2), with almost 80% of the individual *M. alfredi* that were photographed at D'Arros Island being re-sighted on at least one occasion. The consistency of these observations across different components of this study emphasises the significance of D'Arros Island to *M. alfredi* in this remote region of the Western Indian Ocean, and prompt an obvious question: why D'Arros?

Around the world, aggregations of manta rays at tropical locations are commonly associated with foraging opportunities (Anderson et al. 2011a, Couturier et al. 2011, Couturier et al. 2012). It is therefore likely that the availability of prey significantly influences the residency of *M. alfredi* at D'Arros Island. The concurrent collection of movement and environmental data within the acoustic telemetry component of this study (Chapter 3) allowed examination of the temporal and environmental drivers of occurrence of *M. alfredi* at this locality, and consideration of the role of these factors in influencing zooplankton availability at D'Arros Island. Day of year, time of day, fraction of moon illumination, tidal range, time to high tide, wind speed, wind direction and water temperature all influenced the occurrence of acoustically-tagged *M. alfredi* within 2.5 km of the shoreline of D'Arros Island (see Table 3.3). While a large amount of individual variation was also noted to be present in the acoustic detection data, these findings represented a significant first step in understanding the drivers of movement and residency patterns for *M. alfredi* at D'Arros Island and St. Joseph Atoll, and in a remote region of the Western Indian Ocean. Furthermore, these findings provided insight into how zooplankton may accumulate in the water column at D'Arros Island, and indicated the optimal set of conditions under which this may occur.

The hypothesis that foraging opportunities at D'Arros Island drive the high levels of residency and site fidelity of *M. alfredi* observed at this location was further supported by linkages between diet (Chapter 4) and the temporal variation in visits to a cleaning station (Chapters 2 and 3), where individuals are able to have external parasites removed by resident reef fishes (Potts 1973, O'Shea et al. 2010). Stable isotope analyses (Chapter 4) suggested that emergent zooplankton comprises a significant component (~25%) of the diet of *M. alfredi* at D'Arros Island. Additionally, both the

acoustic telemetry and photo-identification studies showed that visits to the cleaning station peaked during the middle hours of the day, and waned at dawn and dusk. Together, these data suggest that *M. alfredi* may prioritise the opportunity to forage on emergent zooplankton from dusk until dawn, only visiting the cleaning station when these communities are no longer accessible as food (i.e. during the day), and cleaner fishes are most active (Potts 1973, Lenke 1988). Furthermore, cleaning stations are hypothesised to serve as important sites for socialising and courtship for manta rays (Deakos et al. 2011, Stevens et al. 2018b, Germanov et al. 2019). Should foraging opportunities drive the initial occupation of *M. alfredi* at D'Arros Island, the subsequent increase in the likelihood of encountering conspecifics at this location may act as additional motivation for individuals to remain in the area.

## 6.2.2 Amirante Islands

In addition to assessing the level of residency of *M. alfredi* to D'Arros Island, this study aimed to examine the movement patterns of this large, pelagic species among the Amirante Islands using acoustic and satellite telemetry (Chapters 3 and 5). Such measures of movement are important to the design of management and conservation strategies, as they indicate the spatial extent of protection required by a species. The contrast in bathymetry between the typically shallow Amirantes Bank (average depth 40 m; Stoddart et al. 1979) upon which the Amirante Islands are located, and the deep water (> 1,000 m) surrounding the Bank is also significant to this study. Deep water has been hypothesised to act as a barrier to the movement of *M. alfredi* (Deakos et al. 2011), however, the extent of this restriction on the movement patterns of *M. alfredi* is still poorly understood.

Medium scale (10 – 100 km) movements by *M. alfredi* away from D'Arros Island and throughout the Amirante Islands occurred infrequently (Chapter 3), and satellite telemetry data suggested that large scale (> 100 km) movements were also uncommon in this population (Chapter 5). The continued occupation of *M. alfredi* within the region of the Amirantes Bank, and lack movement of individuals out of the Seychelles EEZ, highlighted the significance of this shallow plateau, and D'Arros Island in particular, to tagged individuals in Seychelles. It is possible that the deep water surrounding the Bank restricted the movement of *M. alfredi* away from this location and forced the increased residency of individuals to the Amirante Islands. Alternatively, or in addition, the steep bathymetry of the Amirantes Bank may serve to increase zooplankton accumulation and abundance throughout the Amirante Islands by processes including the Island Mass Effect (Doty & Oguri 1956, Hamner & Hauri 1981). This increased prey availability may subsequently promote the high level of residency reported for *M. alfredi* within the Amirante Islands (Chapters 2 and 3), particularly given the oligotrophic nature of the water column away from this



Island Group, and the reduced likelihood of individuals encountering prey fields elsewhere in the open ocean (Sims et al. 2006, Gove et al. 2016).

### 6.2.3 Wider Seychelles

Although the aggregation of *M. alfredi* at D'Arros Island was the primary focus of this research, the collaborative nature of the photo-identification component of this study (Chapter 2) led to the identification of a second aggregation site for *M. alfredi* in Seychelles. A total of 22% of the currently identified population of *M. alfredi* were identified at St. François Atoll within the Alphonse Island Group, suggesting that the lagoon and reef flats at this locality may represent an important habitat for individuals in Seychelles. Additionally, the three recorded movements of *M. alfredi* from D'Arros Island to St. François Atoll (~ 200 km; Chapters 2 and 5) indicated that the Amirante and Alphonse aggregations are connected to a small extent. This suggests that the habitats provided by the St. François Atoll may benefit both individuals that are resident to this site, and those in transit between these Island Groups. As hypothesised for D'Arros Island, St. François Atoll may provide substantial foraging opportunities for *M. alfredi* within a typically oligotrophic region of the Western Indian Ocean (Gove et al. 2016). This is supported by the observation of the largest feeding event on record (40 individuals) for this species in Seychelles along the eastern reef flats of the atoll. It is also possible that the lagoon of St. François may act as a nursery area for *M. alfredi*, given incidental sightings of young individuals (disc width < 1.5 m) at this location during the pilot study conducted in December 2017. Similar hypotheses have been proposed regarding the use of Palmyra Atoll by *M. alfredi* in the Pacific Ocean (McCauley et al. 2014), however, future monitoring will be required to confirm these patterns of habitat use in Seychelles.

The combination of research techniques used in this study, and resultant identification of two key aggregation areas for *M. alfredi* in Seychelles, is not only significant to the assessment of the conservation needs of this species in the Western Indian Ocean. These findings also broaden our understanding of the general movement ecology of *M. alfredi*, and will aid future efforts to study their patterns of movement and residency around the world. Photo-identification techniques have already been shown to be valuable for the study of *M. alfredi* populations (Deakos et al. 2011, Marshall et al. 2011, Marshall & Pierce 2012, Couturier et al. 2014, Germanov & Marshall 2014), and acoustic and satellite telemetry techniques are becoming increasingly popular in the studies of movement ecology of mobulid rays (Croll et al. 2012, Jaine et al. 2014, Thorrold et al. 2014, Stewart et al. 2016a, Couturier et al. 2018, Stewart et al. 2018a). Restricted patterns of movement and high site fidelity have been reported for *M. alfredi* in eastern Australia, Hawaii, Indonesia and the Red Sea (Deakos et al. 2011, Germanov & Marshall 2014, Braun et al. 2015, Kessel et al. 2017, Couturier et al. 2018), and the data presented in this study for the Seychelles population

support these previous findings. Taken together, these studies highlight the significance of aggregation sites to *M. alfredi* populations at a global scale. Individuals visit these sites over long periods of time (weeks to months), in comparison to the short periods (days to weeks) that would be expected for non-aggregating species in transit (Stevens et al. 2010, Ferreira et al. 2015). These extended periods of occupation provide the opportunity to conserve a large number of individuals over relatively small and thus cost-efficient, spatial scales. Knowledge of such movement patterns is particularly valuable in remote archipelagos, including Seychelles, where it is often not possible to survey the waters of islands and reefs spread over thousands of kilometres of ocean. In such situations, the identification of aggregation areas during preliminary surveys can facilitate the early establishment of small- to medium-scale (10 – 100 km) management strategies, while distributions over wider areas are described in the longer term. Furthermore, the deployment of satellite tags during preliminary trips and the resulting data sets may guide the selection of future areas of interest for subsequent surveys, maximising sampling efficiency and the likelihood of identifying new areas of significance to *M. alfredi*.

Finally, the similarity of findings among the photo-identification and telemetry components of this study validate the use of photo-identification to monitor the *M. alfredi* population in Seychelles, and provide cost-effective means of long-term monitoring of residency and patterns of movement of the species. In contrast to photo-identification studies of other elasmobranchs, which tend to under estimate residency (Delaney et al. 2012, Cagua et al. 2015), residency patterns of *M. alfredi* derived from sighting data in Seychelles aligned closely with both acoustic and satellite telemetry data (Chapters 2, 3 and 5). Future photo-identification surveys should be conducted by a network of citizen scientist collaborators distributed widely throughout the islands of Seychelles in order to maximise the coverage of monitoring efforts. Remote camera systems (MantaCam; Chapter 2) could also be used to increase data collection at hotspots (e.g. cleaning stations), particularly when research teams are small. Consistency of this sampling effort among Island Groups will facilitate a more accurate estimation of the Seychelles-wide population size of *M. alfredi*, in addition to providing further insight into the extent and frequency of movements by individuals among islands of the archipelago. Such a monitoring regime would also increase the likelihood of encountering oceanic manta rays (*Mobula birostris*), which were rarely sighted during the current study (Chapter 2). In the immediate future, efforts should be expanded to focus on the *M. alfredi* aggregation at St. François Atoll, and aimed at broadening the current understanding of the role that this location plays in the life history of *M. alfredi* in Seychelles. As a potential nursery area, the establishment of an acoustic receiver array inside and outside of the St. François lagoon, and of an acoustic tagging programme for *M. alfredi*, would be beneficial to understanding the habitat use and movement patterns of individuals at this site.

## 6.3 Feeding ecology

Although feeding opportunities are thought to drive the aggregation of *M. alfredi* at numerous sites around the world (Couturier et al. 2012, Armstrong et al. 2016), only two studies aiming to describe the foraging ecology of this species using stable isotope analyses have been completed to-date (Couturier et al. 2013a, McCauley et al. 2014). These focussed only on *M. alfredi* and potential prey items, providing little information on the trophic role of these animals in the reef environment.

The unique trophic role that *M. alfredi* occupies at D'Arros Island was revealed in this study through extensive sampling of the reef fish community at this locality and the use of stable isotope analyses. Pelagic zooplankton comprised the majority of the diet of *M. alfredi* at D'Arros Island (Chapter 4), a finding consistent with the large number of observations of surface filter-feeding reported at this locality (Chapter 2). The high residency of *M. alfredi* to the reef flats of D'Arros Island (Chapter 3) suggested that the species may play a significant role in distributing nutrients across the reef flats at this locality via defecation after feeding, particularly in the area of cleaning stations (Chapters 2 and 3). Emergent zooplankton comprised a smaller (~25%), yet significant, amount to the diet of *M. alfredi*. As described for the population in eastern Australia (Couturier et al. 2013a), this finding suggested that individuals forage on emergent zooplankton during the night, and is further supported by the lower frequency of crepuscular (Chapter 2) and nocturnal (Chapter 3) visits by *M. alfredi* to the cleaning station at D'Arros Island. By feeding throughout the diel cycle on both pelagic and emergent zooplankton, the contribution of *M. alfredi* to nutrient flow within reefs is expected to be increased, as are any potential trophic effects such, as increased coral growth (Shantz et al. 2015, Williams et al. 2018, Topor et al. 2019).

The contribution of mesopelagic (~17%) zooplankton to the diet of *M. alfredi* at D'Arros Island is also significant here, and provided support for the hypothesis that emergent and mesopelagic zooplankton contribute a larger proportion of the diet of this species than originally thought (Couturier et al. 2013a). Individuals would need to move offshore from D'Arros Island and away from the Amirantes Bank to access mesopelagic zooplankton communities, which typically occur at > 200 m depth during the day (Hays 2003). The diel migration performed by these plankton communities towards the surface during the night (Hays 2003) would then bring mesopelagic prey items within the range of vertical movements of *M. alfredi* in Seychelles (< 50 m depth; Chapter 5). The foraging of individuals on these offshore communities may allow for *M. alfredi* to act as a vector for horizontal nutrient transport on their return to shallow water near D'Arros Island (Papastamatiou et al. 2015a). A similar mechanism of offshore-to-reef nutrient supply has been noted for seabirds at remote archipelagos. Seabird colonies contribute nutrients obtained during offshore foraging journeys to fringing coral reefs by depositing guano on islands (Savage 2019). The resulting provision of nutrients to reef systems has been shown to increase local

productivity and enhance coral growth in Fiji (Savage 2019), Hawaii (Honig & Mahoney 2016), New Caledonia (Lorrain et al. 2017), and at the Chagos Archipelago (Graham et al. 2018). Furthermore, this mechanism of nutrient supply is thought to increase manta ray occurrence at Palmyra Atoll by facilitating a local increase in productivity and subsequently, plankton abundance (McCauley et al. 2012a). In the same way that seabirds foraging offshore return to colonies and defecate, *M. alfredi* may enhance nutrient supply to the coral reefs at D'Arros Island by feeding on mesopelagic zooplankton and then returning to specific aggregation areas (e.g. cleaning stations). This marine-oriented system of offshore-to-reef nutrient transport, coupled with the local residency of *M. alfredi* to D'Arros Island, highlights the unique trophic role that these elasmobranchs may play at this remote reef system.

The insights gained into the foraging behaviour and trophic role of *M. alfredi* at D'Arros Island underscore the value of extensive, yet targeted, sampling of organisms within reef systems for studies involving stable isotope analysis. The sampling strategy used at this locality was motivated by the need to encompass as many trophic guilds within the final isoscape as possible, while minimising the number of animals that were handled throughout the course of the research (Sloman et al. 2019). This was achieved by selecting target species and determining required sample sizes prior to entering the field, facilitating an efficient, but extensive, survey of the reef system at D'Arros Island in a short period of time (< 1 month). Additionally, the samples of muscle tissue from *M. alfredi* collected at D'Arros Island allowed for subsequent handling and processing procedures related to stable isotope analyses to be optimised (Chapter 4). An understanding of the effect of lipid and urea extraction procedures on the isotopic signature of elasmobranch muscle tissue is important in studies of foraging ecology because variations in the stable isotope ratios of carbon ( $\delta^{13}\text{C}$ ) and nitrogen ( $\delta^{15}\text{N}$ ) may influence the interpretation of, and conclusions drawn from, the data (Marcus et al. 2017). Trials that examine the effects of these procedures have been conducted for a number of species of sharks (Hussey et al. 2010, Hussey et al. 2012b, Li et al. 2016, Marcus et al. 2017) but prior to this study, had not yet been completed for a pelagic ray. The findings presented in Chapter 4 indicate that the lipid-extraction procedure was effective at extracting both lipids and urea from the muscle tissue of *M. alfredi*. It should therefore be used in future studies of the foraging ecology of this species using stable isotope analyses to allow for accurate comparisons to be drawn among populations of *M. alfredi* around the world (Stewart et al. 2018a).

## 6.4 Implications for conservation

Global efforts to broaden our understanding of the patterns of movement and foraging ecology of *M. alfredi* have increased markedly over the past two decades, and are driven by the need to

accurately assess the conservation needs of this ‘Vulnerable’ species (IUCN Red List for Threatened Species; Marshall et al. 2018b, Stewart et al. 2018a). Published studies of population size, patterns of residency and movement and feeding behaviour of *M. alfredi* now span the Indian (Kitchen-Wheeler et al. 2012, Germanov & Marshall 2014, Setyawan et al. 2018) and Pacific (Deakos et al. 2011, Couturier et al. 2014, McCauley et al. 2014, Barr & Abelson 2019) Oceans. However, in the Western Indian Ocean, studies are currently limited to coastal aggregation sites (Marshall et al. 2011, Kessel et al. 2017). This study provides insight into the ecology of *M. alfredi* in Seychelles, and represents a first step in assessing the conservation needs of this species in a remote region of the Western Indian Ocean.

The identification of key aggregation sites for *M. alfredi* at D’Arros Island (Amirante Island Group) and St. François Atoll (Alphonse Island Group) in Seychelles, supports the development of Marine Protected Areas at these locations, which would restrict the recreational and commercial use of these areas. Movement data collected using acoustic and satellite telemetry have been shown to benefit conservation and management strategies for marine megafauna (Lea et al. 2016, Hays et al. 2019), and this is expected to be particularly true species that aggregate, including *M. alfredi*, which may be wide-ranging but will often return to specific sites (e.g. cleaning stations; Anderson et al. 2011a, Couturier et al. 2011, Deakos et al. 2011, Germanov & Marshall 2014). In addition to bolstering the protection afforded to *M. alfredi* through listings on the Convention for the International Trade of Endangered Species (CITES; Appendix II) and Convention for Migratory Species (CMS; Appendix I and II), Marine Protected Areas at these locations would also serve to reduce the risk of local-scale anthropogenic threats to individuals. These include, but are not limited to, targeted fishing pressures, by-catch, accidental entanglement, boat strike and entanglement in, or ingestion of, marine debris (Croll et al. 2016, Germanov et al. 2018, Stewart et al. 2018a). The equal proportions of male and female *M. alfredi* reported in the currently identified population of Seychelles suggests that conservation benefits arising from such management strategies would be of equal significance to both sexes. This is particularly significant for a population occurring in a remote region of the Western Indian Ocean, which may face increasing anthropogenic pressures in the future (Temple et al. 2018). Finally, it is important to acknowledge that the establishment of such Marine Protected Areas in Seychelles will also benefit the habitats that they encompass. By conserving key aggregation sites for *M. alfredi*, the nutrient transport processes facilitated by these large zooplanktivores can be protected, and the potential benefits of increased nutrient supply to these reef systems sustained.

On a broader scale, the isolation of this population of *M. alfredi* from the intensive and acute fishing and anthropogenic pressures imposed elsewhere within the Western Indian Ocean (Chapter 2; Croll et al. 2016, Temple et al. 2019) highlights the opportunity for pre-emptive conservation measures to be established for these animals. Although the four satellite tagged individuals in this study remained within the boundary of the Seychelles EEZ while they were

tracked (Chapter 5), these animals represent just a small proportion of the total population (1.7%) identified to date. It is therefore possible that large-scale movements by individuals do occur across international boundaries, albeit infrequently, and may serve to connect populations of *M. alfredi* throughout the Western Indian Ocean. The ability for individuals to undertake such substantial movements was emphasised recently, with a pregnant female being sighted at Cocos Island, Costa Rica, in the eastern Pacific Ocean (Arauz et al. 2019). This encounter expanded the known sighting range of *M. alfredi* by 6,000 km, and is the first record of the species on either side of the American continent (Arauz et al. 2019). Taken together with the widespread occurrence of *M. alfredi* in the Indian and Pacific Oceans, it is therefore possible that conservation measures established for this large zooplanktivore at aggregation sites in Seychelles may benefit vulnerable populations across the Western Indian Ocean.

## 6.5 Limitations and future directions

This study provides insights into the movement patterns, feeding ecology and conservation needs of *M. alfredi* in Seychelles, around which future research and monitoring efforts can be developed and implemented. Key outstanding questions include the: (i) extent of movement of individuals throughout the rest of Seychelles, (ii) presence of additional aggregation and nursery areas, (iii) composition of mesopelagic zooplankton communities at the Amirantes Bank, and (iv) level of connectivity between *M. alfredi* populations in Seychelles and elsewhere in the Western Indian Ocean.

### 6.5.1 Extent of movement of reef manta rays in Seychelles

Satellite tags deployed on four individuals (Chapter 5) provided insight into the extent of movement of *M. alfredi* across the archipelago. Although this tagging was valuable, our inability to physically retrieve the deployed tags restricted our analyses to patterns of horizontal and vertical movement at a broad scale. Additionally, two tags failed to transmit sufficient data, and movement patterns of males and females could not be compared as a result. Future tag deployments on *M. alfredi* in Seychelles should therefore be planned to maximise the resolution of recovered tracking data, and this may be achieved in a number of ways. First, the deployment period of archival pop-up satellite tags could be reduced. This would increase the amount of battery power available after tag release for data transmission, and is currently being trialled for two tags (miniPAT; Wildlife Computers; Redmond, WA, USA) recently deployed on *M. alfredi* at D'Arros Island. Second, alternative tag types that incorporate GPS and Argos technology would

provide more accurate position estimates for tagged individuals, and may also help to increase the amount of high-resolution track data that can be transmitted via satellite. Deployment of such tags would remove the reliance on geolocation to estimate the most probable track paths of tagged individuals, and reduce the errors associated with calculated positions that were highlighted in this study (Chapter 5). Lastly, biologging tags that record the fine scale (metres and seconds) movements of individuals could also be used to improve our current understanding of the movement patterns and energetic requirements of *M. alfredi* (Gleiss et al. 2009, Bograd et al. 2010, Braun et al. 2014). Such tags can be equipped with video cameras that allow for the movement and behavioural patterns evident in accelerometer data to be validated (Jewell et al. 2019, Watanabe et al. 2019), or incorporate additional sensors (e.g. chlorophyll- $\alpha$ , dissolved oxygen) that further differentiate the drivers and energetics of the movements of this species (Teo et al. 2009, Gleiss et al. 2011, Bailleul et al. 2015, Meyer 2017, Andrzejaczek et al. 2018).

### 6.5.2 Additional aggregation and nursery areas for reef manta rays in Seychelles

As discussed above, it is very likely that there are other aggregation and nursery areas for *M. alfredi* beyond our study area in Seychelles. The establishment of a wide ranging network of collaborators and citizen scientists able to collect photo-identification data throughout the archipelago will maximise the likelihood of identifying these locations in the future. Such a network will also aid in producing accurate estimates of population size for *M. alfredi*, and allow for the stability of these estimates to be monitored over time. Additionally, the inclusion of citizen scientists in this process is likely to benefit conservation efforts for *M. alfredi* on a community-level. Engagement in research facilitates an increased awareness of the threats that populations are currently facing, in turn promoting greater conservation efforts and actions (Friedrich et al. 2014, Jefferson et al. 2015, Lawson et al. 2017, Zimmerhackel et al. 2018).

### 6.5.3 Composition of zooplankton communities at the Amirantes Bank

Studies investigating the diet of *M. alfredi* at D'Arros Island through the analysis of fatty acids in muscle tissue and potential prey items are currently underway to compliment the current understanding of the diet of *M. alfredi* gained through stable isotope analyses (Chapter 4; Couturier et al. 2013a, Meyer et al. 2019). Direct records of the foraging behaviours of *M. alfredi*, however, remain challenging to obtain. Technological advances such as animal-borne cameras are expanding our ability to monitor the feeding ecology of *M. alfredi* in the deep sea (Lander et

al. 2015, Stewart et al. 2016b, Edwards et al. 2019). Future research in Seychelles should therefore endeavour to sample potential zooplankton prey items at depth (Stewart et al. 2018a), and couple these efforts with the use of remote cameras and/or tagging devices attached to *M. alfredi* that will confirm linkages between diving events, prey availability and foraging behaviour (Lander et al. 2015, Lawson et al. 2015, Stewart et al. 2016b, Stewart et al. 2018a).

#### 6.5.4 Connectivity of reef manta ray populations in the Western Indian Ocean

Manta rays display a circumtropical distribution but the extent of connectivity between populations is not known. Advances in genetic sequencing processes, including the use of genome-wide Single Nucleotide Polymorphism data, are providing insight into the connectivity of populations on ocean basin scales (Hosegood et al. 2019; Appendix A). The use of these processes to examine the level of genetic connectivity between *M. alfredi* populations of the Western Indian Ocean will be valuable to future conservation efforts implemented for this species in the region. Together with data collected using satellite telemetry, genetic data will further inform the scale at which management strategies should be designed for *M. alfredi* in Seychelles (e.g. national- and/or international-scale plans) relative to the level genetic and geographical isolation that may exist among aggregation sites.



## 6.6 Concluding remarks

The study of animal movement patterns and foraging behaviour in the marine environment remains challenging, but improvements in tracking, biochemical and genetic approaches continue to expand our ability to answer complex questions regarding the conservation needs of vulnerable megafauna (Hays et al. 2016). This study demonstrated the value of using a multi-technique approach to describe the biology and ecology of *M. alfredi* in a remote region of the Western Indian Ocean. A total of 236 individual *M. alfredi* were identified in Seychelles using photo-identification techniques, and aggregation sites were recognised for this population at D'Arros Island and St. Joseph Atoll (Amirante Island Group) and St. François Atoll (Alphonse Island Group). Individuals identified at D'Arros Island and St. Joseph Atoll were largely resident to this location, a finding confirmed by acoustic and satellite telemetry data. Stable isotope analyses were used to examine the feeding preferences and trophic role of *M. alfredi*, and suggested that these large zooplanktivores play a unique role in transporting nutrients within and to the reefs surrounding D'Arros Island and St. Joseph Atoll from mesopelagic habitats. I argue that these findings highlight the potential biological and ecological value of establishing Marine Protected Areas at both D'Arros Island and St. Joseph Atoll, and at St. François Atoll, for *M. alfredi* in Seychelles. Finally, I outline future research directions for studies of *M. alfredi* in Seychelles, and emphasise the importance of collaboration across the archipelago. The increased monitoring capability of a network of researchers and citizen scientists will ensure the greatest chance of success for proposed and future conservation measures aimed at protecting this vulnerable species, and inform the establishment of similar research endeavours elsewhere in the Western Indian Ocean and around the world.

# References

- Agafonkin V, Thieurmél B (2018) suncalc: compute sun position, sunlight phases, moon position and lunar phase. R package version 0.4 <https://CRAN.R-project.org/package=suncalc>
- Alexander R (1996) Evidence of brain-warming in the mobulid rays, *Mobula tarapacana* and *Manta birostris* (Chondrichthyes: Elasmobranchii: Batoidea: Myliobatiformes). *Zool J Linn Soc* 118:151-164
- Allredge AL, King JM (1980) Effects of moonlight on the vertical migration patterns of demersal zooplankton. *J Exp Mar Biol Ecol* 44:133-156
- Allgeier JE, Burkepile DE, Layman CA (2017) Animal pee in the sea: consumer-mediated nutrient dynamics in the world's changing oceans. *Glob Chang Biol* 23:2166-2178
- Amano T, Sutherland WJ (2013) Four barriers to the global understanding of biodiversity conservation: wealth, language, geographical location and security. *Proc R Soc Biol Sci Ser B* 280:20122649
- Anderson RC, Adam MS, Goes JI (2011a) From monsoons to mantas: seasonal distribution of *Manta alfredi* in the Maldives. *Fish Oceanogr* 20:104-113
- Anderson RC, Adam MS, Kitchen-Wheeler A-M, Stevens G (2011b) Extent and economic value of manta ray watching in Maldives. *Tourism Mar Environ* 7:15-27
- Andrzejczek S, Gleiss AC, Jordan LK, Pattiaratchi CB, Howey LA, Brooks EJ, Meekan MG (2018) Temperature and the vertical movements of oceanic whitetip sharks, *Carcharhinus longimanus*. *Sci Rep* 8:8351
- Annasawmy P, Ternon J, Marsac F, Cherel Y, Béhagle N, Roudaut G, Lebourges-Dhaussy A, Demarcq H, Moloney C, Jaquemet S (2018) Micronekton diel migration, community composition and trophic position within two biogeochemical provinces of the South West Indian Ocean: insight from acoustics and stable isotopes. *Deep Sea Res Part 1 Oceanogr Res Pap* 138:85-97
- Arauz R, Chávez EJ, Hoyos-Padilla EM, Marshall AD (2019) First record of the reef manta ray, *Mobula alfredi*, from the eastern Pacific. *Mar Biodivers Rec* 12:3
- Armstrong AO, Armstrong AJ, Jaine FRA, Couturier LIE, Fiora K, Uribe-Palomino J, Weeks SJ, Townsend KA, Bennett MB, Richardson AJ (2016) Prey density threshold and tidal influence on reef manta ray foraging at an aggregation site on the Great Barrier Reef. *PLoS ONE* 11:e0153393
- Armstrong AO, Armstrong AJ, Bennett MB, Richardson AJ, Townsend KA, Dudgeon CL (2019) Photographic identification and citizen science combine to reveal long distance movements of individual reef manta rays *Mobula alfredi* along Australia's east coast. *Mar Biodivers Rec* 12:14

- Bailleul F, Vacquie-Garcia J, Guinet C (2015) Dissolved oxygen sensor in animal-borne instruments: an innovation for monitoring the health of oceans and investigating the functioning of marine ecosystems. *PloS ONE* 10:e0132681
- Bansemer CS, Bennett MB (2011) Sex- and maturity-based differences in movement and migration patterns of grey nurse shark, *Carcharias taurus*, along the eastern coast of Australia. *Mar Freshw Res* 62:596-606
- Barkley AN, Gollock M, Samoilyis M, Llewellyn F, Shivji M, Wetherbee B, Hussey NE (2019) Complex transboundary movements of marine megafauna in the Western Indian Ocean. *Anim Conserv* 22:420-431
- Barr Y, Abelson A (2019) Feeding–cleaning trade off: manta ray ‘decision making’ as a conservation tool. *Front Mar Sci* 6:88
- Barton K, Barton MK (2018) ‘MuMIn’: Multi-model inference. R package, version 1.15.16. <https://CRAN.R-project.org/package=MuMIn>
- Bauer R (2018) RchivalTag: analyzing archival tagging data. R package version 0.0.7 <https://CRAN.R-project.org/package=RchivalTag>
- Bellwood DR, Wainwright PC, Fulton CJ, Hoey AS (2005) Functional versatility supports coral reef biodiversity. *Proc R Soc Biol Sci Ser B* 273:101-107
- Benedetti F, Jalabert L, Sourisseau M, Becker B, Cailliau C, Desnos C, Elineau A, Irisson J-O, Lombard F, Picheral M, Stemmann L, Pouline P (2019) The seasonal and inter-annual fluctuations of plankton abundance and community structure in a North Atlantic Marine Protected Area. *Front Mar Sci* 6:214
- Benoit-Bird K, Au W (2002) Fine-scale diel migration dynamics of an island-associated sound-scattering layer. *J Acoust Soc Am* 112:2208-2208
- Bograd SJ, Block BA, Costa DP, Godley BJ (2010) Biologging technologies: new tools for conservation. Introduction. *Endanger Species Res* 10:1-7
- Braun CD, Skomal GB, Thorrold SR, Berumen ML (2014) Diving behavior of the reef manta ray links coral reefs with adjacent deep pelagic habitats. *PLoS ONE* 9:e88170
- Braun CD, Skomal GB, Thorrold SR, Berumen ML (2015) Movements of the reef manta ray (*Manta alfredi*) in the Red Sea using satellite and acoustic telemetry. *Mar Biol* 162:2351-2362
- Braun CD, Galuardi B, Thorrold SR (2018a) HMMoce: an R package for improved geolocation of archival-tagged fishes using a hidden Markov method. *Methods Ecol Evol* 9:1212-1220
- Braun CD, Skomal GB, Thorrold SR (2018b) Integrating archival tag data and a high-resolution oceanographic model to estimate basking shark (*Cetorhinus maximus*) movements in the Western Atlantic. *Front Mar Sci* 5:25

- Brown AM, Bejder L, Pollock KH, Allen SJ (2016) Site-specific assessments of the abundance of three inshore dolphin species to inform conservation and management. *Front Mar Sci* 3:4
- Burgess KB, Bennett MB (2016) Effects of ethanol storage and lipid and urea extraction on  $\delta^{15}\text{N}$  and  $\delta^{13}\text{C}$  isotope ratios in a benthic elasmobranch, the bluespotted maskray *Neotrygon kuhlii*. *J Fish Biol* 90:417-423
- Burgess KB, Couturier LIE, Marshall AD, Richardson AJ, Weeks SJ, Bennett MB (2016) *Manta birostris*, predator of the deep? Insight into the diet of the giant manta ray through stable isotope analysis. *Royal Soc Open Sci* 3:160717
- Burgess KB, Guerrero M, Richardson AJ, Bennett MB, Marshall AD (2018) Use of epidermal mucus in elasmobranch stable isotope studies: a pilot study using the giant manta ray (*Manta birostris*). *Mar Freshw Res* 69:336-342
- Cagua EF (2012) Factors affecting detection probability of acoustic tags in coral reefs. Master's thesis, King Abdullah University of Science and Technology, Saudi Arabia
- Cagua EF, Cochran JE, Rohner CA, Prebble CE, Sinclair-Taylor TH, Pierce SJ, Berumen ML (2015) Acoustic telemetry reveals cryptic residency of whale sharks. *Biol Lett* 11:1-5
- Calenge C (2006) The package “adehabitat” for the R software: a tool for the analysis of space and habitat use by animals. *Ecol Model* 197:516-519
- Canese S, Cardinali A, Romeo T, Giusti M, Salvati E, Angiolillo M, Greco S (2011) Diving behavior of the giant devil ray in the Mediterranean Sea. *Endanger Species Res* 14:171-176
- Carlisle AB, Litvin SY, Madigan DJ, Lyons K, Bigman JS, Ibarra M, Bizzarro JJ (2016) Interactive effects of urea and lipid content confound stable isotope analysis in elasmobranch fishes. *Can J Fish Aquat Sci* 74:419-428
- Carpenter KE (1988) FAO species catalogue: Fusilier fishes of the world. An annotated and illustrated catalogue of Caesionid species known to date. *FAO Fish Synop* 8:75
- Cerutti-Pereyra F, Thums M, Austin CM, Bradshaw CJA, Stevens JD, Babcock RC, Pillans RD, Meekan MG (2014) Restricted movements of juvenile rays in the lagoon of Ningaloo Reef, Western Australia – evidence for the existence of a nursery. *Environ Biol Fishes* 97:371-383
- Chapman DD, Feldheim KA, Papastamatiou YP, Hueter RE (2015) There and back again: a review of residency and return migrations in sharks, with implications for population structure and management. *Annu Rev Mar Sci* 7:547-570
- Cisneros-Montemayor AM, Barnes-Mauthe M, Al-Abdulrazzak D, Navarro-Holm E, Sumaila UR (2013) Global economic value of shark ecotourism: implications for conservation. *Oryx* 47:381-388
- Clark TB (2010) Abundance, home range, and movement patterns of manta rays (*Manta alfredi*, *M. bistrosis*) in Hawai'i. Doctoral Dissertation, University of Hawai'i, Mānoa, Hawai'i

- Côté IM (2000) Evolution and ecology of cleaning symbioses in the sea. *Oceanogr Mar Biol* 38:311-355
- Couturier LIE, Jaine FRA, Townsend KA, Weeks SJ, Richardson AJ, Bennett MB (2011) Distribution, site affinity and regional movements of the manta ray, *Manta alfredi* (Krefft, 1868), along the east coast of Australia. *Mar Freshw Res* 62:628-637
- Couturier LIE, Marshall AD, Jaine FRA, Kashiwagi T, Pierce SJ, Townsend KA, Weeks SJ, Bennett MB, Richardson AJ (2012) Biology, ecology and conservation of the Mobulidae. *J Fish Biol* 80:1075-1119
- Couturier LIE, Rohner CA, Richardson AJ, Marshall AD, Jaine FRA, Bennett MB, Townsend KA, Weeks SJ, Nichols PD (2013a) Stable isotope and signature fatty acid analyses suggest reef manta rays feed on demersal zooplankton. *PLoS ONE* 8:e77152
- Couturier LIE, Rohner CA, Richardson AJ, Pierce SJ, Marshall AD, Jaine FRA, Townsend KA, Bennett MB, Weeks SJ, Nichols PD (2013b) Unusually high levels of n-6 polyunsaturated fatty acids in whale sharks and reef manta rays. *Lipids* 48:1029-1034
- Couturier LIE, Dudgeon CL, Pollock KH, Jaine FRA, Bennett MB, Townsend KA, Weeks SJ, Richardson AJ (2014) Population dynamics of the reef manta ray *Manta alfredi* in eastern Australia. *Coral Reefs* 33:329-342
- Couturier LIE, Newman P, Jaine FRA, Bennett MB, Venables WN, Cagua EF, Townsend KA, Weeks SJ, Richardson AJ (2018) Variation in occupancy and habitat use of *Mobula alfredi* at a major aggregation site. *Mar Ecol Prog Ser* 599:125-145
- Croll DA, Newton KM, Weng K, Galván-Magaña F, O'Sullivan J, Dewar H (2012) Movement and habitat use by the spine-tail devil ray in the Eastern Pacific Ocean. *Mar Ecol Prog Ser* 465:193-200
- Croll DA, Dewar H, Dulvy NK, Fernando D, Francis MP, Galván-Magaña F, Hall M, Heinrichs S, Marshall A, Mccauley D (2016) Vulnerabilities and fisheries impacts: the uncertain future of manta and devil rays. *Aquat Conserv* 26:562-575
- Csardi G, Nepusz T (2006) The igraph software package for complex network research. *InterJ Complex Syst* 1695:1-9
- Daly R, Froneman PW, Smale MJ (2013) Comparative feeding ecology of bull sharks (*Carcharhinus leucas*) in the coastal waters of the Southwest Indian Ocean inferred from stable isotope analysis. *PLoS ONE* 8:e78229
- Daly R, Smale MJ, Cowley PD, Froneman PW (2014) Residency patterns and migration dynamics of adult bull sharks (*Carcharhinus leucas*) on the east coast of southern Africa. *PLoS ONE* 9:e109357
- Deakos MH, Baker J, Bejder L (2011) Characteristics of a manta ray (*Manta alfredi*) population off Maui, Hawaii, and implications for management. *Mar Ecol Prog Ser* 429:245-260
- Deakos MH (2012) The reproductive ecology of resident manta rays (*Manta alfredi*) off Maui, Hawaii, with an emphasis on body size. *Environ Biol Fishes* 94:443-456

- Delaney DG, Johnson R, Bester MN, Gennari E (2012) Accuracy of using visual identification of white sharks to estimate residency patterns. *PLoS ONE* 7:e34753
- Dent F, Clarke S (2015) State of the global market for shark products. FAO Fisheries and Aquaculture technical paper, No. 590. FAO, Rome
- Dewar H (2002) Preliminary report: Manta harvest in Lamakera. Report from the Pflieger Institute of Environmental Research and the Nature Conservancy, Oceanside, USA
- Dewar H, Mous P, Domeier M, Muljadi A, Pet J, Whitty J (2008) Movements and site fidelity of the giant manta ray, *Manta birostris*, in the Komodo Marine Park, Indonesia. *Mar Biol* 155:121-133
- Doherty PD, Baxter JM, Gell FR, Godley BJ, Graham RT, Hall G, Hall J, Hawkes LA, Henderson SM, Johnson L, Speedie C, Witt MJ (2017) Long-term satellite tracking reveals variable seasonal migration strategies of basking sharks in the north-east Atlantic. *Sci Rep* 7:42837
- Domeier ML, Ortega-Garcia S, Nasby-Lucas N, Offield P (2019) First marlin archival tagging study suggests new direction for research. *Mar Freshw Res* 70:603-608
- Doty MS, Oguri M (1956) The island mass effect. *ICES J Mar Sci* 22:33-37
- Dulvy NK, Fowler SL, Musick JA, Cavanagh RD, Kyne PM, Harrison LR, Carlson JK, Davidson LNK, Fordham SV, Francis MP, Pollock CM, Simpfendorfer CA, Burgess GH, Carpenter KE, Compagno LJV, Ebert DA, Gibson C, Heupel MR, Livingstone SR, Sanciangco JC, Stevens JD, Valenti S, White WT (2014) Extinction risk and conservation of the world's sharks and rays. *eLife* 3:e00590
- Ebert DA, Fowler SL, Compagno LJ (2013) *Sharks of the world: a fully illustrated guide* doi:10.1111/jfb.12250. Wild Nature Press, Plymouth, UK
- Edwards JE, Pratt J, Tress N, Hussey NE (2019) Thinking deeper: uncovering the mysteries of animal movement in the deep sea. *Deep Sea Res Part 1 Oceanogr Res Pap* 146:24-43
- Egbert GD, Erofeeva SY (2002) Efficient inverse modeling of barotropic ocean tides. *J Atmospheric Ocean Technol* 19:183-204
- Estes JA, Heithaus M, McCauley DJ, Rasher DB, Worm B (2016) Megafaunal impacts on structure and function of ocean ecosystems. *Annu Rev Environ Resour* 41:83-116
- Ferreira LC, Thums M, Meeuwig JJ, Vianna GMS, Stevens J, McAuley R, Meekan MG (2015) Crossing latitudes — long-distance tracking of an apex predator. *PLoS ONE* 10:e0116916
- Ferreira LC (2017) Spatial ecology of a top-order marine predator, the tiger shark (*Galeocerdo cuvier*). PhD dissertation, University of Western Australia, Perth, Australia
- Ferreira LC, Thums M, Heithaus MR, Barnett A, Abrantes KG, Holmes BJ, Zamora LM, Frisch AJ, Pepperell JG, Burkholder D (2017) The trophic role of a large marine predator, the tiger shark *Galeocerdo cuvier*. *Sci Rep* 7:7641

- Fleming AH, Kellar NM, Allen CD, Kurle CM (2018) The utility of combining stable isotope and hormone analyses for marine megafauna research. *Front Mar Sci* 5:338
- Friedrich LA, Jefferson R, Glegg G (2014) Public perceptions of sharks: gathering support for shark conservation. *Mar Policy* 47:1-7
- Froese R, Pauly D, Editors. (2018) FishBase. Accessed October 2018. [www.fishbase.org](http://www.fishbase.org)
- Gaines SD, White C, Carr MH, Palumbi SR (2010) Designing marine reserve networks for both conservation and fisheries management. *Proc Natl Acad Sci* 107:18286-18293
- Germanov ES, Marshall AD (2014) Running the gauntlet: regional movement patterns of *Manta alfredi* through a complex of parks and fisheries. *PLoS ONE* 9:e110071
- Germanov ES, Marshall AD, Bejder L, Fossi MC, Loneragan NR (2018) Microplastics: no small problem for filter-feeding megafauna. *Trends Ecol Evol* 33:227-232
- Germanov ES, Bejder L, Chabanne DBH, Dharmadi D, Hendrawan IG, Marshall AD, Pierce SJ, van Keulen M, Loneragan NR (2019) Contrasting habitat use and population dynamics of reef manta rays within the Nusa Penida Marine Protected Area, Indonesia. *Front Mar Sci* 6:1-17
- Giering SLC, Wells SR, Mayers KMJ, Schuster H, Cornwell L, Fileman ES, Atkinson A, Cook KB, Preece C, Mayor DJ (2018) Seasonal variation of zooplankton community structure and trophic position in the Celtic Sea: a stable isotope and biovolume spectrum approach. *Prog Oceanogr* 177:101943
- Gleiss AC, Norman B, Liebsch N, Francis C, Wilson RP (2009) A new prospect for tagging large free-swimming sharks with motion-sensitive data-loggers. *Fish Res* 97:11-16
- Gleiss AC, Wilson RP, Shepard EL (2011) Making overall dynamic body acceleration work: on the theory of acceleration as a proxy for energy expenditure. *Methods Ecol Evol* 2:23-33
- Gliwicz ZM (1986) A lunar cycle in zooplankton. *Ecology* 67:883-897
- Gove JM, McManus MA, Neuheimer AB, Polovina JJ, Drazen JC, Smith CR, Merrifield MA, Friedlander AM, Ehses JS, Young CW, Dillon AK, Williams GJ (2016) Near-island biological hotspots in barren ocean basins. *Nat Commun* 7:10581
- Graham NA, Wilson SK, Carr P, Hoey AS, Jennings S, MacNeil MA (2018) Seabirds enhance coral reef productivity and functioning in the absence of invasive rats. *Nature* 559:250
- Graham RT, Witt MJ, Castellanos DW, Remolina F, Maxwell S, Godley BJ, Hawkes LA (2012) Satellite tracking of manta rays highlights challenges to their conservation. *PLoS ONE* 7:e36834
- Hammerschlag N, Gallagher A, Lazarre D (2011) A review of shark satellite tagging studies. *J Exp Mar Biol Ecol* 398:1-8
- Hammerschlag N, Skubel R, Calich H, Nelson E, Shiffman D, Wester J, Macdonald C, Cain S, Jennings L, Enchelmaier A (2017) Nocturnal and crepuscular behavior in elasmobranchs: a review of movement, habitat use, foraging, and reproduction in the dark. *Bull Mar Sci* 93:355-374

- Hamner W, Hauri I (1981) Effects of island mass: water flow and plankton pattern around a reef in the Great Barrier Reef lagoon, Australia. *Limnol Oceanogr* 26:1084-1102
- Hamylton S, Spencer T, Hagan AB (2012) Coral reefs and reef islands of the Amirantes Archipelago, Western Indian Ocean. In: Harris PT, Baker EK (eds) *Seafloor Geomorphology as Benthic Habitat: GeoHAB Atlas of Seafloor Geomorphic Features and Benthic Habitats*. Elsevier, London, United Kingdom, p 341-348
- Hannides CC, Popp BN, Landry MR, Graham BS (2009) Quantification of zooplankton trophic position in the North Pacific Subtropical Gyre using stable nitrogen isotopes. *Limnol Oceanogr* 54:50-61
- Hays GC (2003) A review of the adaptive significance and ecosystem consequences of zooplankton diel vertical migrations. *Hydrobiologia* 503:163-170
- Hays GC, Ferreira LC, Sequeira AMM, Meekan MG, Duarte CM, Bailey H, Bailleul F, Bowen WD, Caley MJ, Costa DP, Eguíluz VM, Fossette S, Friedlaender AS, Gales N, Gleiss AC, Gunn J, Harcourt R, Hazen EL, Heithaus MR, Heupel M, Holland K, Horning M, Jonsen I, Kooyman GL, Lowe CG, Madsen PT, Marsh H, Phillips RA, Righton D, Ropert-Coudert Y, Sato K, Shaffer SA, Simpfendorfer CA, Sims DW, Skomal G, Takahashi A, Trathan PN, Wikelski M, Womble JN, Thums M (2016) Key questions in marine megafauna movement ecology. *Trends Ecol Evol* 31:463-475
- Hays GC, Bailey H, Bograd SJ, Bowen WD, Campagna C, Carmichael RH, Casale P, Chiaradia A, Costa DP, Cuevas E, Nico de Bruyn PJ, Dias MP, Duarte CM, Dunn DC, Dutton PH, Esteban N, Friedlaender A, Goetz KT, Godley BJ, Halpin PN, Hamann M, Hammerschlag N, Harcourt R, Harrison A-L, Hazen EL, Heupel MR, Hoyt E, Humphries NE, Kot CY, Lea JSE, Marsh H, Maxwell SM, McMahon CR, Notarbartolo di Sciara G, Palacios DM, Phillips RA, Righton D, Schofield G, Seminoff JA, Simpfendorfer CA, Sims DW, Takahashi A, Tetley MJ, Thums M, Trathan PN, Villegas-Amtmann S, Wells RS, Whiting SD, Wildermann NE, Sequeira AMM (2019) Translating marine animal tracking data into conservation policy and management. *Trends Ecol Evol* 34:459-473
- Hazen HD, Harris L (2006) Power of maps:(counter) mapping for conservation. Doctoral Dissertation, University of British Columbia,
- Heinrichs S, O'Malley M, Medd H, Hilton P (2011) Manta ray of hope: global threat to manta and mobula rays. Manta Ray of Hope Project ([www.mantarayofhope.com](http://www.mantarayofhope.com))
- Heupel MR, Semmens J, Hobday A (2006) Automated acoustic tracking of aquatic animals: scales, design and deployment of listening station arrays. *Mar Freshw Res* 57:1-13
- Heupel MR, Carlson JK, Simpfendorfer CA (2007) Shark nursery areas: concepts, definition, characterization and assumptions. *Mar Ecol Prog Ser* 337:287-297
- Heupel MR, Kanno S, Martins APB, Simpfendorfer CA (2018) Advances in understanding the roles and benefits of nursery areas for elasmobranch populations. *Mar Freshw Res* 70:897-907



- Hinojosa-Alvarez S, Walter RP, Diaz-Jaimes P, Galván-Magaña F, Paig-Tran EM (2016) A potential third Manta Ray species near the Yucatán Peninsula? Evidence for a recently diverged and novel genetic Manta group from the Gulf of Mexico. *PeerJ* 4:e2586
- Holden M (1974) Problems in the rational exploitation of elasmobranch populations and some suggested solutions. In: Harden-Jones FR (ed) *Sea fisheries research*. Paul Elek, London, p 117-137
- Homma K, Maruyama T, Itoh T, Ishihara H, Uchida S (1999) Biology of the manta ray, *Manta birostris* Walbaum, in the Indo-Pacific. In: Seret B, Sire JY (eds) *Indo-Pacific fish biology: Proceedings of the 5th Indo-Pacific Fisheries Conference*, Noumea, 1997. Ichthyological Society of France, Paris, p 209-216
- Honig SE, Mahoney B (2016) Evidence of seabird guano enrichment on a coral reef in Oahu, Hawaii. *Mar Biol* 163:22
- Hosegood J, Humble E, Ogden R, de Bruyn M, Creer S, Stevens G, Abudaya M, Bassos-Hull K, Bonfil R, Fernando D, Foote AD, Hipperson H, Jabado RW, Kaden J, Moazzam M, Peel L, Pollett S, Ponzo A, Poortvliet M, Salah J, Senn H, Stewart J, Wintner S, Carvalho G (2019) Genome-wide data for effective conservation of manta and devil ray species. *bioRxiv* doi:10.1101/458141:458141
- How JR, de Lestang S (2012) Acoustic tracking: issues affecting design, analysis and interpretation of data from movement studies. *Mar Freshw Res* 63:312-324
- Hussey N, MacNeil M, Olin J, McMeans B, Kinney M, Chapman D, Fisk A (2012a) Stable isotopes and elasmobranchs: tissue types, methods, applications and assumptions. *J Fish Biol* 80:1449-1484
- Hussey NE, Brush J, McCarthy ID, Fisk AT (2010)  $\delta^{15}\text{N}$  and  $\delta^{13}\text{C}$  diet–tissue discrimination factors for large sharks under semi-controlled conditions. *Comp Biochem Physiol Part A Mol Integr Physiol* 155:445-453
- Hussey NE, Olin JA, Kinney MJ, McMeans BC, Fisk AT (2012b) Lipid extraction effects on stable isotope values ( $\delta^{13}\text{C}$  and  $\delta^{15}\text{N}$ ) of elasmobranch muscle tissue. *J Exp Mar Biol Ecol* 434:7-15
- Hussey NE, MacNeil MA, McMeans BC, Olin JA, Dudley SF, Cliff G, Wintner SP, Fennessy ST, Fisk AT (2014) Rescaling the trophic structure of marine food webs. *Ecol Lett* 17:239-250
- Hussey NE, Kessel ST, Aarestrup K, Cooke SJ, Cowley PD, Fisk AT, Harcourt RG, Holland KN, Iverson SJ, Kocik JF (2015) Aquatic animal telemetry: a panoramic window into the underwater world. *Science* 348:1255-642
- Jackson AL, Inger R, Parnell AC, Bearhop S (2011) Comparing isotopic niche widths among and within communities: SIBER – Stable Isotope Bayesian Ellipses in R. *J Anim Ecol* 80:595-602

- Jacoby DM, Brooks EJ, Croft DP, Sims DW (2012) Developing a deeper understanding of animal movements and spatial dynamics through novel application of network analyses. *Methods Ecol Evol* 3:574-583
- Jaine FRA, Couturier LIE, Weeks SJ, Townsend KA, Bennett MB, Fiora K, Richardson AJ (2012) When giants turn up: sighting trends, environmental influences and habitat use of the manta ray *Manta alfredi* at a coral reef. *PLoS ONE* 7:e46170
- Jaine FRA, Rohner CA, Weeks SJ, Couturier LIE, Bennett MB, Townsend KA, Richardson AJ (2014) Movements and habitat use of reef manta rays off eastern Australia: offshore excursions, deep diving and eddy affinity revealed by satellite telemetry. *Mar Ecol Prog Ser* 510:73-86
- Jefferson R, McKinley E, Capstick S, Fletcher S, Griffin H, Milanese M (2015) Understanding audiences: making public perceptions research matter to marine conservation. *Ocean Coast Manage* 115:61-70
- Jewell OJ, Gleiss AC, Jorgensen SJ, Andrzejczek S, Moxley JH, Beatty SJ, Wikelski M, Block BA, Chapple TK (2019) Cryptic habitat use of white sharks in kelp forest revealed by animal-borne video. *Biol Lett* 15:20190085
- Kashiwagi T, Marshall AD, Bennett MB, Ovenden JR (2011) Habitat segregation and mosaic sympatry of the two species of manta ray in the Indian and Pacific Oceans: *Manta alfredi* and *M. birostris*. *Mar Biodivers Rec* 4:e53
- Kawaley I (1998) Implications of the exclusive economic zone and EEZ management for Seychelles, a small midocean Island Commonwealth Territory. *Ocean Dev & Int'l L* 29:225-264
- Kessel ST, Elamin NA, Yurkowski DJ, Chekchak T, Walter RP, Klaus R, Hill G, Hussey NE (2017) Conservation of reef manta rays (*Manta alfredi*) in a UNESCO World Heritage Site: large-scale island development or sustainable tourism? *PLoS ONE* 12:e0185419
- Keynes Q (1959) Seychelles, Tropic Isles of Eden. *The National Geographic Magazine*, 116:5 p 670-695
- Kim SL, Casper DR, Galván-Magaña F, Ochoa-Díaz R, Hernández-Aguilar SB, Koch PL (2012a) Carbon and nitrogen discrimination factors for elasmobranch soft tissues based on a long-term controlled feeding study. *Environ Biol Fishes* 95:37-52
- Kim SL, del Rio CM, Casper D, Koch PL (2012b) Isotopic incorporation rates for shark tissues from a long-term captive feeding study. *J Exp Biol* 215:2495-2500
- Kitchen-Wheeler A-M (2010) Visual identification of individual manta ray (*Manta alfredi*) in the Maldives Islands, Western Indian Ocean. *Mar Biol Res* 6:351-363
- Kitchen-Wheeler A-M, Ari C, Edwards AJ (2012) Population estimates of Alfred mantas (*Manta alfredi*) in central Maldives atolls: North Male, Ari and Baa. *Environ Biol Fishes* 93:557-575

- Kneebone J, Chisholm J, Skomal G (2014) Movement patterns of juvenile sand tigers (*Carcharias taurus*) along the east coast of the USA. *Mar Biol* 161:1149-1163
- Komdeur J, Daan S (2005) Breeding in the monsoon: semi-annual reproduction in the Seychelles warbler (*Acrocephalus sechellensis*). *J Ornithol* 146:305-313
- Laake JL (2013) RMark: an R interface for analysis of capture-recapture data with MARK. Alaska Fish. Sci. Cent., NOAA, Natl. Mar. Fish. Serv., Seattle, WA
- Lander ME, Lindstrom T, Rutishauser M, Franzheim A, Holland M (2015) Development and field testing a satellite-linked fluorometer for marine vertebrates. *Anim Biotelem* 3:40
- Lawson GL, Hückstädt LA, Lavery AC, Jaffré FM, Wiebe PH, Fincke JR, Crocker DE, Costa DP (2015) Development of an animal-borne “sonar tag” for quantifying prey availability: test deployments on northern elephant seals. *Anim Biotelem* 3:22
- Lawson JM, Fordham SV, O’Malley MP, Davidson LNK, Walls RHL, Heupel MR, Stevens G, Fernando D, Budziak A, Simpfendorfer CA, Ender I, Francis MP, Notarbartolo di Sciarra G, Dulvy NK (2017) Sympathy for the devil: a conservation strategy for devil and manta rays. *PeerJ* 5:e3027
- Lea JSE, Humphries NE, von Brandis RG, Clarke CR, Sims DW (2016) Acoustic telemetry and network analysis reveal the space use of multiple reef predators and enhance marine protected area design. *Proc R Soc Lond B Biol Sci* 283:20160717
- Lea JSE (2017) Migratory behaviour and spatial dynamics of large sharks and their conservation implications. PhD dissertation, University of Plymouth, Plymouth, UK
- Lebreton J-D, Burnham KP, Clobert J, Anderson DR (1992) Modeling survival and testing biological hypotheses using marked animals: a unified approach with case studies. *Ecol Monogr* 62:67-118
- Lenke R (1988) Hormonal control of sleep-appetitive behaviour and diurnal activity rhythms in the cleaner wrasse *Labroides dimidiatus* (Labridae, Teleostei). *Behav Brain Res* 27:73-85
- Li Y, Zhang Y, Hussey NE, Dai X (2016) Urea and lipid extraction treatment effects on  $\delta^{15}\text{N}$  and  $\delta^{13}\text{C}$  values in pelagic sharks. *Rapid Commun Mass Spectrom* 30:1-8
- Logan JM, Lutcavage ME (2010) Stable isotope dynamics in elasmobranch fishes. *Hydrobiologia* 644:231-244
- Lorrain A, Houlbrèque F, Benzoni F, Barjon L, Tremblay-Boyer L, Menkes C, Gillikin DP, Payri C, Jourdan H, Boussarie G, Verheyden A, Vidal E (2017) Seabirds supply nitrogen to reef-building corals on remote Pacific islets. *Sci Rep* 7:3721
- Lysy M, Stasko AD, Swanson HK (2014) nicheROVER: (Niche) (R)egion and Niche (Over)lap Metrics for Multidimensional Ecological Niches. R package version 1.0. <https://CRAN.R-project.org/package=nicheROVER>

- Marcus L, Virtue P, Nichols PD, Meekan MG, Pethybridge H (2017) Effects of sample treatment on the analysis of stable isotopes of carbon and nitrogen in zooplankton, micronekton and a filter-feeding shark. *Mar Biol* 164:124
- Marshall AD, Compagno LJV, Bennett MB (2009) Redescription of the genus *Manta* with resurrection of *Manta alfredi* (Krefft, 1868) (Chondrichthyes; Myliobatoidei; Mobulidae). *Zootaxa* 2301:1-28
- Marshall AD, Bennett MB (2010a) The frequency and effect of shark-inflicted bite injuries to the reef manta ray *Manta alfredi*. *Afr J Mar Sci* 32:573-580
- Marshall AD, Bennett MB (2010b) Reproductive ecology of the reef manta ray *Manta alfredi* in southern Mozambique. *J Fish Biol* 77:169-190
- Marshall AD, Dudgeon CL, Bennett MB (2011) Size and structure of a photographically identified population of manta rays *Manta alfredi* in southern Mozambique. *Mar Biol* 158:1111-1124
- Marshall AD, Pierce SJ (2012) The use and abuse of photographic identification in sharks and rays. *J Fish Biol* 80:1361-1379
- Marshall AD, Bennett MB, Kodja G, Hinojosa-Alvarez S, Galvan-Magana F, Harding M, Stevens G, Kashiwagi T (2018a) *Mobula birostris* (amended version of 2011 assessment). The IUCN Red List of Threatened Species. <http://dx.doi.org/10.2305/IUCN.UK.2018-1.RLTS.T198921A126669349.en>
- Marshall AD, Kashiwagi T, Bennett MB, Deakos M, Stevens G, McGregor F, Clark T, Ishihara H, Sato K (2018b) *Mobula alfredi* (amended version of 2011 assessment). The IUCN Red List of Threatened Species. Accessed 10 February 2019. <http://dx.doi.org/10.2305/IUCN.UK.2011-2.RLTS.T195459A126665723.en>
- Mathies NH, Ogburn MB, McFall G, Fangman S (2014) Environmental interference factors affecting detection range in acoustic telemetry studies using fixed receiver arrays. *Mar Ecol Prog Ser* 495:27-38
- Matley JK, Fisk AT, Tobin AJ, Heupel MR, Simpfendorfer CA (2016) Diet-tissue discrimination factors and turnover of carbon and nitrogen stable isotopes in tissues of an adult predatory coral reef fish, *Plectropomus leopardus*. *Rapid Commun Mass Spectrom* 30:29-44
- McCauley DJ, DeSalles PA, Young HS, Dunbar RB, Dirzo R, Mills MM, Micheli F (2012a) From wing to wing: the persistence of long ecological interaction chains in less-disturbed ecosystems. *Sci Rep* 2:409
- McCauley DJ, Young HS, Dunbar RB, Estes JA, Semmens BX, Micheli F (2012b) Assessing the effects of large mobile predators on ecosystem connectivity. *Ecol Appl* 22:1711-1717
- McCauley DJ, DeSalles PA, Young HS, Papastamatiou YP, Caselle JE, Deakos MH, Gardner JP, Garton DW, Collen JD, Micheli F (2014) Reliance of mobile species on sensitive habitats: a case study of manta rays (*Manta alfredi*) and lagoons. *Mar Biol* 161:1987-1998

- Meekan MG, Fuiman LA, Davis R, Berger Y, Thums M (2015) Swimming strategy and body plan of the world's largest fish: implications for foraging efficiency and thermoregulation. *Front Mar Sci* 2:1-8
- Meyer CG, Papastamatiou YP, Clark TB (2010a) Differential movement patterns and site fidelity among trophic groups of reef fishes in a Hawaiian marine protected area. *Mar Biol* 157:1499-1511
- Meyer CG, Papastamatiou YP, Holland KN (2010b) A multiple instrument approach to quantifying the movement patterns and habitat use of tiger (*Galeocerdo cuvier*) and Galapagos sharks (*Carcharhinus galapagensis*) at French Frigate Shoals, Hawaii. *Mar Biol* 157:1857-1868
- Meyer CG (2017) Electronic tags reveal the hidden lives of fishes. *Bull Mar Sci* 93:301-318
- Meyer JL, Schultz ET, Helfman GS (1983) Fish schools: an asset to corals. *Science* 220:1047-1049
- Meyer L, Pethybridge H, Nichols PD, Beckmann C, Huveneers C (2019) Abiotic and biotic drivers of fatty acid tracers in ecology: a global analysis of chondrichthyan profiles. *Funct Ecol* 33:1243-1255
- Moazzam M (2018) Unprecedented decline in the catches of mobulids: an important component of tuna gillnet fisheries of the Northern Arabian Sea. Working Party on Ecosystems and Bycatch (WPEB). Indian Ocean Tuna Commission. <http://www.iotc.org/documents/unprecedented-decline-catches-mobulids-important-component-tuna-gillnet-fisheries-northern>
- Moss B (2017) Marine reptiles, birds and mammals and nutrient transfers among the seas and the land: an appraisal of current knowledge. *J Exp Mar Biol Ecol* 492:63-80
- Munroe S, Meyer L, Heithaus M (2018) Dietary biomarkers in shark foraging and movement ecology. In: Carrier JC, Heithaus MR, Simpfendorfer CA (eds) *Shark Research: Emerging Technologies and Applications for the Field and Laboratory* doi:10.1201/b21842. CRC Press, Boca Raton, FL, p 1-24
- Musick J, Burgess G, Cailliet G, Camhi M, Fordham S (2000) Management of sharks and their relatives (Elasmobranchii). *Fisheries* 25:9-13
- Nielsen A, Bigelow KA, Musyl MK, Sibert JR (2006) Improving light-based geolocation by including sea surface temperature. *Fish Oceanogr* 15:314-325
- Nielsen A, Sibert JR (2007) State-space model for light-based tracking of marine animals. *Can J Fish Aquat Sci* 64:1055-1068
- Notarbartolo di Sciara G (1987) A revisionary study of the genus *Mobula* Rafinesque, 1810 (Chondrichthyes: Mobulidae) with the description of a new species. *Zool J Linn Soc* 91:1-91
- Nøttestad L, Giske J, Holst JC, Huse G (1999) A length-based hypothesis for feeding migrations in pelagic fish. *Can J Fish Aquat Sci* 56:26-34

- O'Malley MP, Lee-Brooks K, Medd HB (2013) The global economic impact of manta ray watching tourism. *PLoS ONE* 8:e65051
- O'Malley MP, Townsend KA, Hilton P, Heinrichs S, Stewart JD (2017) Characterization of the trade in manta and devil ray gill plates in China and South-east Asia through trader surveys. *Aquat Conserv* 27:394-413
- O'Shea OR, Kingsford MJ, Seymour J (2010) Tide-related periodicity of manta rays and sharks to cleaning stations on a coral reef. *Mar Freshw Res* 61:65-73
- Oliver SP, Grothues TM, Williams AL, Cerna V, Silvosa M, Cases G, Reed M, Christopher S (2019) Risk and resilience: high stakes for sharks making transjurisdictional movements to use a conservation area. *Biol Conserv* 230:58-66
- Palumbi SR (2003) Population genetics, demographic connectivity, and the design of marine reserves. *Ecol Appl* 13:146-158
- Papastamatiou YP, Friedlander AM, Caselle JE, Lowe CG (2010) Long-term movement patterns and trophic ecology of blacktip reef sharks (*Carcharhinus melanopterus*) at Palmyra Atoll. *J Exp Mar Biol Ecol* 386:94-102
- Papastamatiou YP, DeSalles PA, McCauley DJ (2012) Area-restricted searching by manta rays and their response to spatial scale in lagoon habitats. *Mar Ecol Prog Ser* 456:233-244
- Papastamatiou YP, Meyer CG, Kosaki RK, Wallsgrave NJ, Popp BN (2015a) Movements and foraging of predators associated with mesophotic coral reefs and their potential for linking ecological habitats. *Mar Ecol Prog Ser* 521:155-170
- Papastamatiou YP, Watanabe YY, Bradley D, Dee LE, Weng K, Lowe CG, Caselle JE (2015b) Drivers of daily routines in an ectothermic marine predator: hunt warm, rest warmer? *PLoS ONE* 10:e0127807
- Parnell A (2016) *simmr*: A Stable Isotope Mixing Model. R package version 0.3. <https://CRAN.R-project.org/package=simmr>
- Peel LR, Daly R, Daly CAK, Stevens GMW, Collin SP, Meekan MG (2019a) Stable isotope analyses reveal unique trophic role of reef manta rays (*Mobula alfredi*) at a remote coral reef. *Royal Soc Open Sci* 6:190599
- Peel LR, Stevens GMW, Daly R, Keating Daly CA, Lea JSE, Clarke CR, Collin SP, Meekan MG (2019b) Movement and residency patterns of reef manta rays *Mobula alfredi* in the Amirante Islands, Seychelles. *Mar Ecol Prog Ser* 621:169-184
- Pethybridge HR, Choy CA, Polovina JJ, Fulton EA (2018) Improving marine ecosystem models with biochemical tracers. *Annu Rev Mar Sci* 10:199-228
- Pitt KA, Clement A-L, Connolly RM, Thibault-Botha D (2008) Predation by jellyfish on large and emergent zooplankton: implications for benthic–pelagic coupling. *Estuar Coast Shelf S* 76:827-833
- Poortvliet M, Olsen JL, Croll DA, Bernardi G, Newton K, Kollias S, O'Sullivan J, Fernando D, Stevens G, Galván Magaña F, Seret B, Wintner S, Hoarau G (2015) A dated molecular

- phylogeny of manta and devil rays (Mobulidae) based on mitogenome and nuclear sequences. *Mol Phylogenet Evol* 83:72-85
- Post DM (2002) Using stable isotopes to estimate trophic position: models, methods, and assumptions. *Ecology* 83:703-718
- Post DM, Layman CA, Arrington DA, Takimoto G, Quattrochi J, Montaña CG (2007) Getting to the fat of the matter: models, methods and assumptions for dealing with lipids in stable isotope analyses. *Oecologia* 152:179-189
- Potts GW (1973) The ethology of *Labroides dimidiatus* (cuv. & val.) (Labridae, Pisces) on Aldabra. *Anim Behav* 21:250-291
- Prebble CEM, Rohner CA, Pierce SJ, Robinson DP, Jaidah MY, Bach SS, Trueman CN (2018) Limited latitudinal ranging of juvenile whale sharks in the Western Indian Ocean suggests the existence of regional management units. *Mar Ecol Prog Ser* 601:167-183
- R Core Team (2017) R: a language and environment for statistical computing. R Foundation for Statistical Computing, Vienna, Austria <https://www.R-project.org/>
- Rajan P, Sreeraj C, Immanuel T (2012) The goatfishes (Family Mullidae) of Andaman and Nicobar Islands. *Rec Zool Surv India* 111:35-48
- Randall JE (2004) Revision of the goatfish genus *Parupeneus* (Perciformes: Mullidae) with descriptions of two new species. *Indo-Pacific Fishes* 36:1-64
- Roff G, Doropoulos C, Rogers A, Bozec Y-M, Krueck NC, Aurellado E, Priest M, Birrell C, Mumby PJ (2016) The ecological role of sharks on coral reefs. *Trends Ecol Evol* 31:395-407
- Rohner CA, Pierce SJ, Marshall AD, Weeks SJ, Bennett MB, Richardson AJ (2013) Trends in sightings and environmental influences on a coastal aggregation of manta rays and whale sharks. *Mar Ecol Prog Ser* 482:153-168
- Rohner CA, Burgess KB, Rambahiniarison JM, Stewart JD, Ponzio A, Richardson AJ (2017a) Mobulid rays feed on euphausiids in the Bohol Sea. *Royal Soc Open Sci* 4:161060
- Rohner CA, Flam AL, Pierce SJ, Marshall AD (2017b) Steep declines in sightings of manta rays and devil rays (Mobulidae) in southern Mozambique. *PeerJ Preprints* 5:e3051v3051
- Savage C (2019) Seabird nutrients are assimilated by corals and enhance coral growth rates. *Sci Rep* 9:4284
- Schott FA, McCreary Jr JP (2001) The monsoon circulation of the Indian Ocean. *Prog Oceanogr* 51:1-123
- Sequeira A, Heupel M, Lea MA, Eguíluz V, Duarte C, Meekan M, Thums M, Calich H, Carmichael R, Costa D (2019) The importance of sample size in marine megafauna tagging studies. *Ecol Appl*:e01947
- Sequeira AMM, Mellin C, Meekan MG, Sims DW, Bradshaw CJA (2013) Inferred global connectivity of whale shark *Rhincodon typus* populations. *J Fish Biol* 82:367-389

- Sequeira AMM, Rodríguez JP, Eguíluz VM, Harcourt R, Hindell M, Sims DW, Duarte CM, Costa DP, Fernández-Gracia J, Ferreira LC, Hays GC, Heupel MR, Meekan MG, Aven A, Bailleul F, Baylis AMM, Berumen ML, Braun CD, Burns J, Caley MJ, Campbell R, Carmichael RH, Clua E, Einoder LD, Friedlaender A, Goebel ME, Goldsworthy SD, Guinet C, Gunn J, Hamer D, Hammerschlag N, Hammill M, Hückstädt LA, Humphries NE, Lea M-A, Lowther A, Mackay A, McHuron E, McKenzie J, McLeay L, McMahon CR, Mengersen K, Muelbert MMC, Pagano AM, Page B, Queiroz N, Robinson PW, Shaffer SA, Shivji M, Skomal GB, Thorrold SR, Villegas-Amtmann S, Weise M, Wells R, Wetherbee B, Wiebkin A, Wienecke B, Thums M (2018) Convergence of marine megafauna movement patterns in coastal and open oceans. *Proc Natl Acad Sci* 115:3072-3077
- Setyawan E, Sianipar AB, Erdmann MV, Fischer AM, Haddy JA, Beale CS, Lewis SA, Mambrasar R (2018) Site fidelity and movement patterns of reef manta rays (*Mobula alfredi*): Mobulidae using passive acoustic telemetry in northern Raja Ampat, Indonesia. *Nature Conservation Research* 3:1-15
- Shantz AA, Ladd MC, Schrack E, Burkepille DE (2015) Fish-derived nutrient hotspots shape coral reef benthic communities. *Ecol Appl* 25:2142-2152
- Shiple ON, Murchie KJ, Frisk MG, O'Shea OR, Winchester MM, Brooks EJ, Pearson J, Power M (2018) Trophic niche dynamics of three nearshore benthic predators in The Bahamas. *Hydrobiologia* 813:177-188
- Sims DW, Witt MJ, Richardson AJ, Southall EJ, Metcalfe JD (2006) Encounter success of free-ranging marine predator movements across a dynamic prey landscape. *Proc R Soc Biol Sci Ser B* 273:1195-1201
- Skomal GB, Braun CD, Chisholm JH, Thorrold SR (2017) Movements of the white shark *Carcharodon carcharias* in the North Atlantic Ocean. *Mar Ecol Prog Ser* 580:1-16
- Sleeman JC, Meekan MG, Fitzpatrick BJ, Steinberg CR, Ancel R, Bradshaw CJA (2010) Oceanographic and atmospheric phenomena influence the abundance of whale sharks at Ningaloo Reef, Western Australia. *J Exp Mar Biol Ecol* 382:77-81
- Slovan KA, Bouyoucos IA, Brooks EJ, Sneddon LU (2019) Ethical considerations in fish research. *J Fish Biol* 94:556-577
- Stevens GMW (2016) Conservation and population ecology of Manta rays in the Maldives. University of York, York, UK
- Stevens GMW, Fernando D, Dando M, Di Sciara GN (2018a) Guide to the Manta and Devil Rays of the World. Wild Nature Press, Plymouth, UK
- Stevens GMW, Hawkins JP, Roberts CM (2018b) Courtship and mating behaviour of manta rays *Mobula alfredi* and *M. birostris* in the Maldives. *J Fish Biol* 93:344-359



- Stevens JD, Bradford RW, West GJ (2010) Satellite tagging of blue sharks (*Prionace glauca*) and other pelagic sharks off eastern Australia: depth behaviour, temperature experience and movements. *Mar Biol* 157:575-591
- Stewart JD, Beale CS, Fernando D, Sianipar AB, Burton RS, Semmens BX, Aburto-Oropeza O (2016a) Spatial ecology and conservation of *Manta birostris* in the Indo-Pacific. *Biol Conserv* 200:178-183
- Stewart JD, Hoyos-Padilla EM, Kumli KR, Rubin RD (2016b) Deep-water feeding and behavioral plasticity in *Manta birostris* revealed by archival tags and submersible observations. *Zoology* 119:406-413
- Stewart JD, Rohner CA, Araujo G, Avila J, Fernando D, Forsberg K, Ponzo A, Rambahiniarison JM, Kurle CM, Semmens BX (2017) Trophic overlap in mobulid rays: insights from stable isotope analysis. *Mar Ecol Prog Ser* 580:131-151
- Stewart JD, Jaine FRA, Armstrong AJ, Armstrong AO, Bennett MB, Burgess KB, Couturier LIE, Croll DA, Cronin MR, Deakos MH, Dudgeon CL, Fernando D, Froman N, Germanov ES, Hall MA, Hinojosa-Alvarez S, Hosegood JE, Kashiwagi T, Laglbauer BJL, Lezama-Ochoa N, Marshall AD, McGregor F, Notarbartolo di Sciara G, Palacios MD, Peel LR, Richardson AJ, Rubin RD, Townsend KA, Venables SK, Stevens GMW (2018a) Research priorities to support effective manta and devil ray conservation. *Front Mar Sci* 5:314
- Stewart JD, Nuttall M, Hickerson EL, Johnston MA (2018b) Important juvenile manta ray habitat at Flower Garden Banks National Marine Sanctuary in the northwestern Gulf of Mexico. *Mar Biol* 165:111
- Stewart KR, Lewison RL, Dunn DC, Bjorkland RH, Kelez S, Halpin PN, Crowder LB (2010) Characterizing fishing effort and spatial extent of coastal fisheries. *PloS ONE* 5:e14451
- Stoddart DR, Coe MJ, Fosberg FR (1979) D'Arros and St. Joseph, Amirante Islands. *Atoll Res Bull* 223:1-48
- Swanson HK, Lysy M, Power M, Stasko AD, Johnson JD, Reist JD (2015) A new probabilistic method for quantifying n-dimensional ecological niches and niche overlap. *Ecology* 96:318-324
- Syväranta J, Rautio M (2010) Zooplankton, lipids and stable isotopes: importance of seasonal, latitudinal, and taxonomic differences. *Can J Fish Aquat Sci* 67:1721-1729
- Temple AJ, Kiszka JJ, Stead SM, Wambiji N, Brito A, Poonian CNS, Amir OA, Jiddawi N, Fennessy ST, Pérez-Jorge S, Berggren P (2018) Marine megafauna interactions with small-scale fisheries in the southwestern Indian Ocean: a review of status and challenges for research and management. *Rev Fish Biol Fisher* 28:89-115
- Temple AJ, Wambiji N, Poonian CNS, Jiddawi N, Stead SM, Kiszka JJ, Berggren P (2019) Marine megafauna catch in southwestern Indian Ocean small-scale fisheries from landings data. *Biol Conserv* 230:113-121

- Teo SL, Boustany A, Blackwell S, Walli A, Weng KC, Block BA (2004) Validation of geolocation estimates based on light level and sea surface temperature from electronic tags. *Mar Ecol Prog Ser* 283:81-98
- Teo SL, Kudela RM, Rais A, Perle C, Costa DP, Block BA (2009) Estimating chlorophyll profiles from electronic tags deployed on pelagic animals. *Aquat Biol* 5:195-207
- Thorrold SR, Afonso P, Fontes J, Braun CD, Santos RS, Skomal GB, Berumen ML (2014) Extreme diving behaviour in devil rays links surface waters and the deep ocean. *Nat Commun* 5:4274
- Topor ZM, Rasher DB, Duffy JE, Brandl SJ (2019) Marine protected areas enhance coral reef functioning by promoting fish biodiversity. *Conserv Lett* 0:e12638
- Town C, Marshall A, Sethasathien N (2013) Manta Matcher: automated photographic identification of manta rays using keypoint features. *Ecol Evol* 3:1902-1914
- Udyawer V, Dwyer RG, Hoenner X, Babcock RC, Brodie S, Campbell HA, Harcourt RG, Huveneers C, Jaine FRA, Simpfendorfer CA, Taylor MD, Heupel MR (2018) A standardised framework for analysing animal detections from automated tracking arrays. *Anim Biotelem* 6:17
- Valls M, Olivar MP, de Puelles MF, Molí B, Bernal A, Sweeting C (2014) Trophic structure of mesopelagic fishes in the western Mediterranean based on stable isotopes of carbon and nitrogen. *J Marine Syst* 138:160-170
- Venables SK, McGregor F, Brain L, van Keulen M (2016) Manta ray tourism management, precautionary strategies for a growing industry: a case study from the Ningaloo Marine Park, Western Australia. *Pac Conserv Biol* 22:295-300
- Vianna GMS, Meekan MG, Meeuwig JJ, Speed CW (2013) Environmental influences on patterns of vertical movement and site fidelity of grey reef sharks (*Carcharhinus amblyrhynchos*) at aggregation sites. *PLoS ONE* 8:e60331
- Vianna GMS, Meekan MG, Bornovski TH, Meeuwig JJ (2014) Acoustic telemetry validates a citizen science approach for monitoring sharks on coral reefs. *PLoS ONE* 9:e95565
- Ward-Paige CA, Davis B, Worm B (2013) Global population trends and human use patterns of Manta and Mobula rays. *PLoS ONE* 8:e74835
- Ware D (1978) Bioenergetics of pelagic fish: theoretical change in swimming speed and ration with body size. *J Fish Res Board Can* 35:220-228
- Watanabe YY, Payne NL, Semmens JM, Fox A, Huveneers C (2019) Swimming strategies and energetics of endothermic white sharks during foraging. *J Exp Biol* 222:jeb185603
- Webster CN, Varpe Ø, Falk-Petersen S, Berge J, Stübner E, Brierley AS (2015) Moonlit swimming: vertical distributions of macrozooplankton and nekton during the polar night. *Polar Biol* 38:75-85
- Weihs D (1973) Optimal Fish Cruising Speed. *Nature* 245:48

- Weng KC, Boustany AM, Pyle P, Anderson SD, Brown A, Block BA (2007) Migration and habitat of white sharks (*Carcharodon carcharias*) in the eastern Pacific Ocean. *Mar Biol* 152:877-894
- Whitcraft S, O'Malley M, Hilton P (2014) The Continuing Threat to Manta and Mobula Rays: 2013-14 Market Surveys, Guangzhou, China. WildAid, San Francisco, CA
- White GC, Burnham KP (1999) Program MARK: survival estimation from populations of marked animals. *Bird Study* 46:S120-S139
- White TD, Ferretti F, Kroodsma DA, Hazen EL, Carlisle AB, Scales KL, Bograd SJ, Block BA (2019) Predicted hotspots of overlap between highly migratory fishes and industrial fishing fleets in the northeast Pacific. *Sci Adv* 5:eaau3761
- White WT, Giles J, Dharmadi, Potter IC (2006) Data on the bycatch fishery and reproductive biology of mobulid rays (Myliobatiformes) in Indonesia. *Fish Res* 82:65-73
- White WT, Corrigan S, Yang L, Henderson AC, Bazinet AL, Swofford DL, Naylor GJP (2017) Phylogeny of the manta and devilrays (Chondrichthyes: Mobulidae), with an updated taxonomic arrangement for the family. *Zool J Linn Soc* 182:50-75
- Wickham H (2016) ggplot2: Elegant Graphics for Data Analysis doi:10.1007/978-0-387-98141-3. Springer-Verlag New York
- Williams JJ, Papastamatiou YP, Caselle JE, Bradley D, Jacoby DMP (2018) Mobile marine predators: an understudied source of nutrients to coral reefs in an unfished atoll. *Proc R Soc Biol Sci Ser B* 285:20172456
- Wood SN (2017) Generalized additive models: an introduction with R. Chapman and Hall/CRC, New York
- Wyatt ASJ, Matsumoto R, Chikaraishi Y, Miyairi Y, Yokoyama Y, Sato K, Ohkouchi N, Nagata T (2019) Enhancing insights into foraging specialization in the world's largest fish using a multi-tissue, multi-isotope approach. *Ecol Monogr* 89:e01339
- Zimmerhackel JS, Rogers AA, Meekan MG, Ali K, Pannell DJ, Kragt ME (2018) How shark conservation in the Maldives affects demand for dive tourism. *Tourism Manage* 69:263-271
- Zimmerhackel JS, Kragt ME, Rogers AA, Ali K, Meekan MG (2019) Evidence of increased economic benefits from shark-diving tourism in the Maldives. *Mar Policy* 100:21-26
- Zuur A, Ieno E, Walker N, Saveliev A, Smith G (2009) Mixed effects models and extensions in ecology with R. Springer Science & Business Media, New York, NY



# Appendix A

Stewart JD, Jaine FRA, Armstrong AJ, Armstrong AO, Bennett MB, Burgess KB, Couturier LIE, Croll DA, Cronin MR, Deakos MH, Dudgeon CL, Fernando D, Froman N, Germanov ES, Hall MA, Hinojosa-Alvarez S, Hosegood JE, Kashiwagi T, Laglbauer BJL, Lezama-Ochoa N, Marshall AD, McGregor F, Notarbartolo di Sciara G, Palacios MD, Peel LR, Richardson AJ, Rubin RD, Townsend KA, Venables SK, Stevens GMW (2018) Research priorities to support effective manta and devil ray conservation. *Front Mar Sci* 5:314

## Research Priorities to Support Effective Manta and Devil Ray Conservation

### OPEN ACCESS

#### Edited by:

Mark Meekan,  
Australian Institute of Marine Science  
(AIMS), Australia

#### Reviewed by:

Camrin Braun,  
MIT/WHOI Joint Program in  
Oceanography, United States  
Nuno Queiroz,  
Centro de Investigação em  
Biodiversidade e Recursos Genéticos  
(CIBIO), Portugal  
Yannis Peter Papastamatiou,  
Florida International University,  
United States

#### \*Correspondence:

Joshua D. Stewart  
josh@mantatrust.org

#### Specialty section:

This article was submitted to  
Marine Megafauna,  
a section of the journal  
*Frontiers in Marine Science*

Received: 27 June 2018

Accepted: 15 August 2018

Published: 18 September 2018

#### Citation:

Stewart JD, Jaine FRA, Armstrong AJ,  
Armstrong AO, Bennett MB,  
Burgess KB, Couturier LIE, Croll DA,  
Cronin MR, Deakos MH, Dudgeon CL,  
Fernando D, Froman N,  
Germanov ES, Hall MA,  
Hinojosa-Alvarez S, Hosegood JE,  
Kashiwagi T, Laglbauer BJL,  
Lezama-Ochoa N, Marshall AD,  
McGregor F, Notarbartolo di Sciara G,  
Palacios MD, Peel LR, Richardson AJ,  
Rubin RD, Townsend KA,  
Venables SK and Stevens GMW  
(2018) Research Priorities to Support  
Effective Manta and Devil Ray  
Conservation. *Front. Mar. Sci.* 5:314.  
doi: 10.3389/fmars.2018.00314

Joshua D. Stewart<sup>1,2\*</sup>, Fabrice R. A. Jaine<sup>3,4</sup>, Amelia J. Armstrong<sup>5</sup>, Asia O. Armstrong<sup>5</sup>, Michael B. Bennett<sup>5</sup>, Katherine B. Burgess<sup>5,6</sup>, Lydie I. E. Couturier<sup>7</sup>, Donald A. Croll<sup>8</sup>, Melissa R. Cronin<sup>8</sup>, Mark H. Deakos<sup>9</sup>, Christine L. Dudgeon<sup>5</sup>, Daniel Fernando<sup>2,10,11</sup>, Niv Froman<sup>2</sup>, Elitza S. Germanov<sup>5,12</sup>, Martin A. Hall<sup>13</sup>, Silvia Hinojosa-Alvarez<sup>14</sup>, Jane E. Hosegood<sup>2,15</sup>, Tom Kashiwagi<sup>6,16</sup>, Betty J. L. Laglbauer<sup>17</sup>, Nerea Lezama-Ochoa<sup>18</sup>, Andrea D. Marshall<sup>6</sup>, Frazer McGregor<sup>12</sup>, Giuseppe Notarbartolo di Sciara<sup>19</sup>, Marta D. Palacios<sup>20</sup>, Lauren R. Peel<sup>2,21,22,23</sup>, Anthony J. Richardson<sup>24,25</sup>, Robert D. Rubin<sup>26</sup>, Kathy A. Townsend<sup>27</sup>, Stephanie K. Venables<sup>6,21</sup> and Guy M. W. Stevens<sup>2</sup>

<sup>1</sup> Scripps Institution of Oceanography, La Jolla, CA, United States, <sup>2</sup> The Manta Trust, Dorchester, Dorset, United Kingdom, <sup>3</sup> Sydney Institute of Marine Science, Mosman, NSW, Australia, <sup>4</sup> Department of Biological Sciences, Macquarie University, Sydney, NSW, Australia, <sup>5</sup> School of Biomedical Sciences, The University of Queensland, St. Lucia, QLD, Australia, <sup>6</sup> Marine Megafauna Foundation, Truckee, CA, United States, <sup>7</sup> Université de Brest, CNRS, IRD, Ifremer, UMR 6539 LEMAR, Plouzané, France, <sup>8</sup> Coastal Conservation Action Lab, University of California, Santa Cruz, Santa Cruz, CA, United States, <sup>9</sup> Hawaii Association of Marine Education and Research, Lahaina, HI, United States, <sup>10</sup> Department of Biology and Environmental Science, Linnaeus University, Kalmar, Sweden, <sup>11</sup> Blue Resources Trust, Colombo, Sri Lanka, <sup>12</sup> Murdoch University, Perth, WA, Australia, <sup>13</sup> Inter-American Tropical Tuna Commission, La Jolla, CA, United States, <sup>14</sup> Laboratory of Evolutionary Biology and Bioinformatics, University of Barcelona, Barcelona, Spain, <sup>15</sup> Molecular Ecology and Fisheries Genetics Laboratory, Bangor University, Bangor, United Kingdom, <sup>16</sup> Center for Fisheries, Aquaculture & Aquatic Sciences, Southern Illinois University Carbondale, Carbondale, IL, United States, <sup>17</sup> Okeanos Research Centre of the University of the Azores, Horta, Portugal, <sup>18</sup> AZTI - Tecnalia Marine Research Division, Pasaia, Spain, <sup>19</sup> Tethys Research Institute, Milan, Italy, <sup>20</sup> Instituto Politécnico Nacional (CICIMAR), La Paz, Mexico, <sup>21</sup> The School of Biological Sciences and the Oceans Institute, The University of Western Australia, Perth, WA, Australia, <sup>22</sup> Save Our Seas Foundation - D'Arros Research Centre, Geneva, Switzerland, <sup>23</sup> The Australian Institute of Marine Science, Crawley, WA, Australia, <sup>24</sup> Centre for Applications in Natural Resource Mathematics (CARM), School of Mathematics and Physics, The University of Queensland, St. Lucia, QLD, Australia, <sup>25</sup> CSIRO Oceans and Atmosphere, Ecosciences Precinct, Dutton Park, Brisbane, QLD, Australia, <sup>26</sup> Pacific Manta Research Group, Santa Rosa, CA, United States, <sup>27</sup> School of Science and Engineering, University of the Sunshine Coast, Hervey Bay, QLD, Australia

Manta and devil rays are filter-feeding elasmobranchs that are found circumglobally in tropical and subtropical waters. Although relatively understudied for most of the Twentieth century, public awareness and scientific research on these species has increased dramatically in recent years. Much of this attention has been in response to targeted fisheries, international trade in mobulid products, and a growing concern over the fate of exploited populations. Despite progress in mobulid research, major knowledge gaps still exist, hindering the development of effective management and conservation strategies. We assembled 30 leaders and emerging experts in the fields of mobulid biology, ecology, and conservation to identify pressing knowledge gaps that must be filled to facilitate improved science-based management of these vulnerable species. We highlight focal research topics in the subject areas of taxonomy and diversity, life history, reproduction and nursery areas, population trends, bycatch and fisheries, spatial dynamics and

Hosegood J, Humble E, Ogden R, de Bruyn M, Creer S, Stevens G, Abudaya M, Bassos-Hull K, Bonfil R, Fernando D, Foote AD, Hipperson H, Jabado RW, Kaden J, Moazzam M, **Peel LR**, Pollett S, Ponzo A, Poortvliet M, Salah J, Senn H, Stewart J, Wintner S, Carvalho G (2019) Genome-wide data for effective conservation of manta and devil ray species. bioRxiv doi:10.1101/458141:458141

1

2 **Genome-wide data for effective conservation of manta and devil ray**  
3 **species**

4

5 Jane Hosegood<sup>1,2,11</sup> \*, Emily Humble<sup>2,3</sup>, Rob Ogden<sup>3,4</sup>, Mark de Bruyn<sup>1,5</sup>, Si Creer<sup>1</sup>, Guy  
6 Stevens<sup>2</sup>, Mohammed Abudaya<sup>6</sup>, Kim Bassos-Hull<sup>7</sup>, Ramon Bonfil<sup>8</sup>, Daniel Fernando<sup>2,9,10</sup>,  
7 Andrew D. Foote<sup>1</sup>, Helen Hipperson<sup>11</sup>, Rima W. Jabado<sup>12</sup>, Jennifer Kaden<sup>13</sup>, Muhammad  
8 Moazzam<sup>14</sup>, **Lauren Peel<sup>2,15,16,17</sup>**, Stephen Pollett<sup>2</sup>, Alessandro Ponzo<sup>18</sup>, Marloes Poortvliet<sup>19</sup>,  
9 Jehad Salah<sup>20</sup>, Helen Senn<sup>13</sup>, Joshua Stewart<sup>2,21</sup>, Sabine Wintner<sup>22,23</sup> and Gary Carvalho<sup>1</sup>

10

11 <sup>1</sup> Molecular Ecology and Fisheries Genetics Laboratory, Bangor University, Bangor, LL57 2UW, UK

12 <sup>2</sup> The Manta Trust, Catemwood House, Norwood Lane, Dorset, DT2 0NT, UK

13 <sup>3</sup> Royal (Dick) School of Veterinary Studies and the Roslin Institute, University of Edinburgh, Easter  
14 Bush Campus, EH25 9RG, UK

15 <sup>4</sup> TRACE Wildlife Forensics Network, Edinburgh, EH12 6LE, UK

16 <sup>5</sup> The University of Sydney, School of Life and Environmental Sciences, Sydney 2006, NSW, Australia

17 <sup>6</sup> National Research Center, Gaza City-Palestine

18 <sup>7</sup> The Center for Shark Research, Mote Marine Laboratory, 1600 Ken Thompson Parkway, Sarasota, FL  
19 34236, USA

20 <sup>8</sup> Océanos Vivientes A. C. Cerrada Monserrat 9, Col. La Candelaria. CDMX 04380 Mexico.

21 <sup>9</sup> Department of Biology and Environmental Science, Linnaeus University, SE 39182 Kalmar, Sweden

22 <sup>10</sup> Blue Resources Trust, Colombo, Sri Lanka

23 <sup>11</sup> NERC Biomolecular Analysis Facility, Department of Animal and Plant Sciences, University of  
24 Sheffield, Western Bank, Sheffield, S10 2TN, UK

25 <sup>12</sup> Gulf Elasmobranch Project, P.O. Box 29588, Dubai, UAE

26 <sup>13</sup> RZSS WildGenes Lab, Royal Zoological Society of Scotland, Edinburgh EH12 6TS, UK

27 <sup>14</sup> WWF-Pakistan, 46-K, PECHS, Block 6, Karachi 75400, Pakistan

28 <sup>15</sup> School of Biological Sciences, University of Western Australia, Crawley, WA 6009, Australia

29 <sup>16</sup> The Australian Institute of Marine Science, Crawley, WA 6009, Australia

30 <sup>17</sup> Save Our Seas Foundation – D'Arros Research Centre, CH-1201, Geneva, Switzerland

31 <sup>18</sup> Large Marine Vertebrates Research Institute Philippines, Cagulada compound, Jagna, Bohol,  
32 Philippines

33 <sup>19</sup> Tolheksbos 57, 2134 GH Hoofddorp, the Netherlands

34 <sup>20</sup> Ministry of Agriculture Directorate General of Fisheries, Palestine

35 <sup>21</sup> Scripps Institution of Oceanography, La Jolla, CA, United States

36 <sup>22</sup> KwaZulu-Natal Sharks Board, Private Bag 2, Umhlanga Rocks 4320, South Africa

37 <sup>23</sup> School of Life Sciences, University of KwaZulu-Natal, Durban 4000, South Africa

38

39 \*Corresponding author: [bsp420@bangor.ac.uk](mailto:bsp420@bangor.ac.uk) or [jane@mantatrust.org](mailto:jane@mantatrust.org)



40 Abstract

41 Practical biodiversity conservation relies on delineation of biologically meaningful units, particularly  
42 with respect to global conventions and regulatory frameworks. Traditional approaches have  
43 typically relied on morphological observation, resulting in artificially broad delineations and non-  
44 optimal species units for conservation. More recently, species delimitation methods have been  
45 revolutionised with High-Throughput Sequencing approaches, allowing study of diversity within  
46 species radiations using genome-wide data. The highly mobile elasmobranchs, manta and devil rays  
47 (*Mobula* spp.), are threatened globally by targeted and bycatch fishing pressures resulting in recent  
48 protection under several global conventions. However, a lack of global data, morphological  
49 similarities, a succession of recent taxonomic changes and ineffectual traceability measures  
50 combine to impede development and implementation of a coherent and enforceable conservation  
51 strategy. Here, we generate genome-wide Single Nucleotide Polymorphism (SNP) data from among  
52 the most globally and taxonomically representative set of mobulid tissues. The resulting phylogeny  
53 and delimitation of species units represents the most comprehensive assessment of mobulid  
54 diversity with molecular data to date. We find a mismatch between current species classifications,  
55 and optimal species units for effective conservation. Specifically, we find robust evidence for an  
56 undescribed species of manta ray in the Gulf of Mexico and show that species recently synonymised  
57 are reproductively isolated. Further resolution is achieved at the population level, where cryptic  
58 diversity is detected in geographically distinct populations, and indicates potential for future  
59 traceability work determining regional location of catch. We estimate the optimal species tree and  
60 uncover substantial incomplete lineage sorting, where standing variation in extinct ancestral  
61 populations is identified as a driver of phylogenetic uncertainty, with further conservation  
62 implications. Our study provides a framework for molecular genetic species delimitation that is  
63 relevant to wide-ranging taxa of conservation concern, and highlights the potential for genomic data  
64 to support effective management, conservation and law enforcement strategies.

65